Molecular and cellular analysis of adult plant resistance in wheat to *Puccinia graminis* f. sp. *tritici*

Howard Dean Castelyn

A thesis submitted in fulfilment of the requirements for the degree *Philosophiae Doctor*, Department of Plant Sciences, University of the Free State, Bloemfontein, South Africa

2018

Promoter:

Z.A. Pretorius

Department of Plant Sciences, University of the Free State, Bloemfontein, South Africa

Co-promoter:

B. Visser

Department of Plant Sciences, University of the Free State, Bloemfontein, South Africa

Co-promoter:

L.A. Boyd

National Institute of Agricultural Botany, Cambridge, United Kingdom

Table of Contents

Declaration

(i) I, Howard Dean Castelyn, declare that the Doctoral Degree research thesis that I herewith submit for the Doctoral Degree qualification Botany at the University of the Free State is my independent work and that I have not previously submitted it for a qualification at another institution of higher education.

(ii) I, Howard Dean Castelyn, hereby declare that I am aware that the copyright is vested in the University of the Free State.

(iii) I, Howard Dean Castelyn, hereby declare that all royalties as regards intellectual property that was developed during the course of and/or in connection with the study at the University of the Free State, will accrue to the University.

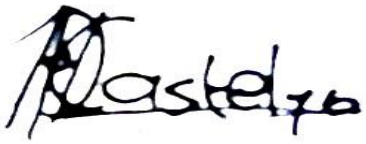

Howard Dean Castelyn

Acknowledgements

I would like to express appreciation to my promoter Prof Zakkie Pretorius and my co-promoters Prof Botma Visser and Dr Lesley Boyd for your guidance. Your expertise in the respective fields was invaluable to my project and your continuous support was crucial to my development as a researcher. I can but only hope to someday emulate your professionalism, work ethic and meticulousness as researchers.

The work was supported in part by the UK Biotechnology and Biological Sciences Research Council (BBSRC) special initiative: Sustainable Crop Production Research for International Development (SCPRID) Project BB/J011525/1. Without this contribution the project would not have been possible.

I am deeply grateful to the Prestige Doctoral Programme and the South African Research Chairs Initiative (SARChI) in Disease Resistance and Quality in Field Crops at the University of the Free State (UFS) for financial assistance during the course of my study.

A travel grant from the European and Mediterranean Cereal Rusts Foundation (EMCRF) allowed me to attend an international conference; an opportunity for which I am truly grateful.

I am grateful to the Department of Plant Sciences (UFS) for the use of their facilities and for creating a work environment that promotes research excellence. Appreciation must be extended to the National Institute of Agricultural Botany (NIAB) for hosting me at your esteemed institution and giving me the opportunity to acquire essential research skills.

Special recognition must go to Dr Nelzo Ereful (NIAB) and Louis Lategan du Preez (UFS) for helping me develop bioinformatics skills and imparting to me a deep admiration for this research tool.

I am eternally thankful to family and friends, whose encouragement gave me personal support beyond the academic field.

My sincerest appreciation goes to my dear wife Sarada for your continuous patience and motivation during the course of my study. Only you know the full extent of the challenges we faced, but together we overcame them all.

List of abbreviations

ABC	Adenosine triphosphate-binding cassette
APR	Adult plant resistance
AR	Acquired resistance
ATP	Adenosine triphosphate
Avr	Avirulence
CC-NB-LRR	Coiled-coil, nucleotide-binding and a leucine-rich repeat
DE	Differentially expressed
DH	Doubled haploid
DMPC	Dimethyldicarbonate
dpi	Days post inoculation
CTP	Chloroplast-targeted proteins
ECM	Extracellular matrix
EDTA	Ethylenediaminetetraacetic acid
EHM	Extrahaustorial matrix
ELISA	Enzyme-linked immunosorbent assay
EST	Expressed sequence tag
ETI	Effector triggered immunity
ETS	Effector triggered susceptibility
FC	Fold change
FDR	False discovery rate
GO	Gene ontology
GWAS	Genome-wide association analysis
HIGS	Host-induced gene silencing

HMC	Haustorial mother cell
hpi	Hours post inoculation
HR	Hypersensitive response
IH	Infection hyphae
JA	Jasmonic acid
LAR	Localised acquired resistance
LB	Lysogeny broth
M	Mean expression stability
MOPS	3-(*N*-Morpholino)propanesulfonic acid
MR	Moderately resistant
MRMS	Moderately resistant to moderately susceptible
MS	Moderately susceptible
NB-LRR	Nucleotide-binding and a leucine-rich repeat
NCBI	National Center for Biotechnology Information
NGS	Next generation sequencing
NHR	Non-host resistance
nt	nucleotides
PAL	Phenylalanine-ammonia lyase
PAMP	Pathogen associated molecular pattern
PCA	Principal component analysis
Pgt	*Puccinia graminis* f. sp. *tritici*
Pgt-BTUB	*Puccinia graminis* f. sp. *tritici β-tubulin*
PR	Pathogen-related
PRR	Pattern-recognition receptor
Pst	*Puccinia striiformis* f. sp. *tritici*
Pt	*Puccinia triticina*
PTI	Pathogen associated molecular pattern triggered immunity

qPCR	Quantitative polymerase chain reaction
QTL	Quantitative trait loci
R	Resistance
RenSeq	Resistance gene enrichment sequencing
RLK	Receptor-like protein kinase
RLP	Receptor-like proteins
RMR	Resistant to moderately resistant
RNA-seq	RNA sequencing
ROS	Reactive oxygen species
rpm	Revolutions per minute
RTP	Rust fungi transferred proteins
RT-qPCR	Reverse transcriptase quantitative polymerase chain reaction
R-Avr	Resistance-avirulence
S	Susceptible
SA	Salicylic acid
SAR	Systemic acquired resistance
SEM	Scanning electron microscopy
SNP	Single nucleotide polymorphism
SSV	Sub-stomatal vesicle
Ta-18S	*Triticum aestivum 18S ribosomal RNA*
Ta-BTUB	*Triticum aestivum β-tubulin*
Ta-CDC	*Triticum aestivum cell division control protein*
Ta-TEF	*Triticum aestivum transcription elongation factor 1 alpha*
TGAC	Centre for Genome Analysis
TIR-NB-LRR	Toll/interleukin receptor-like, nucleotide-binding and a leucine-rich repeat
Tris-HCl	Tris(hydroxymethyl)aminomethane-hydrochloric acid
v	Version
vs	Versus

WGA-FITC	Wheat germ agglutinin fluorescein isothiocyanate conjugate

List of figures

List of tables

List of supplementary material

Supplementary Table S1: Clustered expression profiles in log_2 fold change (FC) of differentially expressed wheat transcripts in the 37-07 line for the time vs. time comparison. The 1 and 3 days post inoculation (dpi) samples were respectively analysed in a pairwise comparison with 0 dpi sample. The five subdivided clusters (A-E) are indicated with the mean log_2FC for all transcripts within that cluster. The Ensembl accessions are reported for the differentially expressed transcripts.

Supplementary Table S2: Clustered expression profiles in log_2 fold change (FC) of differentially expressed wheat transcripts in the W1406 line for the time vs. time comparison. The 1 and 3 days post inoculation (dpi) samples were respectively analysed in a pairwise comparison with 0 dpi sample. The five subdivided clusters (A-E) are indicated with the mean log_2FC for all transcripts within that cluster. The Ensembl accessions are reported for the differentially expressed transcripts.

Supplementary Table S3: Clustered expression profiles in log_2 fold change (FC) of differentially expressed wheat transcripts in the W6979 line for the time vs. time comparison. The 1 and 3 days post inoculation (dpi) samples were respectively analysed in a pairwise comparison with 0 dpi sample. The five subdivided clusters (A-E) are indicated with the mean log_2FC for all transcripts within that cluster. The Ensembl accessions are reported for the differentially expressed transcripts.

Supplementary Table S4: Descriptions, homologies and log_2 fold change (FC) values of differentially expressed wheat transcripts in the 37-07 line for the time vs. time comparison. The Ensembl accessions and descriptions are reported for the all transcripts. Description of homologous genes and associated E values, gene ontology (GO) accessions, InterPro accessions and associated GO accessions were determined with Blast2GO and reported.

Supplementary Table S5: Descriptions, homologies and log_2 fold change (FC) values of differentially expressed wheat transcripts in the W1406 line for the time vs. time comparison. The Ensembl accessions and descriptions are reported for the all transcripts. Description of homologous genes and associated E values, gene ontology (GO) accessions, InterPro accessions and associated GO accessions were determined with Blast2GO and reported.

Supplementary Table S6: Descriptions, homologies and log_2 fold change (FC) values of differentially expressed wheat transcripts in the W6979 line for the time vs. time comparison. The Ensembl accessions and descriptions are reported for the all transcripts. Description of homologous genes and associated E values, gene ontology (GO) accessions, InterPro accessions and associated GO accessions were determined with Blast2GO and reported.

Supplementary Table S7: Clustered expression profiles in log_2 fold change (FC) of differentially expressed *Puccinia graminis* f. sp. *tritici* transcripts in the 37-07 line for the time vs. time comparison. The 1 and 3 days post inoculation (dpi) samples were respectively analysed in a pairwise comparison with 0 dpi sample. The five subdivided clusters (A-E) are indicated with the mean log_2FC for all transcripts within that cluster. The Ensembl accessions are reported for the differentially expressed transcripts.

Supplementary Table S8: Clustered expression profiles in log_2 fold change (FC) of differentially expressed *Puccinia graminis* f. sp. *tritici* transcripts in the W1406 line for the time vs. time comparison. The 1 and 3 days post inoculation (dpi) samples were respectively analysed in a pairwise comparison with 0 dpi sample. The five subdivided clusters (A-E) are indicated with the mean log_2FC for all transcripts within that cluster. The Ensembl accessions are reported for the differentially expressed transcripts.

Supplementary Table S9: Clustered expression profiles in log_2 fold change (FC) of differentially expressed *Puccinia graminis* f. sp. *tritici* transcripts in the W6979 line for the time vs. time comparison. The 1 and 3 days post inoculation (dpi) samples were respectively analysed in a pairwise comparison with 0 dpi sample. The five subdivided clusters (A-E) are indicated with the mean log_2FC for all transcripts within that cluster. The Ensembl accessions are reported for the differentially expressed transcripts.

Supplementary Table S10: Descriptions, homologies and log_2 fold change (FC) values of differentially expressed *Puccinia graminis* f. sp. *tritici* transcripts in the 37-07 line for the time vs. time comparison. The Ensembl accessions and descriptions are reported for the all transcripts. Description of homologous genes and associated E values, gene ontology (GO) accessions, InterPro accessions and associated GO accessions were determined with Blast2GO and reported.

Supplementary Table S11: Descriptions, homologies and log_2 fold change (FC) values of differentially expressed *Puccinia graminis* f. sp. *tritici* transcripts in the W1406 line for the time vs. time comparison. The Ensembl accessions and descriptions are reported for the all transcripts. Description of homologous genes and associated E values, gene ontology (GO) accessions, InterPro accessions and associated GO accessions were determined with Blast2GO and reported.

Supplementary Table S12: Descriptions, homologies and log_2 fold change (FC) values of differentially expressed *Puccinia graminis* f. sp. *tritici* transcripts in the W6979 line for the time vs. time comparison. The Ensembl accessions and descriptions are reported for the all transcripts. Description of homologous genes and associated E values, gene ontology (GO) accessions, InterPro accessions and associated GO accessions were determined with Blast2GO and reported.

Supplementary Table S13: EffectorP predictions for differentially expressed *Puccinia graminis* f. sp. *tritici* transcripts in the 37-07 line for the time vs. time comparison. Transcript products were classified as putative effectors, non-effectors or unlikely effectors based on calculated EffectorP probabilities. Putative sub-cellular localization within the host cell was determined with LOCALIZER as chloroplast, mitochondrion, nucleus or undetermined (-).

Supplementary Table S14: EffectorP predictions for differentially expressed *Puccinia graminis* f. sp. *tritici* transcripts in the W1406 line for the time vs. time comparison. Transcript products were classified as putative effectors, non-effectors or unlikely effectors based on calculated EffectorP probabilities. Putative sub-cellular localization within the host cell was determined with LOCALIZER as chloroplast, mitochondrion, nucleus or undetermined (-).

Supplementary Table S15: EffectorP predictions for differentially expressed *Puccinia graminis* f. sp. *tritici* transcripts in the W1406 line for the time vs. time comparison. Transcript products were classified as putative effectors, non-effectors or unlikely effectors based on calculated EffectorP probabilities. Putative sub-cellular localization within the host cell was determined with LOCALIZER as chloroplast, mitochondrion, nucleus or undetermined (-).

Supplementary Table S16: Clustered expression profiles in $\log_2$ fold change (FC) of differentially expressed wheat transcripts in the W1407 line for the line vs. line comparison. The 0, 1 and 3 days post inoculation (dpi) samples were respectively analysed in a pairwise comparison with same time points in the 37-07 line. The nine subdivided clusters (A-I) are indicated with the mean $\log_2$FC for all transcripts within that cluster. The Ensembl accessions are reported for the differentially expressed transcripts.

Supplementary Table S17: Clustered expression profiles in log_2 fold change (FC) of differentially expressed wheat transcripts in the W6979 line for the line vs. line comparison. The 0, 1 and 3 days post inoculation (dpi) samples were respectively analysed in a pairwise comparison with same time points in the 37-07 line. The nine subdivided clusters (A-I) are indicated with the mean log_2FC for all transcripts within that cluster. The Ensembl accessions are reported for the differentially expressed transcripts.

Supplementary Table S18: Descriptions, InterPro accessions and log_2 fold change (FC) values of differentially expressed wheat transcripts in the W1406 line for the time vs. time comparison. The Ensembl accessions and descriptions are reported for the all transcripts along with InterPro accessions and associated GO accessions.

Supplementary Table S19: Descriptions, InterPro accessions and log_2 fold change (FC) values of differentially expressed wheat transcripts in the W6979 line for the time vs. time comparison. The Ensembl accessions and descriptions are reported for the all transcripts along with InterPro accessions and associated GO accessions.

Supplementary Table S20: Putative nucleotide-binding and a leucine-rich repeat (NB-LRR) domain encoding transcripts in the W1406 line. Differentially expressed wheat transcripts in the time vs. time comparison were analysed by NLR-parser and classified based on the presence of a coiled-coil (CC)-NB-LRR or Toll/interleukin receptor-like (TIR)-NB-LRR domain.

Supplementary Table S21: Putative nucleotide-binding and a leucine-rich repeat (NB-LRR) domain encoding transcripts in the W6979 line. Differentially expressed wheat transcripts in the time vs. time comparison were analysed by NLR-parser and classified based on the presence of a coiled-coil (CC)-NB-LRR or Toll/interleukin receptor-like (TIR)-NB-LRR domain.

Supplementary Table S22: Clustered expression profiles in log_2 fold change (FC) of differentially expressed *Puccinia graminis* f. sp. *tritici* transcripts in the W1407 line for the line vs. line comparison. The 0, 1 and 3 days post inoculation (dpi) samples were respectively analysed in a pairwise comparison with same time points in the 37-07 line. The Ensembl accessions are reported for the differentially expressed transcripts.

Supplementary Table S23: Clustered expression profiles in log_2 fold change (FC) of differentially expressed *Puccinia graminis* f. sp. *tritici* transcripts in the W6979 line for the line vs. line comparison. The 0, 1 and 3 days post inoculation (dpi) samples were respectively analysed in a pairwise comparison with same time points in the 37-07 line. The Ensembl accessions are reported for the differentially expressed transcripts.

Supplementary Table S24: Descriptions, InterPro accessions and log_2 fold change (FC) values of differentially expressed *Puccinia graminis* f. sp. *tritici* transcripts in the W1406 line for the time vs. time comparison. The Ensembl accessions and descriptions are reported for the all transcripts along with InterPro accessions and associated GO accessions.

Supplementary Table S25: Descriptions, InterPro accessions and log_2 fold change (FC) values of differentially expressed *Puccinia graminis* f. sp. *tritici* transcripts in the W6979 line for the time vs. time comparison. The Ensembl accessions and descriptions are reported for the all transcripts along with InterPro accessions and associated GO accessions.

Supplementary Table S26: EffectorP predictions for differentially expressed *Puccinia graminis* f. sp. *tritici* transcripts in the W1406 line for the line vs. line comparison. Transcript products were classified as putative effectors, non-effectors or unlikely effectors based on calculated EffectorP probabilities. Putative sub-cellular localization within the host cell was determined with LOCALIZER as chloroplast, mitochondrion, nucleus or undetermined (-).

Supplementary Table S27: EffectorP predictions for differentially expressed *Puccinia graminis* f. sp. *tritici* transcripts in the W6979 line for the line vs. line comparison. Transcript products were classified as putative effectors, non-effectors or unlikely effectors based on calculated EffectorP probabilities. Putative sub-cellular localization within the host cell was determined with LOCALIZER as chloroplast, mitochondrion, nucleus or undetermined (-).

Abstract

Wheat (*Triticum aestivum* L.) production is affected by fungal diseases such as stem rust caused by *Puccinia graminis* f. sp. *tritici* Erikss. & Henning (*Pgt*). Commercially implemented single gene resistance in wheat may break down with the emergence of new virulent races of *Pgt*. Emergence of the 'Ug99' race group reaffirmed the need for durable stem rust resistance. A paradigm shift is therefore required towards durable types of resistance. Adult plant resistance (APR) may remain durable in the presence of new pathogen races. A preceding project identified two Kenyan wheat lines (W1406 and W6979) from the Genome Resource Unit (Norwich, UK) that exhibited APR to *Pgt*. The aim of this study was to investigate the APR response to *Pgt* race PTKST in W1406 and W6979 compared to a susceptible control (37-07). Four greenhouse trials were done and *Pgt*-inoculated flag leaf sheaths were sampled at selected days post inoculation (dpi). Histological observations using scanning electron microscopy and fluorescence microscopy, described the infection process of *Pgt* on wheat flag leaf sheaths. Fluorescence microscopy in particular showed a significant decrease in *Pgt* colony sizes in the APR lines at 5 dpi. Fungal biomass quantification with a chitin-binding probe and relative expression of the *Pgt β-tubulin* gene distinguished the APR lines from line 37-07 at 5 and 10 dpi. Relative expression of a haustorium-associated gene also distinguished the APR lines from the control line at 5 dpi. Taken together, these findings supported phenotypic evidence that W1406 and W6979 inhibited *Pgt* development, but that the effect was more pronounced in W6979. These results prompted the selection of time points earlier than 5 dpi for RNA-sequencing (RNA-seq) analysis. A time based comparison of differentially expressed (DE) transcripts showed two phases of the APR response at 1 and 3 dpi. The majority of differentially expressed transcripts in W1406 were induced at 3 dpi but in W6979 at 1 dpi. The current hypothesis maintains that the activation of an earlier defence response in W6979 caused a notable decrease of *Pgt* development in this line. The defence response in W1406 was delayed but still significantly decreased *Pgt* development. RNA-seq also identified several transcripts encoding putative effectors in *Pgt*. A comparison of differentially expressed between the APR lines and 37-07 identified a number of candidate APR associated transcripts. The current study therefore delivered a multifaceted description of the APR response in W1406 and W6979 and its effect on *Pgt* development.

Key terms: Adult plant resistance, wheat, *Triticum aestivum*, stem rust, *Puccinia graminis* f. sp. *tritici*, RNA-seq

Chapter 1: Introduction

Wheat (*Triticum aestivum*) production is under constant threat from biotic stress factors such as fungal pathogens. An important fungal pathogen that threatens global wheat production is *Puccinia graminis* f. sp. *tritici* (*Pgt*), the causal agent of stem rust (Dean *et al*., 2012). Global yield losses per year due to stem rust were estimated to be 6.2 million metric tons for the period of 1961-2009 (Pardey *et al*., 2013). These figures correspond to an estimated financial loss of 1.12 billion USD per year. Combatting *Pgt* and other fungal pathogens of wheat is an ongoing objective of farmers, breeders and agricultural researchers.

Resistance in wheat to *Pgt* is largely based on the implementation of *Sr* genes. Products of such resistance genes (*R* genes) recognise products of pathogen avirulence genes (*Avr* genes) in a highly specific plant-pathogen interaction called the R-Avr interaction. Recognition of Avr proteins from the pathogen induces a plant defence response that renders the plant resistant (Van der Biezen and Jones, 1998a). Pathogens such as *Pgt* are therefore under constant selection pressure to negate recognition by the plant and re-establish host compatibility.

The breakdown of resistance genes has received renewed attention since the emergence of the 'Ug99' race of *Pgt*. 'Ug99' was detected in 1998, an isolate collected in Uganda that acquired virulence for the *Pgt* resistance gene *Sr31* (Pretorius *et al.*, 2000). Worldwide resistance to *Pgt* was largely based on *Sr31* and the concern of 'Ug99' spreading beyond Africa re-focussed research on *Pgt*. Here the emergence of 'Ug99' is a key example of the 'boom-and-bust' cycle seen in many plant-pathogen interactions. The widespread use of a single resistance gene, for example *Sr31*, which protects numerous cultivars from a pathogen is referred to as a 'boom'. However, when a pathogen overcomes this resistance gene many cultivars may simultaneously become susceptible, informally referred to as 'bust' (McDonald and Linde, 2002). Furthermore, through step-wise mutations, 'Ug99' has acquired virulence against other *Sr* resistance genes, resulting in a race group with a shared lineage. The 'Ug99' race group consists of 13 races spread across 13 countries in Africa and the Middle East (RustTracker.org, 2016).

Non-'Ug99' races of stem rust have also received attention especially for the potential threat to wheat production in Europe. An outbreak of the TKTTF race occurred in Ethiopia during 2013/2014 (Olivera *et al.*, 2015) and the race has now been detected in North Africa, the Middle East (Singh *et al.*, 2015), Germany (Olivera Firpo *et al.*, 2017) and the United Kingdom (Lewis *et al.*, 2018). An outbreak of another race, TTTTF, has occurred in Sicily

(Bhattacharya, 2017) and may spread further into North Africa and mainland Europe (Hansen, 2017).

The deployment of durable forms of wheat stem rust resistance is required to halt the spread of *Pgt* and reduce the occurrences of new races. Durable resistance is defined as resistance that is effectively granted to a wheat cultivar grown under high disease pressure over an extended period of time (Johnson, 1979). Adult plant resistance (APR) is resistance expressed upon maturation of wheat (Gustafson and Shaner, 1982) and many sources of APR have been proven durable. Unlike *R* gene resistance, effective APR is often based on a number of genes with smaller effects working additively, each genetic region conferring a quantitative phenotype being referred to as quantitative trait loci (QTL) (Kou and Wang, 2010).

To identify potential QTL for *Pgt* resistance, Prins *et al.* (2016) undertook a genome-wide association study (GWAS) of 256 African wheat accessions held at the Genome Resource Unit, Norwich Research Park, United Kingdom. Two wheat lines of Kenyan origin, W1406 and W6979, exhibited APR to races TTKST and PTKST within the 'Ug99' linage. These APR lines were crossed with the stem rust susceptible 37-07 line and two doubled haploid (DH) mapping populations were generated. Five QTL were identified from each mapping population, including one QTL coincident with *Sr57* (*Lr34*/*Yr18*) present in both populations (Prins *et al.,* 2016). In W1406 the four identified QTL were *QSr.ufs-4D, QSr.ufs-2B.1*, *QSr.ufs-3B* and *QSr.ufs-4A*. In field trials *QSr.ufs-4D* had highest logarithm of the odds (LOD) score in most localities and *Sr57* in some. The four identified QTL in W6979 were *QSr.ufs-6A, QSr.ufs-2B.2, QSr.ufs-2D* and *QSr.ufs-3D*. In field trials *QSr.ufs-6A* had highest the LOD score in all of the localities. Both lines therefore expressed APR conferred by complex genetics, based on multiple QTL. The parental lines W1406, W6979 and 37-07 (Prins *et al.* 2016) formed the main focus of the current study.

In South Africa the PTKST race was detected in 2009 (Pretorius *et al.,* 2010) and has been proposed to be a foreign introduction (Visser *et al.,* 2011). In addition to virulence for *Sr31*, PTKST is also virulent for *Sr24* and a number of other *Sr* genes (Pretorius *et al.,* 2010) and 59 of 103 tested South African wheat cultivars/lines were seedling susceptible to PTKST (Pretorius *et al.,* 2012). PTKST has a wide distribution in Africa and has been detected in South Africa, Zimbabwe, Mozambique, Kenya, Ethiopia and Eritrea (RustTracker.org, 2016). Based on its broad virulence and distribution, *Pgt* race PTKST was selected as the inoculum in the current study.

The main aim of the study was to deliver a comprehensive description of the APR response in the W1406 and W6979 wheat lines, compared to the susceptible 37-07 line, upon inoculation with *Pgt* race PTKST, and its effects on the development of the pathogen. To achieve this a number of specific objectives were defined.

The first objective was to generate *Pgt*-inoculated flag leaf sheath samples from adult wheat plants under greenhouse conditions. Since the flag leaf sheath of the last internode is often used for phenotypic scoring of stem rust on adult wheat plants (Roelfs *et al.*, 1992), this tissue was selected for this study. Adult wheat plants were inoculated according to the method developed by Pretorius *et al.* (2007) and modified by Bender *et al.* (2016). The inoculation method was thus tested for effectiveness to reproducibly deliver *Pgt*-inoculated adult wheat plants under controlled conditions. The greenhouse trials also generated *Pgt*-inoculated flag leaf sheath samples for the subsequent time course analyses. Samples were taken at different time points from inoculation up to the appearance of uredinia at 10 days post inoculation (dpi).

The second objective was to investigate the infection process of *Pgt* on the flag leaf sheath of adult wheat plants. Histological studies of the infection process on the flag leaf sheath in particular are scarce and accurate comparisons to the adult plant infection response should refocus research on this tissue. The infection process was investigated for the insights it would provide into the cellular response conferred by APR in W1406 and W6979, and how it affects *Pgt* development.

The third specific objective was to investigate the biomass and haustorium accumulation of *Pgt* in the flag leaf sheath of adult wheat plants by reverse transcriptase quantitative polymerase chain reaction (RT-qPCR) and fluorescence measurement. Such quantitative molecular techniques must be tested for efficacy to follow *Pgt* colonization over the time course of infection and to consistently distinguish APR lines from the susceptible 37-07 line. The identified techniques should support the phenotypic classification and histological observations.

The fourth and final objective was to examine the changes in gene expression in *Pgt*-inoculated adult wheat plants. Next-generation sequencing of RNA was used as the method of choice as this allows large numbers of transcripts to be identified and compared at any given point in time and between wheat lines. Changes in gene expression over the course of infection and comparison of the APR lines to the susceptible control could reveal the

molecular mechanisms underlying the APR response in the W1406 and W6979 lines and the timing of these mechanisms. Currently, there are few published transcriptomic studies of APR to *Pgt* in wheat.

The current study therefore aims to present a multifaceted approach to an understanding of the APR response in wheat against *Pgt* infection. The study delivers both basic and applied scientific research outputs and ultimately contributes to the continued efforts of agricultural scientists to limit the worldwide spread of and damage caused by *Pgt*.

Chapter 2: Literature review

2.1 The impact of rust diseases on wheat production

Wheat (*Triticum aestivum)* is a globally important food crop with 756.5 million metric tons being produced during the 2016/2017 season (USDA, 2018). Recent models have projected that the current annual yield increase is only 38% of that required to double wheat production by 2050 (Ray *et al*., 2013). Thus, farmers and agricultural scientists must continually strive towards increasing wheat production, in part by combating numerous production constraints. Among the significant biotic constraints present are the rust fungi of the genus *Puccinia*. *Puccinia* species are obligate biotrophs of the family Pucciniaceae and the division Basidiomycota. The three *Puccinia* spp. that occur on wheat are *P. triticina* Erikss. (*Pt*), *P. striiformis* f. sp. *tritici* Erikss. (*Pst*) and *P. graminis* f. sp. *tritici* (*Pgt*), the causal agents of leaf (brown) rust, stripe (yellow) rust and stem (black) rust, respectively. The rust fungi of wheat are considered one of the most economically and scientifically important groups of plant pathogens (Dean *et al*., 2012).

2.2 Stem rust on wheat caused by *Puccinia graminis* f. sp. *tritici*

2.2.1 The life cycle of *Puccinia* spp.

Puccinia spp. occurring on wheat are heteroecious, requiring two different hosts for the completion of the sexual life cycle. On wheat *Puccinia* spp. may reproduce exclusively asexually in weather conditions unfavourable for sexual reproduction or in the absence of the alternative host. The asexual cycle involves repeated infection of wheat with urediniospores and can be completed a number of times during the wheat growing season (Voegele *et al*., 2009).

Late in the growing season structures called telia are formed on wheat and teliospores are produced which are required for the start of the sexual life cycle (Voegele *et al*., 2009). *Pgt* will here serve as an example of a sexual life cycle that requires wheat and an alternate host. In the case of *Pgt* the alternate hosts are *Berberis* spp. (barberry) and *Mahonia* spp. (Leonard and Szabo, 2005). The life cycle of *Pgt* completes five different spore stages which include urediniospores, teliospores, basidiospores, pyniospores and aeciospores. During maturation of teliospores the two haploid nuclei fuse in a process called karyogamy and meiosis is initiated. After a period of dormancy, meiosis and associated genetic recombination is completed in the teliospores. Thereafter, the teliospore forms a protruding structure called the basidium. The basidium carries four basidiospores, each spore with one haploid nucleus, which may now

spread to the alternative host of *Pgt*. Infection of the alternative host by basidiospores eventually leads to the formation of pycnia and pycniospores on the adaxial leaf surface of the alternative host. Pycniospores have a single haploid nucleus and are either of the + or - mating type. Pycniospores of one mating type are carried to the pycnial hyphae of the opposite mating type allowing fusion to occur. The fusion of the mating types from potentially different pycnia re-establishes the dikaryotic state and allows for genetic exchange. The resulting dikaryotic hyphae spread through the mesophyll of the alternative host and forms an aecium on the abaxial surface below the pynium. Aecia produce aeciospores on the alternative host, which may once again spread to wheat. Infection of wheat with aeciospores eventually leads to the formation of uredinia. *Pgt* urediniospores can once again complete the asexual life cycle on wheat and if teliospores are formed, the sexual life cycle may start again (Leonard and Szabo, 2005). The life cycle of *P. graminis* is shown in Figure 2.1.

Since the sexual phase allows exchange of genetic information, the life cycle on the alternate host is very important for the generation of new races of *Pgt* that may exhibit increased virulence against its cereal hosts (Jin, 2011). A stem rust epidemic in the United Sates in 1916 prompted a barberry eradication programme aiming to control *Pgt*. This eradication programme, often viewed as one of the most successful interventions in the history of plant disease management, decreased the number of stem rust epidemics, delayed disease onset and decreased the number of *Pgt* races (Roelfs, 1982). Under certain circumstances *Puccinia* spp. can also undergo genetic exchange during the asexual stage in wheat, but except for this and natural mutation, the asexual cycle on wheat remains clonal. The asexual cycle does however allow for rapid dispersal of spores in a wheat field, and if the *Puccinia* spp. are highly virulent on a widely grown cultivar, it could lead to an epidemic (Leonard and Szabo, 2005).

The infection process of *Puccinia* spp. on wheat during the asexual phase is near identical and to illustrate the differentiation of infection structures, *Pgt* will serve as an example. Infection starts with the successful adhesion of an urediniospore to the wheat epidermis. This adhesion is more effective on hydrophobic surfaces, but many spores release molecules that facilitate adhesion. Spores are often dispersed in a state of dormancy and activation is required before germination occurs. The passive hydration of the spore is followed by induction of metabolic processes, but germination is finally marked by the formation of a germ tube (Hardham, 2001; Leonard and Szabo, 2005).

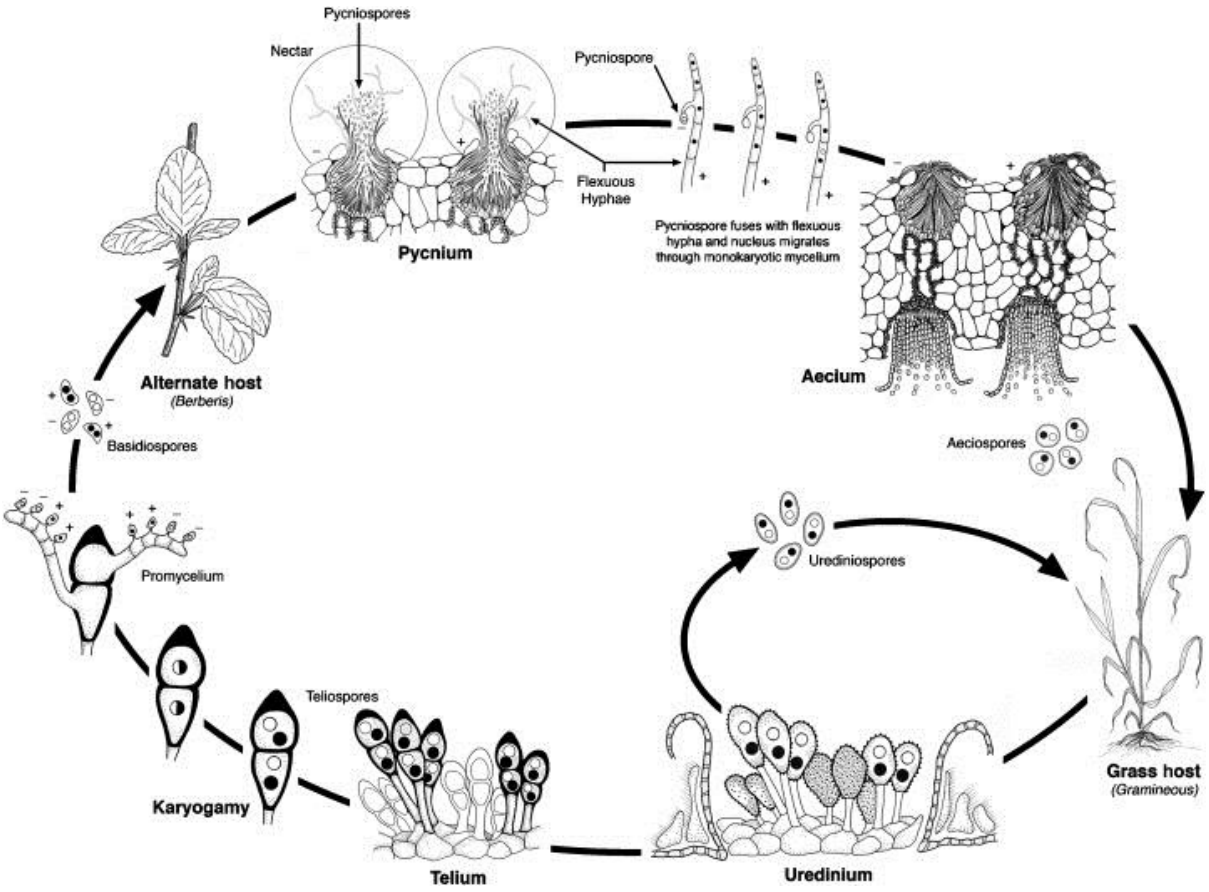

Figure 2.1: The life cycle of *P. graminis* (taken from Leonard and Szabo, 2005). The five spore stages: urediniospores, teliospores, basidiospores, pyniospores and aeciospores are indicated and are successively formed during the stages of the life cycle of *P. graminis*. During the sexual life cycle the fungal pathogen infects the grass host species (*T. aestivum* for *Pgt*), proceeds to infect the alternative host species (*Berberis* spp. and *Mahonia* spp. for *Pgt*) and thereafter infects the grass host species again. The asexual life may be completed through exclusive and continued infection of the grass host species by urediniospores.

Under advantageous conditions the spore germinates and a germ tube grows towards a stoma. The germ tube extends away from the spore with epidermal topography and chemical signals as guiding factors. The germ tube of *Pgt* has long been accepted to exhibit tropism and extend perpendicular to the length of epidermal cells (Johnson, 1934). A germ tube differentiates into an appressorium above the stoma and an infection peg allows the fungus to enter the plant's tissue via the stomatal opening. The infection peg swells into a sub-stomatal vesicle within the stomatal cavity. Infection hyphae grow from the sub-stomatal vesicle and spread through the intercellular spaces of the plant tissue. When infection hyphae reach mesophyll cells, haustorial mother cells differentiate at the tip of the infection hyphae from which a infection peg is formed that finally breaches the plant cell wall via enzymatic actions (Leonard and Szabo, 2005). A structure called a haustorium is formed, in close association with the plant cell. The haustorium does not penetrate the host plasma membrane and is surrounded by an extrahaustorial matrix, which contains proteins and carbohydrates that primarily originate from the host. For obligate biotrophs like *Pgt*, the establishment and maintenance of the interaction between the fungal haustorium and the plant mesophyll cell is crucial for the continued uptake of nutrients (Voegele and Mendgen, 2011). Genes expressed in the haustorium of *Uromyces fabae* encoded amino acid transporters (Hahn and Mendgen, 1997) and in *Pt* various proteins involved in carbohydrate and amino acid metabolism were identified (Song *et al*., 2011). It has thus been established that haustoria absorb simple carbohydrates and amino acids from the plant tissues needed for proliferation of the fungal mycelium (Voegele and Mendgen, 2011). Eventually uredinia are formed which erupt from the epidermis of infected tissue. Mature urediniospores can detach from uredinia to infect the same or other wheat plants, thereby completing the asexual cycle (Hardham, 2001; Leonard and Szabo, 2005).

2.2.2 Race nomenclature systems for *Puccinia graminis* f. sp. *tritici*

Plant resistance genes against *Pt*, *Pst* and *Pgt* are designated as *Lr*, *Yr* and *Sr* respectively, each followed by a number (McIntosh *et al*., 1995). In wheat and other Triticeae, 59 *Sr* genes have been listed (McIntosh *et al.,* 2016). Classification of *Puccinia* spp. races is based on their observed infection type on wheat differential lines that each possesses a known, but different resistance gene. Phenotypically, due to specificity of the interaction between the host and pathogen, the interaction is ranked as either compatible or incompatible. Likewise the fungal race is classified as either virulent or avirulent against the resistance gene in a differential line.

A nomenclature system for 'standard races' using 12 differential lines was proposed by Stakman *et al*. (1962). However, it soon became apparent that this set could not differentiate important new races and modifications were made by rust workers across the globe. The North American system of nomenclature for *Pgt* races was established by Roelfs and Martens (1988). Initially this system considered four groups of four wheat lines, each containing a known *Sr* gene. These sixteen lines are simultaneously infected with a *Pgt* isolate, and depending on its virulence profile on the four wheat lines within each group, a four letter alphabetic code is assigned (Roelfs and Martens, 1988). The Australian nomenclature system retained certain Stakman differentials, but added supplementary lines with the ability to classify *Pgt* races of regional importance (Park, 2007). The South African differential set proposed by Le Roux and Rijkenberg (1987) has since been replaced by the North American series, but also focuses on the South African *Pgt* populations by adding wheat lines of local significance (Terefe *et al*., 2016).

2.2.3 The spread of and recent epidemics of stem rust

2.2.3.1 The 'Ug99' race group

In 1998 severe stem rust infections were observed on wheat lines containing the *Pgt* resistance gene *Sr31* in Uganda. Virulence for *Sr31* was confirmed in 1999, prompting the common referral to the new race as 'Ug99', a name derived from the original isolate number *Pgt*-Ug99 (Pretorius *et al*., 2000). *Sr31* was the basis of much of worldwide *Pgt* resistance and the emergence of 'Ug99' was of concern. Researchers anticipated the spread of 'Ug99' to the Middle-East and Asia and the large wheat producing areas of India, China and Russia (Singh *et al*., 2006). A 2005/2006 survey of cultivars from 18 African and Asian countries estimated that 51.6% of the area under wheat production was susceptible to 'Ug99' (Singh *et al*., 2008). Globally, 66% of wheat grown worldwide is in a climate suitable for stem rust (Pardey *et al*., 2013). When 174 wheat cultivars from the United States of America were tested against the African 'Ug99' races 91.4% were susceptible (Singh *et al*., 2015). These numbers highlighted the potential threat posed to wheat by *Pgt* and the 'Ug99' race group in particular.

The African 'Ug99' race with *Sr31* virulence was initially classified as TTKS (Wanyera *et al*., 2006). The subsequent detection of 'Ug99' variants virulent on wheat containg both *Sr31* and *Sr24* prompted the inclusion of a fifth differential subset and a fifth letter in the North American code, thus distinguishing between TTKSK and TTKST (Jin *et al*., 2008). Through

various step-wise mutations 'Ug99' has acquired virulence for other *Sr* resistance genes, resulting in what is now accepted as a race group with a shared lineage, but different virulence profiles. The hypothetical race PTKSF is considered the ancestor of races in the 'Ug99' lineage (Park *et al*., 2011). Since the nomenclature of *Pgt* races is dependent on a limited number of *Sr* genes in the established differential sets, many races may still remain undescribed, requiring even more refinement of the system. For example, another variant of TTKSF, virulent on the cultivar Matlabas, was detected (Pretorius *et al*., 2012). This race most likely developed due to the breakdown of the *Sr9h* resistance gene (Rouse *et al*., 2014). Even though it was indistinguishable from TTKSF on the current five differential subsets, the addition of Matlabas as part of the differential set labelled it as TTKSF+. Despite these shortcomings, the North American *Pgt* nomenclature system remains robust, recognised and widely implemented, but also under regular revision.

The 'Ug99' race group is spread over a large geographical region; from South Africa, along Eastern Africa and towards Egypt. In Asia 'Ug99' races were detected in Yemen and Iran (Singh *et al.,* 2015). The number of races within the 'Ug99' group is also increasing as *Sr* resistance genes are overcome. In 2014, a *Pgt* race TTKTK (a race within the 'Ug99' lineage) became virulent against the resistance gene *SrTmp* and was identified in Kenya, Uganda, Rwanda and Egypt (Patpour *et al*., 2016). Through such monitoring of 'Ug99', another five races were recently added to the race group, bringing the total up to 13 races spread across 13 countries (RustTracker.org, 2016).

2.2.3.2 Non-'Ug99' races

Pgt races that do not form part of the 'Ug99' lineage have also become important. Olivera *et al.* (2015) showed that breakdown of the *SrTmp* gene for resistance against 'Ug99', may have rendered the Digalu cultivar susceptible to the non-'Ug99' race TKTTF, causing a major epidemic in Ethiopia between 2013/2014. Genotypic and phenotypic characterization identified four *Pgt* races, but race TKTTF was the main cause of the epidemic. Digalu was widely planted in Ethiopia since it had high yield and resistance to races within the known 'Ug99' lineage. The prevalence of Digalu in the field and high disease severity (80-100%) caused yield losses of 51% compared to the previous season. TKTTF has already been detected in Turkey, Iran, Lebanon, Egypt and Ethiopia (Singh *et al*., 2015).

In Germany a stem rust outbreak occurred in 2013, from which six races were detected. Though none of these races were of the 'Ug99' lineage, the TKTTF race was also present

(Olivera Firpo *et al*., 2017). Race TKTTF, or a closely related race, was detected in the United Kingdom in 2013 (Lewis *et al.*, 2018). The susceptibility of wheat varieties in the United Kingdom along with the presence of *Berberis vulgaris* L. and changing climatic conditions favour the spread of stem rust. In 2016, an outbreak of the TTTTF *Pgt* race occurred in Sicily which affected both bread and durum wheat (Bhattacharya, 2017). Spore dispersal models of the TTTTF outbreak in Sicily predicted that this race may spread further to Italy, Greece, Albania, Montenegro, Bosnia and Herzegovina, Croatia, Slovenia, Libya and Tunisia (Hansen, 2017). These findings indicate that *Pgt* may again become problematic in Europe, and highlighted the continued importance of combatting this fungal pathogen.

2.3 Pathogen effectors

2.3.1 Identification and mechanisms of effectors

Molecular studies of *Puccinia* spp. have always been complicated since, as obligate biotrophs, development of the pathogen and the formation of infection structures require a direct association with the host. Though changes in gene expression of *Pgt* transcripts can be followed within axenic cultures and infected plant tissue (Broeker *et al*., 2006) the former method may not fully emulate the colonization process. Voegele *et al.* (2001) identified haustoria as being responsible for active uptake of nutrients from the host. Cell wall strengthening during early infection stages was also associated with the inhibition of haustorium formation (Collins *et al*., 2007). These findings placed haustoria at the forefront in the study of plant-pathogen interactions. A method for haustorium isolation from infected plant tissue was first developed by Hahn and Mendgen (1997) and allowed the identification of infection induced transcripts. This technique allowed for the proteomic analysis of *Pt*-infected wheat and identified 260 proteins of fungal origin of which 50 were secreted (Song *et al*., 2011).

As knowledge of effectors increased, secretion of proteins by the pathogen became a common feature (Rep, 2005). Proteins are secreted to the extracellular matrix of haustoria or the cytosol of the host and function in creating favourable conditions for the pathogen infection within the host cell. Such proteins are classified as effectors.

Rust fungi transferred proteins (RTPs) were some of the first effectors that were shown to pass from the haustorium of *Uromyces* spp. to the host cytosol (Kemen *et al*., 2005). RTPs are so common that they are used as markers to validate haustorium isolation (Puthoff *et al*.,

2008) or to follow fungal infection (Voegele and Schmid, 2011). RTPs occur in numerous members of the Pucciniales, with 28 genes identified in the Order. The N-terminal is highly variable between species but the C-terminal is conserved and shows homology to cysteine protease inhibitors (Pretsch *et al*., 2013). In *Melampsora larici-populina* Kleb., 20 selected effectors were secreted and delivered primarily to the plant cytosol or nucleus and protein interactions with host proteins were confirmed (Petre *et al*., 2015). Interestingly, a small group of *M. larici-populina* effectors called the CTPs (chloroplast-targeted proteins) were delivered to chloroplasts. The CTPs represent effectors that hypothetically mimic host peptides to be delivered with the cell (Petre *et al*., 2016).

Effectors were shown to have a vast array of functions. *FGL1* in *Fusarium graminearum* Schwabe. encodes a lipase (Voigt *et al*., 2005), *AvrP123* in *Melampsora lini* (Ehrenb.) Lév. for a Kazal serine protease inhibitor (Catanzariti *et al*., 2006) and Avr4 in *Cladosporium fulvum* Cooke contains a chitin-binding domain (Van den Burg *et al*., 2003). It was proposed that the binding of Avr4 to chitin in the fungal wall protects it against plant chitinases (Van den Burg *et al*., 2006). Another chitin-binding effector, Slp1 in *Magnaporthe oryzae* (Hebert) Barr, leads to susceptibility in rice when it competes with the chitin oligosaccharide elicitor-binding protein (CEBiP) (Mentlak *et al*., 2012) by being *N*-glycosylated by a fungal Alg3 protein (Chen *et al*., 2014). The current model proposes that Slp1 binds chitin that would otherwise be recognised by CEBiP that would lead to a plant defence response. *Ma. oryzae* thereby evades detection by the host (Mentlak *et al*., 2012). The effectors of biotrophic pathogens are proteins which function allows the fungus to proliferate by suppressing pathogen associated molecular pattern triggered immunity (PTI) and modifying the plant's cellular environment (Vleeshouwers and Oliver, 2014). The Tin2 effector from *Ustilago maydis (DC.) Corda,* binds and stabilises the maize protein kinase ZmTTK1 which in turn activates the anthocyanin biosynthetic pathway. Researchers proposed that the anthocyanin biosynthetic pathway directs precursors away from the lignin biosynthetic pathway and lignification of the host cell walls are thus supressed (Tanaka *et al*., 2014). Many other effectors however remain undiscovered and their mechanisms undescribed.

An important group of effectors are encoded by the avirulence genes (*Avr* genes) that are recognised directly or indirectly by the resistance gene (*R* gene) products (Dodds *et al*., 2007). Once the R-Avr interaction has been established the host induces a defence response called effector triggered immunity (ETI) (Jones and Dangl, 2006). If however non-synonymous mutation alters the protein structure sufficiently to terminate the R-Avr

interaction, infection may proceed as before. Effectors, and *Avr* genes in particular, are therefore of keen importance to research. In *Pgt* two avirulence genes have recently been identified and R-Avr recognition confirmed in wheat between the products of *AvrSr35* and *Sr35* (Salcedo *et al.*, 2017) and *AvrSr50* and *Sr50* (Chen *et al.*, 2017).

2.3.2 Effectoromics

Studies implementing next generation sequencing (NGS) and bioinformatics have narrowed the search for effectors to the secretome (the sum total of secreted proteins). From there the analysis of all effectors of a pathogen (effectoromics) was undertaken which has increased the number of known effectors considerably. In a study by Cantu *et al*. (2011), genome sequencing of *Pst* and prediction of the secretome delivered 1088 putative effectors. Secretome prediction from the publically available *Pgt* genome identified 1463 putative effectors, and the secretomes of *Pst* and *Pgt* shared only 27% similarity. In another study (Duplessis *et al*., 2011), genome sequencing of *M. larici-populina* and *Pgt* delivered 812 and 1184 secreted proteins respectively. Microarray analysis of gene expression also showed only 16% overlap in the top upregulated secreted transcripts. The high diversity found in comparative studies of effectors confirms the high evolution rate of effectors.

Haustorium enrichment and NGS have also been combined. From a transcriptomic study, a total of 437 secreted proteins associated with the haustorium were predicted in *Pst* (Garnica *et al*., 2013). In *Pgt*, 520 haustorium-associated secreted proteins were identified in three races, two of which are more virulent mutants derived from the third race. Reference genome based single nucleotide polymorphism (SNP) analysis of the three races identified mutations in 25 putative effectors that may be responsible for the increased virulence in the two mutants (Upadhyaya *et al*., 2015). A transcriptomic analysis of *Pt* comparing infected tissue to purified haustoria identified 532 predicted secreted proteins, 456 of which were shared between six races. Furthermore, 15 effectors with SNP mutations resulting in non-synonymous codon changes in some races were linked to phenotypic observations. Thus effector gene mutations could be linked to virulence changes that occurred with respect to *Lr* genes (Bruce *et al*., 2014). In *Pst*, out of 2999 proteins in the secretome, five polymorphic effectors were identified in two *Pst* races (Cantu *et al*., 2013).

Comprehensive classification of effectors can now be undertaken by clustering them according to protein domain features. Eight discreet clusters were proposed, namely repeat containing, annotated haustorium expressed, induced during infection, small cysteine rich,

secreted haustoria expressed, rich in effector motifs, haustoria expressed and non-annotated (Saunders *et al*., 2012). Hierarchical clustering analysis of predicted proteins in *Pgt* and *M. larici-populina* (Saunders *et al*., 2012) and *Pst* (Cantu *et al*., 2013) has also been completed. One important class of effectors is the 'rich in cysteine' class that accounts for the largest class of effectors in *Pgt* and *M. larici-populina* (Duplessis *et al*., 2011). The current research focus to identify effectors by searching for secreted proteins has led to the development of bioinformatics tools for effector prediction such as EffectorP (Sperschneider *et al*., 2015). Through such research the list of putative effectors and knowledge of their functioning are continually increasing.

2.3.3 Validation of effector mechanisms

The validation of effector functioning can be done through a RNA-silencing method called host-induced gene silencing (HIGS). A viral vector is used to deliver an antisense nucleotide sequence into the plant which is degraded by the plant RNA-silencing mechanisms. Whereas traditional gene silencing methods were implemented to study the effects of the removal of plant transcripts, HIGS rather targets pathogen transcripts (Nunes and Dean, 2012). Barley stripe mosaic virus based HIGS negated the Avra10 effector and reduced growth of *Blumeria graminis f. sp. hordei* Marchal on barley (Nowara *et al*., 2010). HIGS by particle bombardment was used to screen 50 genes encoding haustorium secreted proteins from *B. graminis* f. sp. *hordei*. Eight genes contributed to infection and one candidate effector, encoding a ribonuclease-like gene, was shown to interfere with the hypersensitive response (HR) mechanisms of the host (Pliego *et al*., 2013).

Silencing of three *Pt* infection-associated genes led to the suppression of this disease on wheat (Panwar *et al*., 2013). Interestingly, silencing of these genes not only supressed the infection of *Pt* but also that of *Pgt* and *Pst*. Likewise, HIGS with barley stripe mosaic virus also showed disease suppression of *Pgt* when 10 haustorium associated genes were silenced (Yin *et al*., 2015). A few of these genes also supressed *Pt* and *Pst* infection when silenced in the respective interactions. HIGS therefore allows the study of effectors but is also a potential method to control a pathogen by exclusion of effectors or other essential pathogenic genes (Nunes and Dean, 2012). HIGS may thus be viewed as an approach to deliver resistance to a range of pathogens, though it may not necessarily be based on the silencing of effectors.

To validate the function of putative effectors, researchers have also used pathogenic bacteria to deliver putative effectors into plants via the type III secretion system. Transformed

Pseudomonas syringae van Hall and *Pseudomonas fluorescens* Migula expressing a *Pst* ToxA effector delivered the effector in wheat that led to the activation of the HR (Yin and Hulbert, 2011). Another bacterium, *Burkholderia glumae* Kurita and Tabei, was transformed and then successfully delivered effectors into rice, wheat and barley (Sharma *et al*., 2013). The *Ps. syringae* system for effector delivery was also used to screen multiple wheat cultivars with known *Sr* genes against putative effectors and the study established an R-Avr interaction between *Sr22* and the *PGTAUSPE-10-1* gene from *Pgt* (Upadhyaya *et al*., 2014).

The continually changing interaction between the plant host and pathogen hinges on the Avr-R gene interaction. Thereby, if a *Puccinia* spp. race can negate the Avr-R interaction by mutation of an effector, it can overcome that resistance gene. If the resistance gene is widely implemented the newly emerged race can quickly become problematic, leading to a classical 'boom and bust' cycle. This is the major disadvantage of *R* gene resistance and cause of the emergence of the 'Ug99' stem rust race group.

2.4 Plant defence

2.4.1 Constitutive defence responses

To combat fungal infections plants have evolved a number of effective constitutive and/or inducible defence responses. Constitutive defence mechanisms include both physical and chemical barriers (Johal *et al*., 1995). The first constitutive defensive barrier is the cuticle of epidermal cells and suberised cell walls that respectively contain the hydrophobic fatty acid-like polymers cutin and suberin. Pathogens evolved specialised enzymes to break through these preformed barriers (Koiattukudy, 1985).

Plant cells may also accumulate secondary metabolites that are directly detrimental to the pathogen with phytoalexins and saponins serving as examples. Various *Arabidopsis* mutants in phytoalexin synthesis pathways were more susceptible to *Hyaloperonospora parasitic*a (Pers.) Constant. (Glazebrook *et al*., 1997) and *Alternaria brassicicola* (Schwein.) Wiltshire infection (Thomma *et al*., 1999). Saponin deficient oat mutants were also shown to be more susceptible to *Gaeumannomyces graminis* (Sacc.) Arx and D.L. Olivier infection (Papadopoulou *et al*., 1999).

2.4.2 Inducible defence responses

Constitutive defences prevent a range of potential pathogens from infecting a plant species. If a pathogen overcomes the constitutive defence mechanisms, an inducible defence response is activated in the plant in order to prevent infection. Recognition of the presence of a potential pathogen is achieved by the plant by perception of small molecules called pathogen associated molecular patterns (PAMPs). PAMPs can either be fungal derived molecules or by-products of plant cell wall damage. Recognition of PAMPs by the plant leads to a signal transduction cascade that induces the basal plant defence responses. This first line of inducible plant defence is referred to as PTI (Jones and Dangl, 2006; Schwessinger and Zipfel, 2008).

Flagellin is a bacterial PAMP that was shown to induce defence responses in tomato, potato, tobacco and *Arabidopsis* (Felix *et al*., 1999). β-Glucan, a component of fungal cell wall degradation, induces defence responses in tobacco (Klarzynski *et al*., 2000) and phytoalexin accumulation rice (Yamaguchi *et al*., 2000). Likewise, chitin, also a component of fungal cell wall, can induce plant cell wall lignification in wheat (Barber and Ride, 1994) and phytoalexin accumulation in rice (Ito *et al*., 1997). These and other PAMPs have been described in numerous plant species (Nürnberger *et al*., 2004) and illustrate the similarity in their identity and their mode of their recognition.

PAMPs are recognised by pattern-recognition receptors (PRRs) in the plant that bind the PAMP, leading to the activation of a PTI signal cascade. PRRs are classified as either receptor-like protein kinases (RLKs) or receptor-like proteins (RLPs) depending on whether an intracellular kinase domain is present or not (Zipfel, 2014). In *Arabidopsis*, the chitin-binding protein was identified by Ito *et al*. (1997) and later described as the CEBiP protein (Kaku *et al*., 2006). However, CEBiP in *Arabidopsis* was not involved in signalling, but rather the CERK1 protein being the crucial receptor (Shinya *et al.*, 2012). In rice CERK1 is responsive to chitin elicitation, and required for the downstream activation of mitogen-activated protein kinases, gene expression and the production of reactive oxygen species (ROS) (Miya *et al*., 2007). CEBiP (structurally a RLP) and CERK1 (structurally a RLK) were shown to interact, forming a dimeric complex. Homo-dimeric CEBiP/CEBiP dominates in the cellular membrane, with chitin inducing the formation of the membrane associated CEBiP/CERK1 complex. The current model of chitin induced PTI in rice proposes the formation of a CEBiP/CERK1 complex, where CEBiP binds chitin and the associated CERK1 activates signal transduction via protein phosphorylation (Shimizu *et al*., 2010).

Pathogens overcome PTI by producing effectors that enable the pathogen to suppress the defence responses (Jones and Dangl, 2006) (see section 2.3.1). In the case of *Puccinia* spp., these effectors are believed to be delivered to the plant cell by the haustorium. By suppressing PTI, effector triggered susceptibility (ETS) is established (Jones and Dangl, 2006) and infection may proceed.

Host plants in turn have evolved *R* genes which may directly or indirectly recognise a specific effector protein. In doing so this effector protein has now become an avirulence factor. This recognition results in the induction of a strong plant defence response called effector triggered immunity (ETI) (Jones and Dangl, 2006). The interaction between the R and Avr proteins (R-Avr interaction) renders a plant resistant and the pathogen avirulent, thereby establishing host incompatibility. These plant-pathogen interactions are therefore referred to as gene-for-gene interactions since products of the *Avr* and *R* genes interact (Van der Biezen and Jones, 1998a).

Fungal pathogens are consequently under a strong selection pressure to negate the R-Avr interaction and establish host compatibility (i.e. ETS). Plants in turn are under strong selection pressure to re-establish host incompatibility (i.e. ETI) via an R-Avr interaction that recognises the presence of pathogens. This continual evolutionary shift between ETS and ETI, based on the specificity of the R-Avr interaction, is called the zig-zag plant defence model (Jones and Dangl, 2006).

The PTI and ETI defence responses share similarities, such as the accumulation of secondary metabolites, but ETI is regularly (although not exclusively) associated with the hypersensitive response (HR) (Jones and Dangl, 2006). The HR is characterised by localised cell death in cells in direct contact with the pathogen and in close proximity to the infection site, and is visible as tissue necrosis on a plant. The cell death effectively restricts the spread of the fungal pathogen and in the case of biotrophs, prevents the uptake of nutrients. The HR is often associated with the so-called oxidative burst, whereby ROS such as hydrogen peroxide (H_2O_2) and the superoxide anion (O_2^-) are formed (Mur *et al.*, 2008). Comparing the incompatible and compatible *Pst* responses in wheat, ROS was closely associated with the HR. The incompatible interaction quickly sees H_2O_2 and O_2^- accumulate at infection sites, whereas the compatible interaction accumulates H_2O_2 much later. In a study by Wang *et al.* (2010) the HR associated with infection sites continually increased during the incompatible interaction to reach 100% of infection sites, while during the same time interval the

compatible interaction showed the HR in less than 5% of infection sites. The delayed HR in the compatible *Pst*-wheat interaction can also be correlated with the delayed induction of H_2O_2 synthesis (Wang *et al*., 2007). In the incompatible interaction the accumulation of H_2O_2 was associated with the cell walls, plasmalemma and intercellular spaces in close proximity to infection sites (Wang *et al*., 2010).

While ROS may be directly detrimental to the pathogen, H_2O_2 is important in cell wall strengthening via the enzymatic action of peroxidases. Peroxidase is associated with cell walls and plasma membranes in wheat cells close to *Pst* infection sites (Wang *et al*., 2010). Peroxidases use H_2O_2 to catalyse the crosslinking of glycoproteins, such as lignin and suberin, in the cell wall (Passardi *et al*., 2004). Lignin is a product of the phenylpropanoid pathway with phenylalanine-ammonia lyase (PAL) being a key enzyme. The inhibition of PAL activity in wheat decreases lignification and the HR associated with *Pgt* infection sites, illustrating the importance of this enzyme (Moerschbacher *et al*., 1990). In barley infected with *B. graminis* f. sp. *hordei*, H_2O_2 is also associated with the deposition of callose and papillae formation to further reinforce the cell wall against penetration (Thordal-Christensen *et al*., 1997). Resistance granted to wheat by *Sr5* and *Sr36* was linked to callose deposition in the guard cells, thereby forming a defensive barrier before appressorium formation. Resistance granted by *Sr6*, *Sr24* and *Sr30* in turn was associated with a HR and lignification (Wang *et al*., 2015).

Peroxidases form one of the classes of pathogen-related (PR) proteins, a group of proteins rapidly induced by pathogen inoculation, which are linked with the inducible defence response and HR (Van Loon *et al*., 2006). These proteins are subdivided into 17 recognised classes, even though the properties of some are still unknown. These include β-1,3-glucanases (PR2), chitinases (PR3, PR4, PR8 and PR11), peroxidases (PR5) and defensins (PR12). β-1,3-glucanases hydrolyses the β-1,3-bonds in glucan, while chitinase in turn hydrolyses the β-1,4-bonds in chitin. Both glucan and chitin are complex polymers present in cell walls of pathogenic fungi. These PR proteins are therefore directly antifungal and effectively degrade the pathogen cell wall (Mauch *et al*., 1988). Characterization of the wheat β-1,3-glucanase activity confirmed higher expression levels during the incompatible interaction with *Pst* and localization in the host cell wall and fungal extrahaustorial matrix (Liu *et al.,* 2010). The products of some enzymatic PR proteins such as β-glucan (Klarzynski *et al*., 2000) and chitin (Barber and Ride 1994) also act as elicitors of further defense response mechanisms. Upon infection by *Pt*, β-1,3-glucanase and chitinase activity is induced

in both resistant and susceptible wheat cultivars, but to greater levels in the resistant cultivar (Anguelova-Merhar *et al*., 2001).

2.4.3 Acquired resistance

The inducible defence responses protect the plant at the site of infection but non-infected plant tissues may also exhibit improved resistance against future pathogenic attack. The feature is called acquired resistance (AR) and ensures that tissues are protected against secondary infection (Van Loon, 1997). However, a distinction must be made between localised acquired resistance (LAR) present in tissues in close proximity to the site of infection, and systemic acquired resistance (SAR) present in distal tissues. In tobacco, LAR was defined as only being present in the region of the leaf surrounding a lesion and SAR as present in the rest of the leaf (Ross, 1961a; Ross, 1961b; Dorey *et al.*, 1997) Alternatively, LAR was defined as being present in the whole leaf where the primary infection occurred (Malamy *et al.,* 1996; Mur *et al.,* 1996). The latter definition of LAR was proposed for barley (Colebrook, 2010). For both definitions, SAR is present on all other leaves of the plant where secondary infection may occur.

SAR has been confirmed in dicotyledonous plants and especially well described in *Arabidopsis* and tobacco (Sticher *et al.*,1997; Gozzo and Faoro, 2013), but limited results exist for monocotyledonous plants. *B. graminis* f. sp. *tritici* infection in barley granted SAR to subsequent *Magnaporthe grisea* (Hebert) Barr infection on secondary leaves (Jarosch *et al.*, 2003). *Ps. syringae* and *Exserohilum tercicum* (Pass.) Leonards and Suggs induced SAR in corn against *Puccinia sorghi* Schw. (Gautam and Stein, 2011). In barley, LAR was confirmed against *Ps. syringae* and *Ma. oryzae* on the same leaf as on which primary infection occurred. However, SAR was not observed for both pathogens on other leaves upon secondary infection (Colebrook *et al.,* 2012). In monocotyledonous plants, SAR therefore requires further investigation.

Numerous systemic signals have been proposed including salicylic acid (SA), the derivative methyl salicylate, jasmonic acid (JA), glycerol-3-phosphate, azelaic acid, dehydroabietinal and pipecolic acid (Dempsey and Klessig, 2012; Gozzo and Faoro, 2013). The JA signalling pathways are associated with the response to necrotrophic pathogens, the SA signalling pathway with the response to biotrophic pathogens (Durrant and Dong, 2004) while the JA and SA signalling pathways work antagonistically under the regulation of the NPR1 protein (Spoel *et al*., 2003).

The signal transduction mechanism of SAR appears to be conserved in dicotyledonous and monocotyledonous plants. The NPR1 signalling pathway is present in both rice (Chern *et al.,* 2001) and wheat (Makandar *et al.,* 2006). Genes induced during LAR in barley against *Ps. syringae* showed high similarity to those associated with SAR in *Arabidopsis* (Colebrook *et al.,* 2012). A systemic leaf extract from *Arabidopsis* could induce a SA signalling dependent defence response in wheat (Chaturvedi *et al.,* 2008) and SAR signals such as JA and SA induced the β-1,3-glucanase accumulation (Liu *et al*., 2010). Putative systemic signals must however be confirmed to be naturally transferred to distal tissue for SAR to be validated in monocotyledonous plants. The potential of putative AR signals to induce a defence response is of importance for crop protection against pathogens.

2.5 Modes of plant resistance

Understanding and applying the plant's defence mechanisms has been of crucial importance for crop protection. Broadly speaking plant resistance may be subdivided into non-host resistance (NHR) and host resistance (Periyannan *et al.,* 2017), although increasing evidence indicates considerable overlap in the two modes of action. The vast majority of potential pathogens do not have the ability to infect the majority of plant species and these are considered non-host species and the resistance is called NHR. Both constitutive defence mechanisms and a range of inducible defence responses are classified as NHR. Where a specific plant-pathogen interaction may lead to susceptibility and disease symptoms the plant is considered a host species (Mysore and Ryu, 2004). The resistance mechanism to counter the pathogen is called host resistance and may be further subdivided into race-specific resistance and race non-specific resistance.

2.5.1 Non-host resistance

In the past the inducible NHR was subdivided into type I NHR, where the HR is absent and type II where the HR is present. Type I NHR has parallels with PTI (Mysore and Ryu, 2004) and limits pathogenic infection during the earlier stages of the interaction. In *Arabidopsis* the *PEN3* gene grants NHR to *B. graminis* f. sp. *hordei* (Stein *et al*., 2006). *PEN3* encodes an ABC transporter that localises to the plant cell membrane and limits pathogen growth by exporting toxins to the apoplast at the site of infection. In turn type II NHR has parallels with ETI (Mysore and Ryu, 2004). The HR was observed in non-host interactions such as barley infected with *B. graminis* f. sp. *tritici* (Hückelhoven *et al*., 2001) and tobacco infected with *Ps. syringae* (Keith *et al*., 2003).

The type I/type II classification has however been replaced by a variable classification system, whereby a continuum of responses exist between host and non-host plants. Atienza *et al.* (2004) showed that phenotypic responses of barley infected with various *Puccinia* spp. were statistically different. Barley was classified a non-host of *Puccinai recondita* Dietel and Holw. and a host to *Puccinia hordei* G.H.Otth. However, when barley is infected with such species such as *Puccinia persistens* Plowr. and *Pt* it may be ranked in an intermediate position on the range of phenotypic responses spanning from host to non-host (Niks *et al*., 2009).

The continuum of responses between host and complete non-host plants was further clarified by a quantitative plant-rust interaction model that was proposed by Bettgenhaeuser *et al*., (2014). Thereby a plant is described as a host if the frequency of colonization and pustule formation is high and nearly all infection sites develop pustules. If the frequency of these traits is less and infection sites without eventual pustules formation are observed, the plant may be called an intermediate host. If pustules formation does not occur, but there are still some occurrences of colonization, a plant may be considered an intermediate non-host. Finally if the frequency of colonization and pustule formation is approaching zero, the plant would be described as a non-host (Bettgenhaeuser *et al*., 2014). A method to validate and further test the model was proposed by Dawson *et al*., (2015) and determines percentage colonization and pustule formation by fluorescence microscopy. The method presents barley as an intermediate host of *Pst* and *Brachypodium distachyon* L. as an intermediate non-host of *Pst.* As previously proposed, the intermediate non-host had exhibited fewer pustules of the pathogen even though colonization did occur.

In rice, NHR effectively limits development of *Puccinia* spp. before the formation of appressorium. However, if appressorium formation does occur, the majority of infection sites develop infection hyphae. NHR in rice to *Pgt*, *Pt*, *Pst* and *P. hordei* involves H_2O_2 accumulation, callose deposition, but infrequent cell death. Even within a single leaf, the NHR response of rice was variable, with a wide range of colony sizes being observed (Ayliffe *et al*., 2011). The continuum therefore also exists between the PTI- and ETI-based mechanisms that may be associated with NHR responses.

The genetic basis of NHR is under investigation since it may potentially convey resistance to a plant that is an established host of a pathogen (Bettgenhaeuser *et al*., 2014). In barley, the *Rps6* locus was identified to contribute to intermediate NHR to *Pst* (Dawson *et al.*, 2016; Li

et al., 2016). Characterizing the gene responsible for barley NHR and transforming it into wheat may grant resistance to *Pst*. Though such advances in the understanding of NHR may prove valuable in the future, historically race-specific resistance was the main focus of research and breeding programmes.

2.5.2 Race-specific/*R* gene resistance

Race-specific resistance is the consequence of the incompatible gene-for-gene interaction seen in plants (Flor, 1971). Genetic resistance implemented in agriculture is largely based on this mode of resistance and is advantageous to breeders since it allows a single *R* gene to be transferred into the genetic background of a high yielding, but potentially susceptible, cultivar. When induced, the HR commonly associated with *R* gene resistance can rapidly limit the spread of a pathogen. Race-specific resistance has also been called seedling resistance, all-stage resistance, major resistance, vertical resistance or *R* gene resistance (Lowe *et al.*, 2011) but some of these descriptions may not hold true. Race-specific resistance is often expressed during all stages of plant growth, thereby providing protection in seedlings and allowing the early screening of resistant lines by breeders. The defence response induced is based on the R-Avr interaction that triggers a defence response (Van der Biezen and Jones, 1998a).

2.5.2.1 *R* gene products as nucleotide-binding and a leucine-rich repeat proteins

The majority of race-specific *R* genes are known to encode proteins with a nucleotide-binding and a leucine-rich repeat (NB-LRR) domain (Jones and Dangl, 2006). These proteins were identified as the major receptors leading to the induction of ETI and the HR associated with the R-Avr interaction (Van der Biezen and Jones, 1998b). NB-LRR proteins therefore stand in contrast with the receptors of PTI that are most often RLKs or RLPs (Zipfel, 2014),

Since NB-LRR domains can hydrolyse adenosine triphosphate (ATP), they are classified as belonging to the STAND (signal transduction ATPases with numerous domains) family of proteins (Lukasik and Takken, 2009). In *Arabidopsis*, close to 200 genes encoding NB-LRR proteins have been identified (Meyers *et al*., 2003). More recently, 1117 NB-LRR encoding genes were identified in the wheat genome (Peng and Yang, 2017). The existing diversity within NB-LRR domains most likely recognises various potential pathogenic challenges.

In general, NB-LRR proteins have one of two additional N-terminal domains and are therefore described as either Toll/interleukin receptor-like (TIR)-NB-LRR proteins (Meyers

et al., 1999) or coiled-coil (CC)-NB-LRR proteins (Pan *et al.*, 2000). NB-LRR proteins in plants can be further grouped into four subclasses based on the presence of various domains and their arrangement (Li *et al*., 2015). Typical NB-LRR proteins have a TIR or CC N-terminal domain and other domains common to these classes of proteins. Truncated NB-LRR proteins have lost one or more of these domains. NB-LRR proteins may also have an unusual additional domain on the N-terminal or C-terminal side of the protein. Lastly NB-LRR proteins may have unusual assemblies where domains have been rearranged and even duplicated.

Comparative studies of the NB-LRR proteins in monocotyledonous and dicotyledonous plants show independent evolutionary paths since divergence of these two groups of flowering plants. In cereals, the TIR-NB-LRR subgroup appears to be absent (Pan *et al.*, 2000; Bai *et al.*, 2002). CC-NB-LRR proteins and truncated NB-LRR proteins, lacking the LRR domain, are however well represented (Bai *et al.*, 2002). Further studies in other monocotyledonous species also showed no TIR-NB-LRR proteins to be present (Tarr and Alexander, 2009).

The NB domain is in close proximity to the ARC domain and these domains are collectively called the NB-ARC domain (Van der Biezen and Jones, 1998b). ARC domains form protein interactions with the LRR domain and assure auto-inhibition of the NB domain. Resistance genes induce the HR and regulation of signal transduction is crucial to prevent unnecessary cell death. Therefore NB-LRR proteins are in a default state of auto-inhibition. The presence of pathogenic effectors cause conformational changes of the NB-LRR proteins, thereby releasing the auto-inhibitory effect of the LRR domain, leaving the NB domain free to interact with signalling proteins (Lukasik and Takken, 2009).

The strong association of NB-LRR domains with disease perception has placed the focus on genes encoding these domains. Bioinformatics techniques can be used to predict the NB-LRR domains within plant proteins. Computationally, a total of 438 genes with NB-LRR domains were identified in potato (Jupe *et al*., 2012), which increased to 755 when resistance gene enrichment sequencing (RenSeq) was used. The identified potato NB-LRR proteins were used to computationally predict 394 putative NB-LRR proteins in tomato (Jupe *et al*., 2013). RenSeq in tomato could directly annotate only 355 NB-LRR proteins, which is less than half of potato, but still includes 105 novel tomato NB-LRR proteins (Andolfo *et al*., 2014). The bioinformatics tool NLR-parser has now been developed to predict NB-LRR proteins in any

plant (Steuernagel *et al*., 2015). A further variation on RenSeq, called Mut RenSeq, has allowed the identification the *Sr22* and *Sr45* genes from wheat as encoding NB-LRR (Steuernagel *et al*., 2016).

2.5.2.2 Functioning of nucleotide-binding and a leucine-rich repeat proteins

NB-LRR proteins function cooperatively. In wheat, the *Lr10* resistance gene encodes a CC-NB-LRR protein that lies in close genetic proximity to a *resistance gene analog* 2 (*RGA2*) gene (Feuillet *et al*., 2003). The resistance conferred by *Lr10* is dependent on *RGA2*. The N terminus domain of *Lr10* is under selection pressure, identifying it as the effector interacting protein, while RGA2 may act downstream during signal transduction (Loutre *et al.,* 2009). Likewise resistance conferred by *rpg4* to barley against *Pgt* is dependent on three genes in close genetic proximity, namely *Rpg5* (a resistance gene against *Puccinia graminis* f. sp. *secalis* Erikss. and Henning), *HvRga1* (another NB-LRR encoding gene) and *HvAdf3* (a gene with homology to actin depolymerizing factors) (Wang *et al.,* 2013).

The cooperative function of NB-LRR proteins also works through the formation of polymeric complexes. In rice RGA4 and RGA5 are both required to induce a HR in the presence of the *Ma. oryzae* effector AVR1-CO39. Recognition of AVR1-CO39 and another effector (AVR-Pia) occurs directly by the C-terminal domain of RGA5. This supports a direct R-Avr interaction and recognition of multiple effectors by a single NB-LRR (Césari *et al*., 2013). RGA4 is essential for the induction of the HR while RGA5 most likely negatively regulates RGA4. Furthermore, RGA4 and RGA5 form both homo- and hetero-dimeric complexes though the interaction of their N-terminal CC domains. The model proposes that in the RGA4/RGA5 dimer complex, RGA5 recognises effectors through the C-terminal RATX1 domain, where after conformational changes release the negative regulation of RGA4 that leads to signal transduction and the eventual HR (Césari *et al*., 2014b). In *Arabidopsis,* the PopP2 effector from *Ralstonia solanacearum* Smith and the RRS1 resistance protein directly interact. This R-Avr interaction does not involve the additional C-terminal domain in RRS1, a WRKY domain (Deslandes *et al.,* 2003). RRS1 and another resistance protein RPS4 also form a dimeric complex that interacts at the N-terminal TIR domain. In this model the RPS4/RRS1 dimer conformation inhibits ETI signal transduction via the TIR domain of RPS4, but recognition of an effector by RRS1 releases inhibitory conformation (Williams *et al*., 2014).

The nature of the R-Avr interaction is under continual investigation to determine whether this interaction is direct or indirect. The former proposes a protein-protein interaction between the R and Avr gene products within the host plant (Dangl and Jones, 2001). Direct protein-protein interaction was shown in the interaction of flax (*Linum usitatissimum* L.) and the causal agent of flax rust (*M. lini*) (Dodds *et al*., 2006). Positive interactions in the yeast two-hybrid system between AvrL567 avirulence protein variants and L resistance proteins corresponded to the phenotypic responses of flax lines when exposed to the corresponding avirulence protein variants.

An indirect R-Avr interaction in turn was first proposed by Van der Biezen and Jones (1998a). The guard model proposes that the *R* gene product recognises the modification made by an effector to another protein, rather than the effector directly. The modified protein is called the guardee and the alteration is perceived by the *R* gene product (Dangl and Jones, 2001). Formally the model is based on a number of principles. Firstly, the effector targets one or multiple guardees in the plant host. Secondly, alteration of the guardees leads to susceptibility of the host in the compatible interaction. Finally, alteration of a guardee generates a molecular pattern that may be perceived by a corresponding R protein in the incompatible interaction.

Validation of the guard model can be seen for *Arabidopsis* protein RIN4 and its role during *Ps. syringae* infection. RIN4 is required for resistance granted by the RPS2. The RIN4 and RPS2 proteins are membrane associated (Axtell *et al*., 2003a) and directly interact (Mackey *et al*., 2003). RIN4 serves to negatively regulate RPS2 activity when the pathogen is absent (Belkhadir *et al*., 2004). However, RIN4 is targeted and degraded by the AvrRpt2 effector (Axtell *et al*., 2003a; Mackey *et al*., 2003). AvrRpt2 is a cysteine protease (Axtell *et al*., 2003b) that cleaves RIN4 and potentially a large number of other *Arabidopsis* proteins containing the target cleavage site (Chisholm *et al*., 2005). The action of AvrRpt2 shows that the putative function of the effector in virulence is by protein degradation (Chisholm *et al*., 2005). Degradation of RIN4 in particular releases the inhibition of RPS2, which leads to the induction of defence (Day *et al.*, 2005). RIN4 therefore acts as the guardee, which when modified, activates RPS2, triggering defence responses leading to resistance.

The existence of both direct and indirect R-Avr interactions may be explained by host specificity. By this hypothesis an indirect R-Avr interaction is associated with pathogens that infect multiple hosts such as *Ps. syringae*. A direct R-Avr interaction is associated with a

pathogen that is specialised for a single plant host, with strong selection pressure driving the co-evolution of *R* and *Avr* genes (Dodds *et al*., 2006; Jones and Dangl, 2006). However, the RPS4/RRS1 NB-LRR dimer grants resistance in *Arabidopsis* to *Colletotrichum higginsianum*, *Ralstonia solanacearum* and *Ps. syringae* (Narusaka *et al*., 2009). The interaction between RRS1 and some effectors are known to be direct (Deslandes *et al.*, 2003), challenging the association of direct effector recognition and a single specific plant-pathogen interaction.

Further modes of interaction between the *R* and *Avr* gene products that are variations of the guard model, have also been proposed. The decoy model proposes that along with the target of an effector protein, a number of decoy targets may also exist. Modification of target proteins by an effector typically leads to increased pathogenicity, but the modification of a decoy does not. The presence of these decoys theoretically then improves the chance of the R protein perceiving the modification made by an effector (Van der Hoorn and Kamoun, 2008).

Support for the decoy model is found during the infection of tomatoes (*Solanum lycopersicum* L.) with *C. fulvum* (Shabab *et al*., 2008). The fungus produces the AVR2 effector, a protease inhibitor that targets two papain-like cysteine proteases PIP1 and RCR3. Both are transcriptionally induced during benzothiadiazole treatment, but PIP1 protein levels are more abundant and most likely the target of AVR2. RCR3 is required by the Cf-2 resistance protein for resistance against *C. fulvum* (Dixon *et al*., 2000). RCR3, like PIP1, is under strong selection pressure. Therefore RCR3 may act as a decoy that induces the defence response when modified by AVR2, although PIP1 is the true target (Shabab *et al*., 2008).

The integrated decoy hypothesis proposes that a decoy may be incorporated into a NB-LRR as an additional domain. The effector directly modifies this domain by binding, resulting in conformational changes that start a signalling cascade (Césari *et al*., 2014a). The integrated decoy model is based on dimeric NB-LRR proteins such as RGA4/RGA5 in rice (Césari *et al*., 2014b) and RPS4/RRS1 in *Arabidopsis* (Williams *et al*., 2014). In such a NB-LRR dimer, one element acts as 'receptor' NB-LRR and has an additional or unusual domain that act as the decoy. The other protein in the dimer is the 'signalling' NB-LRR protein that, once activated by the first NB-LRR, leads to signal transduction (Césari *et al*., 2014a). Commentary on the integrated decoy hypothesis highlighted that domains that sense effector modification need not necessarily be decoys and may still have functionality. If functionality

was lost, it is also unknown if this occurred before or after incorporation into NB-LRR proteins (Wu *et al*., 2015). These hypotheses must however be tested further.

2.5.2.3 Durability of *R* gene resistance

The specificity of the R-Avr interaction determines which race of the pathogen is virulent on which plant cultivar, hence the term race-specific resistance. The defence response places the particular race of the pathogen under a selection pressure to negate the interaction and re-establish virulence. New races of fungal pathogens develop when selection pressure leads to the breakdown of the effectiveness of *R* genes. The 'Ug99' race group of *Pgt* developed with the breakdown of a number of widely implemented *Sr* genes (see section 2.2.3.1). This highlights a disadvantage associated with *R* gene resistance. Though some of these *Sr* genes may have become ineffective, resistance is still granted to the 'Ug99' race group by a provisional list of 39 known *Sr* genes (Singh *et al*., 2015). However, if *R* genes are not correctly utilised, new races of *Puccinia* spp. will continue to emerge and if an *R* gene is widely implemented epidemics may occur. When researchers implement resistance genes irresponsibly a continued 'boom-and-bust' cycle may occur (McDonald and Linde, 2002). A paradigm shift is therefore required to shift away from the widespread implementation of single gene resistance.

Multiple *R* genes may be combined to attempt to assure durability in wheat. The approach is called gene pyramiding or stacking and is based on the principle that multiple resistance genes require multiple mutations within the pathogen to overcome resistance, thereby decreasing the likelihood of the emergence of a new virulent race (Joshi and Nayak, 2010). Identifying and linking *R* genes on a large genome such as wheat have proven to be challenging (Hulbert and Pumphrey, 2014). *Sr24* has however been successfully pyramided in various combinations with *Sr26*, *Sr31*, and *SrR* (Mago *et al.*, 2011).

A key theme in combatting resistance breakdown and potential rust epidemics is the implementation of durable resistance. Durable resistance is resistance that is effectively granted to a plant cultivar over an extended period of time in an environment usually suitable for disease development (Johnson, 1979). Plant resistance may be seen as a continuum from most to least durable, with NHR considered most durable and race-specific resistance non-durable (Gurr and Rushton, 2005). Another type of host resistance, termed race non-specific resistance (Periyannan *et al.*, 2017) has the immediate potential of practical durability in current wheat breeding programmes.

2.5.3 Race non-specific/adult plant resistance

Race non-specific resistance has also been called slow-rusting resistance, partial resistance, field resistance, horizontal resistance or adult plant resistance (APR) (Lowe *et al.*, 2011). APR is resistance that is only effective at later plant growth stages, with resistance often becoming more effective as the plant matures (Gustafson and Shaner, 1982). APR is usually partial and often race non-specific. Many forms of rust APR are slow-rusting, working by slowing down the development of the disease. Although multiple race non-specific resistance genes are usually required to achieve an effective level of resistance, it is worth noting genes such as *Rpg1*, *Lr34*, *Yr36* and *Lr67* that may convey effective resistance on their own.

Rpg1 in barley encodes two tandem protein kinase domains (Brueggeman *et al.*, 2002). In wheat, *Lr34* encodes an adenosine triphosphate-binding cassette (ABC) transporter protein (Krattinger *et al.*, 2009), *Yr36* for a kinase with a START domain (Fu *et al.*, 2009) and *Lr67* is for a hexose transporter protein (Moore *et al.*, 2015). Though these single race non-specific resistance genes have diverse protein products, all lack the NB-LRR domain characteristic of known *R* gene products in wheat, barley and maize (Singh *et al.*, 2015). These genes are not only race non-specific but may also be species non-specific. For example, *Lr67* not only grants resistance to *Pt* but also *Pst*, *Pgt* and *B. graminis* f. sp. *tritici* (Hiebert *et al.*, 2010; Herrera-Foessel *et al.*, 2011; Herrera-Foessel *et al.*, 2014) and has subsequently been synonymised with *Yr46*, *Sr55* and *Pm46*. Importantly all these genes grant APR and have proven durable thus far.

The *Lr34* gene in wheat also grants resistance against all three *Puccinia* spp. and *B. graminis* f. sp. *tritici* (Krattinger *et al.*, 2009). As an ABC transporter, *Lr34* shows similarity to *PEN3* in *Arabidopsis* identified by Stein *et al.* (2006) which grants NHR by exporting toxins to the apoplast. *Pt* infection of *Lr34* containing wheat differentially expressed 151 genes compared to uninfected resistant wheat. Upregulated genes included those encoding PR proteins, signal transduction components and enzymes responsible for energy production and metabolism that points to a high energy demand during the induced defence response (Bolton *et al.*, 2008). *Lr34* transformed barley exhibited *Lr34* resistance and inhibited the growth of *P. hordei*, *B. graminis* f. sp. *hordei* and *Pgt* (Risk *et al.*, 2013). Rice transformed with *Lr34* gained partial resistance to *M. oryzae* that was associated with maturation in the plant (Krattinger *et al.*, 2016).

The *Yr39* resistance gene restricted fungal growth shortly after infection of wheat with *Pst* and potentially before haustorium formation (Coram *et al*., 2008). The APR response induced 99 transcripts encoding PR proteins, enzymes of the phenylpropanoid pathway and R protein analogs. Transcriptomic analysis of *Pst*-infected wheat with the single APR gene *Yr39*, compared to the race-specific *Yr5* resistance gene, showed a greater diversity of transcripts with the APR response. Along with β-1,3-glucanase and PAL, a total of nine *R* gene analogs were also induced. It was proposed that the R proteins are all under the regulation of *Yr39* and that they additively contribute to durability, since each may regulate different defence components (Chen *et al*., 2013).

Of the 39 known *Sr* genes that are considered effective against the 'Ug99' race group, only five confer APR, namely *Sr2*, *Sr55*, *Sr56*, *Sr57* and *Sr58* (Singh *et al*., 2015). *Sr2* independently conveys partial resistance and under high inoculation levels may exhibit a susceptible phenotype (Ellis *et al*., 2014). However, *Sr2* is considered the most important *Pgt* resistance gene (McIntosh *et al*., 1995) due to its continued durability and incorporation into breeding programmes. *Sr2* is often combined with other genes in a *Sr2*-complex, but the identity of this gene combination is not always known (Ellis *et al*., 2014).

Durable resistance is usually based on numerous genes working additively. The identification of a genetic region within the plant genome that contributes a partial, quantitative resistance is referred to as quantitative trait loci (QTL). *Lr34* and *Yr36* are examples of single genes that appear as QTL. Some researchers have designated a QTL that explains greater than 10% of the phenotypic response as a major QTL and less than 10% of the phenotypic response a minor QTL (Kou and Wang, 2010). APR in the South African wheat cultivar Kariega based on two major and two minor QTL acted additively when conferring resistance to *Pst* (Moldenhauer *et al*., 2008).

A review of APR identified, over a period of 15 years, 80 QTL for *Pt* resistance and 119 QTL for *B. graminis* f. sp. *tritici* resistance (Li *et al*., 2014). Breeders therefore have a large collection of QTL to utilise. However, not all resistance QTL will be durable. Mapping techniques have shifted away from linkage mapping to genome-wide association analysis (GWAS) (Li *et al*., 2014). Modelling predicts GWAS to be an effective approach for the mapping of QTL for APR against *Pgt* within International Maize and Wheat Improvement Center germplasm. Interestingly, the *Sr2* region on chromosome 3B of wheat remains crucial for APR within this germplasm (Rutkoski *et al*., 2014).

Gene pyramiding must be applied to both race specific and race non-specific resistance genes. The advantage of gene pyramiding can be seen in resistance against *Pt* which is much greater in wheat cultivars when *Lr34* is combined with other *Lr* genes (Kloppers and Pretorius, 1997). QTL have been successfully combined for resistance to the three *Puccinia* spp. along with grain quality traits (Tyagi *et al.*, 2014). Only with such advances may durable resistance in wheat be assured.

Searching for new APR wheat cultivars and mapping QTL have great value for the future of resistance breeding. Identification of QTL is of importance since it increases the pool of genes/loci that a plant breeder can use to select from. New gene combinations can be explored and placed into high yielding cultivar backgrounds. Recent developments in NGS have allowed the generation of large data sets for detailed genetic studies, but a more multifaceted and integrated approach to understanding plant-pathogen interactions is needed (Saunders, 2015). APR must likewise be investigated and not only aim to identify genetic sources of resistance but also to describe molecular and cellular mechanisms underlying the APR response.

Chapter 3: Experimental layout of greenhouse trials and inoculation methods

3.1 Introduction

Fungal diseases that affect wheat (*Triticum aestivum*) include stem rust caused by *Puccinia graminis* f. sp. *tritici* (*Pgt*). On wheat, *Pgt* infection causes brown uredinia (pustules) on the surfaces of leaves, stems, leaf sheaths, spikes, glumes, awns and grains (Roelfs *et al.*, 1992; Leonard and Szabo, 2005). As an obligate biotroph, the successful infection and colonisation of wheat requires *Pgt* to absorb nutrients from its host. By directing photosynthetic products away from host tissue, *Pgt* infection affects wheat development and ultimately agricultural productivity (Leonard and Szabo, 2005). *Pgt* causes epidemics if susceptible cultivars are widely deployed. Recently, wheat yield losses of 51% caused by *Pgt* were reported (Olivera *et al*., 2015). Farmers in turn aim to reduce losses in wheat production by planting resistant cultivars. Adult plant resistance (APR) is a type of resistance which is more effective in older plants, typically conferring no protection at the seedling stage.

Seedling infection types produced by *Pgt*, as well as *P. triticina* (*Pt*) and *P. striiformis* f. sp. *tritici* (*Pst*), are commonly assessed on primary seedling leaves (Roelfs *et al.*, 1992). Scoring of infection types on differential sets of wheat varieties is the basis of *Pgt* race classification, e.g. as used by the North American system of nomenclature (Roelfs and Martens, 1988). However, phenotypic scoring of seedlings cannot be used to classify APR, which typically shows a susceptible infection type during the seedling phase. A noteworthy exception is the APR gene *Sr2*, which is linked to chlorosis in seedling leaves. Seedling chlorosis associated with *Sr2* proved an effective phenotypic marker for this gene, but its expression is subject to environmental variation (Brown, 1997).

Phenotypic scoring of *Pgt* infection on adult plants is usually done on the flag leaf sheath and true stem. In contrast, *Pt* and *Pst* are scored on the flag leaf, but the entire plant may be considered for *Pst* scoring (Roelfs *et al.*, 1992). Any study of APR mechanisms is underpinned by an understanding and classification of the APR phenotype.

The aim of this chapter was to firstly generate *Pgt*-inoculated adult wheat plants under greenhouse conditions. Secondly, to describe and score the adult plant infection responses on the flag leaf sheath of a number of APR lines. Throughout the study the APR lines were compared to a susceptible wheat line. Lastly, the aim was to generate *Pgt*-inoculated flag leaf sheath samples for subsequent experimentation.

3.2 Materials and methods

3.2.1 Plant and pathogen materials

Two Kenyan wheat lines, W1406 (Kenya_TK_42) and W6979 (Kenya-Popo) from the Genome Resource Unit, Norwich Research Park, United Kingdom (Prins *et al.*, 2016) were selected for detailed analysis. These lines previously exhibited APR in the field to a race from the 'Ug99' race group (Prins *et al.*, 2016). The 37-07 line was selected from the 2007 International Stem Rust Trap Nursery (entry 37) for its susceptible field response. The 37-07 line was used as the stem rust susceptible control in all experiments. Doubled haploid (DH) entries from mapping populations generated by Prins *et al.* (2016) were also included. Lines DH1.43 and DH1.50 were selected from the W1406 x 37-07 cross and DH2.31 and DH2.38 from the W6979 x 37-07 cross. Pavon-76, Francolin-1 and Kingbird, cultivars with a known APR response, were also included. Stem rust race PTKST (UFS isolate UVPgt60) was used for all inoculation studies. The *Pgt* urediniospores were multiplied on the susceptible cultivar McNair-701. The pedigrees of the lines and cultivars used are given in Table 3.1. Quantitative trait loci (QTL) present in DH entries used in the current study are summarised in Tables 3.2 and 3.3.

3.2.2 Wheat growing conditions and urediniospore multiplication

Wheat was grown in a rust-free greenhouse under natural light conditions at 18-25°C (night-day cycle). For urediniospore multiplication and seedling trials, seeds were planted in a sterilised soil-peat moss mixture in plastic pots (8 cm height x 10 cm diameter), whereas for the adult plant trials, three seeds were planted per plastic pot, each measuring 16 cm in height x 15 cm in diameter. Plants were fertilised with Multifeed Classic™ (N:P:K ratio 19:8:16 plus micronutrients) at a concentration of 8 g/l twice a week. Urediniospores were multiplied on McNair-701 seedlings treated with 0.3 g/l maleic hydrazide five days after planting to inhibit growth beyond primary leaf development. Ten-day-old seedlings were inoculated for both spore multiplication and the experimental seedling trial. For multiplication purposes, urediniospores stored in cryovials at -80°C were heat shocked in a water bath at 48°C for 6 min before inoculation of seedlings. For all other experiments freshly collected urediniospores were used.

Table 3.1: Pedigrees of wheat lines used in the current study. Information was either retrieved from the Genetic Resources Information System for Wheat and Triticale, available at http://wheatpedigree.net/ [accessed 03-04-2017] or was previously reported in Prins *et al.* (2016).

Line/Cultivar	Pedigree
37-07	Kasyob/Genaro-81//Cham4
W1406	Penjamo-62/908-Frontana-1//Kentana-54-B
W6979	Klein-Atlas/Tobari-66//Centrifen/3/Bluebird/4/Kenya-Fahari
Pavon-76	Icam-71//Ciano-67/Siete-Cerros-66/3/Kalyansona/Bluebird
Francolin-1	Waxwing*2/Vivitsi
Kingbird	Tam-200/Tui/6/Pavon-76//Car-422/Anahuac-75/5/Bobwhite/Crow//Buckbuck/Pavon-76/3/Yecora-70/4/Trap-1
McNair-701	(S)McNair-2203

Table 3.2: Quantitative trait loci linked to the adult plant resistance response to *Puccinia graminis* f. sp. *tritici* in two doubled haploid wheat lines, DH1.43 and DH1.50. Positive symbols (+) indicate the presence of a quantitative trait loci and negative symbols (-) the absence. Doubled haploid entries were derived from a W1406 x 37-07 mapping population and quantitative trait loci were identified by Prins *et al.* (2016).

Entry	*Lr34/Yr18/Sr57*	*QSr.ufs-4D*	*QSr.ufs-2B.1*	*QSr.ufs-3B*	*QSr.ufs-4A*
DH1.43	-	+	+	+	-
DH1.50	-	-	+	+	+

Table 3.3: Quantitative trait loci linked to the APR response to *Puccinia graminis* f. sp. *tritici* in two doubled haploid wheat lines, DH2.31 and DH2.38. Positive symbols (+) indicate the presence of a quantitative trait loci and negative symbols (-) the absence. Doubled haploid entries were derived from the W6979 x 37-07 mapping population and quantitative trait loci were identified by Prins *et al.* (2016).

Entry	*Lr34/Yr18/Sr57*	*QSr.ufs-6A*	*QSr.ufs-2B.2*	*QSr.ufs-2D*	*QSr.ufs-3D*
DH2.31	+	+	+	+	-
DH2.38	+	-	+	+	+

3.2.3 Seedling trial

The inoculation method described by Browder (1971), where urediniospores are suspended in light mineral oil (Soltrol-130™) to a final concentration of 1 mg/ml, was used. A spore suspension volume of 800 µl was used to inoculate four pots of seedlings. The spore suspension was transferred into a gelatin capsule that was attached to an atomiser, and using a pressure pump sprayed onto seedlings on a platform rotating at 14 rpm. After drying off the plants for 2 h at 25°C under fluorescent lighting, seedlings were incubated for 16 h in the dark in a dew chamber at 20-23°C. Before transferring seedlings back to the greenhouse, they were dried off at 20°C for 2 h under fluorescent lighting. First leaves were collected at designated hours post inoculation (hpi)/days post inoculation (dpi) for further experimentation. Phenotypic observations were done at 12 dpi and infection types scored according to Stakman *et al.* (1962).

3.2.4 Adult plant trials

For adult plant trials, seedlings were thinned to two plants per pot. Wheat plants were grown until the milk to dough stage (Zadoks scale 77-83; Zadoks *et al.*, 1974) and inoculated according to the method developed by Pretorius *et al.* (2007) and modified by Bender *et al.* (2016). Freshly collected urediniospores were suspended in distilled water containing 0.003% (v/v) Tween 20® (polyoxyethylene (20) sorbitan monolaurate) to a final concentration of 0.7 mg/ml. A spore suspension of 80 ml was used to inoculate plants in seven randomised pots. A compressed air sprayer (spray-gun and compressor) at 250 kPa was used to apply the spore suspension uniformly on adult plants. Inoculated plants were incubated in chambers measuring 100 cm x 85 cm x 60 cm that were constructed from an aluminium frame covered with 200 µm plastic sheeting (Bender *et al.*, 2016). The chambers were submerged in 5 cm water to assure high humidity. Pots were randomly placed on a metal grid raised above the water line with 28 pots in each chamber. Plants within chambers were kept under greenhouse conditions and natural light for 20 h. During incubation, the temperature fluctuated between 20 and 28˚C within the chambers. After removal, plants were grown under greenhouse conditions as previously described in section 3.2.2.

The last internode was sampled since this section is routinely used for phenotypic scoring of stem rust on adult wheat plants (Roelfs *et al.*, 1992). The wheat stem was cut just below the flag leaf and above the flag-1 leaf with the head and peduncle being discarded (Figure 3.1). The flag leaf sheaths of the last internode were collected at selected hpi/dpi. Phenotypic observations of the last internode were done at 14 dpi and the adult plant infection response scored using the method of Roelfs *et al.* (1992). Adult wheat trials were independently replicated in the greenhouse, and details of respective trials and methods used are given in Table 3.4.

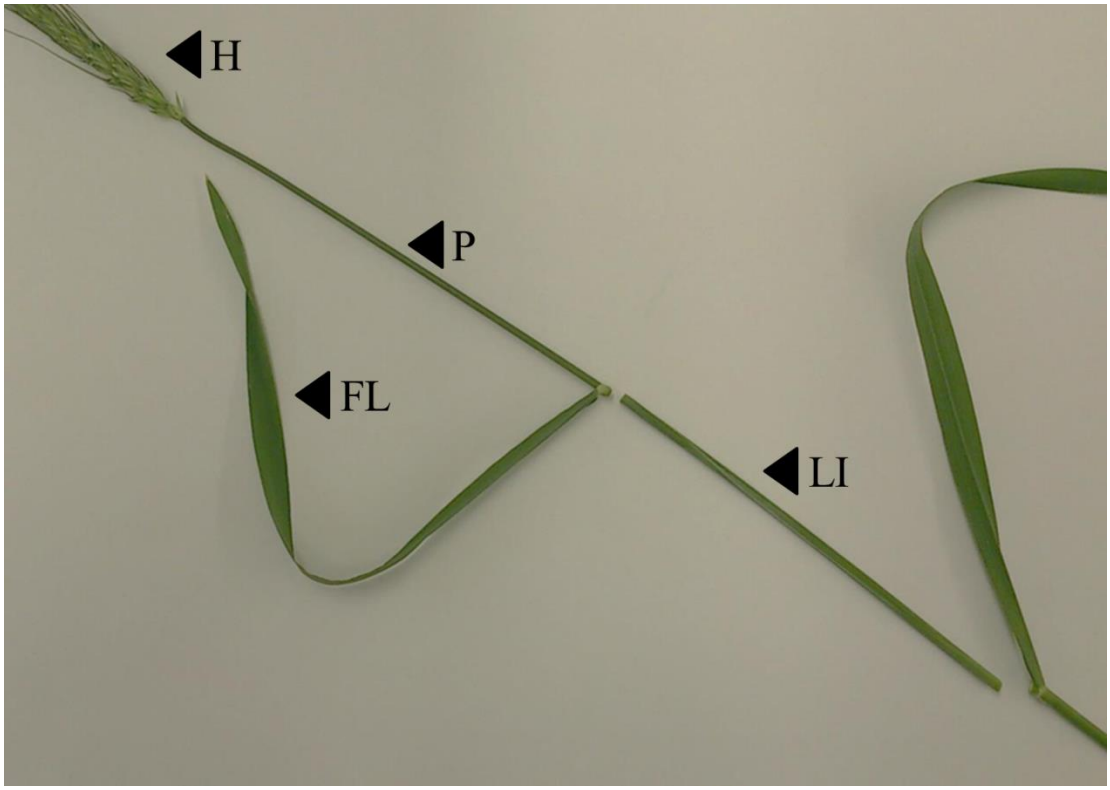

Figure 3.1: Sampling of the leaf sheath from adult wheat plants. The head (H), peduncle (P), flag leaf (FL) and last internode (LI) are indicated.

Table 3.4: Summary of greenhouse trials performed and methods used to investigate generated samples. One seedling trial and four adult trial replicates (Adult trial 1-4) with lines 37-07, W1406 and W6979 were conducted. Of these, two adult plant trials included additional doubled haploid entries (Adult trial 3-4). Two other replicate trials (Adult trial 5-6) made use of the 37-07 line, and the Pavon-76, Francolin-1 and Kingbird cultivars.

Trial	Line/Entry/Cultivar	Methods used for investigation
Seedling trial	37-07, W1406, W6979	Phenotype, reverse transcriptase quantitative polymerase chain reaction (RT-qPCR)
Adult trial 1	37-07, W1406, W6979	Phenotype, histology, chitin biomass, RT-qPCR, Illumina sequencing, Ion Torrent sequencing
Adult trial 2	37-07, W1406, W6979	Phenotype, histology, chitin biomass, RT-qPCR, Ion Torrent sequencing
Adult trial 3	37-07, W1406, DH1.43, DH1.50, W6979, DH2.31, DH2.38	Phenotype, RT-qPCR, Ion Torrent sequencing (excluding DH entries)
Adult trial 4	37-07, W1406, DH1.43, DH1.50, W6979, DH2.31, DH2.38	Phenotype, RT-qPCR
Adult trial 5	37-07, Pavon-76, Francolin-1, Kingbird	Phenotype, RT-qPCR
Adult trial 6	37-07, Pavon-76, Francolin-1, Kingbird	Phenotype, RT-qPCR

3.3 Results

3.3.1 Seedling trial

The seedling infection types of wheat lines 37-07, W1406 and W6979 are shown in Figure 3.2. Large uredinia, typical of *Pgt* infection were observed on the primary leaves of all three lines. Based on the phenotypic classification system of Stakman *et al.* (1962), the 37-07 and W1406 lines showed an infection type of 4, while the W6979 line showed an infection type of 3++.

3.3.2 Adult plant trials

Uredinia developed on flag leaf sheaths of all lines used in this study but levels of infection differed between lines. The adult plant infection response of the wheat lines 37-07, W1406 and W6979 are shown in Figures 3.3, 3.4, 3.5 and 3.7, each showing phenotypes observed in one of the four biological replicate trails (Adult trial 1-4, respectively). Figures 3.6 and 3.8 show wheat lines DH1.43, DH1.50, DH2.31 and DH2.38 included in the third and fourth biological replicates (Adult trial 3 and 4). Finally, the adult plant infection response of wheat lines 37-07, Pavon-76, Francolin-1 and Kingbird are indicated in Figures 3.9 and 3.10. These observed phenotypes represent the two biological replicates done for additional APR cultivars (Adult trial 5 and 6).

Adult plant infection responses were phenotypically classified based on the system of Roelfs *et al.* (1992) and results are summarised in Table 3.5. The phenotypic response of the 37-07 line was scored susceptible (S) in all six trials, with this line having the highest levels of *Pgt* infection. The phenotypic response of the W1406 line varied from moderately resistant (MR) to moderately susceptible (MS), and the infection response of line W6979 varied from resistant to moderately resistant (RMR) to MR. Both lines therefore had a lower level of *Pgt* infection than 37-07, but W1406 had a marginally higher level of infection compared to W6979.

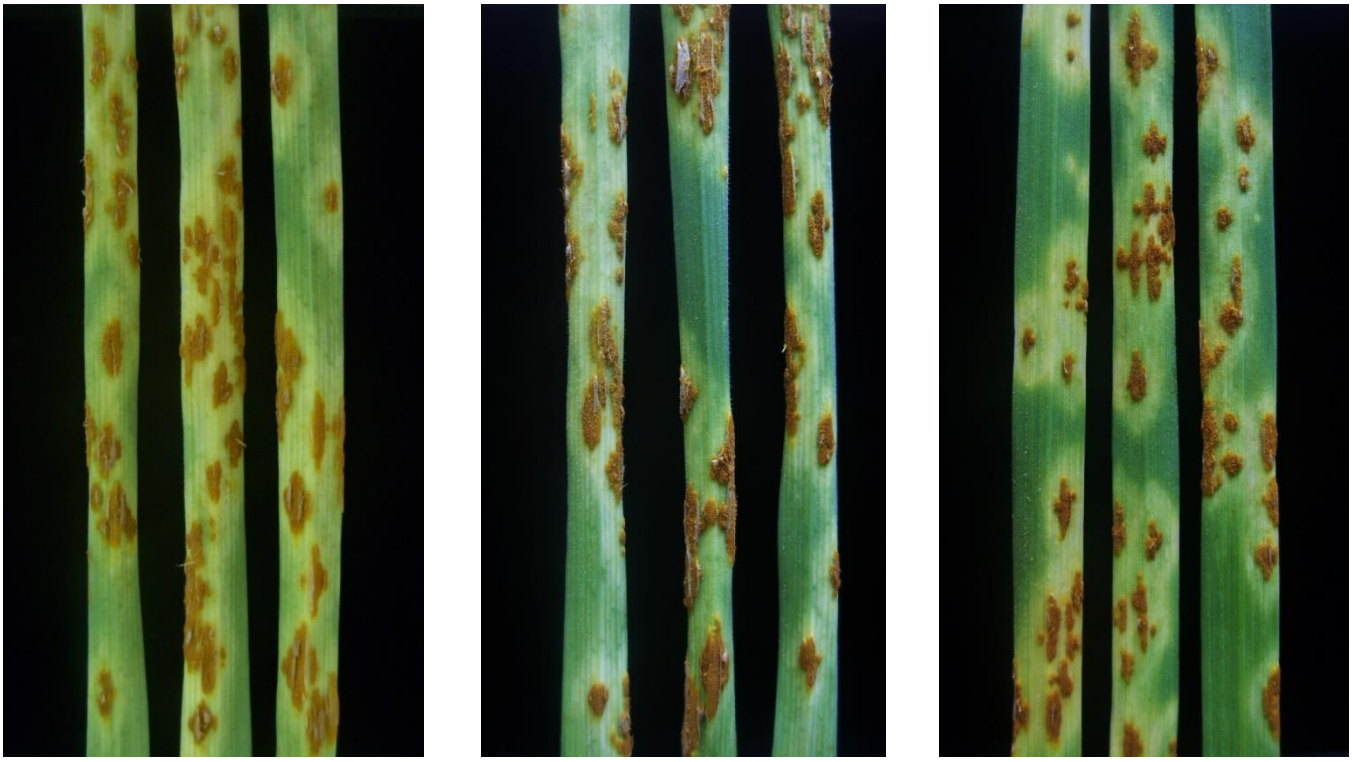

37-07
(4)

W1406
(4)

W6979
(3++)

Figure 3.2: Seedling infection types of three wheat lines (37-07, W1406 and W6979) when inoculated with *Puccinia graminis* f. sp. *tritici* race PTKST. Photographs represent the abaxial surface of primary leaves at 12 dpi. The infection types of seedlings were scored according to the method of Stakman *et al.* (1962) and are indicated in brackets.

37-07 (S) | W1406 (MR) | W6979 (RMR)

Figure 3.3: Adult plant infection response of the three wheat lines 37-07, W1406 and W6979 inoculated with *Puccinia graminis* f. sp. *tritici* race PTKST. Photographs represent the flag leaf sheath of the last internode at 14 dpi. Lines were inoculated for the first biological replicate (Adult trial 1). Adult plant infection responses were scored according to the method of Roelfs *et al.* (1992) and are indicated in brackets: resistant to moderately resistant (RMR), moderately resistant (MR) or susceptible (S).

37-07
(S)

W1406
(MR)

W6979
(MR)

Figure 3.4: Adult plant infection response of the three wheat lines 37-07, W1406 and W6979 inoculated with *Puccinia graminis* f. sp. *tritici* race PTKST. Photographs represent the flag leaf sheath of the last internode at 14 dpi. Lines were inoculated for the second biological replicate (Adult trial 2). Adult plant infection responses were scored according to the method of Roelfs *et al.* (1992) and are indicated in brackets: moderately resistant (MR) and susceptible (S).

37-07
(S)

W1406
(MRMS)

W6979
(MR)

Figure 3.5: Adult plant infection response of the three wheat lines 37-07, W1406 and W6979 inoculated with *Puccinia graminis* f. sp. *tritici* race PTKST. Photographs represent the flag leaf sheath of the last internode at 14 dpi. Lines were inoculated for the third biological replicate (Adult trial 3). Adult plant infection responses were scored according to the method of Roelfs *et al.* (1992) and are indicated in brackets: moderately resistant (MR), moderately resistant to moderately susceptible (MRMS) and susceptible (S).

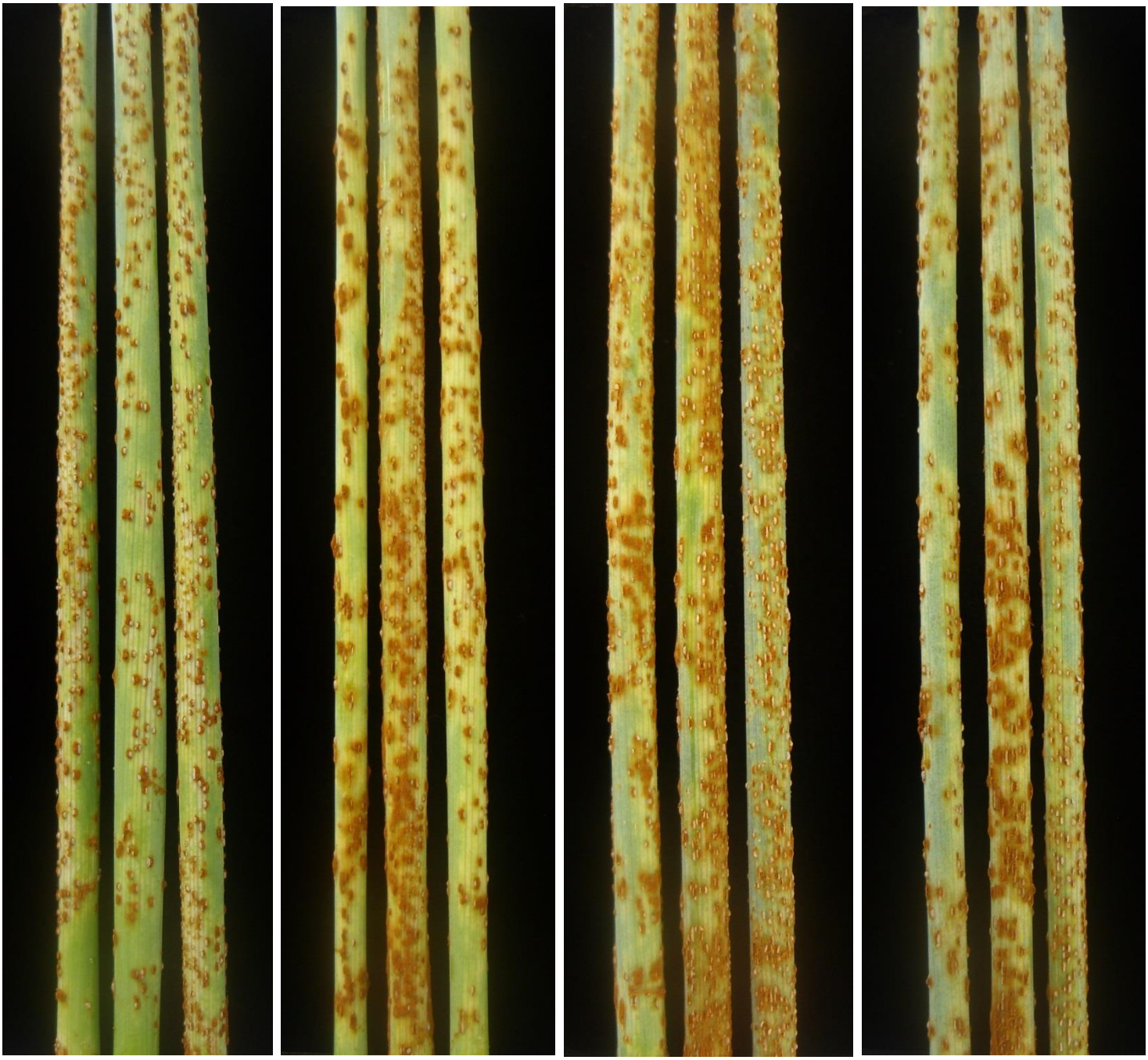

DH1.43 (MR) | DH1.50 (MS) | DH2.31 (MS) | DH2.38 (MS)

Figure 3.6: Adult plant infection response of the four doubled haploid wheat lines DH1.43, DH1.50, DH2.31 and DH2.38 inoculated with *Puccinia graminis* f. sp. *tritici* race PTKST. Photographs represent the flag leaf sheath of the last internode at 14 dpi. Lines were inoculated for the third biological replicate (Adult trial 3). Adult plant infection responses were scored according to the method of Roelfs *et al.* (1992) and are indicated in brackets: moderately resistant (MR) and moderately susceptible (MS).

37-07
(S)

W1406
(MS)

W6979
(MR)

Figure 3.7: Adult plant infection response of the three wheat lines 37-07, W1406 and W6979 inoculated with *Puccinia graminis* f. sp. *tritici* race PTKST. Photographs represent the flag leaf sheath of the last internode at 14 dpi. Lines were inoculated for the fourth biological replicate (Adult trial 4). Adult plant infection responses were scored according to the method of Roelfs *et al.* (1992) and are indicated in brackets: moderately resistant (MR), moderately susceptible (MS) and susceptible (S).

DH1.43 (MRMS) | DH1.50 (MR) | DH2.31 (MS) | DH2.38 (MS)

Figure 3.8: Adult plant infection response of the four doubled haploid wheat lines DH1.43, DH1.50, DH2.31 and DH2.38 inoculated with *Puccinia graminis* f. sp. *tritici* race PTKST. Photographs represent the flag leaf sheath of the last internode at 14 dpi. Lines were inoculated for the third biological replicate (Adult trial 4). Adult plant infection responses were scored according to the method of Roelfs *et al.* (1992) and are indicated in brackets: moderately resistant (MR), moderately resistant to moderately susceptible (MRMS) and moderately susceptible (MS).

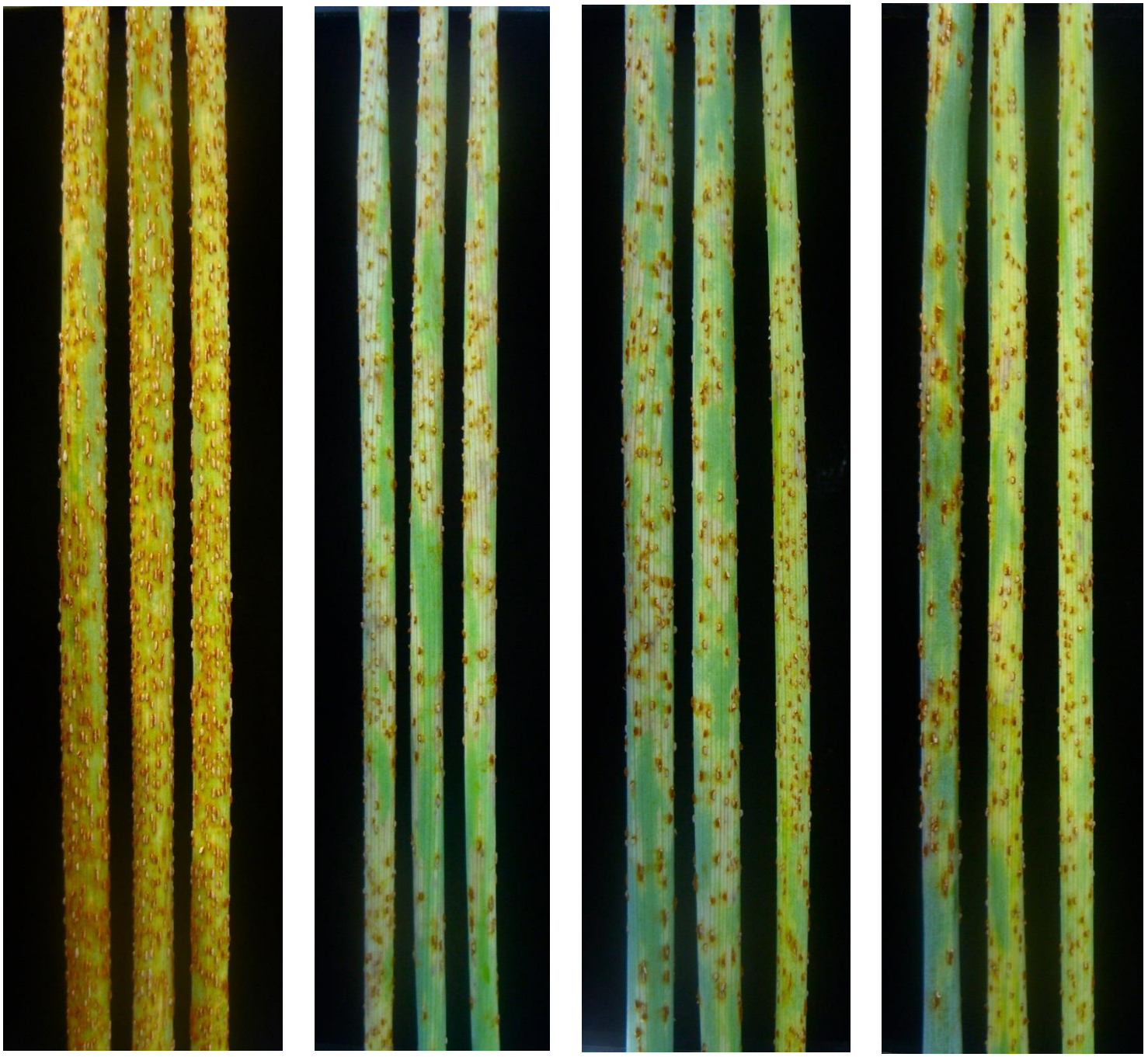

37-07 (S) | Francolin-1 (MR) | Kingbird (MR) | Pavon-76 (MR)

Figure 3.9: Adult plant infection response of the four wheat lines 37-07, Francolin-1, Kingbird and Pavon-76 inoculated with *Puccinia graminis* f. sp. *tritici* race PTKST. Photographs represent the flag leaf sheath of the last internode at 14 dpi. Lines were inoculated for the fifth biological replicate (Adult trial 5). Adult plant infection responses were scored according to the method of Roelfs *et al.* (1992) and are indicated in brackets: moderately resistant (MR) and susceptible (S).

37-07
(S)

Francolin-1
(MR)

Kingbird
(MR)

Pavon-76
(MR)

Figure 3.10: Adult plant infection response of the four wheat lines 37-07, Francolin-1, Kingbird and Pavon-76 inoculated with *Puccinia graminis f. sp. tritici* race PTKST. Photographs represent the flag leaf sheath of the last internode at 14 dpi. Lines were inoculated for the sixth biological replicate (Adult trial 6). Adult plant infection responses were scored according to the method of Roelfs *et al.* (1992) and are indicated in brackets: moderately resistant (MR) and susceptible (S).

Table 3.5: Adult plant infection responses of wheat lines used in the current study. The method of Roelfs *et al.* (1992) was used to score the *Puccinia graminis* f. sp. *tritici* infection on flag leaf sheaths. Scoring abbreviations are as follows: resistant to moderately resistant (RMR), moderately resistant (MR), moderately resistant to moderately susceptible (MRMS), moderately susceptible (MS) and susceptible (S).

Line/Entry/Cultivar	Adult trial 1	Adult trial 2	Adult trial 3	Adult trial 4	Adult trial 5	Adult trial 6
37-07	S	S	S	S	S	S
W1406	MR	MR	MRMS	MS	-	-
W6979	RMR	MR	MR	MR	-	-
DH1.43	-	-	MR	MRMS	-	-
DH1.50	-	-	MS	MR	-	-
DH2.31	-	-	MS	MS	-	-
DH2.38	-	-	MS	MS	-	-
Pavon-76	-	-	-	-	MR	MR
Francolin-1	-	-	-	-	MR	MR
Kingbird	-	-	-	-	MR	MR

The DH entries showed adult plant infection responses intermediate between those of their susceptible (37-07) and APR (W1406 and W6979 respectively) parental lines. The DH1.43 entry had a phenotypic response that varied from moderately resistant to moderately susceptible (MRMS) to MR, while line DH1.50 had an infection phenotype that varied from MS to MR. In both the biological replicates DH1.50 had a higher level of infection. DH lines DH2.31 and DH2.38 showed a phenotypic response of MS in both biological replicates. When comparing the two biological replicates neither of the DH entries could be confirmed as having a higher level of infection relative to the other.

The phenotypic response of Pavon-76, Francolin-1 and Kingbird was scored as MR. The level of infection on these APR cultivars corresponded well between the two biological replicates.

3.4 Discussion

The W1406 and W6979 wheat lines, which are the main focus of the current study, exhibited a susceptible seedling infection type. As seedlings these lines were as susceptible as the control line, 37-07, with W6979 only displaying a marginally lower infection type. In four biological replicates, W1406 and W6979 showed partial resistance as adult wheat plants. Prins *et al.* (2016) reported the adult plant infection responses of W1406 and W6979 in two locations for three growing seasons. W1406 was scored as 0R, 5R en 10R and W6979 as 0R, 5R and 40RMR. Based on those scores these two lines were equally resistant but W6979 was more susceptible at one location. Over two growing seasons, Soko *et al.* (2018) also showed a higher stem rust coefficient of infection and area under disease progress curve in the W6979 line. This was contradicted under greenhouse conditions where the APR response in W6979 appeared more effective in restricting *Pgt* development than W1406 in three of the four trials. Expression of an APR phenotype in W1406 and W6979, as reported by Prins *et al.* (2016), was however confirmed under greenhouse conditions. The 37-07 line was confirmed as an effective susceptible control.

The DH entries exhibited an APR response but in all cases this was intermediate between the parental lines. DH lines DH1.43 and DH1.50 each had one QTL absent; the *QSr.ufs-4D* QTL was only present in DH1.43 and the *QSr.ufs-4A* QTL was only present in DH1.50. Based on the phenotypic observations of these two DH entries, the APR response appeared consistently more effective in DH1.43. Therefore, the *QSr.ufs-4D* QTL appeared to convey a more effective APR response. This corresponds to the study of Prins *et al.* (2016) which identified *QSr.ufs-4D* as a major QTL with the largest effect in the W1406 line.

Similarly, DH lines DH2.31 and DH2.38 differed by one QTL. The *QSr.ufs-6A* QTL was only present in DH2.31 and *QSr.ufs-3D* only in DH2.38. Based on the phenotypic observations, neither of these two DH entries appeared to consistently have a more effective APR response. The two biological replicates showed contradicting results, and the QTL that possibly conveys a more effective APR response could not be identified in the current study. However the DH mapping study of Prins *et al.* (2016) identified *QSr.ufs-6A* as a major QTL with the largest effect in the W6979 line.

The APR response of the additional wheat cultivars Pavon-76, Francolin-1 and Kingbird was confirmed under greenhouse conditions. These cultivars were more effective in restricting *Pgt* development than either W1406 or W6979, or the DH entries derived from these wheat

lines. The APR response of the additional wheat cultivars Pavon-76, Francolin-1 and Kingbird was confirmed under greenhouse conditions. These cultivars were more effective in restricting *Pgt* development than either W1406 or W6979, or the DH entries derived from these wheat lines. Three stem rust resistance QTL were identified by Njau *et al.* (2012) in Pavon-76 and occur on chromosomes 1B (possibly *Sr58/Lr46*), 3B (possibly *Sr2*) and 3D. *Sr2* is likely present in Francolin-1 (Lan *et al.*, 2014, Pretorius *et al.*, 2015) along with a *Pt* resistance QTL pointing to the presence of *Sr58/Lr46* (Lan *et al.*, 2014). In Kingbird, QTL on chromosomes 2B, 2D, 3B (*Sr2*), 5D, 7B, and 7D (*Sr57/Lr34*) were reported by Gambone (2016). As previously reported in the Chapter 1, *Sr57* is present in both W1406 and W6979 but does not convey the greatest *Pgt* resistance effect (Prins *et al.*, 2016). In many of the APR lines included in current study *Sr2* appears to be the foundation of *Pgt* resistance, but additional QTL contribute to resistance. However, *Sr2* is not present in the W1406 and W6979 lines, which is the main focus of the study.

Across all trials of the current study the expression of an APR response against *Pgt* was confirmed in a number of wheat lines under greenhouse conditions. The inoculation method developed by Pretorius *et al.* (2007) and modified by Bender *et al.* (2016) for *Pgt* remained an effective tool to study APR under greenhouse conditions. In the current study, the flag leaf sheaths could be phenotypically scored and the inoculation method allowed plant tissue sampling for subsequent experimentation. The adult plant infection response never exhibited a full resistance phenotype and was scored as an intermediate category, indicative of the partial resistance response typical of APR.

Chapter 4: Histological observations of *Puccinia graminis* f. sp. *tritici* colonization in adult wheat lines

4.1 Introduction

The economic importance of wheat (*Triticum aestivum*) and the threat of fungal pathogens such as *Puccinia* spp. have focused research on the biology and management of rust diseases for many years. Histological investigations of the infection process are often the first step to understand the specialised interaction between host and pathogen. Evans (1907) provided one of the first detailed descriptions of the infection process of the stem rust fungus *Puccinia graminis* f. sp. *tritici* (*Pgt*) on wheat. Parallels can also be drawn with other species within the Pucciniales that have similar infection processes. The development of infection structures on artificial supports has also given insight into the process. These methods use growth media (Hurd-Karrer and Rodenhiser, 1947) or artificial surfaces such as membranes (Dickenson, 1949). As fabrication techniques improved, artificial surfaces started to feature microtopographies which are informative for understanding fungal behaviour (Hoch *et al.*, 1987; Read *et al*., 1997).

Infection of wheat represents the asexual phase of *Pgt*. On a susceptible or partially susceptible wheat cultivar, hyphal proliferation and uredinia (pustules) formation will occur. As an obligate biotroph *Pgt* must extract nutrients from its host and complete the infection process without causing the death of the host. Wheat must counteract this process by halting or impeding the infection process. If colonisation is successful in wheat, uredinia will form and the asexual life cycle on wheat can recommence (Leonard and Szabo, 2005).

The infection process begins with the deposition and adhesion of urediniospores on the host epidermis. Germination of urediniospores is signified by the formation of a germ tube. The adhesion of urediniospores of *Uromyces appendiculatus* F. Strauss and subsequent formation of infection structures are more effective on hydrophobic surfaces (Terhune and Hoch, 1993). Urediniospores therefore initially attach to the epicuticular waxes on the host epidermis via a hydrophobic interaction. Urediniospores from *Uromyces viciae-fabae* (Pers.) Schroet will attach to various surfaces, but humid conditions are required for germination (Beckett *et al.*, 1990). Under humid conditions *U. viciae-fabae* urediniospores form an adhesion pad where they come in contact with the epidermal cuticle of broad bean plants (Deising *et al.*, 1992). The adhesion pad is composed of extracellular matrix (ECM) material and is secreted by urediniospores to facilitate the adhesion of the spore. The ECM also encloses the germ tube and ensures adhesion of the developing germ tube to the host epidermis (Beckett *et al.*, 1990). The ECM of *U. viciae-fabae* can be observed as a hydrophobic region surrounding the spore

and germ tube (Clement *et al.*, 1994). A clear distinction can therefore be made between passive adhesion during spore deposition and active adhesion, whereby secreted ECM facilitates the adhesion (Clement *et al.*, 1993). Adhesion ensures that germ tubes develop further on the host epidermis.

The urediniospores of *Pgt* have 3-5 equatorial pores (Baum and Savile, 1985) from where the germ tube develops. The urediniospore initially forms two germ tubes but the development of one is later halted. The one germ tube then develops by extending away from the urediniospore and becoming branched (Evans, 1907). The germ tubes of *Pgt* must reach a stomatal opening before the infection process can continue.

Pgt exhibits tropism as observed by the perpendicular extension of a germ tube in relation to the long axis of the leaf. In wheat, the stomata together with epidermal cells and vascular bundles are orientated parallel to the long axis of the leaf. By orientating germ tube growth perpendicular to the epidermal cells, the probability of reaching stomata may be increased (Johnson, 1934). It is important to note that though chemical and physical factors may induce spore germination and differentiation, the germ tube does not seem to grow directly towards the stomata. Thigmotropic growth only increases the probability of the germ tube finding a stomatal opening (Lewis and Day, 1972). Directional growth of *Pgt* was confirmed on wheat (Lewis and Day, 1972; Lennox and Rijkenberg, 1989; Read *et al*., 1997) and artificial microtopographies (Setten *et al*., 2015). Lewis and Day (1972) argued that the lattice of wax crystals that covers the epidermis is the thigmotropic stimulus for directional growth of a germ tube. Removal of the epicuticular wax layer by organic solvents not only prevented successful adhesion of germ tubes, but the growth of these germ tubes also became non-directional (Wynn and Wilmot 1977). The observation that *Pgt* exhibits directional growth on artificial microtopographies (Setten *et al*., 2015) that lack epicuticular wax indicates that microscopic ridges most likely also contribute to urediniospore thigmotropism.

When a germ tube reaches the stomatal opening it swells and forms a structure called the appressorium. The cytoplasmic content of the germ tube then migrates into the appressorium. An infection peg develops from the appressorium and grows through the stomatal opening (Evans, 1907). Appressorium formation in *Pgt* is also responsive to microtopographies (Dickenson, 1949; Staples *et al*., 1983). Fixed widths of the microtopographies that mimic the close spacing of the stomatal guard cell walls can cause appressorium differentiation (Read *et al*., 1997). Physical signals therefore appear crucial for appressorium development.

In addition to physical signals, chemical signals may induce development of various infection structures, and volatile compounds have been particularly well studied. Nonanal induces urediniospore germination in *Pgt* (French, 1992). Trans-2-hexen-1-ol acts synergistically with both ridges on microtopographies (Collins *et al.*, 2001) and a heat shock treatment (Wiethölter *et al*., 2003) to induce appressorium formation in *Pgt*. Nonanal, decanal and hexenyl acetate induce the colonization of plant hosts by numerous Pucciniales, including wheat by *Pgt* (Mendgen *et al*., 2006).

The tip of the infection peg develops into a sub-stomatal vesicle (SSV) and the cytoplasmic contents of the appressorium migrate into the SSV. The SSV of *Pgt* is cylindrical and non-septate, with its long axis parallel to the long axis of the stomatal opening (Evans, 1907). From the SSV, infection hyphae (IH) develop that spread through the intercellular spaces of the host mesophyll. The first IH to form is called the primary IH, subsequently followed by secondary IH. For *Pgt*, a single primary IH emerging from either pole of the SSV was reported by Hurd-Karrer and Rodenhiser (1947). In contrast, a low number of primary IH and the ability to form a haustorial mother cell (HMC) directly from a SSV without primary IH formation were noted by Niks (1986). Furthermore, the apparent absence of a primary IH in *Pgt* was considered of potential taxonomic use as other *Puccinia* spp. form a prominent primary IH. The SSV forms the primary IH which differentiates a HMC at its hyphal tip and the elongation at the opposite axis of the SSV is simply an appendix (Niks, 1986; Lennox and Rijkenberg, 1989). IH originating from both ends of a SSV were reported for *Pgt* on growth media (Dickenson, 1949; Williams, 1971; Wiethölter *et al*., 2003), but this has not been reported on wheat. When appressoria are formed on microtopographies, development will often proceed further, forming SSV and IH. Read *et al*. (1997) hypothesised that once appressorium formation has occurred, the pathogen is set on differentiation up to the point of IH.

The HMC, usually separated from the IH by a septum, forms a penetration peg that breaches the plant cell wall (Niks, 1986). A specialised structure called a haustorium develops at the end of the penetration peg, pushing back the plant cell plasma membrane, but maintaining its integrity. The haustorium forms a close association with the plant cell, and does not penetrate the host plasma membrane. The haustorium is surrounded by an extrahaustorial matrix (EHM), which contains proteins and carbohydrates primarily from the host and is viewed as an essential component for successful biotrophic interaction (Voegele and Mendgen, 2011). *Pgt* generally forms haustoria within mesophyll cells to establish the biotrophic interaction.

However, *Pgt* readily forms a haustorium within the epidermal cells from the primary IH (Evans, 1907; Tiburzy *et al*., 1990). This may explain the rapid development of a HMC from the primary IH as reported by Niks (1986).

Though the haustorium has long been considered the structure by which the pathogen absorbs nutrients from the host, it was only with molecular techniques that the interaction was confirmed. In the membrane of *U. viciae-fabae*, H^+-ATPase activity is higher in the haustorium than the spore and germ tube, resulting in a H^+ gradient between the EHM and haustorium (Struck *et al*., 1996). Among genes that are expressed in the haustorium of *U. fabae* are two putative amino acid transporters (*AAT1* and *AAT2*). The product of *AAT2* is localised in the haustorial membrane. The model proposes that the H^+ gradient across the haustorial membrane drives the uptake of amino acids (Hahn *et al*., 1997). The product of *AAT1*, AAT1p, was shown to transport a number of amino acids, but showed highest affinity for histidine and lysine (Struck *et al*., 2002). From the haustorium associated genes reported by Hahn and Mendgen (1997), *HXT1* showed homology to hexose transporters encoding genes. The product of *HXT1*, HXT1p, was also localised on the haustorial membrane of *U. fabae* and showed highest affinity for glucose and fructose (Voegele *et al*., 2001). The function of such proteins confirms that the haustoria formed by members of the Pucciniales take up amino acids and simple carbohydrates from their hosts.

Upon establishment of the first haustorium, the pathogen absorbs nutrients from its host for further development. The HMC can then form secondary IH that can in turn form its own HMC and haustorium. Hughes and Rijkenberg (1985) hypothesised that the formation of secondary IH is based on the successful establishment of a primary haustroium. IH spread through the extracellular spaces and continue to form HMC and haustoria. The pathogen effectively diverts nutrients produced during photosynthesis away from host cells (Mendgen, 1981). Eventually, the extensive hyphal colonies form sporogenous cells that in turn start to develop into urediniospores. The collection of urediniospores that are carried on the uredinium then erupts through the plant epidermis. Upon maturation, the urediniospores detach from their pedicels, thereby completing the asexual life cycle on wheat (Kolmer *et al*., 2009). The complete infection process of the asexual life cycle of a *Puccinia* sp. is summarised in Figure 4.1.

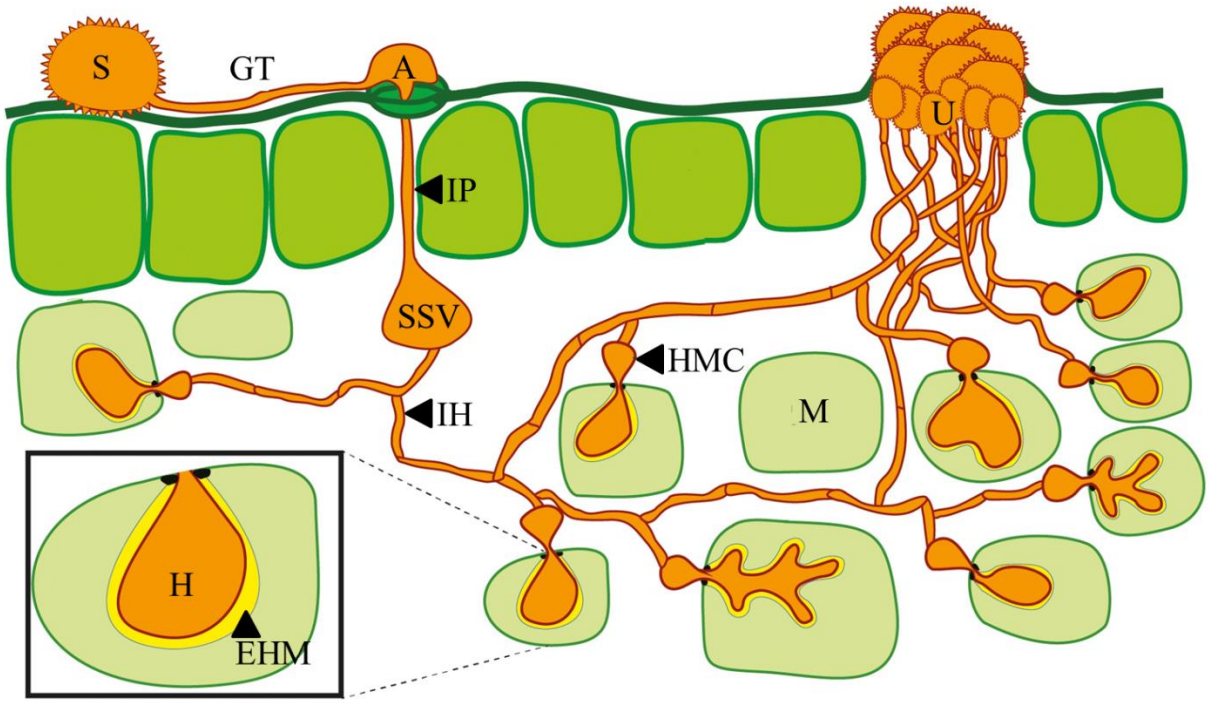

Figure 4.1: Schematic representation of the infection process of *Puccinia* spp. on wheat (taken from Garnica *et al.*, 2013 with modification to labels). The fungal urediniospore (S) forms of a germ tube (GT) on the host epidermis that extends towards a stoma. The germ tube develops into an appressorium (A) and an infection peg (IP) which allows the fungus to enter the plant via the stomatal opening. The infection peg develops into a sub-stomatal vesicle (SSV). An infection hypha (IH) spreads through the intercellular spaces of the plant tissue. Upon reaching a mesophyll cell (M), the infection hypha differentiates into a haustorial mother cell (HMC). A haustorium is subsequently formed but does not penetrate the host plasma membrane. The haustorium is surrounded by an extrahaustorial matrix (EHM) which acts as an essential interface for the absorption of nutrients from a mesophyll cell. Through the establishment of a biotrophic relationship between the haustorium and mesophyll cell, energy is derived for the proliferation of the pathogen. Subsequently infection hyphae spread through the plant mesophyll and more haustoria are formed. Eventually the fungal mycelium may form an uredinium (U) from where urediniospores are released.

Mendgen *et al*. (1988) divided the infection process from germination to haustorium formation and the establishment of biotrophy into a number of phases: the recognition, signalling and parasitic phases. The host plant has a defence mechanism that may impede fungal development at each of these stages. The recognition phase proceeds from germination to appressorium formation, and the plant defence mechanism is typically general and constitutive. The signalling phase proceeds from SSV formation to the initiation of haustorium development during which the pathogen starts releasing effectors to suppress the defence response. The likelihood of the host recognizing the presence of the pathogen also increases. The parasitic phase is characterised by the establishment of haustoria and the biotrophic relationship with its host. During the parasitic phase a race-specific defence response may be induced to restrict haustorium formation. Therefore, if the means of absorbing nutrients from the host is impeded, development of the pathogen will be inhibited and the pathogen may perish.

Germination of *Pgt* urediniospores has also been studied on a number of non-host cereal plants. In general, infection proceeds as described on wheat up to the point of appressorium formation (Lennox and Rijkenberg, 1989). On sorghum, primary IH form but further development is halted. In maize, a primary HMC and secondary IH are formed at the site of infection. In barley, as in wheat, intracellular hyphae and HMCs are observed. As the evolutionary distance between the non-host species increases from wheat, the potency of non-host resistance (NHR) to restrict the spread of *Pgt* also increases (Lennox and Rijkenberg, 1989). On rice, the early infection process of *Pgt* is identical to wheat, with NHR mostly halting the infection process at appressorium formation. If appressorium formation does occur, the majority of infection sites develop IH, but haustoria are seldom seen. NHR in rice to *Pgt* is associated with H_2O_2 accumulation, callose deposition and infrequent cell death (Ayliffe *et al*., 2011).

The defence mechanisms induced by all stage *Sr* resistance genes that impede *Pgt* colonization have been well characterised in wheat seedlings. The presence of the *Sr5* resistance gene activated the hypersensitive response (HR) in epidermal cells of *Pgt*-inoculated wheat and restricted the establishment of the first HMC and haustorium (Tiburzy *et al*., 1990). *Sr5* and *Sr36* have similar effects in wheat. Both induce an early HR to avirulent races and few haustoria are formed. Interestingly, both resistance genes induce callose deposition in the stomatal guard cells, which was hypothesised to impede penetration by closing the stomatal opening. The signal of this race-specific resistance response prior to

haustorium formation is, however, unknown (Wang *et al*., 2015). Contradicting results were reported for *Sr5*, with no differences in infection structures during the early infection process (Lennox and Rijkenberg, 1994). The number of germ tubes, appressoria, SSV and HMC did not differ, although no significant statistical analysis supported these observations. *Sr6* caused a rapid HR in host cells and necrosis of *Pgt* HMC and haustoria associated with these cells. The number of haustoria in the resistant line was thereby reduced but the HMC septum prevented that the necrosis spread to the hyphae (Skipp *et al*., 1974). *Sr6*, *Sr24* and *Sr30* have similar effects in wheat, leading to the HR and lignification after inoculation with *Pgt*. This response was however only partially effective to restrict further colonization. For these resistance genes, the response comes into effect after haustorium formation (Wang *et al*., 2015). A clear distinction can therefore be made between pre-haustorial and post-haustorial defence responses.

Microscopic investigation of the *Pgt* infection process has been effectively completed on wheat seedlings (Skipp *et al*., 1974; Tiburzy *et al*., 1990; Wang *et al*., 2015) and seedlings of non-host plants (Lennox and Rijkenberg, 1989; Ayliffe *et al*., 2011). However, information is lacking on the infection process of *Pgt* on adult plants. The focus on wheat seedlings allows the histological characterisation of defence mechanisms induced by all stage *Sr* resistance genes. The histological characterisation of the adult plant resistance (APR) response upon *Pgt* colonization, however, needs further description. The phenotypic characterization of *P. triticina* (*Pt*) and *P. striiformis* f. sp. *tritici* (*Pst)* infection on adult wheat uses flag leaves. Flag leaves have also been effectively used for microscopic observation of the infection process of *Pt* (Wesp-Guterres *et al*., 2013) and *Pst* (Moldenhauer *et al*., 2006; Coram *et al*., 2008; Moldenhauer *et al*., 2008; Zhang *et al*., 2012; Segovia *et al*., 2014). In contrast, the flag leaf sheath of the last internode is used for the phenotypic characterization of *Pgt* infection response on adult wheat plants. Insufficient information on the *Pgt* infection process complicates any comparison to phenotypic scoring and characterisation of the APR response.

The aim of this chapter was therefore to investigate the infection process of *Pgt* on the flag leaf sheath of the last internode of adult wheat plants, in particular for the susceptible line (37-07). In addition, the *Pgt* infection process in the 37-07 line was compared with two APR lines, W1406 and W6979.

4.2 Materials and methods

4.2.1 Biological material

For histological observations, samples were generated as described in Chapter 3. The 37-07, W1406 and W6979 lines from the first two adult plant trials (Adult trial 1-2) were included. The last internode below the flag leaf was collected as described, but the internal stem was not initially removed. The last internode was cut into manageable sections depending on the technique implemented. The stem assured structural integrity of samples, but was usually removed during further processing. The external surface of the flag leaf sheath was the focus for histological observations as this surface was exposed to *Pgt* inoculation.

4.2.2 Scanning electron microscopy

Samples for scanning electron microscopy (SEM) were taken at 6 hpi, 12 hpi and 1 dpi for epidermal observations and at 1 dpi, 36 hpi and 2 dpi for sub-epidermal observations. The last internodes of inoculated wheat were randomly cut along the length into 5 mm sections. Internode sections were placed in 3% (v/v) glutaraldehyde in a sodium phosphate buffer (0.1 M, pH 7.0) and stored until processing. Sections were washed in a 0.1 M sodium phosphate buffer for 10 min and then fixed in 1% (w/v) osmium tetroxide in 0.1 M sodium phosphate buffer for 1 h. Sections were then washed twice for 10 min in the phosphate buffer. Sections were dried with a graded ethanol series of 50%, 70% and 95% (v/v) in distilled water for 20 min with a final 100% ethanol stage for 1 h which was repeated twice. Sections were thereafter dried in a Tousimis critical point drier (Rockville, Maryland, United States of America) using carbon dioxide drying gas.

For epidermal observations, the dried intact internode sections were mounted on aluminium stubs (Cambridge pin type 10 mm) with epoxy glue. The Bio-Rad coating system (London, United Kingdom) was used for gold sputter coating of the sample with a layer of approximately 60 nm. Observations of spore differentiation on the epidermal layer were made with a Shimadzu SSX-550 (Kyoto, Japan) scanning electron microscope.

For sub-epidermal observations of the leaf sheath, the fractioning method of Hughes and Rijkenberg (1985) was used with modifications. Leaf sheaths were removed from the dried internode sections and laid flat on an aluminium stub using double-sided tape. Another aluminium stub with double sided tape was then pressed directly on top of the leaf sheath sections, effectively sandwiching the leaf sheath between two layers of double sided tape and

the flat ends of two aluminium stubs. Pulling these two stubs apart separated the two epidermal layers, each to a different stub. Excess mesophyll tissue was removed with a scalpel blade and sections were gold sputter coated with an approximately 60 nm layer using the Bio-Rad coating system. Thereby, the sub-stomatal chambers and any potential infection structures were exposed for observation using the Shimadzu SSX-550 scanning electron microscope.

4.2.3 Fluorescence microscopy

Sections of the last internode were sampled for fluorescence microscopy at 1, 2, 3, 5 and 10 dpi. Samples were prepared with a modified method of Rohringer *et al*. (1977) as described by Moldenhauer *et al*. (2006). Uvitex 2B (Polysciences Inc., United States of America) was used to stain fungal colonies and observations were made using the Olympus AX70 (Tokyo, Japan) microscope. The blue wavelength (WB) epifluorescence cube with an excitation filter of 330-385 nm and barrier filter of 420 nm showed the fluorescence of stained fungal tissue. The ultraviolet wavelenghth (WU) epifluorescence cube with an excitation filter of 450-480 nm and barrier filter of 515 nm showed autofluorescence in wheat tissue, as an indication of cell death. Mounted samples were subsequently stained with phloroglucinol-HCl, as a test for lignin formation. The method is based on that of Sherwood and Vance (1976) but was modified by Moldenhauer *et al*. (2006) to use Uvitex 2B-stained tissue for subsequent testing. However, these methods were later abandoned in favour of the wheat germ agglutinin fluorescein isothiocyanate conjugate (WGA-FITC*)* staining method as described below.

The samples mentioned above were also processed according to a modified method of Ayliffe *et al*. (2011) using WGA-FITC (Sigma-Aldrich, St Louis, Missouri, United States of America). Sections of the last internode were placed in 1 M KOH and 0.05% (v/v) Silwet L-77 (SouthernChem, Sandton, South Africa) directly after sampling and incubated at 37°C for 16 h. Samples were washed thrice with a 50 mM tris(hydroxymethyl)aminomethane-hydrochloric acid (Tris-HCl) buffer (pH 7.0) and the flag leaf sheaths removed from the stem for further processing. Leaf sheaths were stained for 16 h with 20 µg/ml (w/v) WGA-FITC in the Tris-HCl buffer. Samples were washed twice with the Tris-HCl buffer and the leaf sheaths were mounted on microscope slides. Fluorescence observations were made with an Olympus AX70 microscope using the WU epiflorescence cube with an excitation filter of 450-480 nm and barrier filter of 515 nm. Micrographs were taken with the fitted Olympus CC12 camera (Olympus Soft Imaging Solutions, Japan) and Olympus AnalySIS LS Research

v 2.2 software. The size of fungal colonies at 5 dpi was determined and the means calculated. Colony sizes were statistically analysed by Tukey's multiple comparison test using GraphPad Prism v 6.01. The mean colony size of each line was compared to the mean colony size of every other line. The confidence level for the test was set at 99%.

4.2.4 Cross-sectioning of last internodes

To investigate the cross section (transverse plane) of the last internode of inoculated wheat, the paraffin wax impregnation technique of Johansen (1940) was used with some modifications. Samples of the last internode were taken at 10 dpi from the susceptible 37-07 line. The last internodes were randomly cut along the length into 5 mm sections and placed in 3% (v/v) glutaraldehyde in a sodium phosphate buffer (0.1 M) at pH 7.0. Sections were dehydrated in a tertiary butyl alcohol series (Johansen, 1940). Two additional steps were included; firstly a 50:50 volume of tertiary butyl alcohol and liquid paraffin and secondly pure liquid paraffin.

For impregnation the total volume liquid paraffin was gradually replaced with melted paraffin wax over the course of 5 days while samples were kept at 60°C. Last internode sections in the paraffin wax suspension were cast in plastic moulds (15 x 15 x 15 mm) and orientated to allow for the cutting of transverse sections. After setting, the paraffin block containing the embedded tissue was trimmed and mounted unto small wooden blocks (20 x 20 x 20 mm). Cross-sectioning of tissue was done with a rotary microtome (Model 45; Lipshaw Manufacturing Company, Detroit, Michigan, United States of America) equipped with the standard blade. Cross sections of 5-10 μm (typically 6 μm) were made and affixed to microscope slides with Entellan® (Merck KGaA, Darmstadt, Germany). The cross sections were stained with Safranin O/Fast Green FCF (Johansen, 1940) or WGA-FITC.

The Safranin O staining solution was prepared by dissolving 1.0% (w/v) Safranin O (Sigma-Aldrich, St. Louis, Missouri, United States of America) in a 2:1:1 methyl cellosolve, ethanol and water solution with 1.0% (w/v) sodium acetate and 2.0% (w/v) formalin. The Fast Green FCF staining solution consisted of 0.5% (w/v) Fast Green FCF (Sigma-Aldrich) dissolved in a 1:1:1 methyl cellosolve, ethanol and clove oil solution. For Safranin O/Fast Green FCF staining of cross sections, the microscope slides were processed with the following solutions: xylene (10 min), 1:1 xylene and ethanol (10 min), ethanol (10 min), 50% (v/v) ethanol in water (5 min), Safranin O staining solution (30 min), twice with ethanol, Fast Green FCF staining solution (as needed), 1:1 xylene and ethanol solution and finally xylene (10 min).

Cover slips were permanently fixed with Entallan and observations made under white light with the Olympus AX70 microscope.

For WGA-FITC staining of cross sections, the microscope slides were transferred through the following solutions: xylene (10 min), 1:1 xylene and ethanol (10 min), ethanol (10 min), 50% (v/v) ethanol in 50 mM Tris-HCl buffer at pH 7.0 (10 min), the Tris-HCl buffer (10 min) and finally 20 μg/ml (w/v) WGA-FITC (16 h) in the Tris-HCl buffer. Slides were washed with the Tris-HCl buffer and fluorescence observations made with the Olympus AX70 microscope as described in section 4.2.3.

4.3 Results

4.3.1 Initial microscopic experimentation

Fluorescence microscopy using Uvitex 2B only partially allowed the observation of infection structures of *Pgt* in the adult plant tissues of wheat lines 37-07, W1406 and W6979. High background fluorescence of wheat tissue made observations of especially internal infection structures difficult. Initial optimization however showed that Uvitex 2B staining of inoculated seedling tissue does show internal infection structures. Autofluorescence, indicative of cell death associated with infection sites was neither observed in the susceptible nor the APR lines at all tested time points up to 5 dpi. Lignin formation associated with infection sites was likewise not observed for all tested time points up to 5 dpi, in all three lines. The wheat sclerenchymatous fibres associated with vascular bundles did however show the reddish-brown colour as a positive test for lignin and indicated that staining was successful. Results for Uvitex 2B staining, autofluorescence and lignin staining of *Pgt* infection sites are not shown.

4.3.2 Scanning electron microscopy

Observations made by SEM allowed the description of the early stages of the *Pgt* infection process. Epidermal micrographs showed germination of urediniospores on all three wheat lines by 6 hpi (Figures 4.2, 4.6 and 4.10). The germ tubes extended away from the urediniospore and had a swollen appearance. No further structures were visible. By 12 hpi appressoria were observed on all lines at a stomatal opening, as illustrated by a typical appressorium in Figure 4.3. The appressoria were cylindrical and covered a large section of the stomatal opening (Figures 4.5, 4.9 and 4.13). The developing germ tubes started to collapse and only stayed swollen at the distal points (Figures 4.7 and 4.11). At 1 dpi the germ tubes associated with appressoria were invariably collapsed (Figures 4.5, 4.9 and 4.13) and germ tubes that have not reached a stomatal opening at 1 dpi had also collapsed (Figures 4.4, 4.8 and 4.12). Adhesion pads and ECM associated with urediniospores were not observed.

From a single urediniospore two germ tubes typically developed (Figure 4.8). One germ tube did not develop as extensively as the other. No directional development of germ tubes of *Pgt* was observed on the epidermis in any of the three lines. Germ tubes were also extensively branched. In some instances the lateral branch could not be clearly differentiated from the principal germ tube with two developing points being equally pronounced (Figure 4.7). The

wheat epidermal surface also varied slightly. At times longitudinal ridges were prominent (Figures 4.2, 4.7 and 4.11) but at other times not (Figures 4.4 and 4.8). Epicuticular wax was prominent on the epidermal surface.

Sub-epidermal observations of the *Pgt* infection process on the susceptible 37-07 line were also carried out. Observations of internal infection structures were rare, but possible. Mesophyll cells and sub-stomatal chambers were readily exposed, but observed infection sites rare. Where infection sites were observed within the sub-stomatal chamber it showed the clear development of a SSV by 1 dpi (Figure 4.14). Similar to the appressorium, the SSV was cylindrical and covered a large section of the internal stomatal opening. The SSV elongated at both ends by 36 hpi (Figures 4.15 and 4.16), indicating possible IH. One of the elongated ends however developed a pronounced septum, indicating the formation a HMC by 36 hpi (Figures 4.15 and 4.16). No extensive primary IH was found developing in the mesophyll intracellular spaces. At 2 dpi further IH were observed forming just below the septum of the first HMC and showed a double branched structure (Figure 4.17).

4.3.3 Fluorescence microscopy

Preparation for fluorescence microscopy destained wheat tissue effectively but some background fluorescence was still seen. Binding of chitin by WGA-FITC allowed internal fungal infection structures to be observed. At 1 dpi, appressorium development was observed in all three lines (Figure 4.18). At a different focal plane, corresponding to the deeper sub-epidermal mesophyll layer, a SSV was observed in all infection sites that had an appressorium. Some SSV also showed a clear septum indicative of HMC formation, but primary IH were not well defined. No noteworthy differences in the infection process were observed for the three lines at this time point.

By 2 dpi the infection sites showed the development of IH branching out, close to the first HMC (Figure 4.19). The IH associated with the first HMC invariably had a double branched structure. From these IH the development of further HMC was observed. Here too, no noteworthy differences in the infection process were observed among the three lines. The IH had spread through the mesophyll cells and further HMC developed by 3 dpi (Figure 4.20). The infection sites on the three lines at 3 dpi showed no differences that could be quantified. Colonies of *Pgt* were well established by 5 dpi and radiated from the stomata where infection had begun (Figure 4.21).

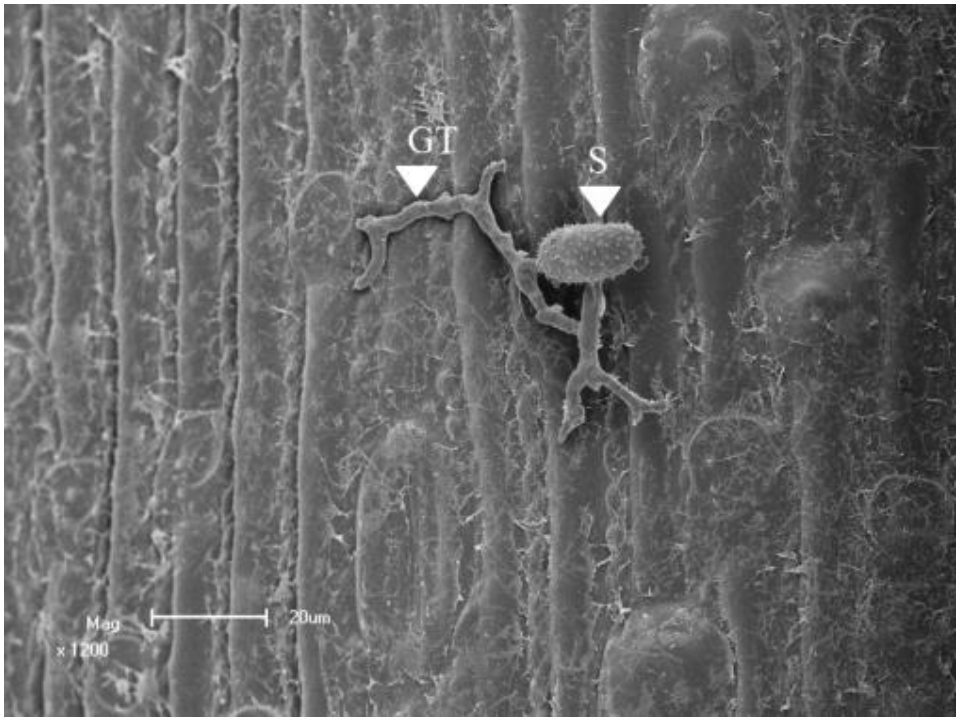

Figure 4.2: Scanning electron micrograph of the *Puccinia graminis* f. sp. *tritici* infection process on the flag leaf sheath of the 37-07 wheat line at 6 hours post inoculation. The urediniospore (S) and developing germ tube (GT) are indicated.

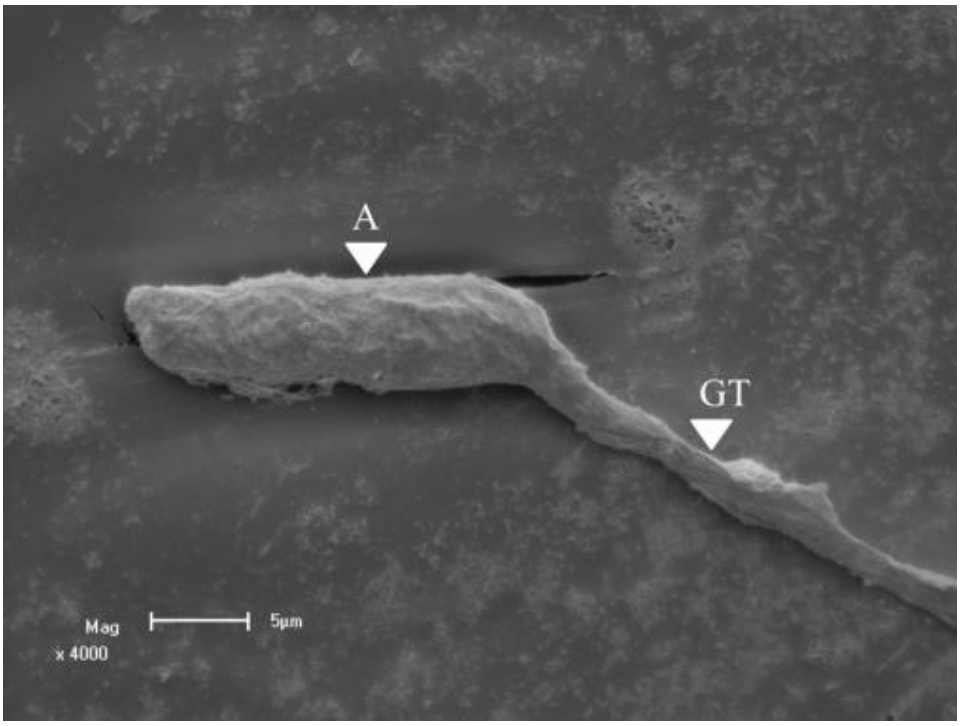

Figure 4.3: Scanning electron micrograph of the *Puccinia graminis* f. sp. *tritici* infection process on the flag leaf sheath of the 37-07 wheat line at 12 hours post inoculation. The germ tube (GT) and appressorium (A) are indicated.

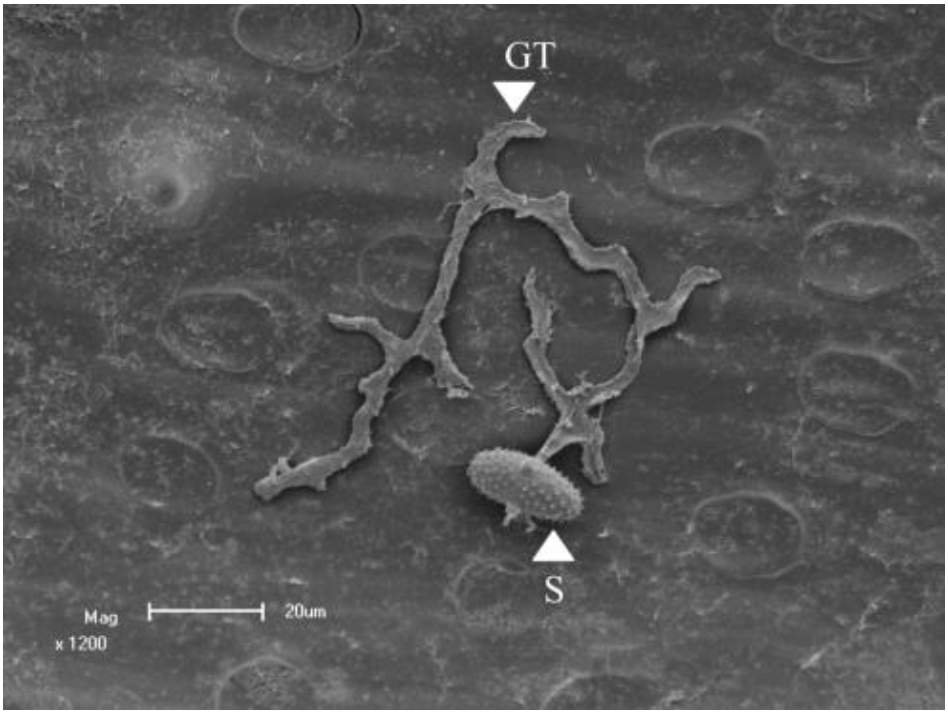

Figure 4.4: Scanning electron micrograph of the *Puccinia graminis* f. sp. *tritici* infection process on the flag leaf sheath of the 37-07 wheat line at 1 day post inoculation. The urediniospore (S) and developing germ tube (GT) are indicated.

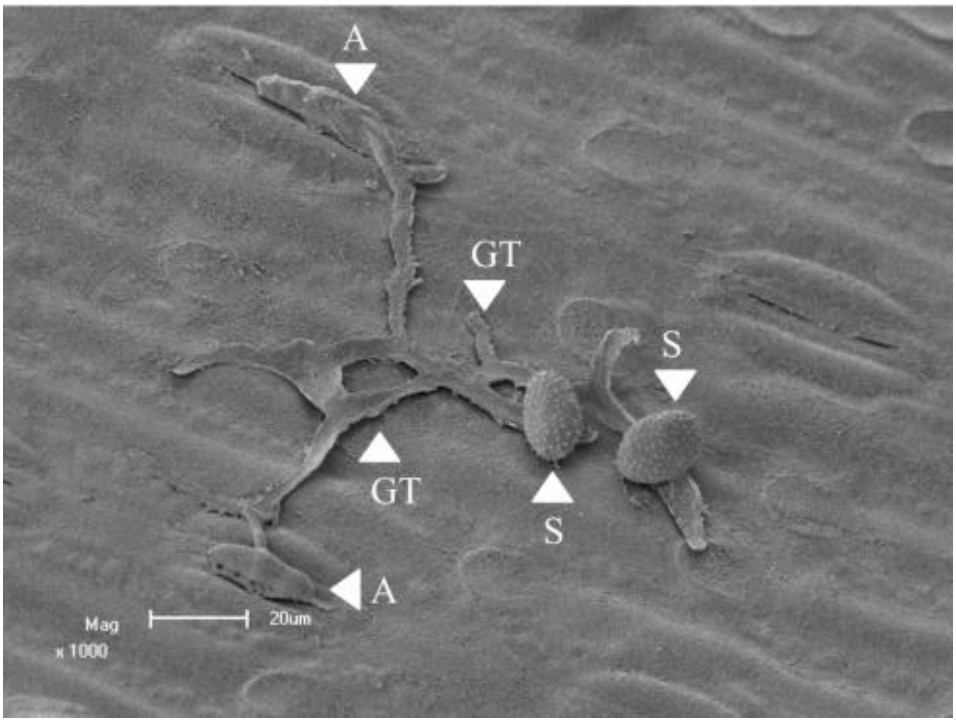

Figure 4.5: Scanning electron micrograph of the *Puccinia graminis* f. sp. *tritici* infection process on the flag leaf sheath of the 37-07 wheat line at 1 day post inoculation. Urediniospores (S), developing germ tubes (GT) and appressoria (A) are indicated.

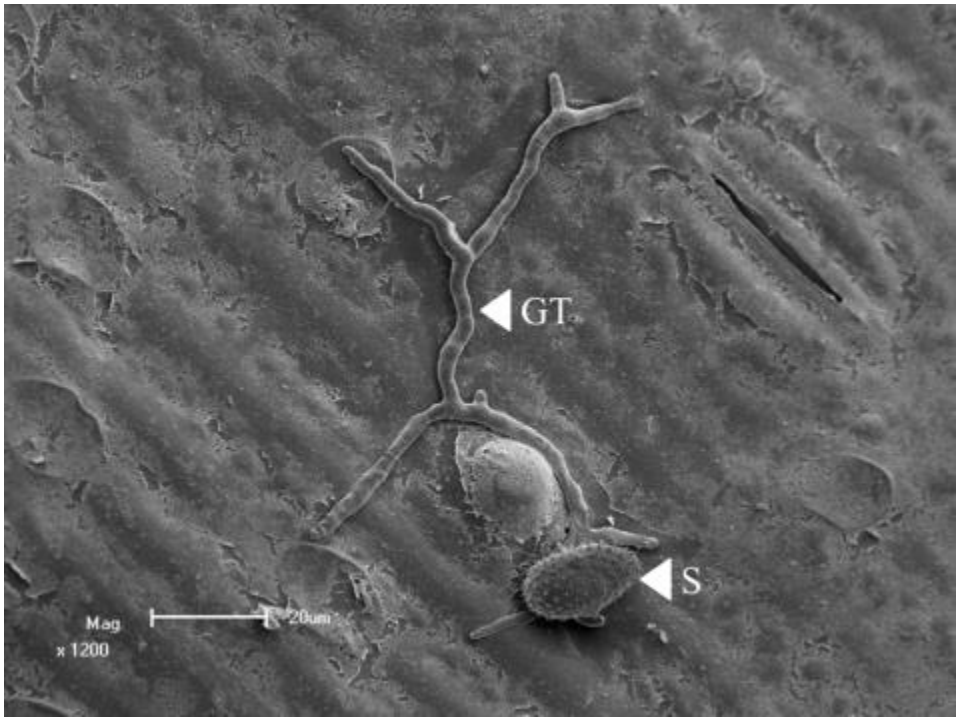

Figure 4.6: Scanning electron micrograph of the *Puccinia graminis* f. sp. *tritici* infection process on the flag leaf sheath of the W1406 wheat line at 6 hours post inoculation. The urediniospore (S) and developing germ tube (GT) are indicated.

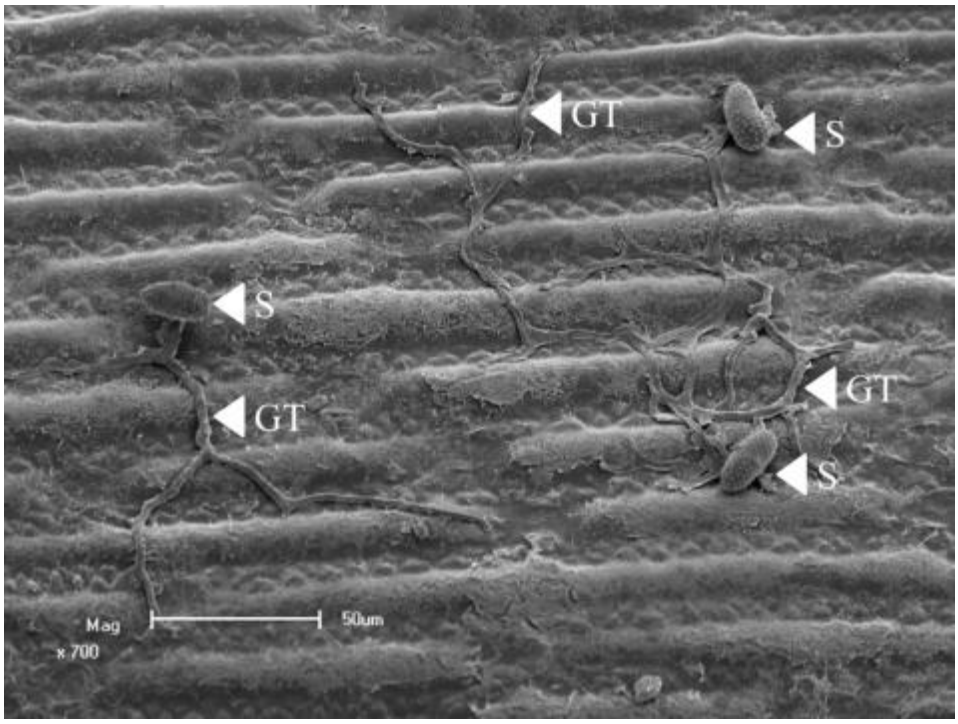

Figure 4.7: Scanning electron micrograph of the *Puccinia graminis* f. sp. *tritici* infection process on the flag leaf sheath of the W1406 wheat line at 12 hours post inoculation. The urediniospore (S) and developing germ tube (GT) are indicated.

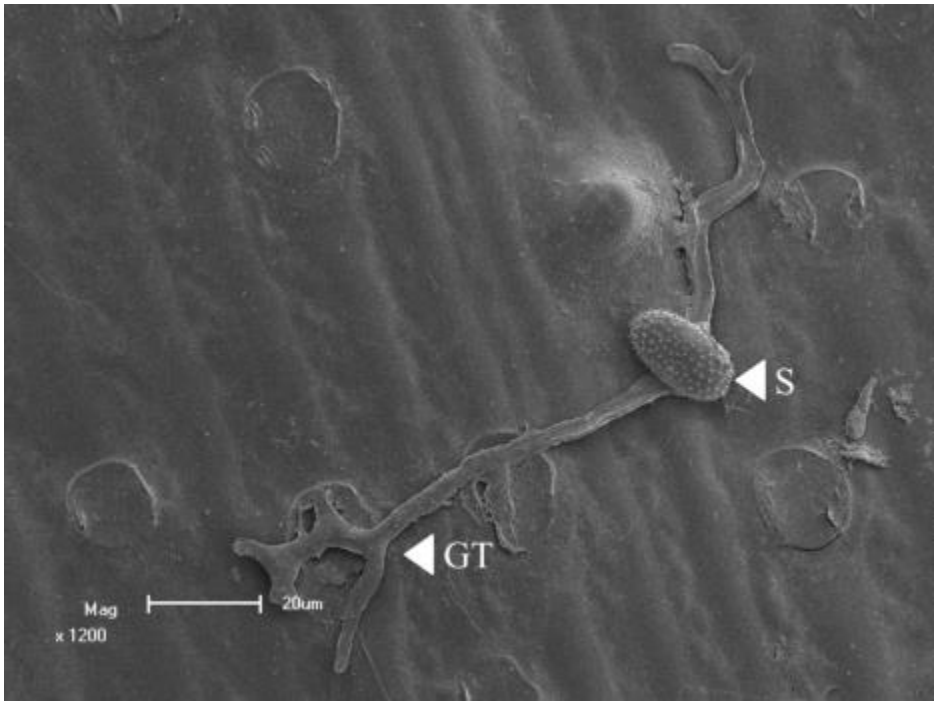

Figure 4.8: Scanning electron micrograph of the *Puccinia graminis* f. sp. *tritici* infection process on the flag leaf sheath of the W1406 wheat line at 1 day post inoculation. The urediniospore (S) and developing germ tube (GT) are indicated.

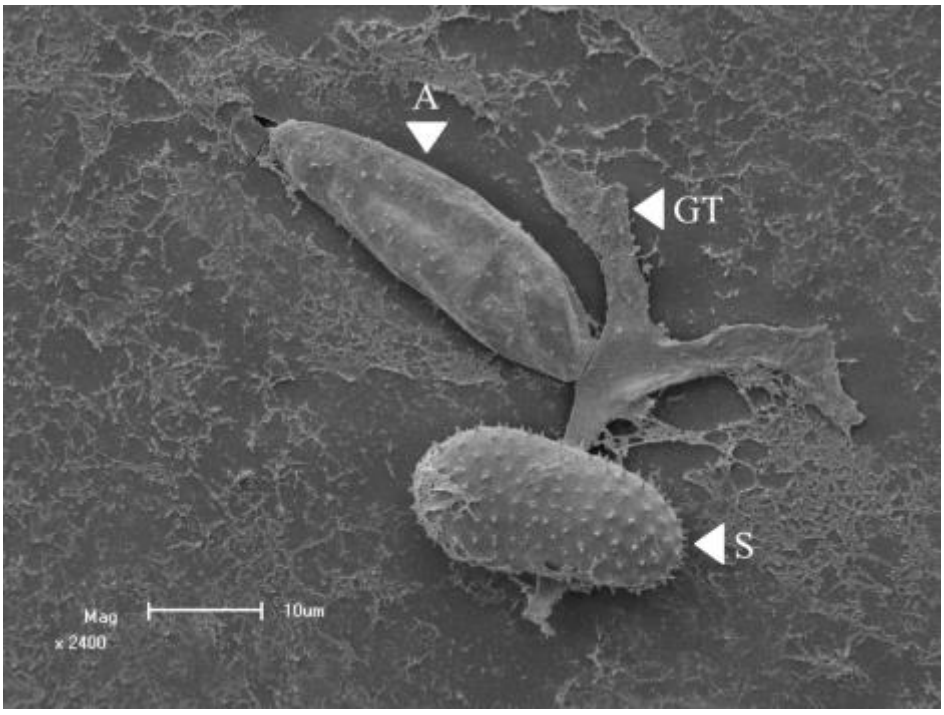

Figure 4.9: Scanning electron micrograph of the *Puccinia graminis* f. sp. *tritici* infection process on the flag leaf sheath of the W1406 wheat line at 1 day post inoculation. The urediniospore (S), developing germ tube (GT) and appressorium (A) are indicated.

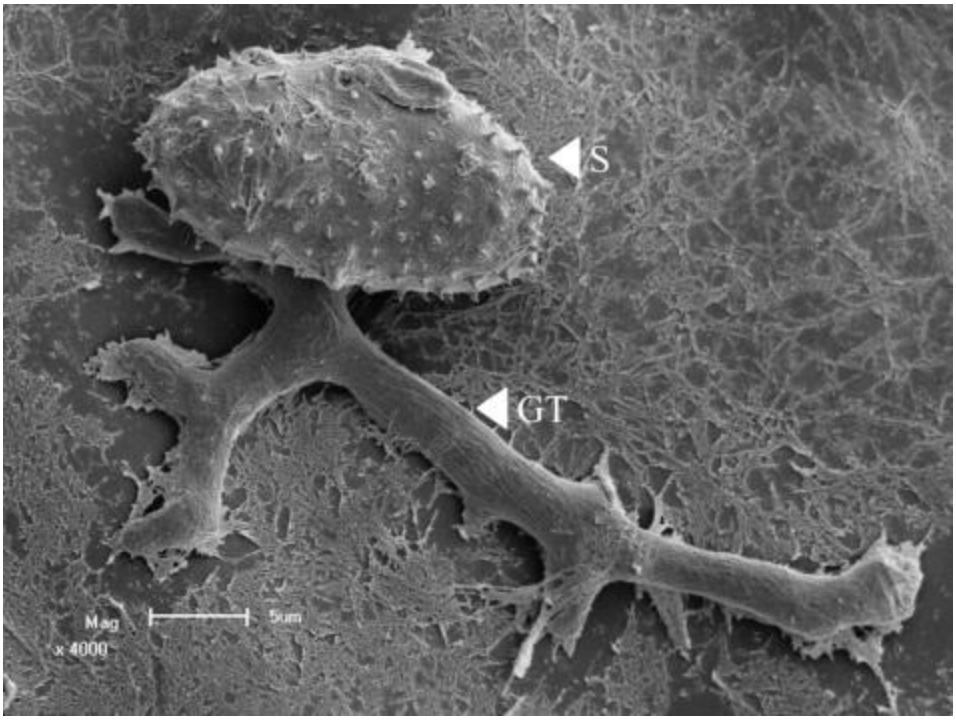

Figure 4.10: Scanning electron micrograph of the *Puccinia graminis* f. sp. *tritici* infection process on the flag leaf sheath of the W6979 wheat line at 6 hours post inoculation. The urediniospore (S) and developing germ tube (GT) are indicated.

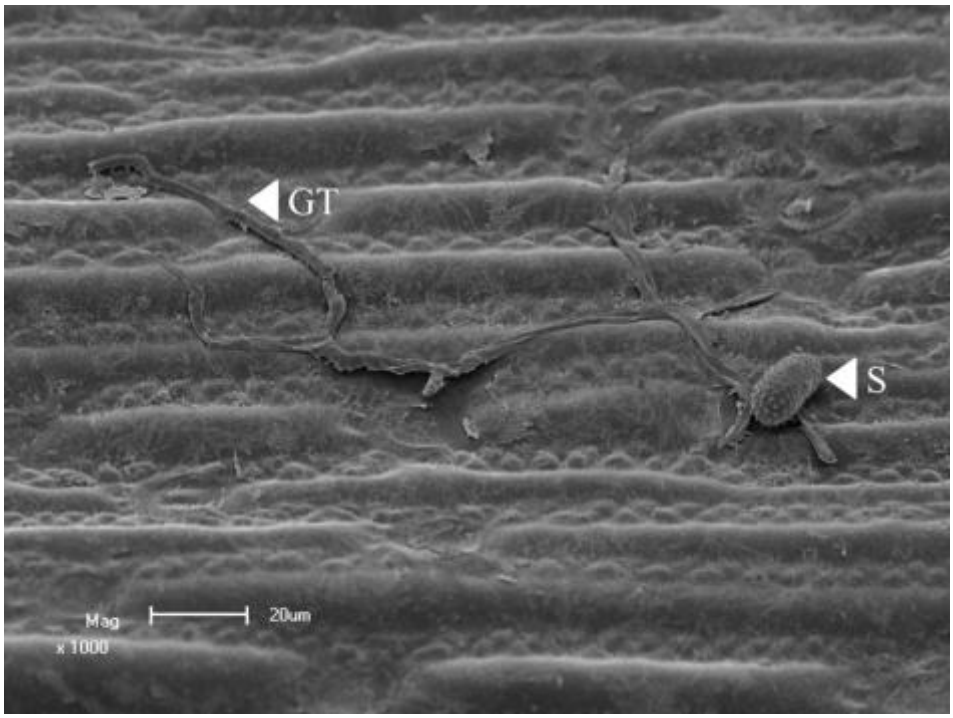

Figure 4.11: Scanning electron micrograph of the *Puccinia graminis* f. sp. *tritici* infection process on the flag leaf sheath of the W6979 wheat line at 12 hours post inoculation. The urediniospore (S) and developing germ tube (GT) are indicated.

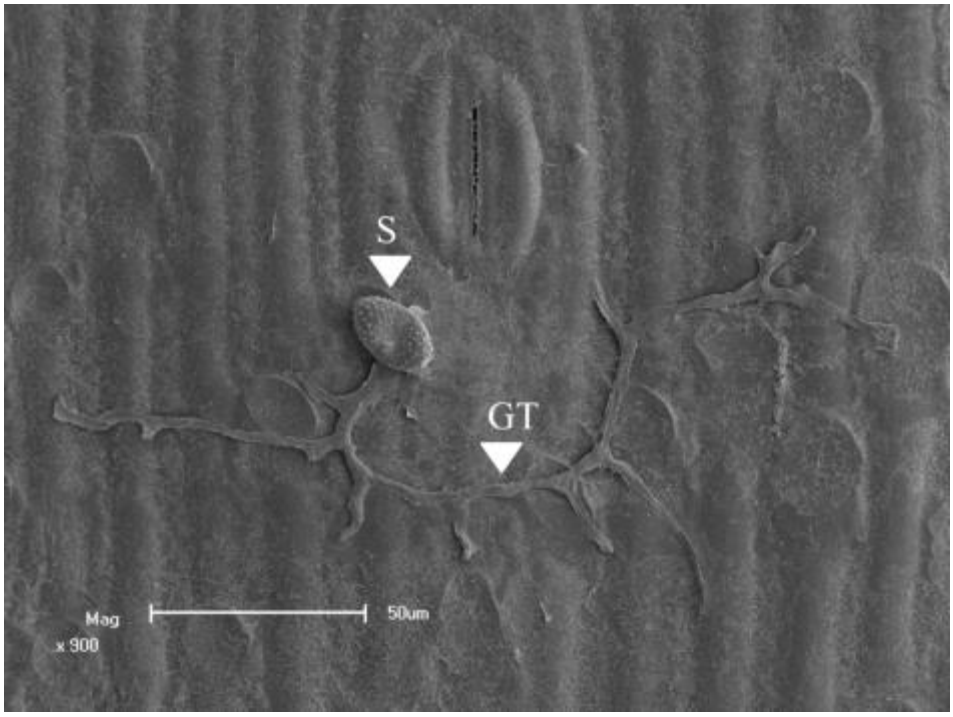

Figure 4.12 Scanning electron micrograph of the *Puccinia graminis* f. sp. *tritici* infection process on the flag leaf sheath of the W6979 wheat line at 1 day post inoculation. The urediniospore (S) and developing germ tube (GT) are indicated.

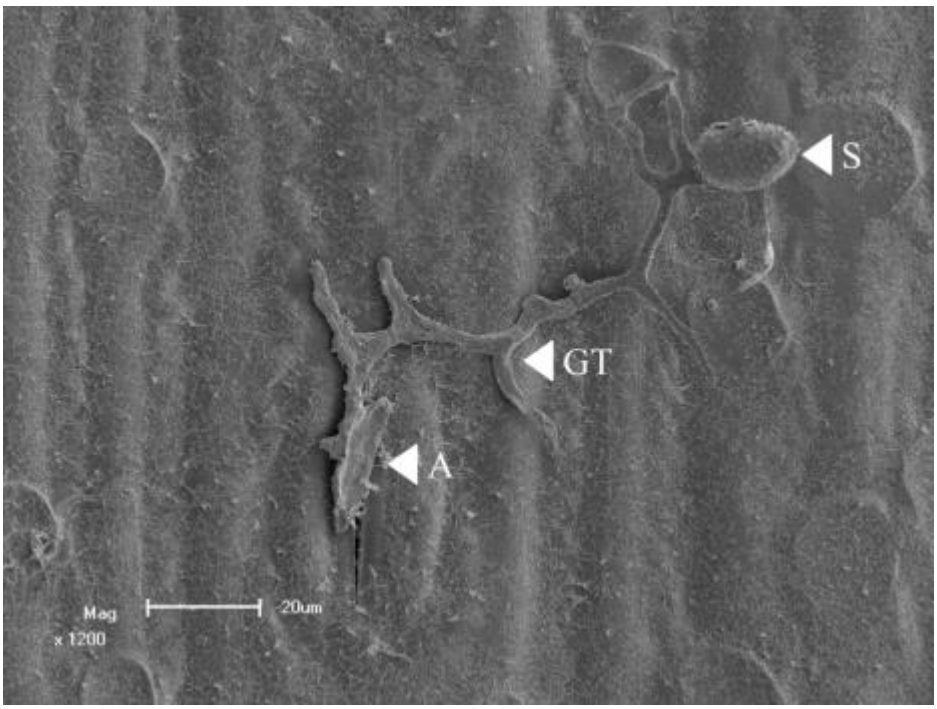

Figure 4.13: Scanning electron micrograph of the *Puccinia graminis* f. sp. *tritici* infection process on the flag leaf sheath of the W6979 wheat line at 1 day post inoculation. The urediniospore (S), developing germ tube (GT) and appressorium (A) are indicated.

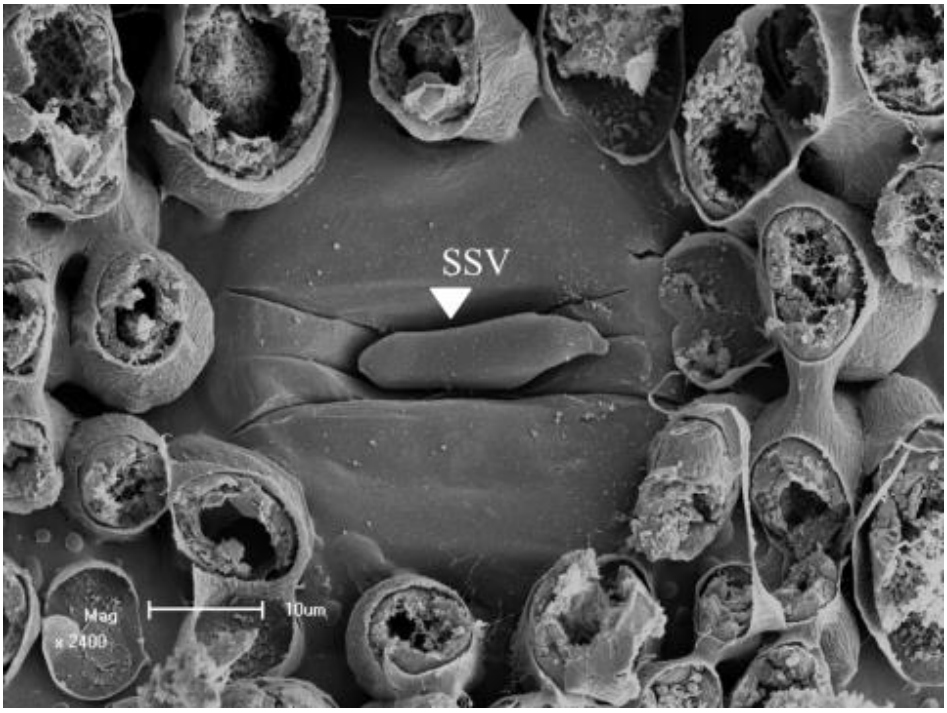

Figure 4.14: Sub-epidermal scanning electron micrograph of the *Puccinia graminis* f. sp. *tritici* infection process on the flag leaf sheath of the 37-07 wheat line at 1 day post inoculation. The sub-stomatal vesicle (SSV) is indicated.

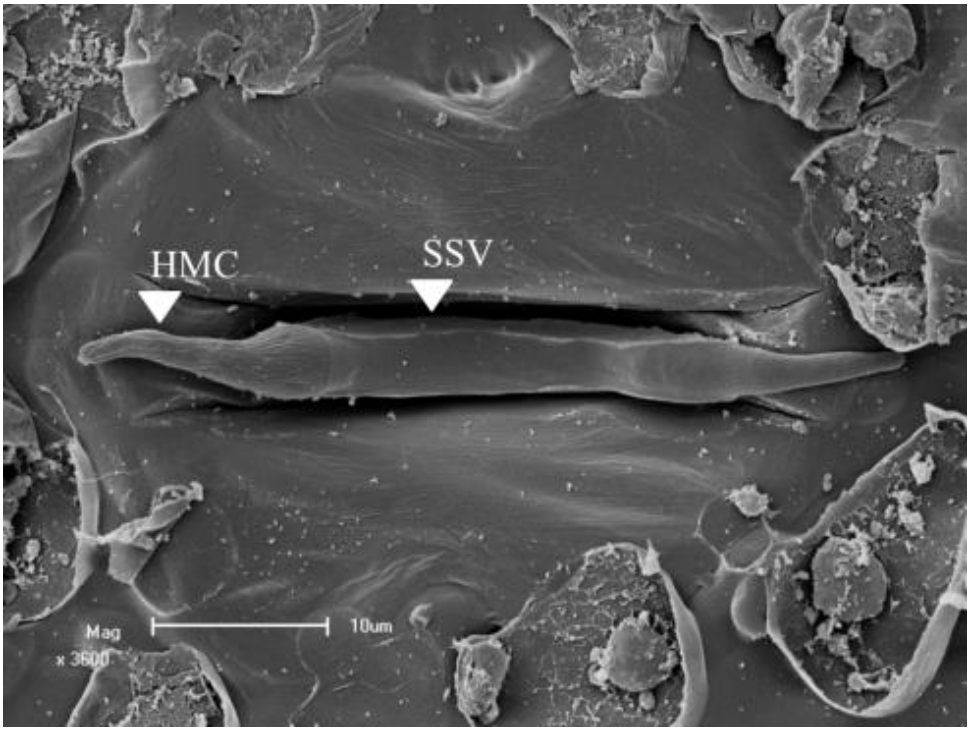

Figure 4.15: Sub-epidermal scanning electron micrograph of the *Puccinia graminis* f. sp. *tritici* infection process on the flag leaf sheath of the 37-07 wheat line at 36 hours post inoculation. The sub-stomatal vesicle (SSV) and haustorial mother cell (HMC) are indicated.

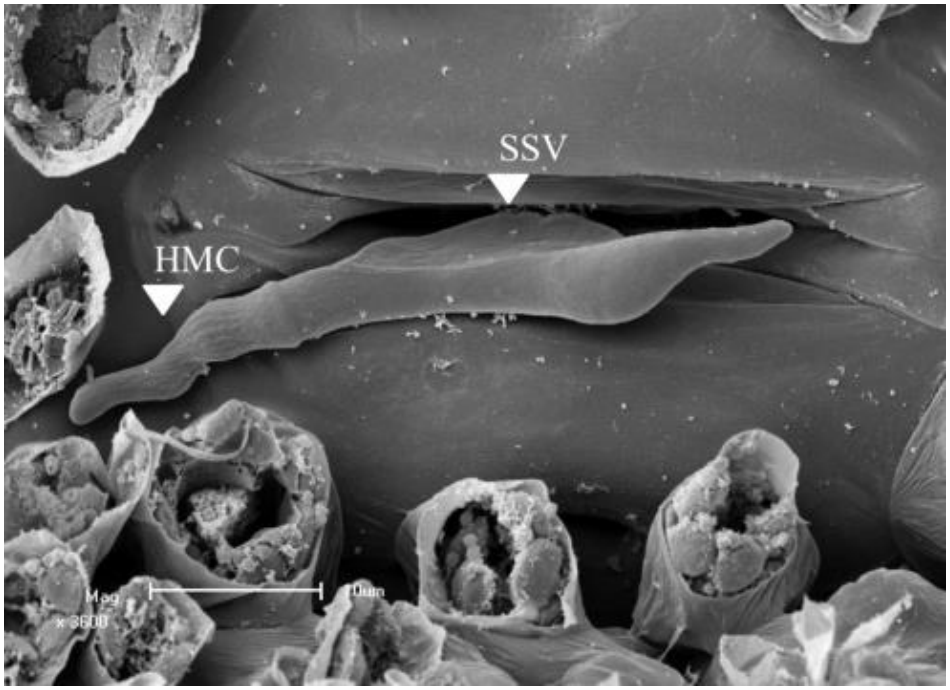

Figure 4.16: Sub-epidermal scanning electron micrograph of the *Puccinia graminis* f. sp. *tritici* infection process on the flag leaf sheath of the 37-07 wheat line at 36 hours post inoculation. The sub-stomatal vesicle (SSV) and haustorial mother cell (HMC) are indicated.

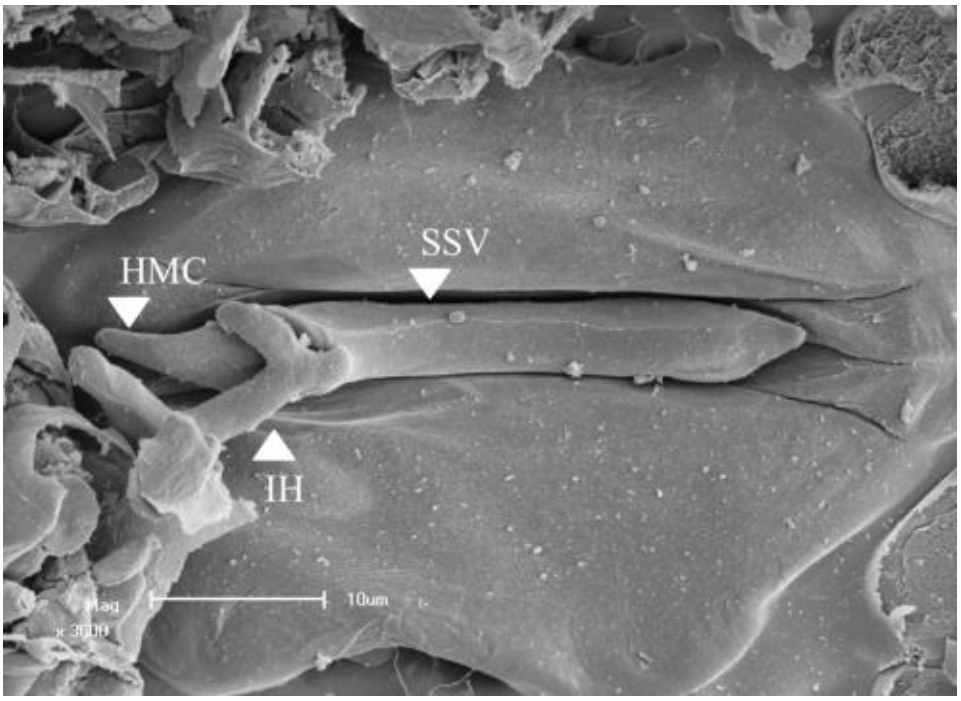

Figure 4.17: Sub-epidermal scanning electron micrograph of the *Puccinia graminis* f. sp. *tritici* infection process on the flag leaf sheath of the 37-07 wheat line at 2 days post inoculation. The sub-stomatal vesicle (SSV), haustorial mother cell (HMC) and infection hypha (IH) are indicated.

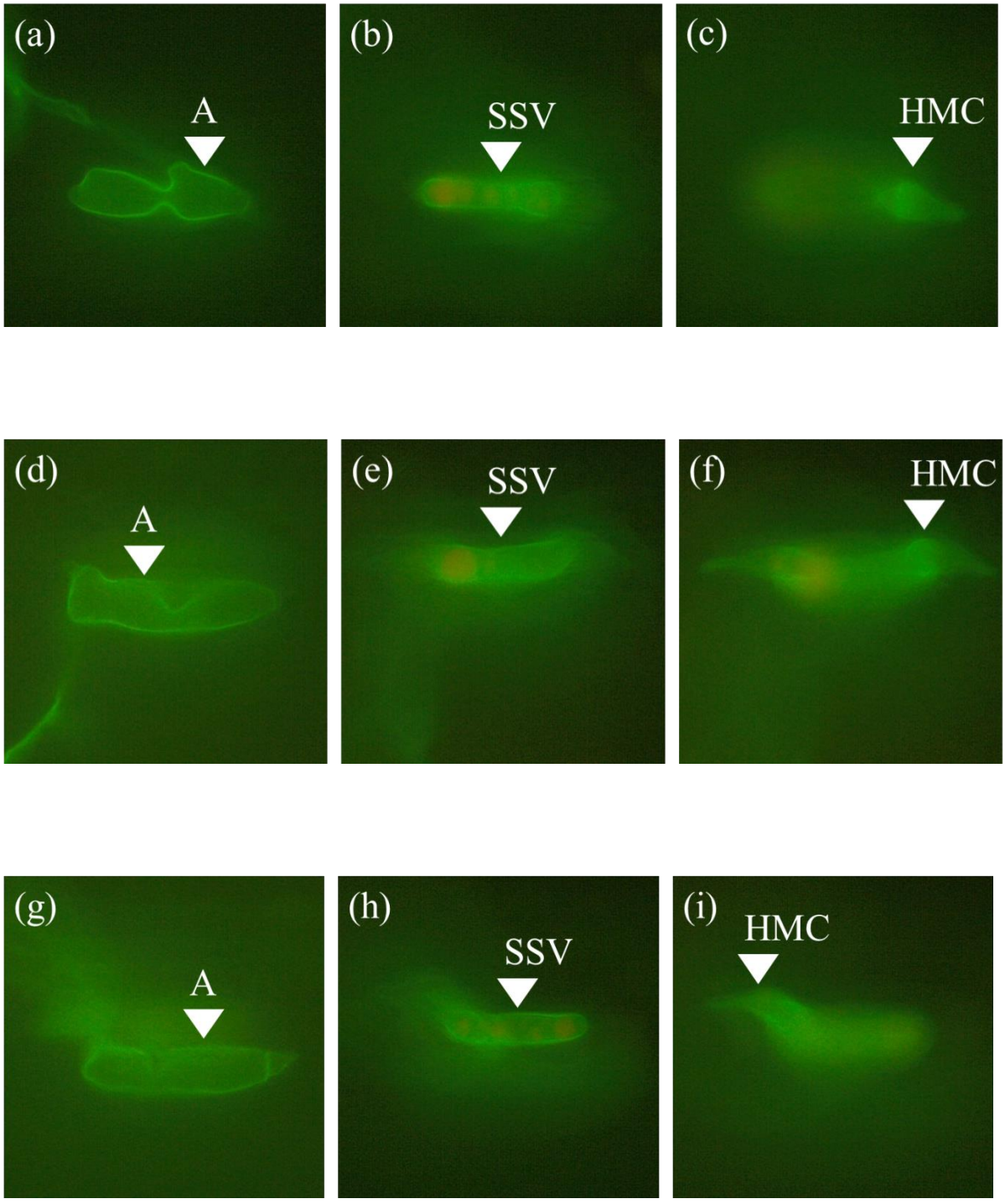

Figure 4.18: Fluorescence micrograph of *Puccinia graminis* f. sp. *tritici* infection sites on the flag leaf sheath at 1 day post inoculation. Each set of three micrographs represents a single *Puccinia graminis* f. sp. *tritici* infection site at different focal planes as seen on the 37-07 (a-c), W1406 (d-f) and W6979 (g-i) wheat lines. The appressoria (A), sub-stomatal vesicles (SSV) and haustorial mother cells (HMC) are indicated.

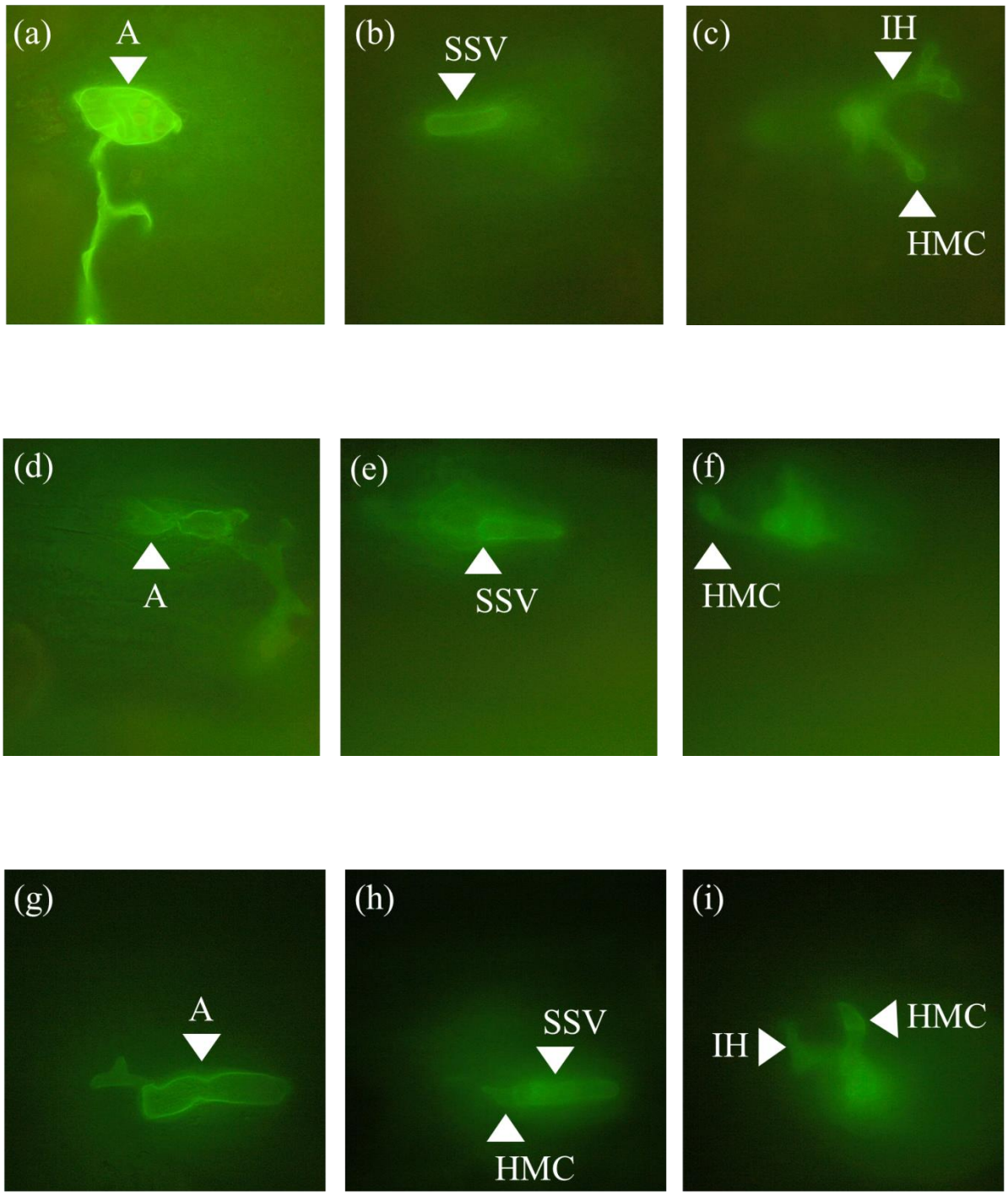

Figure 4.19: Fluorescence micrograph of *Puccinia graminis* f. sp. *tritici* infection sites on the flag leaf sheath at 2 days post inoculation. Each set of three micrographs represents a single *Puccinia graminis* f. sp. *tritici* infection site at different focal planes as seen on the 37-07 (a-c), W1406 (d-f) and W6979 (g-i) wheat lines. The appressoria (A), sub-stomatal vesicles (SSV), infection hyphae (IH) and haustorial mother cells (HMC) are indicated.

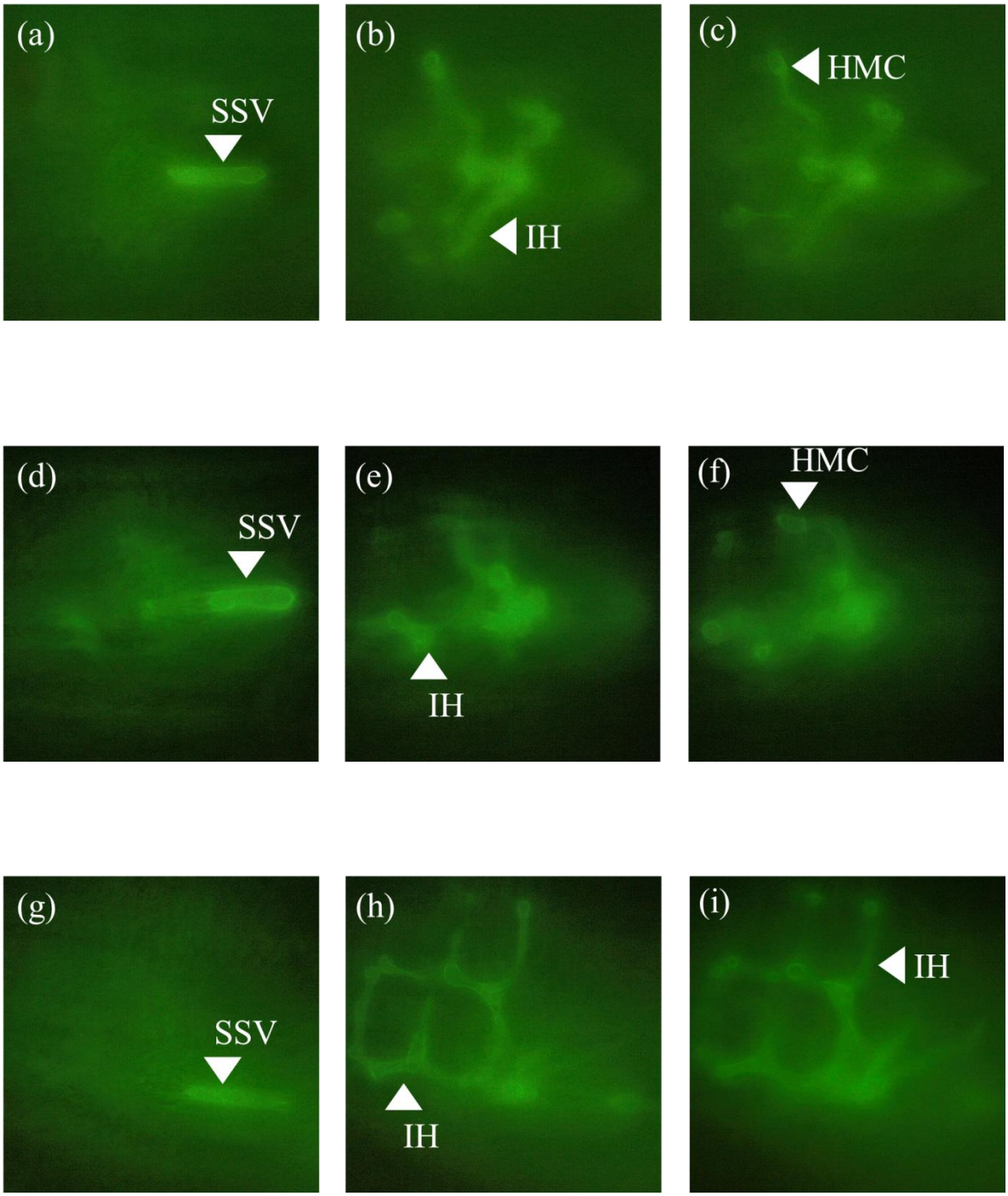

Figure 4.20: Fluorescence micrograph of *Puccinia graminis* f. sp. *tritici* infection sites on the flag leaf sheaths at 3 days post inoculation. Each set of three micrographs represents a single *Puccinia graminis* f. sp. *tritici* infection site at different focal planes as seen on the 37-07 (a-c), W1406 (d-f) and W6979 (g-i) wheat lines. The sub-stomatal vesicles (SSV), infection hyphae (IH) and haustorial mother cells (HMC) are indicated.

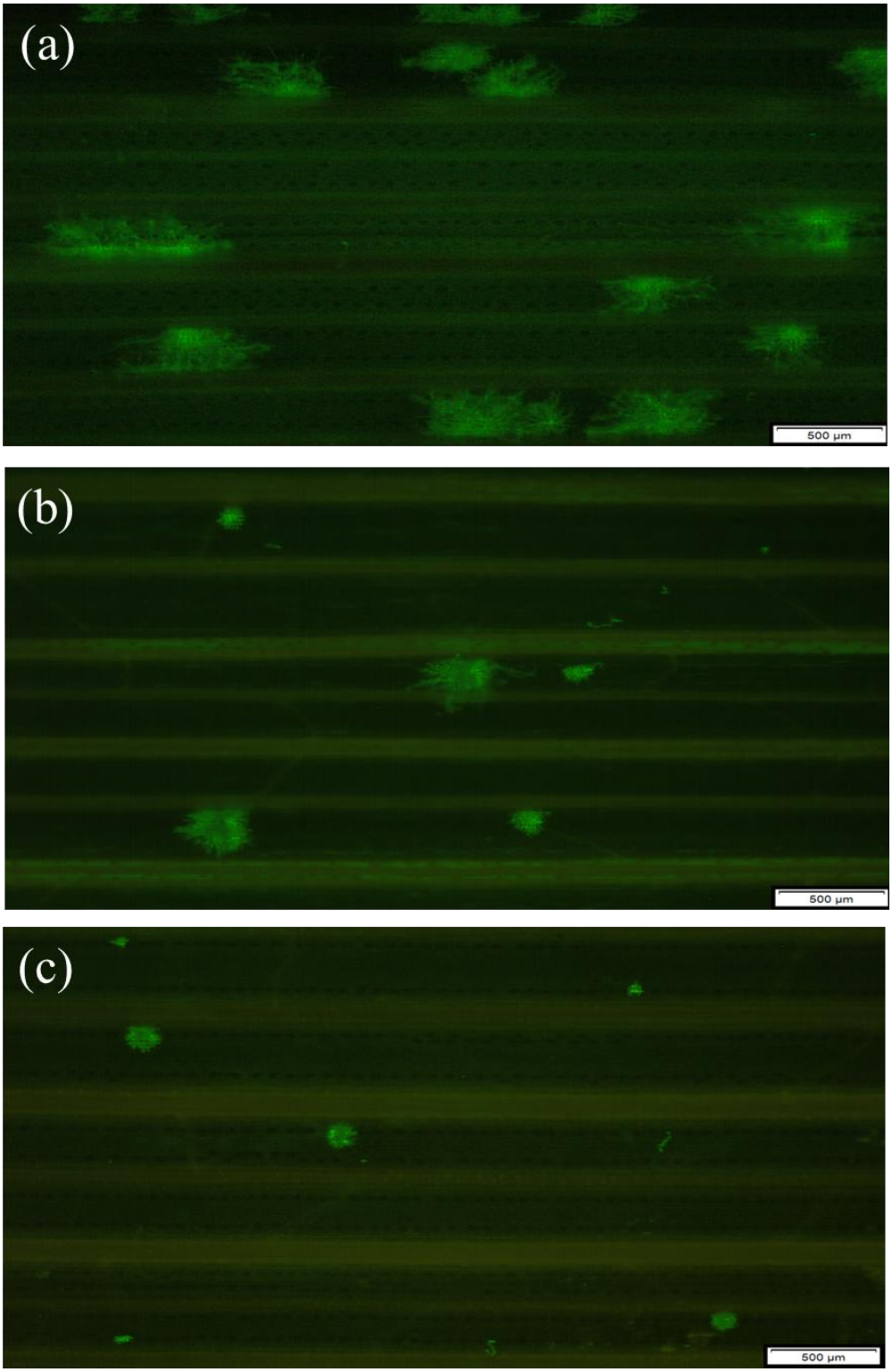

Figure 4.21: Fluorescence micrograph of *Puccinia graminis* f. sp. *tritici* colonies in the flag leaf sheath at 5 days post inoculation. The leaf sheaths of the 37-07 (a), W1406 (b) and W6979 (c) wheat lines are shown.

At 5 dpi, the colony sizes showed a marked difference between the wheat lines which was quantifiable. The mean colony size of *Pgt* on the three lines is indicated in Figure 4.22. The mean colony size was significantly different between all treatments as indicated by a Tukey's multiple comparison test (Table 4.1). The mean colony size on 37-07 was the largest, followed by W1406 and W6979 (Figure 4.22). Likewise, the 37-07 line had the greatest variation, followed by W1406 and W6979.

By 10 dpi, colonies of *Pgt* had spread through the mesophyll tissue and sporulation was observed (Figure 4.23). The development of a colony was longitudinal, parallel with the long axis of the leaf sheath. The development of the colony was restricted by the sclerenchymatous fibres of the vascular bundles. The mycelium had also differentiated to form uredinia containing urediniospores that lifted the wheat epidermal cells. These features were observed in all three lines (Figure 4.23). Visually, W1406 and W6979 showed smaller colonies and less sporulation. However, the proliferation of *Pgt* mycelium at 10 dpi was such that a single colony originating from a stoma could not be differentiated from another, and further quantification was not possible.

4.3.4 Cross-sectioning of last internodes

The larger colonies of 37-07 simplified the cross sectioning of the mycelium and only this line was investigated at 10 dpi (Figures 4.24 - 4.27). In cross section, the last internode clearly showed the hollow stem surrounded by two layers of leaf sheath (Figures 4.24 and 4.25). Using Safranin O/Fast Green FCF staining (Figure 4.24) and WGA-FITC staining (Figure 4.25) a number of uredinia were observed. Under higher magnification (Figures 4.26 and 4.27) the urediniospores and ruptured epidermis are visible. In cross section the sclerenchymatous fibres are clearly restricting the lateral development of colonies.

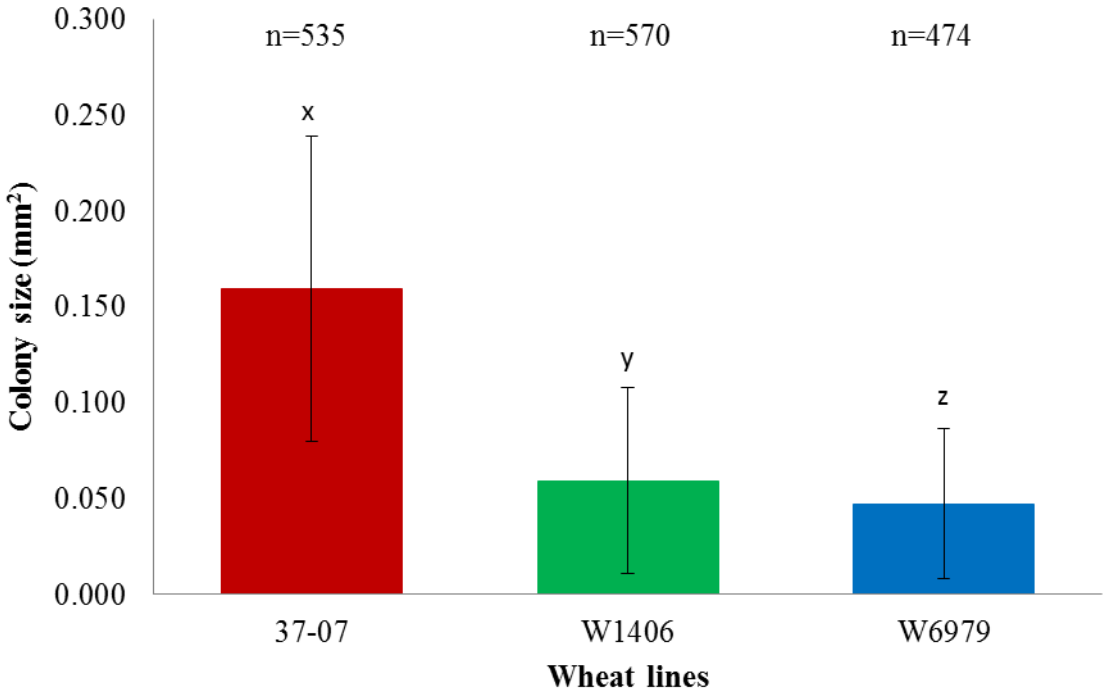

Figure 4.22: Mean colony size (mm^2) of *Puccinia graminis* f. sp. *tritici* colonies at 5 days post inoculation. The mean colony size on the 37-07, W1406 and W6979 wheat lines are indicated, with the respective sample sizes (n) and standard deviation as error bars. Corresponding alphabetic symbols indicate samples with no significant differences as confirmed by Tukey's multiple comparison test (see Table 4.1)

Table 4.1: Tukey's multiple comparison test results for mean colony size of *Puccinia graminis* f. sp. *tritici* on wheat lines at 5 days post inoculation. The mean colony size on 37-07, W1406 and W6979 was compared to the mean colony size of every other line. Confidence level for the test was 99%.

Sample comparisons	Sample size (n)	Mean difference	Confidence interval of difference
37-07 vs W1406	535	0.0997	0.0894 to 0.1100
37-07 vs W6979	570	0.1118	0.1010 to 0.1226
W1406 vs W6979	474	0.0121	0.0014 to 0.02270

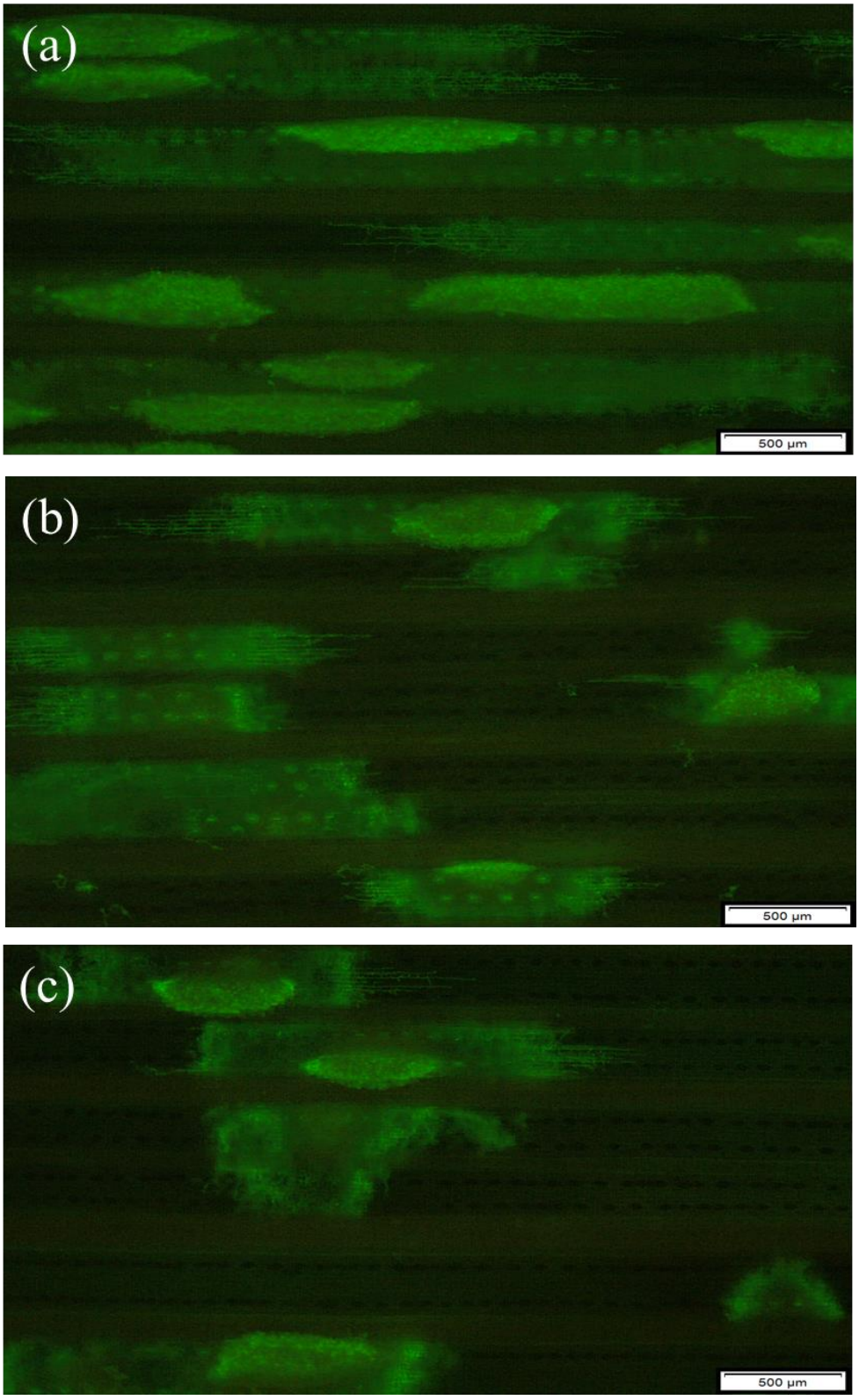

Figure 4.23: Fluorescence micrograph of *Puccinia graminis* f. sp. *tritici* colonies in the flag leaf sheath at 10 days post inoculation. The leaf sheath of the 37-07 (a), W1406 (b) and W6979 (c) wheat lines are shown.

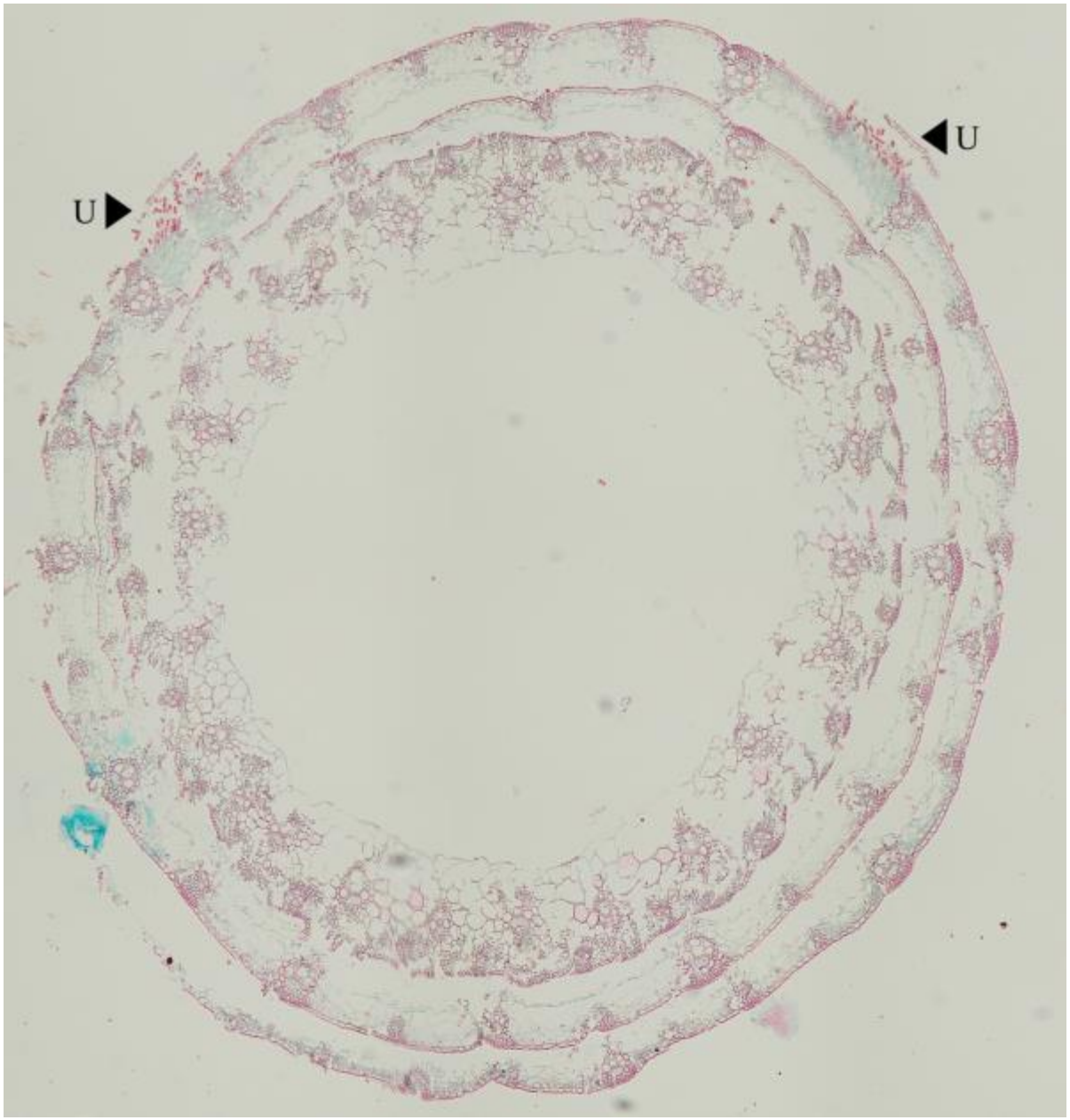

Figure 4.24: Light micrograph of the cross section of a *Puccinia graminis* f. sp. *tritici*-inoculated last internode. The 37-07 line is shown at 10 days post inoculation and uredinia (U) are indicated.

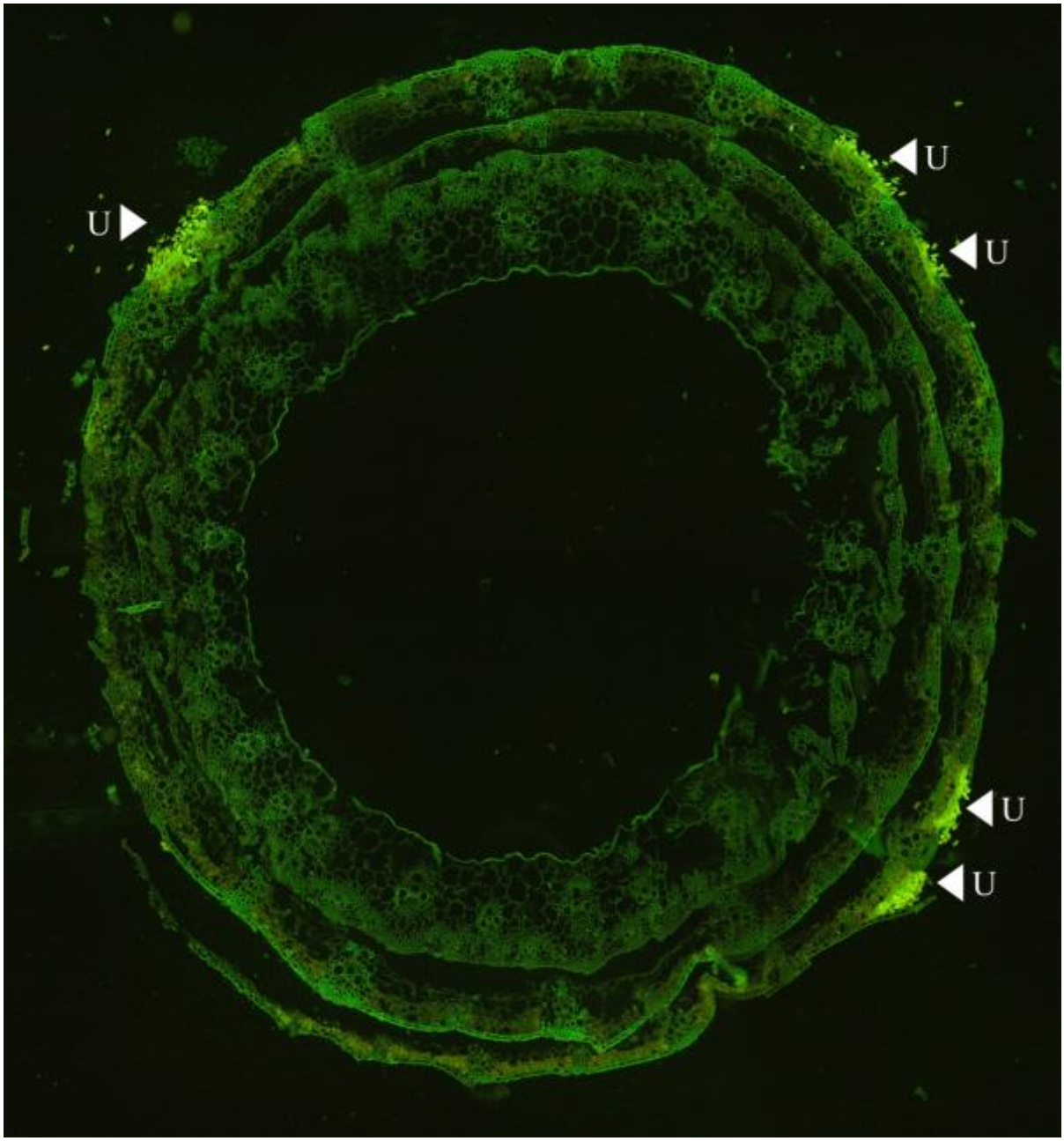

Figure 4.25: Fluorescence micrograph of the cross section of a *Puccinia graminis* f. sp. *tritici*-inoculated last internode. The 37-07 line is shown at 10 days post inoculation and uredinia (U) are indicated.

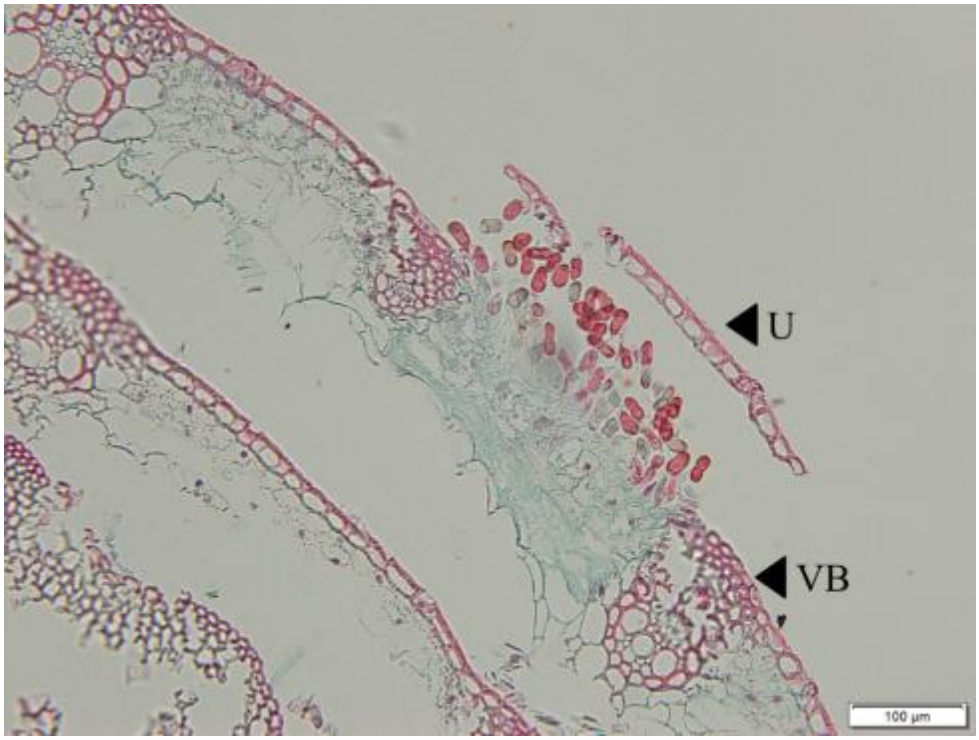

Figure 4.26: Light micrograph of the cross section of a *Puccinia graminis f. sp. tritici*-inoculated last internode. The 37-07 line is shown at 10 days post inoculation and an uredinium (U) and vascular bundle (VB) are indicated.

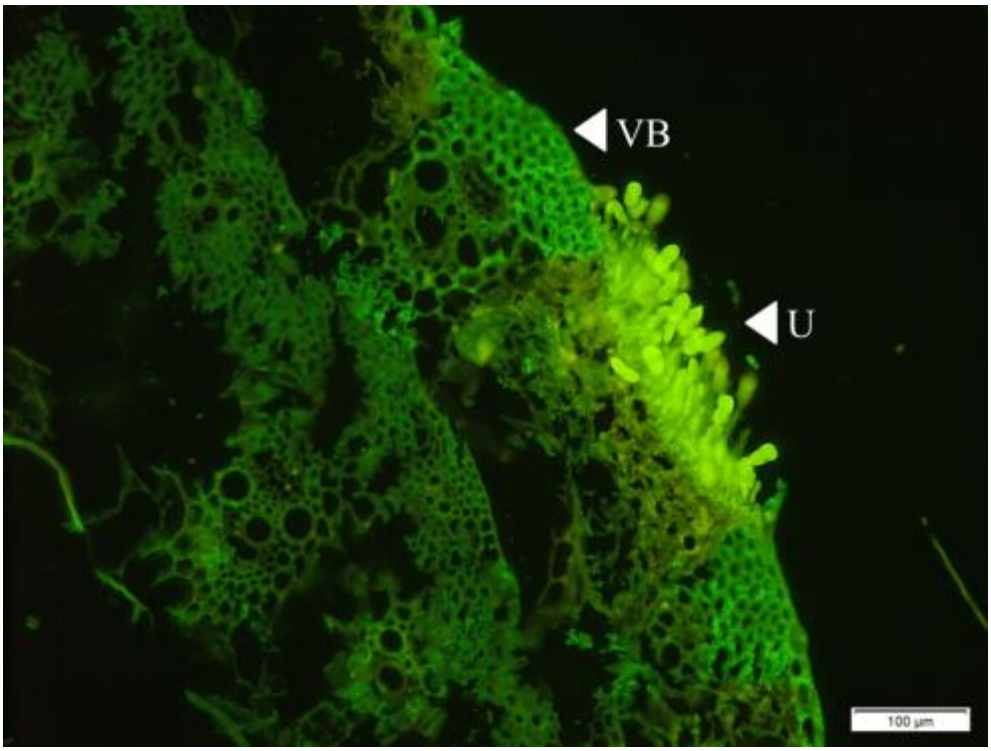

Figure 4.27: Fluorescence micrograph of the cross section of a *Puccinia graminis* f. sp. *tritici*-inoculated last internode. The 37-07 line is shown at 10 days post inoculation and an uredinium (U) and vascular bundle (VB) are indicated.

4.4 Discussion

The microscopic investigation of the *Pgt* infection process on flag leaf sheaths of the last internode presented a number of challenges. The sclerenchymatous fibres associated with vascular bundles in wheat were resilient to destaining, particularly during preparation for fluorescence microscopy. Excessive destaining, may however, disintegrate the tissue. The cylindrical structure of the leaf sheath also complicated the mounting of samples. Any future work on this tissue must involve optimization of sample preparation for microscopy. However, microscopic observations were successfully made during this study and gave insights into the *Pgt* infection process on adult wheat plants.

Evans (1907) reported that germination of *Pgt* urediniospores on wheat occurred by 1 dpi. In the current study, germination had occurred as early as 6 hpi, as confirmed by SEM, an observation reported previously (Lennox and Rijkenberg, 1989). Adhesion pads and ECM associated with urediniospores could not be confirmed, but these structures are assumed to be present. SEM processing seldom caused the spore and germ tube to separate from the epidermis, suggesting strong adhesion. The initial development of two germ tubes in *Pgt*, as reported by Evans (1907), was also confirmed.

During the course of the early infection process, an important observation was made regarding the directional development of germ tubes on the leaf sheath epidermis. The germ tubes did not appear to develop at right angles to the longitudinal wall of epidermal cells. This observation contradicts ‘common knowledge’ of germ tube development of *Pgt* that have been previously reported (Johnson, 1934; Lewis and Day, 1972; Lennox and Rijkenberg, 1989; Read *et al*., 1997). Importantly, past research was done on inoculated wheat seedling leaves and not adult leaf sheaths.

The non-directional growth as reported in the current study has various hypothetical explanations. The germ tubes of *Uromyces phaseoli* (Pers.) G. Winter exhibit directional growth on its host but on the non-host wheat, germ tube development becomes non-directional (Wynn, 1976). The hypothesis was that the adhesion of germ tubes from *U. phaseoli* was ineffective due to the waxes on the wheat leaf surface. The directional growth of *Pgt* germ tubes has however been confirmed in a number non-host cereal species (Lennox and Rijkenberg, 1989). Non-directional growth must therefore be attributed to another feature since *Pgt* adhesion on the wheat host appeared normal.

On the abaxial surface of rye grass (*Lolium perenne* L.) leaves, the germ tubes of *Puccinia graminis* Pers., *Puccinia coronata* Corda and *Puccinia loliina* Sydow and Sydow all exhibit non-directional growth (Roderick and Thomas, 1997). In contrast, on the adaxial surface typical directional growth was observed. Here it was argued that the abaxial surface has less rigid topography and lacks epicuticular wax crystals, but rather has an amorphous wax layer that may lead to the non-directional growth. However, on wheat, *Pgt* exhibits directional growth on both the adaxial and abaxial surfaces of wheat seedling leaves (Lewis and Day, 1972). Features of the epicuticular waxes on the flag leaf sheath may however have caused the non-directional growth observed in this project.

The leaf sheath has a lower rate of transpiration than the flag leaf (Clarke and Richards, 1988) and structural and chemical factors may account for this difference in transpiration. The composition of the waxes on the leaf sheath was shown to differ from that on the leaf blades. In the leaf sheath β-diketones are dominant, while alcohols are dominant in the leaf blades (Tulloch, 1973). Epicuticular wax composition varies greatly in wheat cultivars (Uddin and Marshall, 1988). In the current study, non-directional growth was observed on all three wheat lines and even if epicuticular wax content differs, the development of germ tubes seems to have non-directional growth as a common feature on wheat leaf sheaths.

At times, ridges were observed running parallel to the stomata but in other cases prominent ridges were absent. Even when longitudinal ridges were observed, they appeared less pronounced on the leaf sheath in comparison to the ridges reported on seedling leaves (Lewis and Day, 1972). The less pronounced epidermal ridges may therefore also contribute to the non-directional growth of *Pgt* germ tubes seen on flag leaf sheaths.

Quantifying the directional growth of germ tubes from SEM observations remains complex but novel techniques have been developed. The RIMAPS (Rotated Image with Maximum Average Power Spectrum) technique coupled with SEM allowed the orientation of epicuticular wax (Favret and Pidal, 2013) and *Pt* germ tubes on microtopographies (Setten *et al*., 2015) to be quantified. The epicuticular wax of susceptible and resistant wheat cultivars is near identical with a rigid angular distribution pattern (Favret and Pidal, 2013). *Pt* germ tube orientates at a perpendicular angle to a parallel microtopographical surface but the germ tube development is non-directional on a smooth surface (Setten *et al*., 2015). Such approaches may add statistical support to non-directional growth of *Pgt* on wheat leaf sheaths.

Appressorium formation was observed at 12 hpi in the current study, as opposed to 6 hpi as reported by Lennox and Rijkenberg (1989) on wheat seedlings. This discrepancy in appressorium formation may be explained by probability of observing an appressorium, which should decrease at earlier time points. How the non-directional growth of germ tubes may potentially delay the infection process is also worth investigating. Furthermore, it is conceivable that different incubation environments will have a strong influence on the chronological development of infection structures.

In the current study, appressorium formation was observed in 37-07, W1406 and W6979 by 12 hpi, but the APR response does not appear to restrict appressorium development. Likewise, the presence of the APR gene, *Yr39*, made no difference to the germination and formation of appressoria of *Pst* (Coram *et al*., 2008). At 12 hpi these structures formed on cultivars that had either the functional or non-functioning APR allele. However, only external microscopic observation of the epidermis was made. Since pustule formation was observed by 15 dpi in the susceptible cultivar but not in the APR cultivar, the defence response must have inhibited the infection process of *Pst*.

Sub-epidermal observations of infection structures using SEM and leaf fractioning were only done for the susceptible 37-07 line. WGA-FITC staining and fluorescence microscopy allowed the resolution of internal infection structures and were used to study the infection process at 1 dpi and onwards. Both SEM and fluorescence microscopy showed SSV development at 1 dpi but fluorescence microscopy showed HMC development too. Clear HMC development was only seen by 36 hpi using SEM. The discrepancy between SEM and fluorescence microscopy may be based on disadvantages associated with the former. Though SEM delivers better resolution and magnification, infection sites are seldom observed and required meticulous observation. Fluorescence microscopy allowed large sections of the leaf sheath to be rapidly examined, but insufficient destaining affected resolution. These techniques confirmed that HMC are formed from 24-36 hpi. Formation of HMC was observed by 40 hpi by Niks (1986) but as early as 12 hpi by Lennox and Rijkenberg (1989).

Both SEM and fluorescence microscopy showed the SSV forming a septum, indicating the formation of HMC. The formation of a primary IH could not be confirmed and was less pronounced as reported by Lennox and Rijkenberg (1989). The clear distinction between the primary IH and secondary IH is therefore not made from the observations reported in the current study. Tiburzy *et al*. (1990) indicated that the first HMC formed by *Pgt* within the

sub-stomatal chamber penetrates an epidermal cell from beneath, in which it establishes a haustorium. In the current study the formation of the first HMC was observed just within the sub-stomatal chamber. The first HMC may form a haustorium that penetrates the epidermal cell and then acts as a first point for nutrient uptake by the pathogen. Both SEM and fluorescence microscopy showed the formation of IH off this first HMC by 2 dpi, confirming this point as crucial in the initiation of the biotrophic relationship. Cells of the epidermis may well be the first host cells to be penetrated but as the current study did not observe haustorium formation at 2 dpi, the hypothesis cannot be confirmed. In wheat seedlings inoculated with *Pgt*, secondary IH formation with HMC was seen at 1 dpi (Lennox and Rijkenberg, 1989). Both SEM and fluorescence microscopy showed that the IH invariably had a double branched structure and similar secondary IH were noted by Lennox and Rijkenberg (1989).

For fluorescence microscopy of inoculated flag leaf sheaths of wheat, Uvitex 2B staining proved to be an inadequate approach. Previously, Uvitex 2B was effective for the staining of *Pst* colonies on the flag leaves of APR wheat lines (Moldenhauer *et al*., 2006; Moldenhauer *et al*., 2008). The destaining of the flag leaf sheath of the last internode is problematic and the method must be therefore be further optimised if Uvitex 2B is to be used. The Uvitex 2B staining method is advantageous as it can be combined with an autofluorescence test for the HR, and a test for lignin formation. Subsequent testing of Uvitex 2B stained *Pst*-inoculated flag leaves showed the HR and lignin formation associated with colonies on the APR line Kariega (Moldenhauer *et al*., 2006). Microscopic observations of the APR W1406 and W6979 lines showed no cell death or lignin formation at any time point up to 5 dpi. Therefore the HR and lignification may not form part of the early defence mechanism in these two lines. The quantitative trait loci (QTL) present in the APR line Kariega were varyingly linked with lignification upon *Pst* inoculation (Moldenhauer *et al*., 2008). The presence of *QYr.sgi-7D* resulted in lignification in wheat but this did not restrict fungal growth. However, the presence of *QYr.sgi-2B.1* resulted in occasional lignification but the presence of the QTL effectively restricted fungal growth. Therefore, before the absence of the HR and lignification can be confirmed in W1406 and W6979, further testing is required.

If the destaining of flag leaf sheaths can be improved, microscopic techniques with better resolution may be used. Two-photon excitation microscopy was shown to give excellent resolution of infection structures including haustoria (Sørensen *et al*., 2012). Haustoria were seldom observed in the current study and other techniques need to be investigated. In both

susceptible and race-specific resistant lines infection sites with more than one haustorium were only observed from 32 hpi onwards, and greatly increased from 32 to 44 hpi (Skipp *et al*., 1974). The formation of HMC from 24-36 hpi and IH associated with the first HMC in the current study suggests that the biotrophic relationship between the wheat lines and *Pgt* was established at 1 dpi, but conclusively at 2 dpi.

Proliferation of intracellular IH and further HMC formation was seen by 3 dpi using fluorescence microscopy. Furthermore, no quantifiable differences in the infection process of *Pgt* on the three lines were observed in any time point up to 3 dpi. The adult plant infection response observed in W1406 and W6979 (Chapter 3, Table 3.5) can therefore not be related to histological observations at these time points. The potential of a decrease in *Pgt* development could not be excluded and techniques should be improved further on leaf sheaths. However, in the current study, the defence response appears to be induced after the formation of the first HMC. Although HMC and haustorium formation was not quantified, a pre-haustorial defence response coupled with the APR in W1406 and W6979 could not be confirmed.

By 5 dpi the biotrophic relationship becomes even more apparent with many infection structures becoming indistinguishable in the mass of fungal mycelium within the leaf sheath tissue. At this time colony size differed between the two APR lines and the susceptible control line. The mean colony size differed significantly within a large sampling pool. The APR response is therefore clearly restricting *Pgt* growth at 5 dpi. The two APR lines also differed significantly, which corresponds to the phenotypic scores of the infection responses shown in Chapter 3 (Table 3.5). W6979 showed a stronger APR response than W1406, but W1406 could still effectively restrict *Pgt* development.

The inhibition of fungal development at later time points was also seen in other *Puccinia* spp. At 5 dpi adult wheat plants with *Lr34* showed significantly smaller *Pt* colonies as compared to the susceptible control (Rubiales and Niks, 1995). The early infection structures of *Pt* were studied on a susceptible cultivar and two race-specific resistant cultivars (based on *Lr19* and *Lr21* respectively) using SEM (Hu and Rijkenberg, 1998). There were no significant differences between the susceptible and resistant lines in the formation of SSV, primary IH, secondary IH and HMC up to 4 dpi. However, these lines could be differentiated by the number of uredinia formed by 6 dpi, indicating that resistance is expressed only after HMC formation (Hu and Rijkenberg, 1998). Similarly, *Pst*-inoculated doubled haploid lines with

varying numbers of QTL originating from Kariega could only be distinguished from 6 dpi onwards (Moldenhauer *et al*., 2008). Such a defence response at these points, as seen in the current study is clearly post-haustorial in character.

By 10 dpi all three lines exhibited sporulation. On a visual basis the largest amount of sporulation was seen in 37-07, followed by W1406 and W6979. Though colonization was not quantified at 10 dpi it was clear that the APR response that restricted *Pgt* colonization at 5 dpi still delayed development by 10 dpi and is probably responsible for the observed phenotype. Dawson *et al.* (2015) described a method for *Pst* quantification on the non-host seedlings using WGA-FITC staining. Percentage colonization and pustule formation at 14 dpi were correlated with the adult plant infection responses. In the current study, quantification of *Pgt* colony size at 5 dpi directly corresponded with the phenotypic scoring at 14 dpi (Chapter 3; Table 3.5) and quantification of sporulation was not required. Quantification of *Pgt* colony size therefore served as an effective tool to distinguish wheat lines nine days earlier than phenotypic scoring.

The 37-07 line used for cross-sectioning of the last internodes confirmed sporulation by 10 dpi. Fluorescence microscopy proved as effective as the traditionally used Safranin O/Fast Green FCF staining. The maturation of spores in the uredinium may be easily followed in cross section. Uredinium formation may also vary along the length of the leaf sheath and cross-sectioning may assist in elucidating these effects. Cross-sectioning of the last internode may also lead to further analyses beyond microscopic observations. Hacquard *et al*. (2010) impregnated *Melampsora larici-populina* inoculated leaves with paraffin and the fungal tissue associated with pustules was then separated and collected by laser capture microdissection. RNA was extracted from these sections and used for downstream analyses, comparing expression in the sub-epidermal uredinium to the fungal tissue in the infected spongy and palisade mesophyll. Microdissection should therefore be considered for further investigations of the *Pgt* infection process.

The APR response that effectively restricted *Pgt* colonization by 5 dpi could not be elucidated using microscopic techniques. However, microscopic techniques have given insight into the APR response compared to other *Puccinia* spp. A Brazilian wheat cultivar Toropi also exhibits APR against *Pt* and restricts the development of infection structures from appressorium formation onwards (Wesp-Guterres *et al*., 2013) indicating a pre-haustorial defence mechanism. The HR is observed only in 37% of infection sites as late as 5

dpi, indicating that a post-haustorial defence mechanism is also present. The APR cultivar Xingzi 9104 inhibits *Pst* haustorium and secondary IH formation along with the accumulation of H_2O_2 and O_2^-, and associated cell death (Zhang *et al*., 2012), indicating a pre-haustorial defence mechanism. In contrast, the APR response in Guardian to *Pst* and *Pt* is only expressed much later and was shown to affect sporulation but not earlier fungal development (Boyd and Minchin, 2001). Cell death and peroxidase activity were not observed in Guardian (Melichar *et al*., 2008) indicating a post-haustorial defence mechanism. APR may thus include either pre- and post-haustorial defence mechanisms or both, and the response is exceptionally varied.

In Chapter 3 (Table 3.5) the phenotypic scoring of *Pgt*-inoculated leaf sheaths indicated expression of an APR response in W1406 and W6979. Though the mechanism of APR in the W1406 and W6979 lines was not clarified by microscopic observations in the current study, the timing of the response was illustrated. The APR lines effectively inhibited colonisation in the APR lines by 5 dpi and implied a defence response being induced earlier than 5 dpi. The microscopic techniques may allow for better quantification of the *Pgt* infection process on leaf sheaths. Other techniques, such as gene expression analysis, are available to researchers and may also allow for quantification. Histological observation should however remain the initial basis of any investigation of plant-pathogen interactions.

Microscopic observations made during the current study led to two major conclusions. Firstly, the methods used proved successful to describe the infection process of *Pgt* on the flag leaf sheath of the last internode of adult wheat. The microscopic observations therefore gave an insight into the infection process on the tissue type that is used for phenotypic scoring. The study also opens the door for future work on *Pgt*-inoculated flag leaf sheaths. Secondly, the time point whereby the APR W1406 and W6979 lines restricted *Pgt* development was identified. Due to the importance of haustoria in the infection process, the defence response is usually separated into pre-haustorial and post-haustorial defence mechanisms. Microscopic observations confirmed that both the W1406 and W6979 lines exhibit post-haustorial defence mechanisms. Though the defence mechanism could not be elucidated by microscopic observations, colonization was found to be significantly inhibited by the APR lines. The inhibition of *Pgt* colonization on the flag leaf sheaths matches phenotypic scoring and is the result of the APR response in W1406 and W6979.

Chapter 5: Molecular quantification of *Puccinia graminis* f. sp. *tritici* biomass and haustorium formation in adult wheat plants

5.1 Introduction

The symptoms of rusts on wheat (*Triticum aestivum*) are caused by infection of fungal pathogens of the *Puccinia* spp.. *Puccinia triticina* (*Pt*), *P. striiformis* f. sp. *tritici* (*Pst*) and *P. graminis* f. sp. *tritici* (*Pgt*) are the causal agents of wheat leaf rust, stripe rust and stem rust respectively (Dean *et al*., 2012). Wheat host plants may however impede the infection process of these pathogens by inducing a defence response that often becomes visible as a quantifiable resistance phenotype. Variation of the disease symptoms manifested by *Puccinia* spp. infection has been classified by phenotypic scoring conventions. The phenotypic response of wheat may be classified according to Stakman *et al.* (1962) for seedlings and Roelfs *et al.* (1992) for adult plants. Phenotypic scoring may, however, be critiqued for being subjective. More objective techniques to describe the infection phenotype have however been implemented. Conversely, these methods are often destructive to plant tissue, slow and labour-intensive.

Microscopic observation of the infection process is more objective and remains a primary method to describe the plant-pathogen interaction. The infection process of *Pgt* has been thoroughly explained through histological investigations (Leonard and Szabo, 2005). Using microscopic techniques, the infection structures of fungal pathogens can be directly observed, described and quantified. While microscopic observations are less subjective it remains laborious.

Methods beyond phenotypic scoring and microscopy may be used by researchers to quantify the infection processes of fungal plant pathogens. These methods are classified as direct or indirect (Sankaran *et al.,* 2010). Direct methods are based on the exact detection of the pathogen and indirect methods rather on the host plant response when challenged by infection. In the current chapter, focus was given to direct molecular methods that allow infection to be quantified and followed over time, particularly in the Pucciniales.

Quantitative polymerase chain reaction (qPCR) based methods were proposed as crucial tools to detect plant pathogens on hosts (Schena *et al.,* 2004). A method for absolute fungal DNA quantification was used by Jackson *et al.* (2006) to quantify *Puccinia coronata* f. sp. *avenae* infection on inoculated oat seedlings and flag leaves. In that study, fungal genomic markers were analysed by qPCR and DNA quantified from a qPCR standard curve. Absolute fungal DNA quantification by qPCR was also used for *Pst* (Gao *et al.,* 2016). The number of nuclei observed in *Pst* during colonization varied greatly especially in haustorial mother cells

(HMC) and non-sporogenous mycelium (Chong *et al.*, 1992). Voegele and Schmid (2011) argued that due to this difference in the number of nuclei, absolute DNA quantification may not be an accurate method to follow the development of multinucleate fungi on hosts. In the *P. coronata* f. sp. *avenae* - oat interaction a relative qPCR quantification method expressing the marker of Jackson *et al.* (2006) versus the oat *β-actin* gene proved as successful as absolute DNA quantification (Acevedo *et al.*, 2010).

Relative quantification of pathogen versus host genes analysed by qPCR has subsequently been widely implemented. Relative quantification of the rRNA intergenic *ITS* region of both the pathogen and host was used to follow *Melampsora larici-populina* development on poplar cuttings (Rinaldi *et al.*, 2007; Hacquard *et al.*, 2011). The pathogen rRNA intergenic *ITS* region versus the host *ubiquitin* gene was used to follow *Pgt* colonization in barley seedlings (Zurn *et al.*, 2015). DNA quantification can thereby be used to infer fungal biomass and follow its accumulation over the course of infection.

RNA quantification by reverse transcriptase qPCR (RT-qPCR) was proposed as the alternative to absolute DNA quantification (Voegele and Schmid, 2011). *β-tubulin* and two uncharacterised genes (Hahn and Mendgen, 1997) allowed the quantification of *Uromyces fabae* development on broad bean plants (Voegele and Schmid, 2011). Relative quantification of pathogen genes is informative of the infection process of fungal pathogens and was used to infer fungal biomass of *Pst* on wheat (Coram *et al.*, 2008). Relative gene quantification analysis by RT-qPCR has also found application in the analysis of haustorium associated transcripts to infer its formation in *Uromyces appendiculatus* (Puthoff *et al.*, 2008) and *Pst* (Yin *et al.*, 2009).

In addition, direct quantification of fungal proteins by immunological based methods is possible. Monoclonal antibodies for urediniospores were generated for *Pst* (Skottrup *et al.*, 2007) and *Pt* (Gao *et al.*, 2013) and used to detect urediniospores by an enzyme-linked immunosorbent assay (ELISA). Immunological based methods have however not been applied to quantify *Puccinia* spp. infection on hosts.

Another direct quantification method of fungal pathogen infection was described by Ayliffe *et al.* (2013). The method is based on the binding of wheat germ agglutinin fluorescein conjugate (WGA-FITC) to fungal chitin. Fluorescence measurement of bound WGA-FITC allows chitin quantity, and by extension fungal biomass quantification. The method can be applied to any plant-fungal interaction, but cannot distinguish species. Ayliffe *et al.* (2013)

successfully applied the method to wheat inoculated with *Pgt*, *Pst*, *Pt* and *Blumeria graminis* f. sp. *tritici*. The method has been widely implemented to study the various interactions of *Puccinia* spp. with wheat (Moore *et al.*, 2015; Hiebert *et al.*, 2016; Rinaldo *et al.*, 2017) and maize (Sucher *et al.*, 2017).

Numerous methods are therefore available to follow fungal infection, but these have not been extensively applied in *Pgt* infected flag leaf sheaths of adult wheat plants. The flag leaf sheath is used for phenotypic scoring of stem rust on adult wheat plants (Roelfs *et al.*, 1992), and methods to detect and quantify *Pgt* infection must therefore sample leaf sheaths to allow direct comparison to the phenotypic scoring.

The aim of this chapter was to identify the time point whereby *Pgt* colonization is inhibited in adult plant resistant (APR) wheat lines. Particular focus was given to the W1406 and W6979 lines under investigation. To achieve the aim, two objectives were defined. Firstly, to investigate molecular methods to quantify *Pgt* infection on inoculated flag leaf sheaths of adult wheat plants. Secondly, to determine if the implemented methods can follow *Pgt* development over the course of infection and consistently distinguish APR wheat from susceptible wheat.

5.2 Materials and methods

5.2.1 Biological material

For molecular analysis, *Pgt*-inoculated wheat samples were generated as described in Chapter 3. Unless otherwise stated, all wheat lines, entries or cultivars from the seedling and six adult plant trials (Adult trials 1-6) were included. The flag leaf sheath of the last internode was collected as previously described and further processed. The 0 days post inoculation (dpi) sample was collected directly following inoculation. Samples were thereafter taken at 1, 3, 5 and 10 dpi.

5.2.2 Chitin quantification by fluorescence analysis

For chitin quantification, the method of Ayliffe *et al.* (2013) was used with modifications relevant to processing wheat leaf sheaths. Samples were collected for the first two adult plant trials (Adult trials 1 and 2; see Chapter 3) which included the 37-07, W1406 and W6979 lines. The last internode (leaf sheath and stem) was cut into manageable sections and placed directly in 1 M KOH containing 0.05% (v/v) Silwet L-77 (SouthernChem, Sandton, South Africa). The stem assured structural integrity of samples. Samples were autoclaved at 120°C and 1.0 kg/cm^2. Sections were thereafter washed thrice with a 50 mM tris(hydroxymethyl)aminomethane-hydrochloric acid (Tris-HCl) buffer (pH 7.0), the internal stems removed and the flag leaf sheaths further processed. Flag leaf sheath samples were adjusted to a ratio of 200 mg to 1 ml 50 mM Tris-HCl buffer (pH 7.0).

The flag leaf sheaths required maceration by a polytron blender to achieve a uniform suspension. Samples were further processed as described by Ayliffe *et al.* (2013) and chitin probed by WGA-FITC (Sigma-Aldrich, St Louis, Missouri, United States of America). Fluorescence was measured in 200 µl of macerated sample using a Zenyth 3100 multimode detector (Anthos Labtec Instruments, Salzburg, Austria). Fluorescence measurements were done in quadruplicate with excitation at 485 nm and emission at 535 nm with an integration time of 1 sec. An uninoculated flag leaf sheath sample was used to generate a fluorescence versus chitin standard curve. Chitin from crab shells (Sigma-Aldrich, St. Louis, Missouri, United States of America) of 0-100 µg was added to the uninoculated sample and fluorescence measured as before.

5.2.3 Relative gene quantification analysis

5.2.3.1 Total RNA extraction

For RNA sampling, the flag leaf sheath was gently removed and the stem discarded at the moment of collection. Samples were collected for the seedling trial and all adult plant trials (Adult trials 1-6; see Chapter 3). Leaf sheath samples were immediately frozen in liquid nitrogen. Tissue was ground to a fine powder in liquid nitrogen using a mortar and pestle and thereafter stored at -80°C. All experimentation described hereafter relating to RNA was done using nuclease free water. The nuclease free water was prepared by adding 0.1% (v/v) dimethyldicarbonate (DMPC) to deionised water and leaving it overnight at room temperature. The water was finally autoclaved twice to destroy the DMPC.

Total RNA was extracted from 100 mg ground wheat leaf sheath tissue using TRIzol™ reagent (Chomczynski and Sacchi, 1987), keeping to the manufacturer's instructions (Thermo Fisher Scientific, Waltham, Massachusetts, United States of America). After finally dissolving the RNA in 200 µl DMPC-treated water, the concentration was determined using the NanoDrop 2000 Spectrophotometer (Thermo Fisher Scientific). RNA quality was assessed by separating 200 ng RNA on a 1.0% (w/v) denaturing agarose gel (Sambrook *et al.*, 1989) prepared in a 3-(N-morpholino)propanesulfonic acid (MOPS) buffer (20 mM MOPS pH 7.0, 5 mM sodium acetate, 1 mM ethylenediaminetetraacetic acid (EDTA)). The RNA was dissolved in 1x MOPS buffer, 50% (v/v) formamide, 6.5% (v/v) formaldehyde and 50 µg/ml ethidium bromide, denatured at 65°C for 15 min and separated using 1x MOPS running buffer. The gel was observed under ultraviolet light illumination (302 nm) using the GelDoc XR+ system (Bio-Rad, Hercules, California, United States of America).

5.2.3.2 Reverse transcriptase quantitative polymerase chain reaction

The expression of six gene transcripts (four reference transcripts from wheat and two experimental transcripts from *Pgt*) was determined by RT-qPCR. The primer sequences of these transcripts are reported in Table 5.1 and were derived from literature or designed using PrimerQuest (https://eu.idtdna.com/Primerquest/Home/Index). The KAPA SYBR® FAST One-Step RT-qPCR kit (Kapa Biosystems, Wilmington, Massachusetts, United States of America) was used for amplification from 10 ng total RNA as per the manufacturer's instructions. Amplification was done with the C1000 thermal cycler and the CFX96 real-time

attachment (Bio-Rad). The amplification protocol was 42°C for 10 min, 95°C for 3 min, 40 cycles of 95°C for 10 sec and the specific primer annealing temperature (Table 5.2) for 30 sec. Primer specificity was confirmed using a melt curve analysis from 65-95°C at 0.5°C/5 sec. Optimal annealing temperatures were determined from a gradient RT-qPCR and the range of linear amplification determined from a 3:1 total RNA serial dilution, Cq versus log starting quantity standard curve. Each RT-qPCR run included a no template control to confirm primer specificity and absence of DNA or RNA contamination.

The RT-qPCR amplicons were separated on a 2.0% (w/v) agarose gel prepared in 0.5x TAE buffer (20 mM Tris-HCl pH 8.0, 0.5 mM EDTA, 0.28% (v/v) acetic acid) containing 0.5 µg/ml ethidium bromide (Sambrook *et al.,* 1989). The gel was observed under ultraviolet light illumination using the GelDoc XR+ system (Bio-Rad) to confirm the amplification of a single product. Melt curves were further validated by comparison to predicted melt curves as generated by uMELT v 2.0 (https://www.dna.utah.edu/umelt/umelt.html) (Dwight *et al*., 2011).

All gene quantification analyses were done using qBasePlus v 2.6 (Biogazelle, Gent, Belgium) (Hellemans *et al.,* 2007). Reference gene validation was done for four transcripts from wheat: *18S ribosomal RNA* (*Ta-18S*), *β-tubulin* (*Ta-BTUB*), *cell division control protein* (*Ta-CDC*) and *transcription elongation factor 1 alpha* (*Ta-TEF*). All samples from Adult trials 1-6 were included for reference gene validation with the exception of the doubled haploid (DH) entries. Due to differences in wheat samples included in trials, Adult trials 1-4 and Adult trials 5-6 were analysed separately. Cq values were imported into the geNorm module of qBasePlus and the mean expression stability (M) values calculated based on the method of Vandesompele *et al.* (2002). The M value allows a group of selected candidate reference genes to be ranked based on their expression stability in a given experiment. A lower M value corresponds to higher stability of a reference gene. Furthermore, if a gene has an M value greater than 1.0 it is considered unstable and should not be selected as a candidate reference gene.

Relative gene quantification was done for two experimental transcripts from *Pgt*: *β-tubulin* (*Pgt-BTUB*) and a transcript encoding an uncharacterised protein (*PGTG_11318*). The *Pgt-BTUB* transcripts level was expressed relative to the level of *Ta-TEF* transcripts as based on the method of Coram *et al.* (2008). The *PGTG_11318* gene was selected as a putative marker for haustorium formation in the current study. *PGTG_11318* encodes an uncharacterised

protein and the transcript was highly upregulated in *Pgt* infected wheat tissue at 8 dpi compared to urediniospores (Duplessis *et al.,* 2011). Furthermore, *PGTG_11318* had homology to ten expressed sequence tags (EST) in a haustorial library. The *PGTG_11318* transcript level was expressed relative to the level of the *Pgt-BTUB* transcript.

Normalised relative quantity of the two experimental transcripts was calculated in qBasePlus based on the method of Pfaffl (2001). For both reference gene validation and relative gene quantification analyses, replicate variability was set to a maximum limit of 0.5 Cq values and significant outliers were excluded for each set of four technical replicates. The RT-qPCR analyses were done in compliance to the essential Minimum Information for Publication of Quantitative Real-Time PCR Experiments (MIQE) recommendations (Bustin *et al.,* 2009; Taylor *et al.,* 2010).

The mean normalised relative quantities from Adult trials 1-4 for the 37-07, W1406 and W6979 lines were statistically analysed by a Tukey's multiple comparisons test using GraphPad Prism v 6.01. The mean normalised relative quantity of each line was compared to the mean normalised relative quantity of every other line at every time point. The confidence level for the test was set at 99%. The 37-07 line for the seedling and six adult plant trials was used to model the normalised relative quantities over the course of infection. The non-linear regression equations from GraphPad Prism were used to determine the best fit model. The least squares method was used to fit the model and determine the graph equation with a confidence level of 95%. An additional sum of squares *F* test was included to determine if a single model may accurately describe all the independent trials.

5.2.4 Sequence analysis of *PGTG_11318*

5.2.4.1 Sequencing of *PGTG_11318*

Specific amplification of *PGTG_11318* was confirmed by cloning and sequencing the amplicon. RNA samples from the first four biological replicates (Adult trials 1-4) at 3 dpi from the 37-07 line were used for a non-quantitative RT-PCR. The RobusT II RT-PCR kit (Finnzymes, Espoo, Finland) was used per the instruction manual using 10 ng of total RNA. The amplification protocol was identical to the RT-qPCR protocol (see section 5.2.3.2) but excluded a melt curve analysis. A subset of the RT-PCR products were separated on a 2.0% (w/v) agarose gel and observed using the GelDoc XR+ system (Bio-Rad) (see section 5.2.3.2) to confirm the amplification of a single product.

The remaining RT-PCR products were ligated into pGEM®-T Easy vector (Promega, Madison, Wisconsin, United States of America) as per the instruction manual. Plasmids were transformed into the JM109 strain of *Escherichia coli* competent cells. Five µl of the ligation reaction was added to 80 µl competent cells and incubated for 30 min on ice. Thereafter the suspension was heat shocked at 42°C for 45 sec and again incubated for 2 min on ice. To the suspension, 900 µl lysogeny broth (LB) medium consisting of 1.0% (w/v) tryptone, 0.5% (w/v) yeast extract and 1.0% (w/v) NaCl, was added and incubated at 37°C for 90 min. The suspension was thereafter plated on LB plates (LB medium with the addition of 1.5% (w/v) agar, 2.0% (w/v) 5-bromo-4-chloro-3-indolyl-β-D-galactopyranoside (X-gal) and 2.0% (w/v) isopropyl β-D-1-thiogalactopyranoside (IPTG)). Plates were incubated at 37°C for 12 h and subjected to blue-white selection. Selected colonies were inoculated in 5 ml LB medium and incubated at 37°C for 16 h. After centrifugation for 5 min at 12 000g, the pelleted cells were suspended in DMPC treated water and incubated for 5 min at 94°C. The suspension was centrifuged for 5 min at 12 000g and the extracted plasmids was directly used for PCR.

The KAPA Taq PCR kit (Kapa Biosystems) was used per the instruction manual using 10 pmol of the *PGTG_11318* primers. The PCR protocol was 95°C for 3 min, 40 cycles of 95°C for 10 s and 62°C for 30 s. The PCR products were separated on a 2.0% (w/v) agarose gel and observed using the GelDoc XR+ system (Bio-Rad) (see section 5.2.3.2) to confirm the amplification of a single product. The remaining PCR products were purified with the FavorPrep™ Gel/ PCR Purification kit (Favorgen Biotech Corporation, Pingtung City, Taiwan) as per the instruction manual.

Purified PCR products were sequenced using the BigDye® Terminator v. 3.1 Cycle Sequencing Kit (Applied Biosystems, Foster City, California, United States of America) as per the instruction manual. PCR products were sequenced using 3.2 pmol of the forward primer for *PGTG_11318*. The sequencing PCR protocol was 96°C for 1 min, 25 cycles of 96°C for 10 sec, 50°C for 10 sec and 60°C for 4 min. The sequenced PCR products were purified by adding 5 µl 125 mM EDTA and 60 µl 100% ethanol to each tube. Samples were incubated at room temperature for 15 min, and then centrifuged for 15 min at 12 000g. The supernatant was discarded and the pellet washed with 70% (v/v) ethanol. Thereafter each reaction was centrifuged for 5 min at 12 000g, the supernatant discarded and the pellet dried. Eeactions were separated on a 3130xl Genetic Analyzer (Applied Biosystems) with the StdSeq50_POP7 sequencing run module. Sequencing was done at the facilities of the

Department of Microbial, Biochemical and Food Biotechnology (University of the Free State).

5.2.4.2 Computational analysis of *PGTG_11318*

To elucidate the possible function of PGTG_11318, the protein sequence was aligned against the Ensembl database for fungal species (http://fungi.ensembl.org) limited to the Pucciniales. The Ensembl database was also used to search for homologues of PGTG_11318. National Center for Biotechnology Information (NCBI) Blast (https://blast.ncbi.nlm.nih.gov/Blast.cgi) was used to search for ESTs with homology to the *PGTG_11318* coding sequence. Online programmes (Table 5.3) were used to elucidate the putative subcellular localization and function of PGTG_11318 from the protein sequence.

Table 5.1: Primer sequences of analysed transcripts used for reverse transcriptase quantitative polymerase chain reaction. Forward (F) and reverse (R) primer sequences are shown. References for published primer sequences and accession for designed primers are indicated; the Ensembl accession firstly and the National Center for Biotechnology Information accession in brackets.

Transcripts	Primer sequence (5' → 3')	Reference/ Accession number
Ta-18S	F: GTGACGGGTGACGGAGAATT R: GACACTAATGCGCCCGGTAT	Jarošová and Kundu (2010)
Ta-BTUB	F: CAAGGAGGTGGACGAGCAGATG R: GACTTGACGTTGTTGGGGATCCA	Jarošová and Kundu (2010)
Ta-CDC	F: CAAATACGCCATCAGGGAGAACATC R: CGCTGCCGAAACCACGAGAC	Paolacci *et al.* (2009)
Ta-TEF	F: GCCCTCCTTGCTTTCACTCT R: AACGCGCCTTTGAGTACTTG	Giménez *et al.* (2011)
Pgt-BTUB	F: CTCGATCGTGATGAGTGGGA R: AGTGCAATCGAGGGAAAGGA	*PGTG_12204* (XM_003330619.2)
PGTG_11318	F: AACGGTGGCATGAACACTAT R: GAAGACTTGGGAGCCTTGTT	*PGTG_11318* (XM_003329520.2)

Table 5.2: Reverse transcriptase quantitative polymerase chain reaction details for transcripts analysed in the current study. Confirmed amplicon sizes in number of nucleotides (nt) and annealing temperatures are shown. Efficiencies and coefficients of determination (R^2-values) established from Cq versus log starting quantity standard curves for each respective transcript are indicated.

Transcripts	Amplicon size (nt)	Annealing temperature (°C)	Efficiency (%)	Coefficient of determination (R^2-value)
Ta-18S	151	65	110.3	0.999
Ta-BTUB	84	64	103.3	0.999
Ta-CDC	227	64	107.0	0.996
Ta-TEF	91	60	98.6	0.993
Pgt-BTUB	107	56	107.1	0.984
PGTG_11318	120	62	99.7	0.943

Table 5.3: Programmes used for the analysis of the predicted PGTG_11318 protein sequence. Respective references and websites accessed are indicated.

Programme	Reference	Website
EffectorP v 2.0	Sperschneider *et al.* (2018)	http://effectorp.csiro.au
InterPro v 5.25	Jones *et al.* (2014)	https://www.ebi.ac.uk/interpro
Phobius v 1.01	Käll *et al.* (2007)	http://phobius.sbc.su.se
SignalP v 4.1	Petersen *et al.* (2011)	http://www.cbs.dtu.dk/services/SignalP
TargetP v 1.1	Emanuelsson *et al.* (2000)	http://www.cbs.dtu.dk/services/TargetP
TMHMM v 2.0	Krogh *et al.* (2001)	http://www.cbs.dtu.dk/services/TMHMM
WoLF PSORT v 0.2	Horton *et al.* (2007)	https://wolfpsort.hgc.jp

5.3 Results

5.3.1 Chitin quantification by fluorescence analysis

The fluorescence versus chitin standard curve exhibited a linear correlation (R^2 = 0.9178) between fluorescence and amount of added chitin up to a maximum quantity of 100 µg (results not shown). At the maximum amount of chitin, the measured fluorescence units were approximately 700 000. All subsequent fluorescence measurements fell within the linear range of the standard curve.

The binding of WGA-FITC to chitin in fungal tissue and the resulting fluorescence measurements allowed chitin amount to be inferred in *Pgt*-inoculated adult wheat over time. In both Adult trial 1 and 2 the chitin quantity increased from 0 to 10 dpi in the susceptible (37-07) and APR lines (W1406 and W6979) (Figure 5.1). For Adult trial 1 (Figure 5.1 a) the greatest increase of chitin quantity was observed in the time interval from 0 to 1 dpi, but such a rapid increase was not observed for the same time interval in Adult trial 2 (Figure 5.1 b). All samples showed the highest chitin quantity at 10 dpi (approximately 400 000 fluorescence units). The general pattern of chitin accumulation over time corresponded well between the two trials.

In both trials the tested wheat lines could not be distinguished at 0, 1 or 3 dpi. However, at 5 and 10 dpi the three wheat lines could be clearly distinguished with the exception of the 37-07 and W1406 lines at 5 dpi in Adult trial 2 (Figure 5.1 b). In both trials at 5 dpi the 37-07 line had the highest chitin quantity followed by W1406, with W6979 having the lowest. The ranking of the three wheat lines was maintained at 10 dpi, and was identical in both trials.

5.3.2 General reverse transcriptase quantitative polymerase chain reaction results and reference gene validation

Amplification of a single product during RT-qPCR was observed for all six tested primer pairs. Melt curves of amplicons corresponded to predicted melt curves generated by uMELT and showed a single peak for all six amplicons (results not shown). Amplification occurred within the linear range, as confirmed by the standard curve of Cq versus log starting quantity. The R^2-values (Table 5.2) were above the desired value of 0.980 for all transcripts with the exception of *PGTG_11318*. The amplification efficiency values (Table 5.2) were all within the desired range of 90-110% for all transcripts, with the exception of *Ta-18S*.

The M values determined by the geNorm analysis for the four reference transcripts are reported in Figure 5.2 for Adult trails 1-4 and Figure 5.3 for Adult trails 5-6. These two groups of trials were analysed and reported separately based on the wheat lines/cultivars used in the respective trials. The M values for Adult trails 1-4 were all below the 1.0 cut-off for heterogeneous samples. *Ta-TEF* had the lowest M value, followed by *Ta-18S*, *Ta-CDC* and finally *Ta-BTUB*. Three of the four reference transcripts for Adult trails 5-6 fell below the 1.0 cut-off, with *Ta-BTUB* having an M value greater than 1.0. The M values determined for Adult trails 5-6 were much higher than the M values of Adult trail 1-4. *Ta-TEF* again had the lowest M value, but was then followed by *Ta-CDC* and *Ta-18S*, with *Ta-BTUB* having the highest M value.

5.3.3 *Puccinia graminis* f. sp. *tritici β-tubulin* transcript quantification

Quantification of the *Pgt-BTUB* transcript relative to the *Ta-TEF* reference transcript allowed the *Pgt* biomass in inoculated wheat to be inferred. The seedling trial (Figure 5.4), in which all three wheat lines are susceptible to *Pgt*, showed an increase in *Pgt-BTUB* transcripts over the course of infection. The three lines were not distinguishable from 0 to 5 dpi; but at 10 dpi the *Pgt-BTUB* transcript levels indicated that W1406 had higher fungal biomass than 37-07 and W6979, but these two lines could not be distinguished from each other.

The *Pgt* biomass in the flag leaf sheaths of inoculated adult plants are indicated in Figures 5.5-5.9. The analysis of the 37-07, W1406 and W6979 lines of Adult trials 1-4 are indicated in Figure 5.5. These lines were not distinguishable based on *Pgt* biomass from 0 to 3 dpi. However, at 5 dpi differences between lines were distinguishable, but results were variable. Adult trial 4 (Figure 5.5 d) showed *Pgt-BTUB* transcript levels highest in the 37-07 line, followed by W1406 and then W6979. In the other trials, two of the three lines could not be distinguished at 5 dpi. At 10 dpi the *Pgt* biomass greatly increased and the three lines were clearly distinguishable. Consistently, the 37-07 line had the highest *Pgt-BTUB* transcript levels followed by W1406 and finally W6979. The ranking of these APR lines at 10 dpi, based on inferred biomass, was consistent in Adult trial 1-4.

The mean transcript levels of *Pgt-BTUB*, in the four biological replicates over the course of infection are indicated in Figure 5.6. The ranking of wheat lines as 37-07, W1406 and W6979, based on inferred biomass was possible at 5 and 10 dpi. However, a Tukey's multiple comparison test (Table 5.4) indicated that each line could only be statistically distinguished from the other two at 10 dpi.

Adult trials 3 and 4 included four DH entries in the analysis of *Pgt-BTUB* transcripts (Figures 5.7 and 5.8). These entries were DH1.43, DH1.50, DH2.31 and DH2.38, indicated with their respective parental lines. As before, no entries could be distinguished from the parental lines from 0 to 3 dpi. Analyses of the DH1.43 and DH1.50 biomass showed that these entries, along with W1406, were distinguishable from 37-07 at 5 dpi. In Adult trial 3 (Figure 5.7 a), ranking of lines and entries at 10 dpi showed 37-07 had the highest *Pgt-BTUB* transcript levels followed by DH1.50, then W1406 and finally DH1.43. In Adult trial 4 ranking of the lines and entries were: 37-07, DH1.50, DH1.43 and W1406 (Figure 5.7 b).

Biomass analyses of the other two DH entries, DH2.31 and DH2.38, showed that these entries could not be consistently distinguished at 5 dpi (Figure 5.8). In Adult trial 3 (Figure 5.8 a) DH2.31, DH2.38 and the parental lines were distinguishable at 5 dpi, but in Adult trial 4 (Figure 5.8 b) only 37-07 was distinguishable and showed the highest *Pgt-BTUB* transcript levels. At 10 dpi all lines and entries were distinguishable. In Adult trial 3 the ranking of biomass from highest to lowest was: 37-07, DH2.31, DH2.38 and W6979, but the DH entries could not be distinguished from one another. In Adult trial 4 at 10 dpi, the highest *Pgt-BTUB* transcript levels were in 37-07, and were followed by DH2.38, then DH2.31 and finally W6979 as before.

Adult trials 5 and 6 (Figure 5.9) included the Pavon-76, Francolin-1 and Kingbird cultivars along with the 37-07 line. These cultivars were not distinguishable based on *Pgt* biomass from 0 to 3 dpi. At 5 dpi in Adult trial 5 (Figure 5.9 a), these cultivars remained indistinguishable. In Adult trial 6 (Figure 5.9 b) however, 37-07 and Francolin-1 could be clearly distinguished from the other cultivars. At 10 dpi the ranking of cultivars based on *Pgt-BTUB* transcripts was identical for both trials, but some cultivars were not distinguishable. The 37-07 line had the highest *Pgt-BTUB* transcript levels and was distinguishable in both trials at 10 dpi. Pavon-76, Francolin-1 and Kingbird had less *Pgt-BTUB* transcripts. In Adult trial 5 (Figure 5.9 a), Pavon-76 and Francolin-1 could not be distinguished at 10 dpi but Kingbird was distinguishable and had the lowest *Pgt* biomass. However, in Adult trial 6 (Figure 5.9 b) Pavon-76, Francolin-1 and Kingbird could not be distinguished from one another.

The change in normalised relative quantities of *Pgt-BTUB* in the 37-07 line in the seedling and all adult wheat trials was used to fit a non-linear regression equation. Due to rapid increase of *Pgt-BTUB* transcripts from 5 to 10 dpi, an exponential growth equation was

selected (Figure 5.10). A sum of squares *F*-test indicated that a single equation could not accurately describe all the independent trials simultaneously. Independent trials were separately fitted to an exponential growth equation using the least squares method with a confidence level of 95%. All trials fitted this model except the seedling trial and Adult trial 5, where the fit was ambiguous and outside the predetermined confidence level. The R^2-values of the fitted non-linear regression equations ranged from 0.9902 to 0.9998.

5.3.4 Sequence analysis of *PGTG_11318*

PGTG_11318 encodes a single transcript with no known splice variants and an uncharacterised protein. The NCBI GenBank accession is XM_003329520.2. The *PGTG_11318* product had homology to a number of sequences within the Ensembl database. Hits were found in *Pgt*, *Pst*, *Pt* and *P. hordei* and all were uncharacterised proteins. No hits were found in *M. larici-populina*. *PGTG_11318* had five paralogues in *Pgt* (*PGTG_11320*, *PGTG_11179*, *PGTG_00415*, *PGTG_11182* and *PGTG_11180)*. *PGTG_11318* and had three orthologues in related species (*VP01_3521g1* and *VP01_1186g7* in *P. sorghi* and *maker-PST130_11738-snap-gene-0.3-mRNA-1* in *Pst*). *PGTG_11318* had high homology with two ESTs from *Pgt* namely CV191731 (E value = 0.0) and CV191667 (E value = $9e^{-114}$), most likely originating from the same transcript.

EffectorP analysis predicted that PGTG_11318 is not an effector protein (*p*-value = 0.623). SignalP results (maximum raw cleavage site score = 0.197, maximum signal peptide score = 0.187, maximum combined cleavage site score = 0.274) indicated PGTG_11318 as a non-secreted protein. A signal domain, transmembrane helix and extracellular domain were predicted by TMHMM and confirmed by Phobius, with good posterior probabilities across the length of the protein sequence. WoLF PSORT predicted PGTG_11318 to be an extracellular protein, but TargetP results indicated the protein to be localised in the mitochondrion (neural network score = 0.863). The mitochondrion was ranked second most probable subcellular localization predicted by WoLF PSORT. InterPro could not identify protein family membership, domains or repeats. However, regions on the protein corresponded to signal peptide, transmembrane, non-cytoplasmic and intrinsically disordered protein sequences.

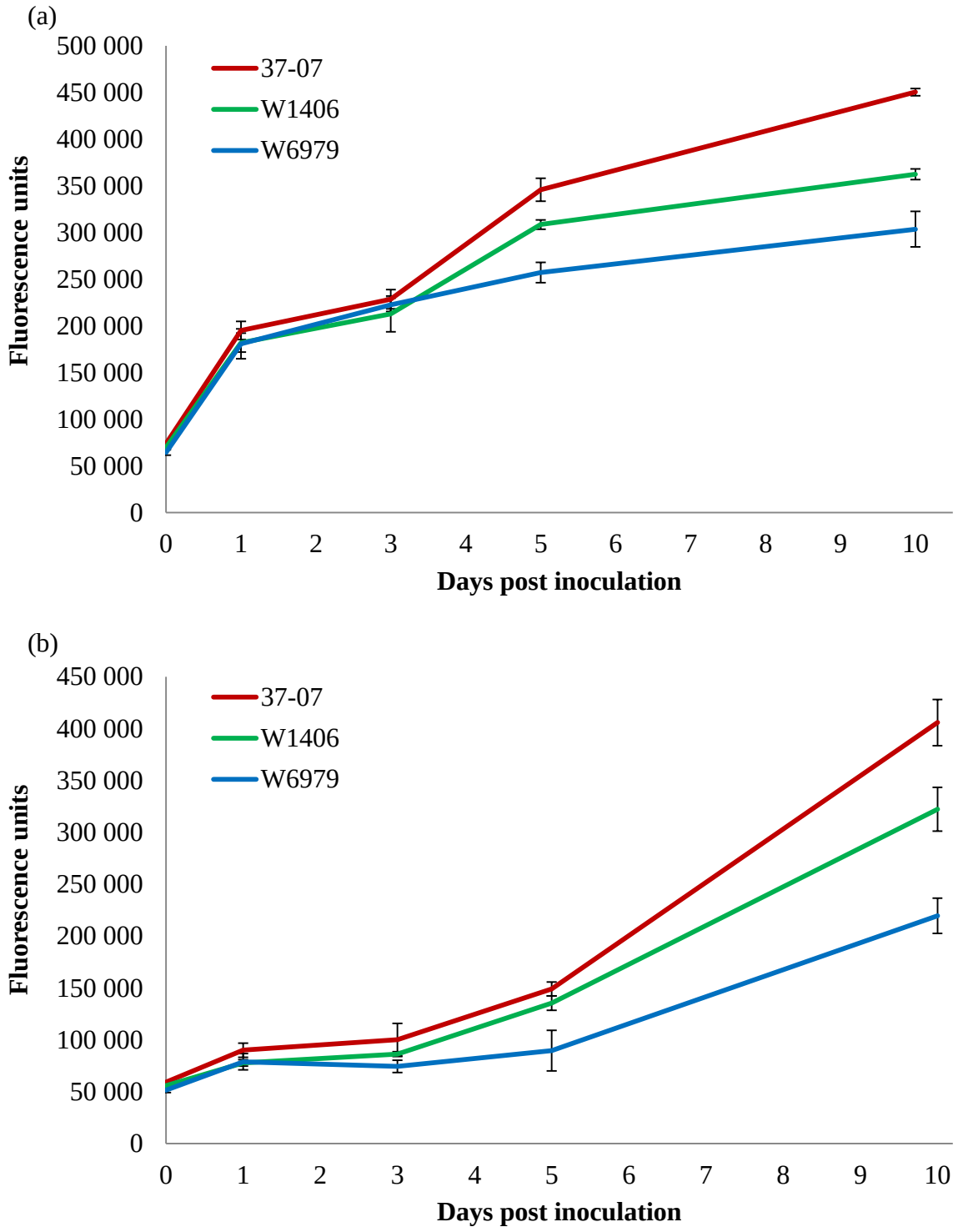

Figure 5.1: Quantification of chitin in *Puccinia graminis* f. sp. *tritici*-inoculated wheat lines tested in Adult trial 1 (a) and Adult trial 2 (b). Mean fluorescence units are plotted with standard error (n = 4) at the indicated days post inoculation. Fluorescence was measured after the binding of wheat germ agglutinin fluorescein isothiocyanate conjugate to *Puccinia graminis* f. sp. *tritici* on inoculated wheat.

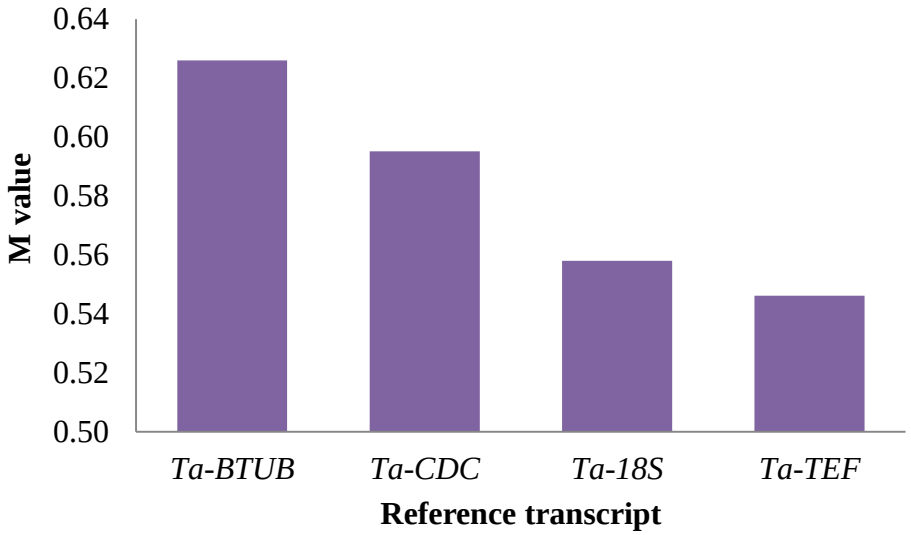

Figure 5.2: Mean expression stability (M value) of four reference genes in *Puccinia graminis* f. sp. *tritici*-inoculated wheat lines tested in Adult trials 1-4. The expression of the *18S ribosomal RNA* (*Ta-18S*), *β-tubulin* (*Ta-BTUB*), *cell division control protein* (*Ta-CDC*) and *transcription elongation factor 1 alpha* (*Ta-TEF*) transcripts were analysed by the geNorm package of qBasePlus.

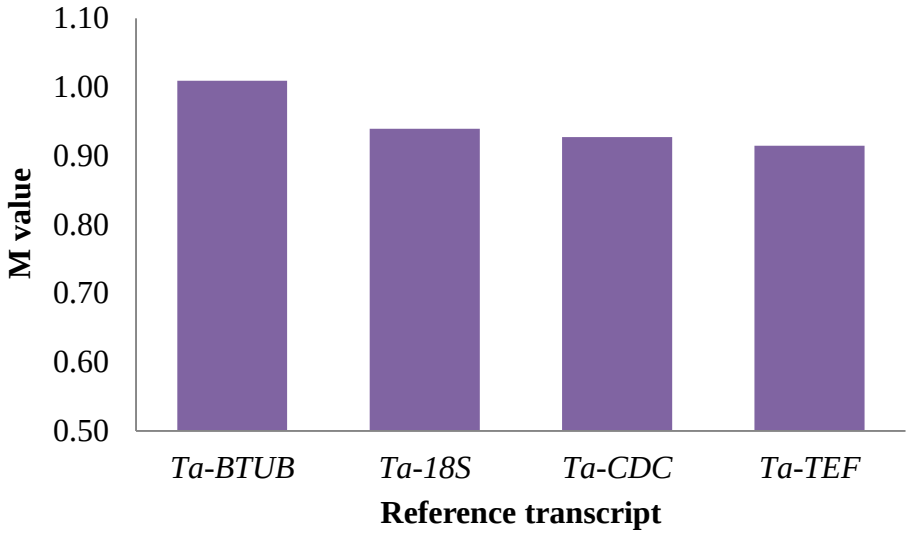

Figure 5.3: Mean expression stability (M value) of four reference genes in *Puccinia graminis* f. sp. *tritici*-inoculated wheat lines tested in Adult trials 5 and 6. The expression of the *18S ribosomal RNA* (*Ta-18S*), *β-tubulin* (*Ta-BTUB*), *cell division control protein* (*Ta-CDC*) and *transcription elongation factor 1 alpha* (*Ta-TEF*) transcripts were analysed by the geNorm package of qBasePlus.

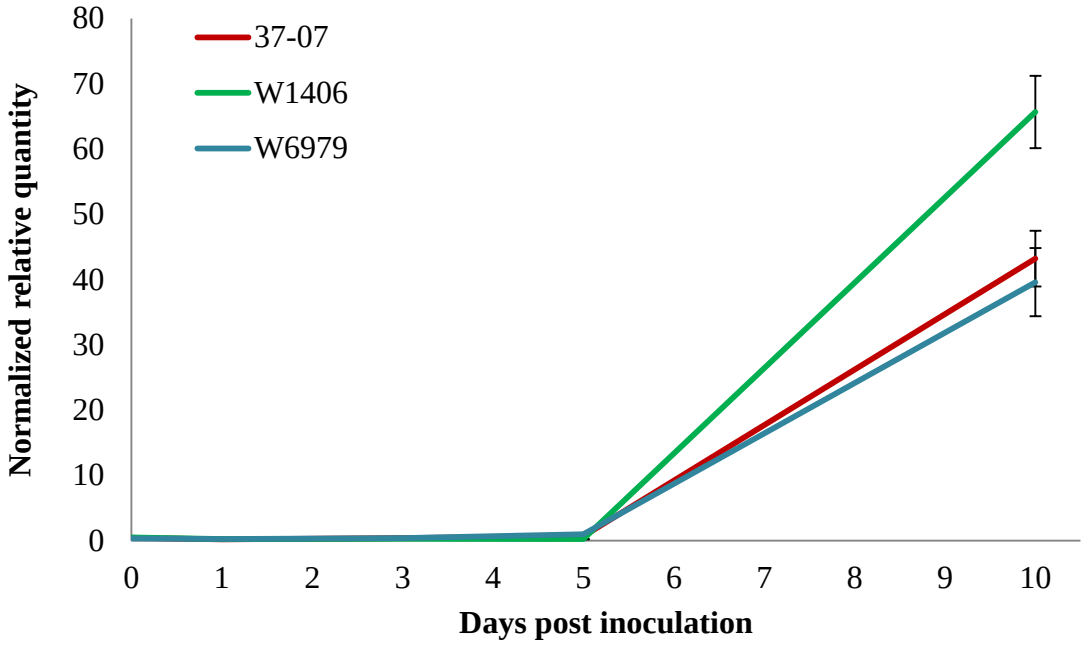

Figure 5.4: Normalised relative quantity of *Puccinia graminis* f. sp. *tritici β-tubulin* transcripts in inoculated wheat lines tested in the seedling trial. Points show normalised relative quantity mean with standard error (n = 4) at indicated days post inoculation. *Puccinia graminis* f. sp. *tritici β-tubulin* transcripts were expressed relative to *Triticum aestivum transcription elongation factor 1 alpha* transcripts and Cq values were determined by reverse transcriptase quantitative polymerase chain reaction.

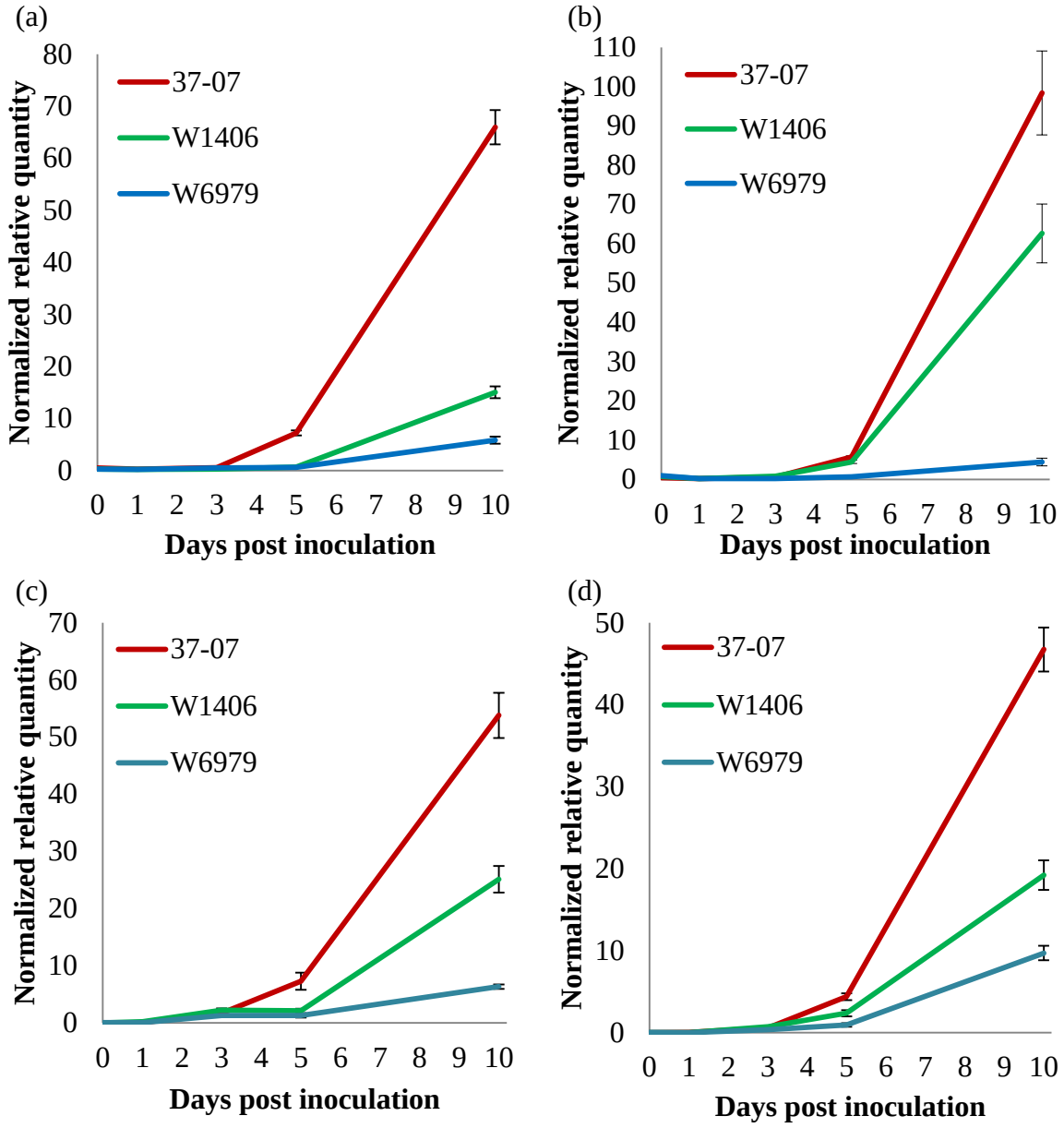

Figure 5.5: Normalised relative quantity of *Puccinia graminis* f. sp. *tritici β-tubulin* transcripts in inoculated wheat lines tested in four biological replicates. Respective figures are shown for Adult trial 1 (a), Adult trial 2 (b), Adult trial 3 (c) and Adult trial 4 (d). Points show normalised relative quantity mean with standard error (n = 4) at indicated days post inoculation. Cq values were determined by reverse transcriptase quantitative polymerase chain reaction and *Puccinia graminis* f. sp. *tritici β-tubulin* transcripts were expressed relative to *Triticum aestivum transcription elongation factor 1 alpha* transcripts.

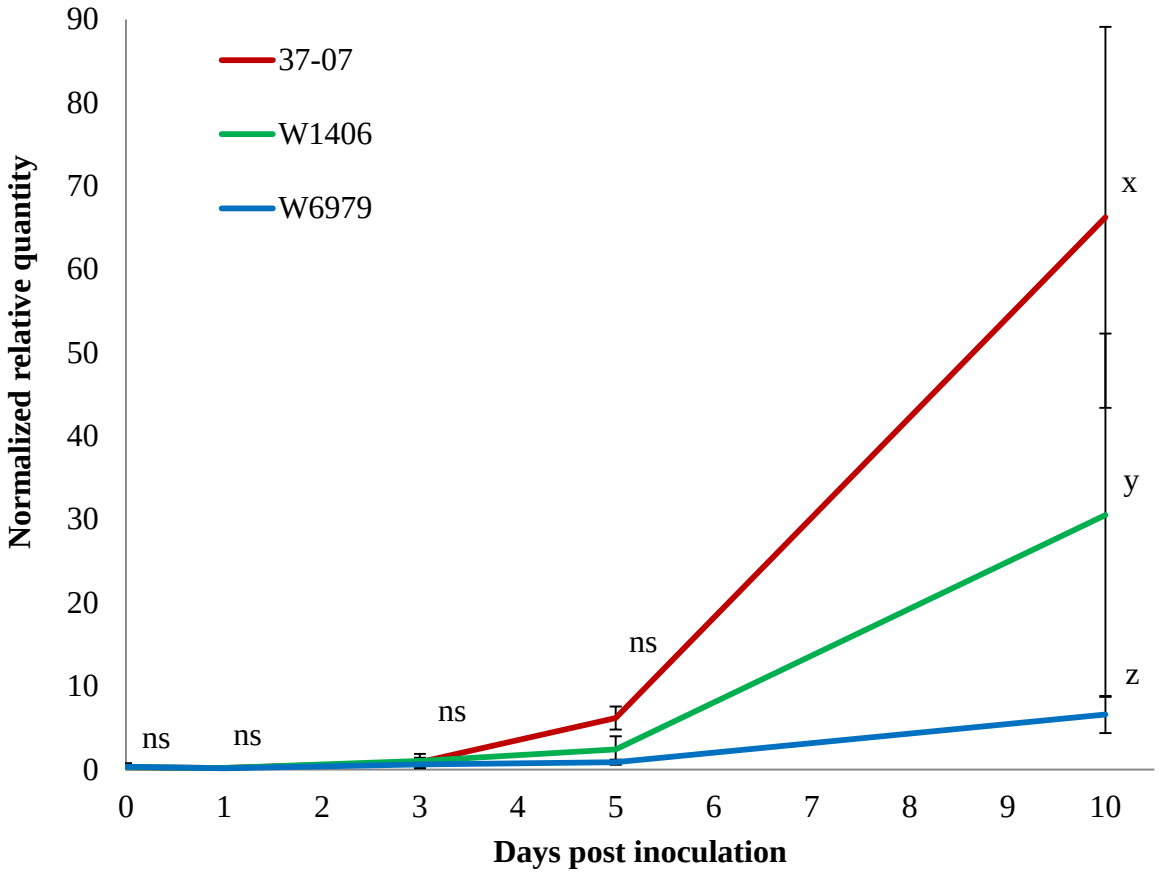

Figure 5.6: Mean normalised relative quantity of *Puccinia graminis* f. sp. *tritici β-tubulin* transcripts in inoculated wheat lines tested for four biological replicates (Adult trials 1-4). Points show normalised relative quantity mean with standard error (n = 4 trials) at indicated days post inoculation. Different alphabetic symbols indicate samples with significant differences for a time point as confirmed by a Tukey's multiple comparison test (see Table 5.4). Time points with no significant differences for all sample comparisons were indicated as non-significant (ns).

Table 5.4: Tukey's multiple comparison test results for mean normalised relative quantity of *Puccinia graminis* f. sp. *tritici β-tubulin* transcripts in *Puccinia graminis* f. sp. *tritici*-inoculated wheat. Means were calculated from four biological replicates (Adult trials 1-4). The mean normalised relative quantity of 37-07, W1406 and W6979 was compared to every other line, at every time point. Confidence level for the test was 99%. Sample comparisons are indicated as significant (*) or non-significant (ns).

Sample comparisons	Mean difference	Confidence interval of difference	Significant
0 dpi			
37-07 vs W1406	-0.02288	-17.82 to 17.77	ns
37-07 vs W6979	-0.09386	-17.89 to 17.70	ns
W1406 vs W6979	-0.07098	-17.87 to 17.72	ns
1 dpi			
37-07 vs W1406	-0.006238	-17.80 to 17.79	ns
37-07 vs W6979	0.04084	-17.75 to 17.84	ns
W1406 vs W6979	0.04708	-17.75 to 17.84	ns
3 dpi			
37-07 vs W1406	-0.1732	-17.97 to 17.62	ns
37-07 vs W6979	0.2433	-17.55 to 18.04	ns
W1406 vs W6979	0.4165	-17.38 to 18.21	ns
5 dpi			
37-07 vs W1406	3.761	-14.03 to 21.56	ns
37-07 vs W6979	5.298	-12.50 to 23.09	ns
W1406 vs W6979	1.537	-16.26 to 19.33	ns
10 dpi			
37-07 vs W1406	35.72	17.93 to 53.52	*
37-07 vs W6979	59.65	41.85 to 77.44	*
W1406 vs W6979	23.92	6.128 to 41.72	*

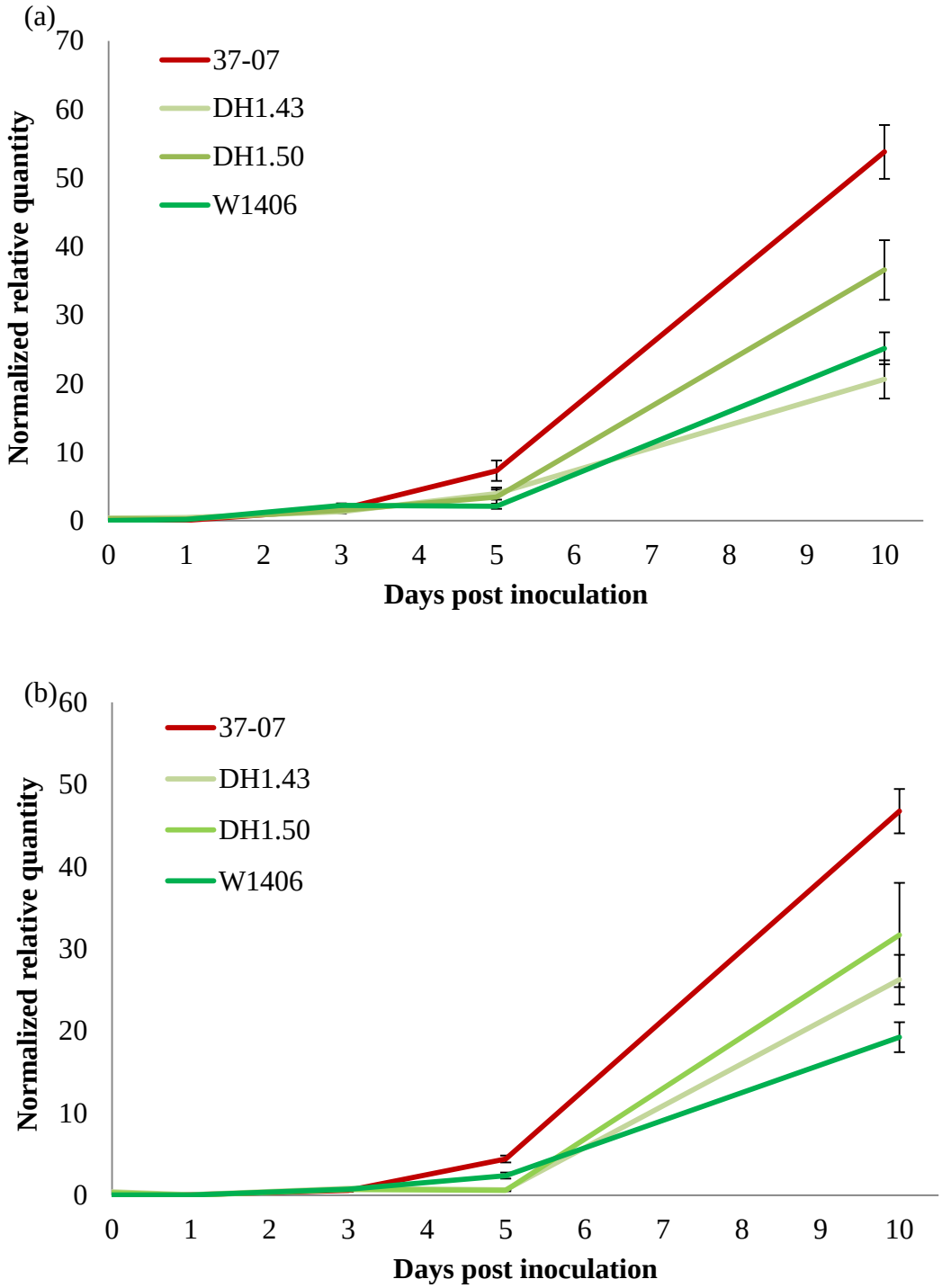

Figure 5.7: Normalised relative quantity of *Puccinia graminis* f. sp. *tritici β-tubulin* transcripts in inoculated doubled haploid wheat lines from the W1406 x 37-07 cross tested in Adult trial 3 (a) and Adult trial 4 (b). Points show normalised relative quantity mean with standard error (n = 4) at indicated days post inoculation. *Puccinia graminis* f. sp. *tritici β-tubulin* transcripts were expressed relative to *Triticum aestivum transcription elongation factor 1 alpha* transcripts and Cq values were determined by reverse transcriptase quantitative polymerase chain reaction.

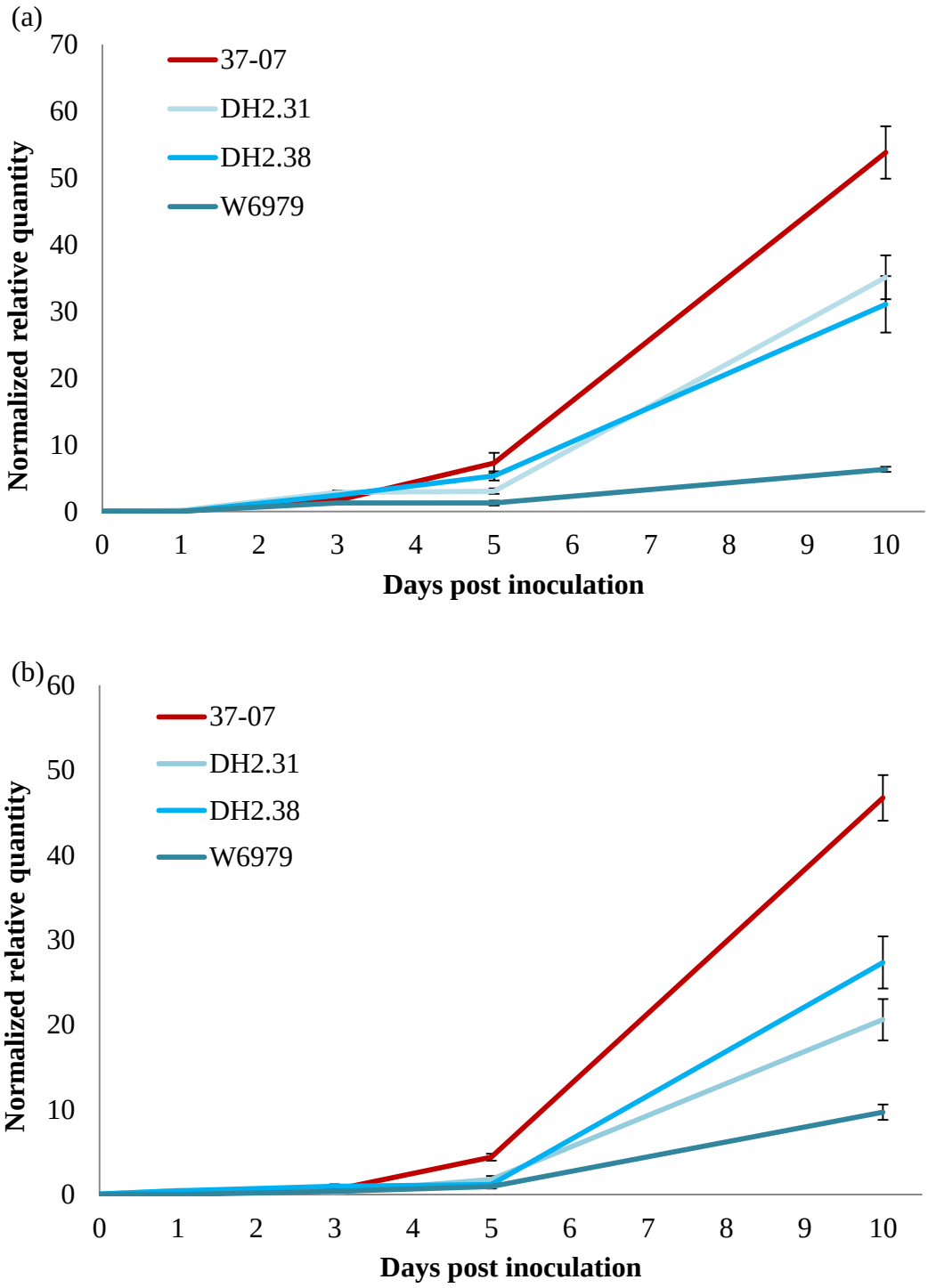

Figure 5.8: Normalised relative quantity of *Puccinia graminis* f. sp. *tritici β-tubulin* transcripts in inoculated doubled haploid wheat lines from the W6979 x 37-07 cross tested in Adult trial 3 (a) and Adult trial 4 (b). Points show normalised relative quantity mean with standard error (n = 4) at indicated days post inoculation. *Puccinia graminis* f. sp. *tritici β-tubulin* transcripts were expressed relative to *Triticum aestivum transcription elongation factor 1 alpha* transcripts and Cq values were determined by reverse transcriptase quantitative polymerase chain reaction.

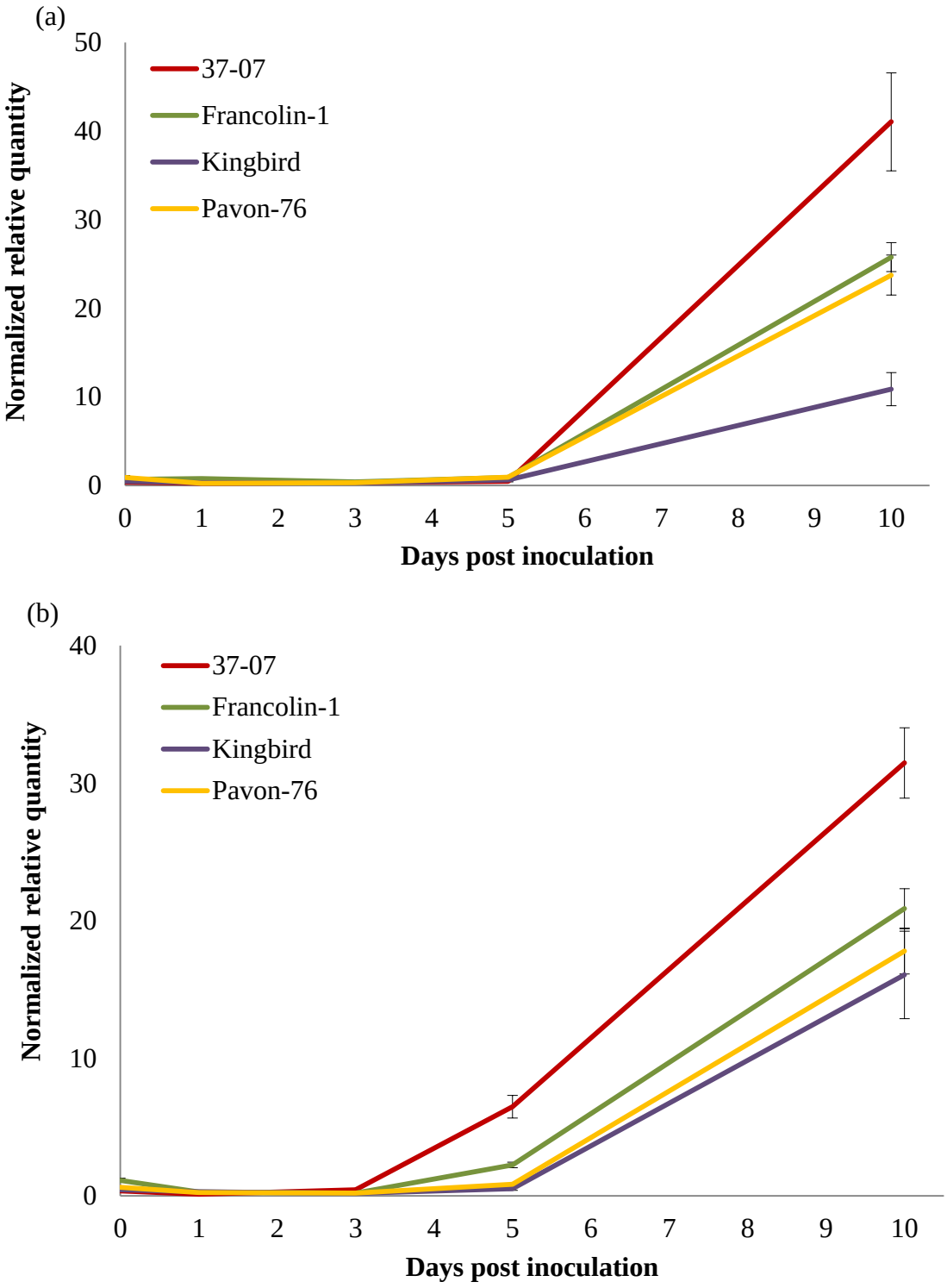

Figure 5.9: Normalised relative quantity of *Puccinia graminis* f. sp. *tritici β-tubulin* transcripts in inoculated wheat lines tested in Adult trial 5 (a) and Adult trial 6 (b). Points show normalised relative quantity mean with standard error (n = 4) at indicated days post inoculation. *Puccinia graminis* f. sp. *tritici β-tubulin* transcripts were expressed relative to *Triticum aestivum transcription elongation factor 1 alpha* transcripts and Cq values were determined by reverse transcriptase quantitative polymerase chain reaction.

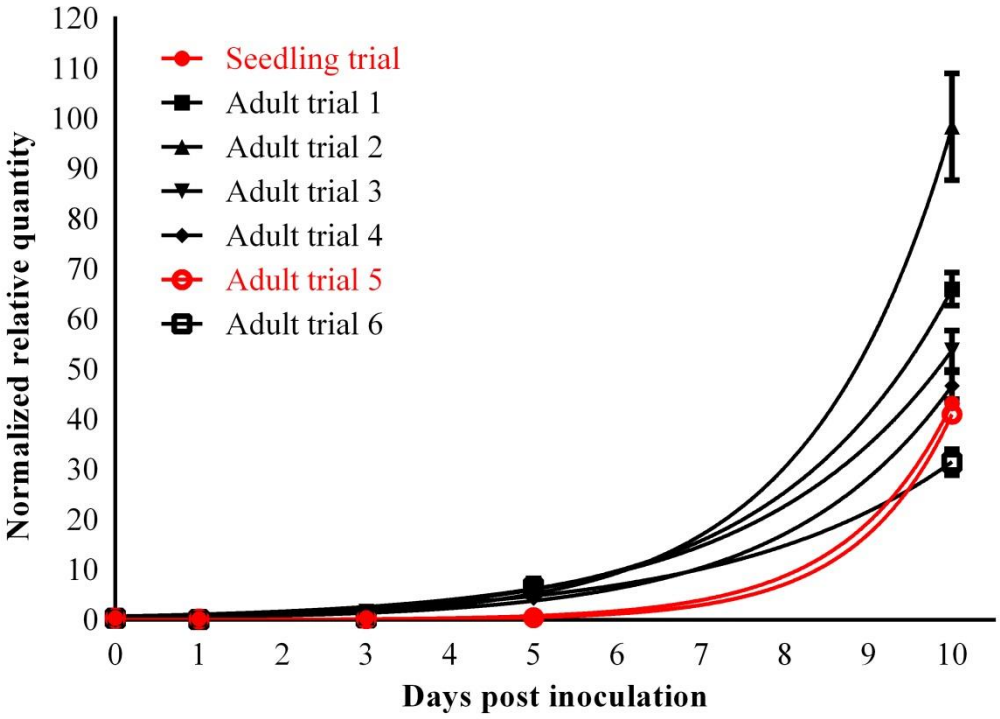

Figure 5.10: Non-linear regression graphs of normalised relative quantity of *Puccinia graminis* f. sp. *tritici β-tubulin* transcripts in the inoculated 37-07 wheat line. Points show normalised relative quantity mean with standard error (n = 4) at indicated days post inoculation. The seedling trial and six adult plant trials (Adult trials 1-6) were modelled separately using an exponential growth equation (confidence level = 95%). Trials indicated in red had an ambiguous fit to the selected model.

5.3.5 *PGTG_11318* transcript quantification

The quantification of the *PGTG_11318* transcript relative to *Pgt-BTUB* allowed haustorium formation in *Pgt*-inoculated wheat, over time, to be inferred. The *PGTG_11318* transcript levels in the seedling trial (Figure 5.11) showed an increase from 0 to 5 dpi, but a decrease from 5 to 10 dpi. The 37-07, W1406 and W6979 lines were not distinguishable from 0 to 3 dpi. The *PGTG_11318* transcript levels at 5 dpi were highest in the W1406 line, thereafter W6979 and finally 37-07. At 10 dpi the tested lines could not be distinguished.

The transcript levels of *PGTG_11318* in the flag leaf sheaths of adult wheat plants are indicated in Figures 5.12-5.16. The analysis of the 37-07, W1406 and W6979 lines of Adult trials 1-4 are indicated in Figure 5.12. The relative quantity of transcripts invariably increased over the course of infection up to 5 dpi. Lines were not distinguishable based on *PGTG_11318* transcript levels from at 0 or 1 dpi, and in some trials not at 3 dpi. However, at 5 dpi lines were clearly distinguishable in three of the four trials. Consistently the level of the *PGTG_11318* transcripts was highest in the 37-07 line, lower in W1406, and lowest in W6979. The only exception was Adult trial 3 (Figure 5.12 c) where W1406 and W6979 were not distinguishable at 5 dpi. *PGTG_11318* transcripts decreased from the 5 to 10 dpi, and the ranking of *PGTG_11318* transcript levels varied between the first four trials at 10 dpi.

In Figure 5.13 the mean transcript levels of *PGTG_11318* of the four biological replicates over the course of infection are indicated. At 5 dpi, the wheat lines are ranked as 37-07, W1406 and W6979, but different rankings were observed at 3 and 10 dpi. Furthermore, a Tukey's multiple comparison test (Table 5.5) indicated the 37-07 line could only be statistically distinguished from the other two lines at 5 dpi, while W1406 and W6979 could not be statistically distinguished from each other at that time point. At all other time points the lines could not be statistically distinguished

The transcript levels of *PGTG_11318* for the DH entries of Adult trials 3 and 4 are indicated in Figures 5.14 and 5.15. The quantity of transcripts increased from 0 to 5 dpi and decreased from 5 to 10 dpi. In Adult trial 3 (Figure 5.14 a) DH1.43, DH1.50 and W1406 were not distinguishable at any time point, but had lower transcript levels than 37-07, with the exception of 10 dpi. Similarly, in Adult trial 4 (Figure 5.14 b) DH1.43, DH1.50 and W1406 were not distinguishable at 3 or 5 dpi, but the *PGTG_11318* transcripts were less than in the 37-07 line at both time points.

The relative quantification analysis of *PGTG_11318* in the DH2.31 and DH2.38 entries from Adult trial 3 and 4 showed no point where these entries and the parental lines were distinguishable, with the exception of 5 dpi. In Adult trial 3 (Figure 5.15 a) 37-07, DH2.31 and DH2.38 could not be distinguished at 5 dpi, but the transcript levels in W6979 were lower and distinguishable. At 5 dpi in Adult trial 4 (Figure 5.15 b) 37-07, DH2.31 and DH2.38 were not distinguishable. However, W6979 again had less transcripts and was distinguishable. Interestingly, the DH2.38 entry had the highest transcript levels of *PGTG_11318* at 3 dpi, but it could not be distinguished from 37-07 in Adult trial 4 at that time point.

The transcript levels of *PGTG_11318* for Pavon-76, Francolin-1 and Kingbird along with the 37-07 line from Adult trials 5 and 6 are indicated in Figure 5.16. As with the other trials, the *PGTG_11318* transcripts increased from 0 to 5 dpi and decreased from 5 to 10 dpi. The results of Adult trial 5 and 6 were only comparable in some regards, including the general pattern of transcript quantification, and the 37-07 line consistently showing the highest transcript levels at 5 dpi. In Adult trials 5 (Figure 5.16 a) cultivars could be clearly distinguished at 5 dpi. However, in Adult trial 6 (Figure 5.16 b) cultivars were distinguishable as early as 3 dpi. The ranking of cultivars based on *PGTG_11318* transcript levels also differed. Consistently, at 5 dpi, the 37-07 line showed the highest transcript levels of *PGTG_11318* followed by Pavon-76. In Adult trial 5 Francolin-1 had more transcripts than Kingbird, while in Adult trial 6 the ranking was reversed, but the two cultivars could not be distinguished at 5 dpi.

The change in normalised relative quantities of *PGTG_11318* in the 37-07 line in all trials was also used to fit a non-linear regression equation. Due to the increase of *PGTG_11318* transcripts from 0 to 5 dpi, but a decrease thereafter, a Gaussian equation was selected (Figure 5.17). A sum of squares *F*-test indicated that a single equation could not accurately describe all the independent trials simultaneously. Independent trials were separately fitted to a Gaussian equation using the least squares method with a confidence level of 95%. All trials were found to fit this model and the R^2-values ranged from 0.9857 to 0.9996.

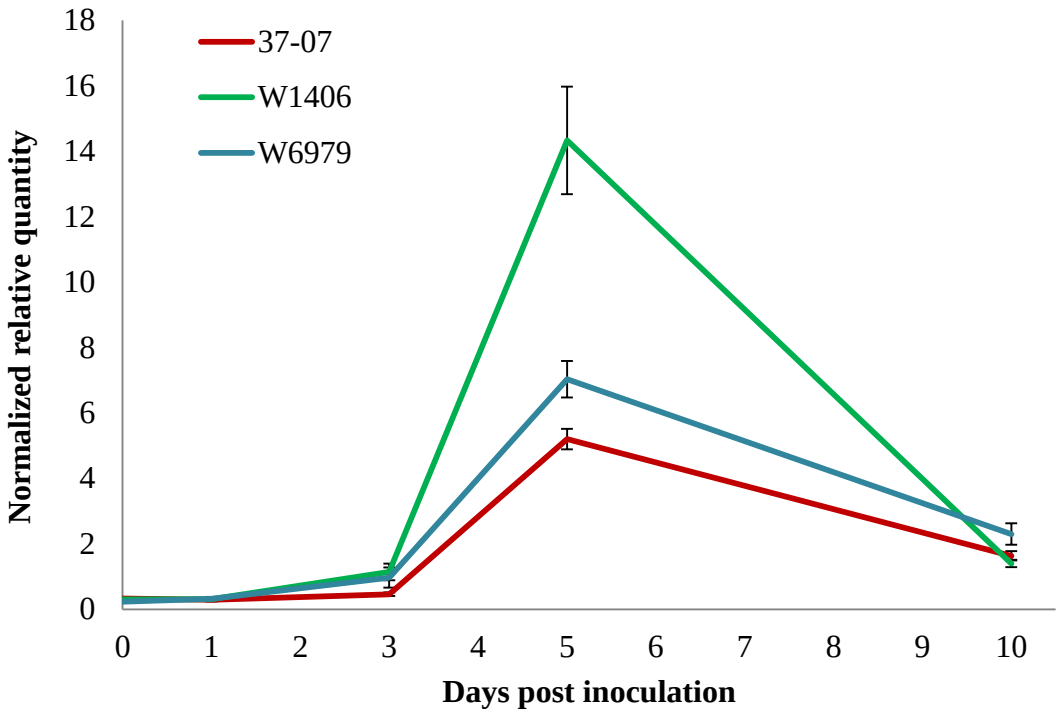

Figure 5.11: Normalised relative quantity of *PGTG_11318* transcripts in inoculated wheat lines tested in the seedling trial. Points show normalised relative quantity mean with standard error (n = 4) at indicated days post inoculation. *PGTG_11318* transcripts were expressed relative to *Pgt-BTUB* transcripts and Cq values were determined by reverse transcriptase quantitative polymerase chain reaction.

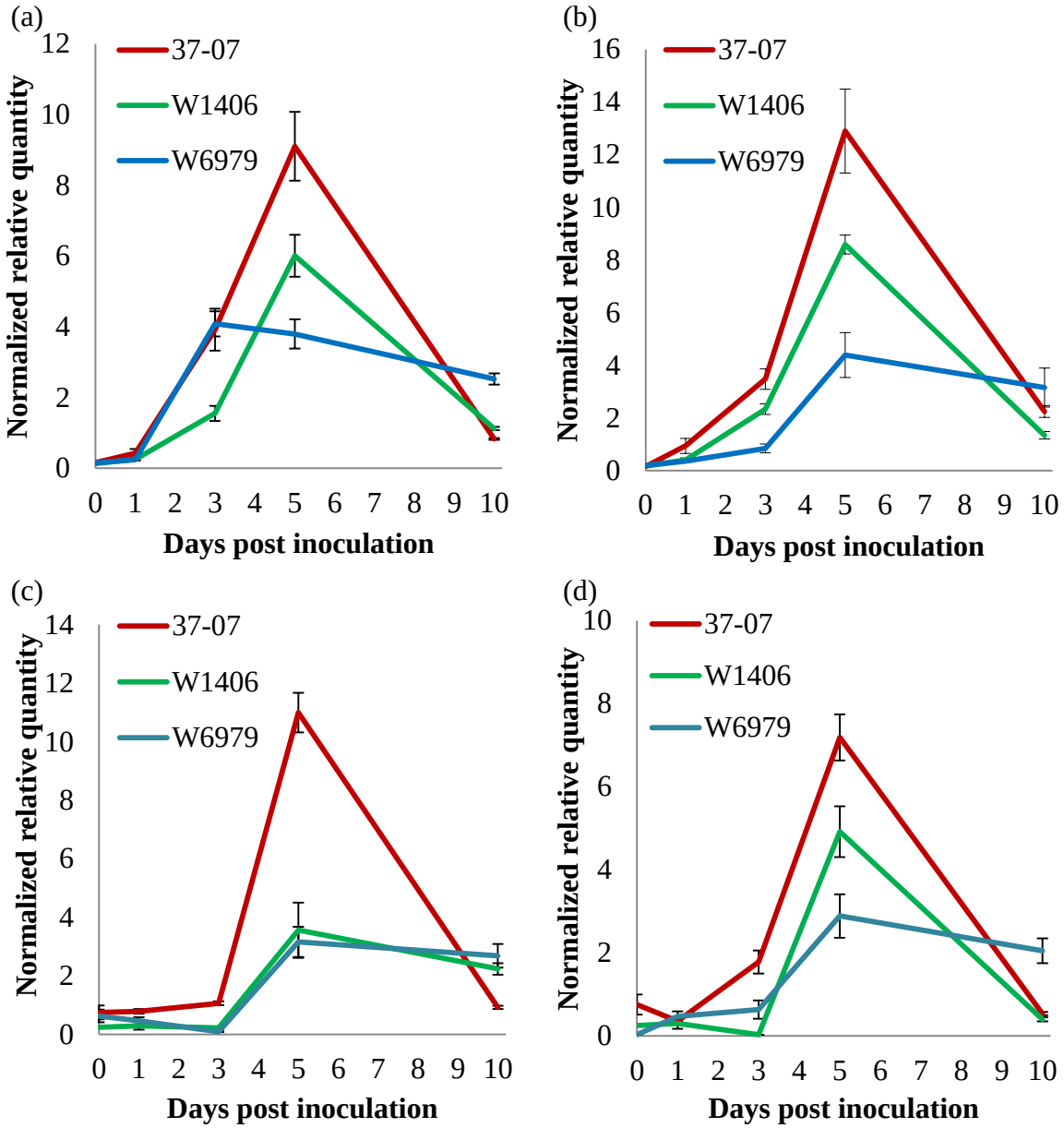

Figure 5.12: Normalised relative quantity of *PGTG_11318* transcripts in inoculated wheat lines tested in four biological replicates. Respective figures are shown for Adult trial 1 (a), Adult trial 2 (b), Adult trial 3 (c) and Adult trial 4 (d). Points show normalised relative quantity mean with standard error (n = 4) at indicated days post inoculation. Cq values were determined by reverse transcriptase quantitative polymerase chain reaction and *PGTG_11318* transcripts were expressed relative to *Puccinia graminis* f. sp. *tritici β-tubulin* transcripts.

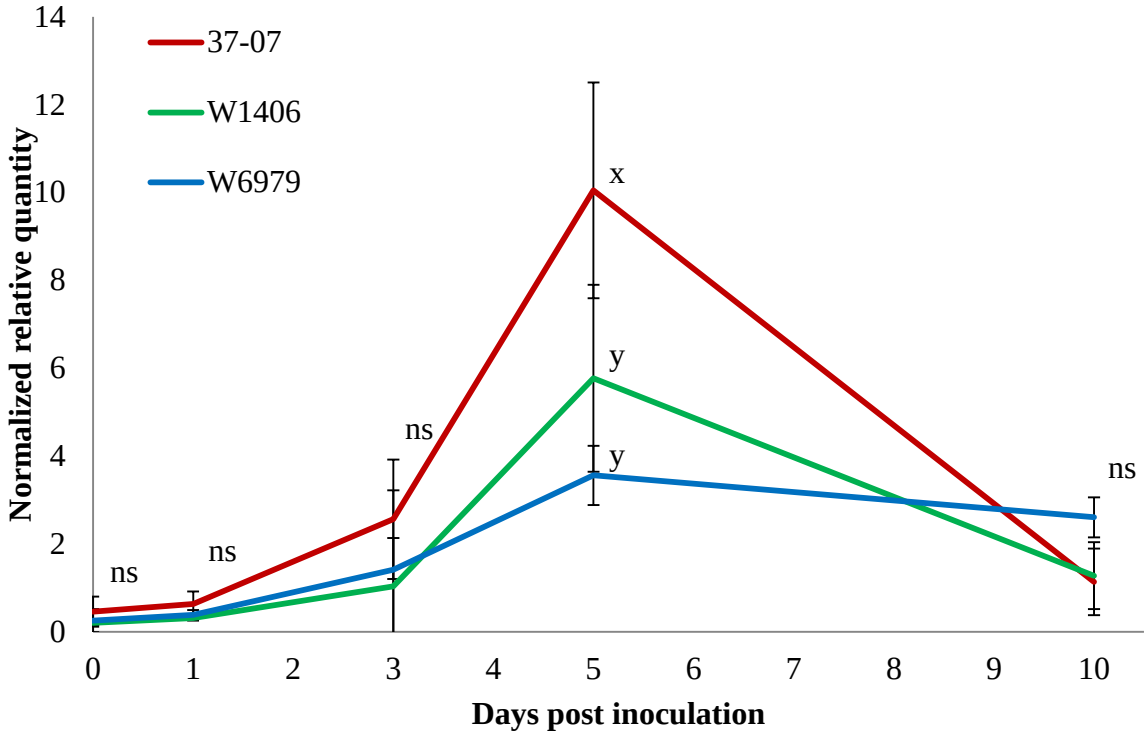

Figure 5.13: Mean normalised relative quantity of *PGTG_11318* transcripts in inoculated wheat lines tested for four biological replicates (Adult trials 1-4). Points show normalised relative quantity mean with standard error (n = 4 trials) at indicated days post inoculation. Corresponding alphabetic symbols indicate samples with no significant differences for a time point as confirmed by a Tukey's multiple comparison test (see Table 5.5). Time points with no significant differences for all sample comparisons were indicated as non-significant (ns).

Table 5.5: Tukey's multiple comparison test results for mean normalised relative quantity of *PGTG_11318* transcripts in *Puccinia graminis* f. sp. *tritici*-inoculated wheat. Means were calculated from four biological replicates (Adult trials 1-4). The mean normalised relative quantity of 37-07, W1406 and W6979 was compared to every other line, at every time point. Confidence level for the test was 99%. Sample comparisons are indicated as significant (*) or non-significant (ns).

Sample comparisons	Mean difference	Confidence interval of difference	Significant
0 dpi			
37-07 vs W1406	0.2545	-2.187 to 2.696	ns
37-07 vs W6979	0.2055	-2.236 to 2.647	ns
W1406 vs W6979	-0.04894	-2.491 to 2.393	ns
1 dpi			
37-07 vs W1406	0.3177	-2.124 to 2.759	ns
37-07 vs W6979	0.2434	-2.198 to 2.685	ns
W1406 vs W6979	-0.07424	-2.516 to 2.367	ns
3 dpi			
37-07 vs W1406	1.527	-0.9145 to 3.969	ns
37-07 vs W6979	1.146	-1.295 to 3.588	ns
W1406 vs W6979	-0.3806	-2.822 to 2.061	ns
5 dpi			
37-07 vs W1406	4.276	1.835 to 6.718	*
37-07 vs W6979	6.488	4.046 to 8.930	*
W1406 vs W6979	2.212	-0.2301 to 4.653	ns
10 dpi			
37-07 vs W1406	-0.1417	-2.583 to 2.300	ns
37-07 vs W6979	-1.470	-3.911 to 0.9718	ns
W1406 vs W6979	-1.328	-3.770 to 1.114	ns

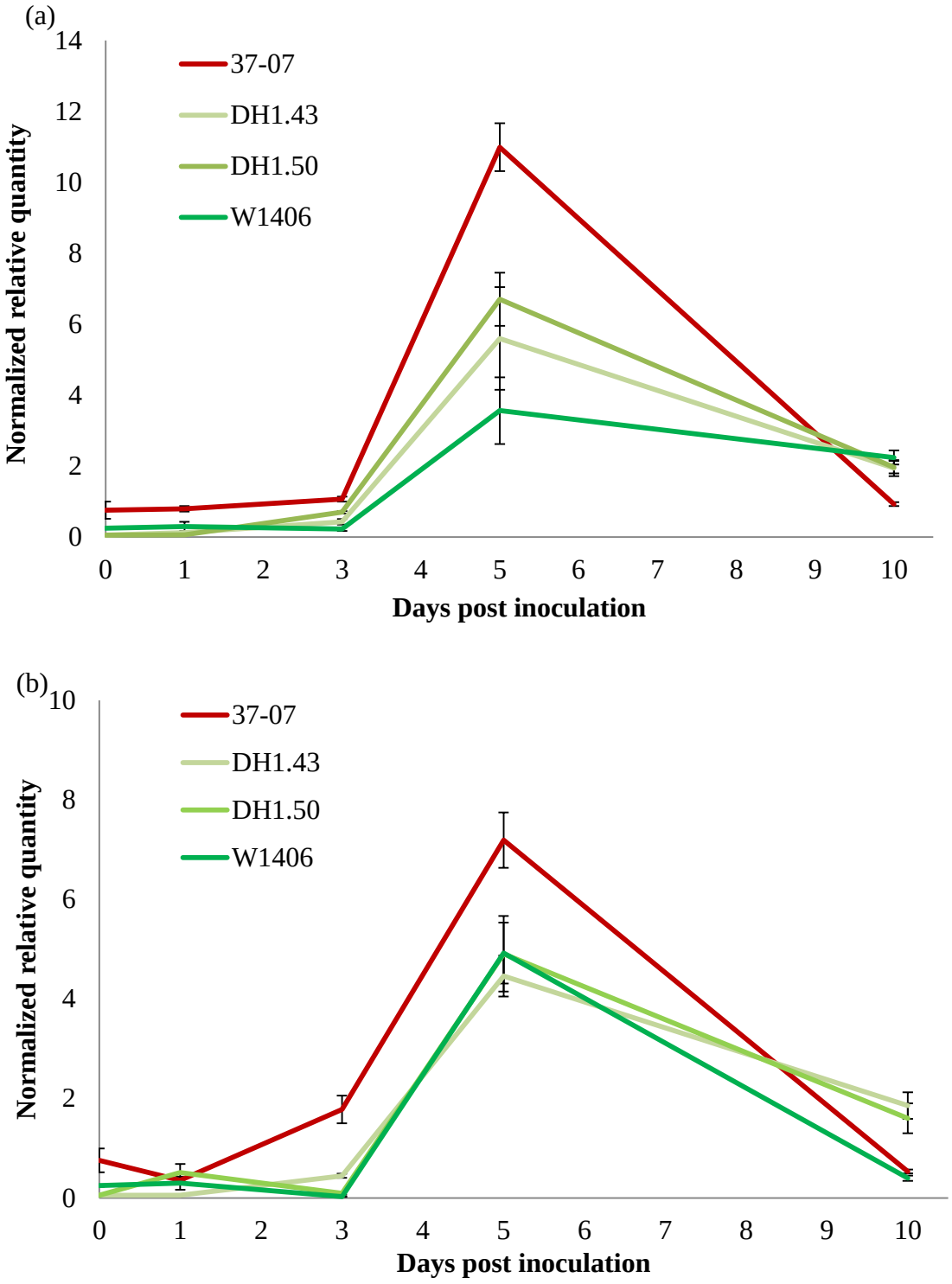

Figure 5.14: Normalised relative quantity of *PGTG_11318* transcripts in inoculated doubled haploid wheat lines from the W1406 x 37-07 cross tested in Adult trial 3 (a) and Adult trial 4 (b). Points show normalised relative quantity mean with standard error (n = 4) at indicated days post inoculation. *PGTG_11318* transcripts were expressed relative to *Puccinia graminis* f. sp. *tritici β-tubulin* transcripts and Cq values were determined by reverse transcriptase quantitative polymerase chain reaction.

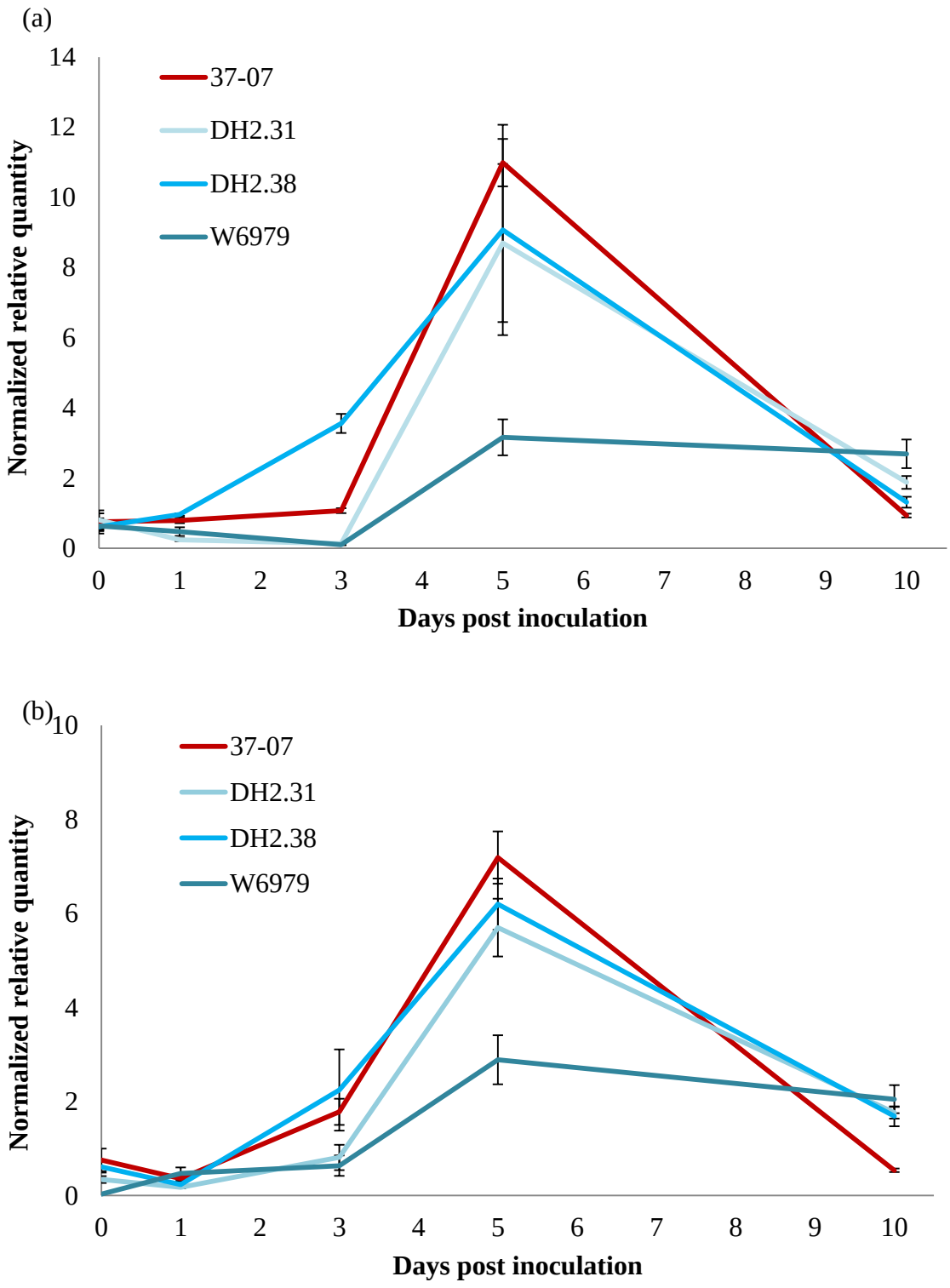

Figure 5.15: Normalised relative quantity of *PGTG_11318* transcripts in inoculated doubled haploid wheat lines from the W6979 x 37-07 cross tested in Adult trial 3 (a) and Adult trial 4 (b). Points show normalised relative quantity mean with standard error (n = 4) at indicated days post inoculation. *PGTG_11318* transcripts were expressed relative to *Puccinia graminis* f. sp. *tritici β-tubulin* transcripts and Cq values were determined by reverse transcriptase quantitative polymerase chain reaction.

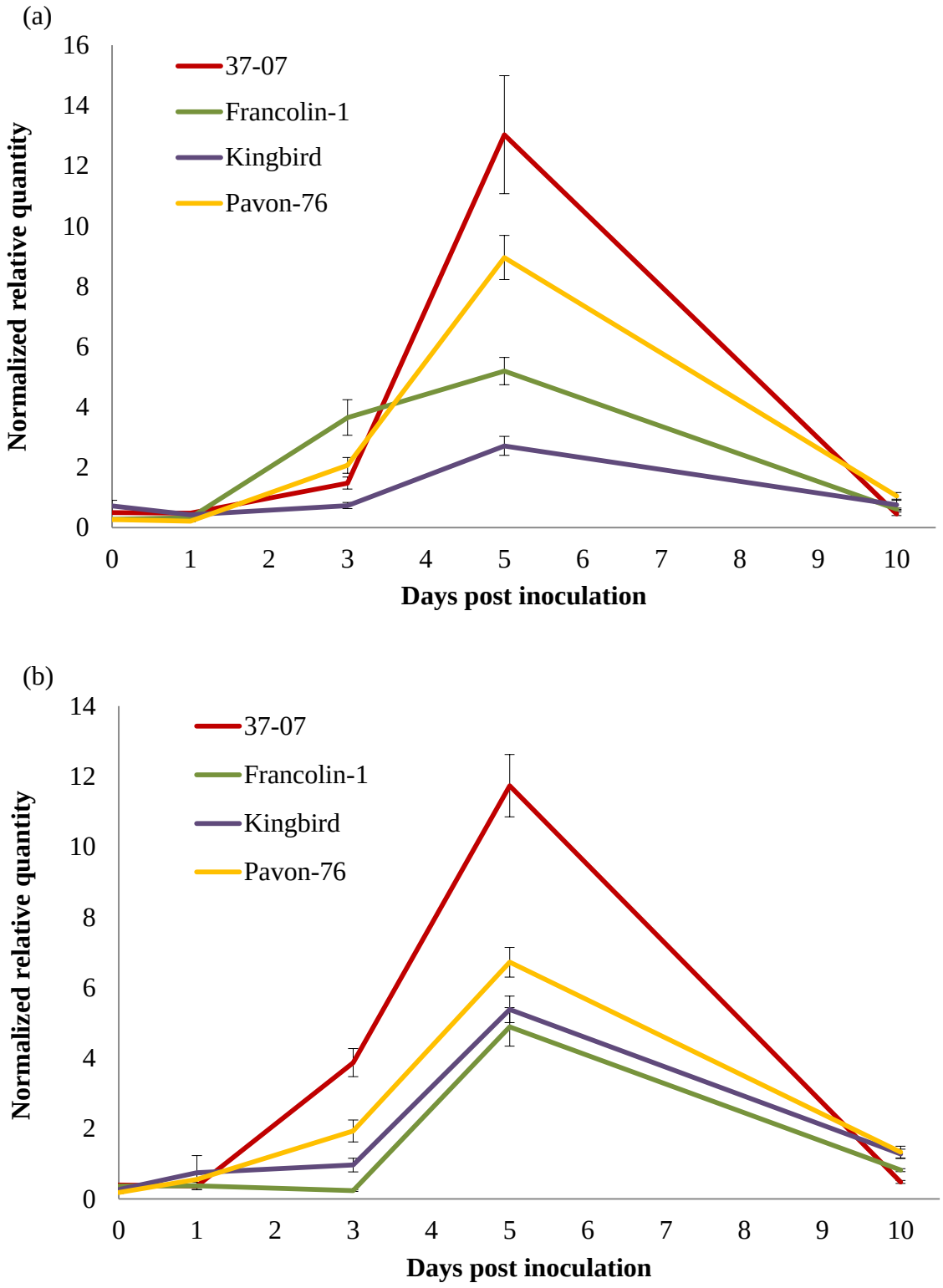

Figure 5.16: Normalised relative quantity of *PGTG_11318* transcripts in inoculated wheat lines tested in Adult trial 5 (a) and Adult trial 6 (b). Points show normalised relative quantity mean with standard error (n = 4) at indicated days post inoculation. *PGTG_11318* transcripts were expressed relative to *Puccinia graminis* f. sp. *tritici β-tubulin* transcripts and Cq values were determined by Reverse transcriptase quantitative polymerase chain reaction.

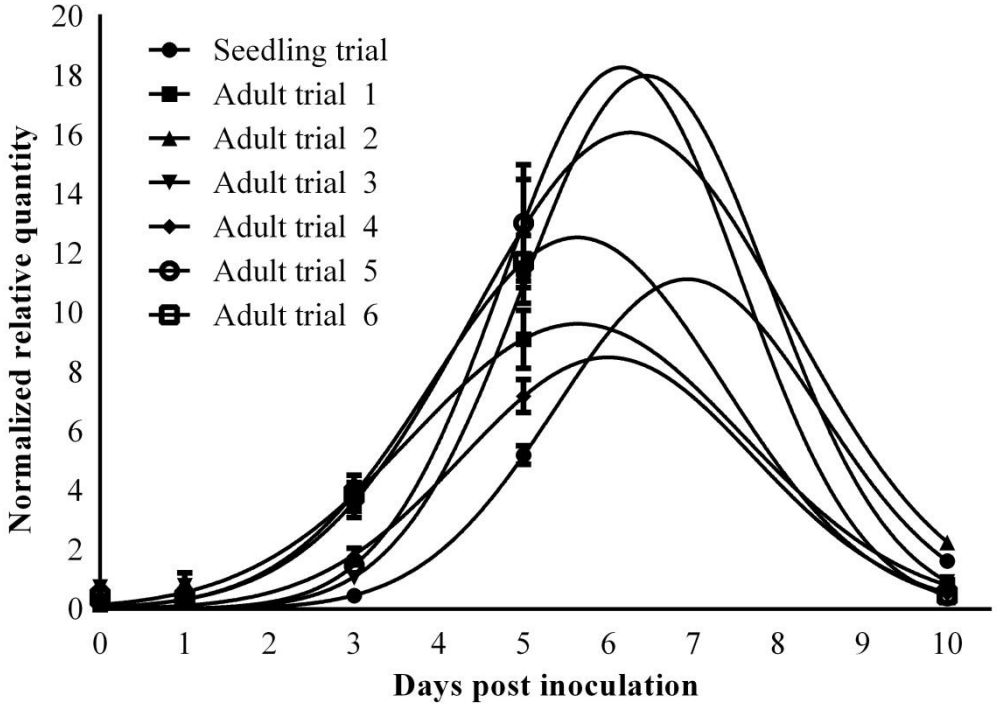

Figure 5.17: Non-linear regression graphs of normalised relative quantity of *PGTG_11318* transcripts in the inoculated 37-07 wheat line. Points show normalised relative quantity mean with standard error (n = 4) at indicated days post inoculation. The seedling trial and six adult plant trials (Adult trials 1-6) were modelled separately using a Gaussian equation (confidence level = 95%).

5.4 Discussion

Methods used in the current chapter successfully quantified *Pgt* biomass in inoculated adult wheat plants. These methods allowed the infection process to be followed, and showed at which time point the APR response could be distinguished from the susceptible response.

The presence of chitin in the cell walls of fungi, combined with the binding of WGA-FITC and resulting fluorescence measurement, underpins the quantification method of Ayliffe *et al.* (2013) and presents an effective tool for chitin quantification. The linear correlation between fluorescence and chitin was proven by Ayliffe *et al.* (2013), which indicated 40 µg of chitin and the corresponding 200 000 fluorescence units as the maximum value for this linear range. WGA-FITC binding was reported to become limiting above 40 µg of chitin. In the current study 100 µg of chitin and approximately 700 000 fluorescence units were shown as the maximum for the linear range. However, chitin measurements in technically replicated samples showed high variation and the fluorescence versus chitin standard curve was therefore not used for absolute quantification of chitin.

In the current study, the method of Ayliffe *et al.* (2013) was effectively used to infer *Pgt* biomass in inoculated adult wheat plants. Results obtained for the two independent trials (Adult trials 1 and 2) were similar, indicating good reproducibility. Any differences in the pattern of chitin quantity over time could be attributed to effects of biological or environmental variation. The ranking of tested wheat lines from Adult trials 1 and 2 was identical, with 37-07 having the greatest chitin quantity, W1406 being intermediate and W6979 having the lowest chitin quantity. Measurements therefore indicated the 37-07 line as most susceptible to *Pgt* and the W1406 and W6979 lines comparably less susceptible. Measurements confirmed the adult plant infection response observed in the W1406 and W6979 lines (Chapter 3; Table 3.5). The APR response in the tested lines was thus confirmed to effectively restrict the *Pgt* colonization process.

Chitin quantification was previously used by Ayliffe *et al.* (2013) to follow *Pgt* infection on wheat seedlings. The method was used to distinguish susceptible and resistant wheat lines quantitatively at 9 dpi. The current application could distinguish test lines at 5 dpi, but most clear differentiation only occurred at 10 dpi. Though the method was previously applied to *Pgt*-inoculated wheat seedlings (Ayliffe *et al.,* 2013; Hiebert *et al.,* 2016) the current application to *Pgt*-inoculated flag leaf sheaths of adult wheat plants is the first known report.

The binding of WGA-FITC is not only used for chitin quantification but also for histological studies (Ayliffe *et al.*, 2011). WGA-FITC was used for microscopic observation of the *Pgt* infection process on the tested APR lines (Chapter 4). Distinguishing wheat lines by colony size at 5 dpi (Chapter 4; Figure 4.22) was directly comparable to chitin quantification at the same time point, in the same trials. Both methods indicated the 37-07 line as most susceptible, the W1406 line as intermediate and the W6979 line as the least susceptible. Chitin quantification also has the advantage of allowing *Pgt* infection to be quantified at 10 dpi, which was not accomplished by colony sizes (Chapter 4).

Before the relative quantification of *Pgt* biomass by RT-qPCR was undertaken, reference gene validation was required. A previous validation of reference gene stability in *Pgt*-inoculated wheat seedlings showed *Ta-18S*, *Ta-BTUB* and *Ta-CDC* (in that order) as the most stable transcripts (Scholtz and Visser, 2013). In their study, only *Ta-18S* had an M value lower than the 0.5 cut-off for homogeneous samples, and with the inclusion of the other two transcripts were deemed sufficient for expression analysis. The *Ta-18S* transcript was previously used for expression analysis in *Pst*-inoculated wheat seedlings (Bozkurt *et al.*, 2007). These findings served as the rationale for inclusion of *Ta-18S*, *Ta-BTUB* and *Ta-CDC* as candidates for reference gene validation in the current study. *Ta-TEF* was included as a fourth candidate since it was previously used as a reference gene to infer fungal biomass (Coram *et al.*, 2008) and was confirmed a stable reference gene in *Pt*-inoculated adult wheat flag leaves (Casassola *et al.*, 2015).

In the current study the transcripts reported by Scholtz and Visser (2013) were sufficiently stable for gene expression analyses in *Pgt*-inoculated wheat flag leaf sheaths. This finding was supported in two different experimental layouts using different wheat lines/cultivars (Adult trials 1-4 and Adult trials 5-6) which showed comparable results. *Ta-TEF*, *Ta-18S* and *Ta-CDC* proved sufficiently stable in both experiments though the ranking of the latter two genes was different between the two experiments. The higher M values in Adult trials 5-6 and the exclusion of *Ta-BTUB* may be attributed to fewer biological replicates and high sample heterogeneity (i.e. genetic difference) in wheat from these trials. In Adult trials 1-4, three APR lines were analysed and in Adult trial 5-6 four APR lines/cultivars were analysed, potentially adding to the effect of sample heterogeneity in the latter experiment.

Ta-TEF was the most stable reference gene throughout all experimentation and showed the importance of reference gene validation. Numerous other reference genes remain to be tested

and may prove even more stable during *Pgt* inoculation. Scholtz and Visser (2013) also reported stable reference transcripts during *Pst* and *Pt* inoculation of wheat seedlings, although reference gene validation for adult wheat for these two species still needs to be undertaken. Here presented, however, is the first known reference gene validation study for adult wheat inoculated with *Pgt*.

Vandesompele *et al.* (2002) proposed that three to five stable reference genes should be selected for accurate expression analysis. The current findings indicated that for large scale gene expression analysis of *Pgt*-inoculated wheat flag leaf sheaths, *Ta-TEF*, *Ta-18S* and *Ta-CDC* may be used. *Ta-BTUB* is another candidate transcript to be considered. However, for quick and routine gene expression analyses, as used for determining *Pgt* development, a single reference transcript is suggested. *Ta-TEF* was thus subsequently used as a reference transcript since it proved most stable in all trials.

The expression of *Pgt-BTUB* relative to *Ta-TEF* to assess *Pgt* biomass in inoculated wheat flag leaf sheaths was based on a method of Coram *et al.* (2008). The method was effectively used to infer biomass in *Pgt*-inoculated adult wheat over the course of infection. In general tested cultivars, lines and entries were not distinguishable at the 0 - 3 dpi time points. In the study of Coram *et al.* (2008), the wheat line with the *Yr39* APR gene could be distinguished from the susceptible line from 2 dpi onwards when inoculated with *Pst* using relative *β-tubulin* expression. A qPCR based method could distinguish *Pgt*-inoculated barley lines/cultivars as early as 1 dpi, and though it corresponded to the fluorescence microscopy results, it was contradicted by the infection types on inoculated seedlings (Zurn *et al.*, 2015). A pre-haustorial defence response that may be overcome by *Pgt* was hypothesised to account for this discrepancy.

In the current study, at 5 dpi some of the tested samples could be distinguished, but results were variable. Results imply that *Pgt* biomass must pass some threshold in the flag leaf sheath for the effect of the APR response to be accurately measured. This hypothesis applies to both the chitin quantification by fluorescence and the *Pgt-BTUB* transcript quantification by RT-qPCR. In most trials, a clear ranking of *Pgt-BTUB* transcript levels was established at 10 dpi. The *Pgt* biomass on inoculated flag leaf sheaths increased over the course of infection, but most rapidly from 5 to 10 dpi. For future quantification it is therefore suggested that 5 dpi and later be considered to allow wheat cultivars or lines to be effectively

distinguished, with 10 dpi as the best time point. The inclusion of more time points in future studies may shift this to an earlier time interval.

At 10 dpi, the 37-07 line had the highest *Pgt* biomass, confirming this line as the most susceptible. The W1406 and W6979 lines were by extension less susceptible, with W1406 being intermediate. Differences in transcript levels were statistically significant only at 10 dpi. The ranking of these lines are supported by phenotypic scoring of the adult plant infection responses at 14 dpi (Chapter 3; Table 3.5). The APR response in W1406 and W6979 was thereby confirmed to restrict the *Pgt* colonization process.

The DH entries delivered variable results for *Pgt-BTUB* transcript quantification at 10 dpi. The ranking of DH1.43 and DH1.50 differed between the two trials and from the phenotypic scoring (Chapter 3; Table 3.5). These lines could not be distinguished based on phenotypic scoring (Chapter 3; Table 3.5) but in Adult trial 4 these lines were distinguishable by *Pgt-BTUB* transcript quantification, alluding to the potential of the method. However, the method proved less accurate when analysing DH lines. A connection between the respective quantitative trait loci (QTL) in the DH entries and the putative effects on *Pgt* biomass could not be established. Regardless, the DH entries were confirmed to effectively restrict the *Pgt* colonization process.

Results of *Pgt* biomass at 10 dpi indicated that other APR cultivars were distinguishable and *Pgt-BTUB* transcript levels ranked the tested cultivars from 37-07 (most susceptible) to Francolin-1, Pavon-76 and Kingbird (least susceptible). The APR cultivars could not be distinguished by phenotypic scoring of the adult plant infection responses at 14 dpi (Chapter 3; Table 3.5). Therefore, *Pgt-BTUB* transcript quantification again allowed cultivars to be distinguished that was otherwise difficult by phenotypic scoring. The low *Pgt* biomass in Kingbird was attributed to the presence of strong APR including the *Sr2* gene (Maré, 2017).

Theis method to infer fungal biomass in inoculated adult wheat was also used by Maré (2017). Quantification of *β-tubulin* from *Puccinia* spp. relative to *Ta-TEF* was analysed at 5 dpi intervals for *Pt-*, *Pst-* and *Pgt*-inoculated wheat and showed that 10 dpi was the best time point to distinguish inoculated lines/cultivars. Results confirmed the efficacy of the method to infer biomass in adult wheat plants and the choice of 10 dpi as the most effective time point for distinguishing the APR response.

Due to the confirmed effects of the APR cultivars, lines and entries, these transcript levels were not considered to model a non-linear equation. The infection process on the susceptible 37-07 line was assumed to be the best representation of the infection process on the flag leaf sheaths of wheat. Most of the trials fitted the exponential growth equation and confirmed the rapid accumulation of *Pgt* biomass over the course of infection. The exclusion of the seedling trial and Adult trial 5 from this model implied that the exponential growth equation may not be the ideal model. Inclusion of more time points over the course of infection and time points after 10 dpi may improve the model.

The biomass quantification of *U. fabae* on broad bean inferred by RT-qPCR appeared to fit a sigmoidal growth curve (Voegele and Schmid, 2011). At early time points gene expression was in the lag phase, but from 4 to 9 dpi expression may be described as proceeding through an exponential phase. In the current study, parallels can be drawn with the exponential growth equation of *Pgt* development and the rapid increase of transcript levels from 5 to 10 dpi. In *U. fabae* at 9 dpi, gene expression entered the steady-state phase that was maintained until 18 dpi (Voegele and Schmid, 2011). A sigmoidal growth equation may thus accurately describe *Pgt* development on adult wheat, but requires more time points after 10 dpi to confirm a steady-state phase.

Maré (2017) included a 15 dpi time point in the analysis of fungal *β-tubulin* transcripts in *Pgt*-inoculated adult wheat. The fungal *β-tubulin* transcript levels in most lines/cultivars continued to increase from 10 to 15 dpi, but the most susceptible line showed decreased transcripts at 15 dpi. The decrease was reported for certain susceptible lines/cultivars at 10 dpi in *Pt*-inoculated adult wheat and at 15 dpi in *Pst*-inoculated adult wheat. Results implied a sigmoidal growth curve with a decline phase of fungal development in *Puccinia* spp., especially on inoculated susceptible adult wheat. From these findings it seems unlikely that an unified model of fungal *β-tubulin* transcript levels on inoculated adult wheat could be applied to all the *Puccinia* spp. and even within *Pgt*. The transcript levels of *β-tubulin* seem variable.

Another transcript, *PGTG_11318,* was selected to quantify haustoria development in inoculated wheat. The gene encodes a putative haustorium associated protein and the transcript was highly upregulated in *Pgt* infected wheat tissue (Duplessis *et al.,* 2011). In the current study TMHMM, Phobius and InterPro indicated that PGTG_11318 may be membrane bound with a large extracellular region. The protein may thus be associated with transport

across the membrane or recognition of an extracellular signal. Haustoria were established as important in the uptake of simple carbohydrates and amino acids from the host (Voegele and Mendgen, 2011). Alternatively, PGTG_11318 may be localised in mitochondria as indicated by TargetP and WoLF PSORT. Mitochondria were proven to accumulate in the haustoria of *Pgt* (Ehrlich and Ehrlich, 1963). The expression of the *PGTG_11318* transcript may thus be associated haustorial mitochondria and the proliferation thereof during the *Pgt* infection process.

PGTG_11318 was homologous to two ESTs reported in Broeker *et al.* (2006), and both are likely encoded by *PGTG_11318*. The ESTs were highly expressed during *Pgt* infection and reported to share homology to *INF24* encoding infection structure-specific protein 24 from *U. appendiculatus*. However, homology of *PGTG_11318* to *INF24* could not be confirmed. Based on the reports of Duplessis *et al.* (2011) and Broeker *et al.* (2006) PGTG_11318 was therefore assumed to be associated with haustorium formation in *Pgt,* although not assumed to be exclusively expressed in the haustorium. Its function could, however, not be elucidated.

PGTG_11318, unlike *Pgt-BTUB*, was not expressed relative to the *Ta-TEF* reference transcript. Since *PGTG_11318* was assumed to be associated with a particular infection structure in *Pgt*, this transcript was expressed relative to *Pgt-BTUB*. As discussed in section 5.4.2.2, *Pgt-BTUB* was induced over the course of infection and may not be a stable reference gene. The quantity of *PGTG_11318* transcripts relative to *Pgt-BTUB* transcripts does however give an indication of the relationship of haustoria to fungal biomass. The expression of a number of haustorial ESTs has previously been quantified relative to *β-tubulin, elongation factor 1 alpha* and *actin* in *Pst* (Yin *et al.*, 2009).

In the current study the tested lines were distinguishable from 3 - 10 dpi, but results were variable. A clear ranking of *PGTG_11318* transcript levels was established at 5 dpi in most trials and this time point was thus considered the most appropriate for accurate quantification of haustorium formation. A ranking of most lines, entries or cultivars was possible at 5 dpi when *PGTG_11318* transcripts were quantified.

At 5 dpi, the 37-07 line had the highest transcript levels, implying greater haustorium formation and confirming this line as the most susceptible. The W1406 and W6979 lines were by extension less susceptible, with the W1406 line being intermediate between 37-07 and W6979. The differences in transcript levels were statistically significant only at 5 dpi. The ranking by *PGTG_11318* transcript levels does however differ from the ranking

determined in the seedling trials; thereby indicating the defence response associated with adult phase of the W1406 and W6979. The APR response in these lines was thereby confirmed to restrict the *Pgt* colonization process, possibly by restricting haustorium formation.

Analysis of the *PGTG_11318* transcripts in the DH entries delivered comparable results at 5 dpi, but clearly distinguishing all entries was not possible. DH1.43 and DH1.50 could not be distinguished from the W1406 line, while DH2.31 and DH2.38 could not be distinguished from 37-07. These results imply that DH1.43 and DH1.50 potentially restrict haustorium formation to the same extent as in the W1406 line. DH2.31 and DH2.38 could not restrict haustorium formation to the same extent as W6979. Furthermore, results implied that while haustorium formation may be restricted by both W1406 and W6979, the QTL interactions may have a crucial effect.

Results of *PGTG_11318* transcript quantification analysis at 5 dpi could not consistently distinguish Francolin-1, Pavon-76 and Kingbird. The ranking of cultivars, in turn, differed from the ranking seen in the analysis of *Pgt-BTUB* transcripts. Generally, Kingbird was considered to have the lowest *PGTG_11318* and *Pgt-BTUB* transcript levels. The APR cultivars could not be distinguished by phenotypic scoring of the adult plant infection responses at 14 dpi (Chapter 3; Table 3.5). The tested cultivars may therefore overlap in the intensity of APR response, but not necessarily in the mechanism. All cultivars had lower quantities of *PGTG_11318* transcripts than the 37-07 line confirming the APR response in these cultivars. The restriction of haustorium formation was thus a possible contributing factor to the inhibition of *Pgt* colonization.

PGTG_11318 transcript levels showed that the APR response in most of the tested cultivars, lines and entries inhibited haustorium formation from 3 dpi onwards, but particularly at 5 dpi. Quantifiable differences in haustorium formation could not be confirmed by microscopic observation. Results imply a post-haustorial defence response in the tested lines/cultivars that may restrict *Pgt* proliferation. A pre-haustorial defence response cannot be completely ruled out, but quantification of haustorium formation at early time points requires an improvement of the sensitivity of the current methods.

The transcript levels of *PGTG_11318* showed a fixed pattern in all trials. *PGTG_11318* transcripts started low, increased over the course of infection, peaked at 5 dpi, but deceased thereafter. At the early time intervals the infection process is starting and fungal biomass is

low, as confirmed by chitin quantification and biomass analysis. Though HMC formation was confirmed by microscopic observations at 1 dpi (Chapter 4; Figure 4.18), the quantity of haustoria is assumed to be too low to be detected by RT-qPCR of *PGTG_11318*. These initial phases were classified as recognition, signalling and parasitic by Mendgen *et al.* (1988). During the parasitic phase the pathogen establishes a biotrophic relationship through haustorium formation. The tested haustorium-associated transcript therefore accumulates in proportion to total biomass and increases as *Pgt* proliferates.

From 5 to 10 dpi the transcript levels of *PGTG_11318* decreased, however fungal biomass still increased exponentially. This observation implies that haustorium formation was proportionally low at 10 dpi and that fungal development may have shifted away from the parasitic phase. Microscopic observations confirmed that uredinia were formed from 5 to 10 dpi, and that sporulation occurred by 10 dpi (Chapter 4, Figure 4.23). It is hypothesised that the proportion of haustoria in the total *Pgt* biomass decreased from 5 to 10 dpi. Sporulating mycelium and urediniospores increased in the proportion to the total *Pgt* biomass at 10 dpi. The peak of *PGTG* transcripts therefore neatly separates the phases into establishment of the pathogen, proliferation of haustoria and sporulation.

A similar pattern of expression for haustorium-associated transcripts was reported by Puthoff *et al.* (2008) in *U. appendiculatus*. The *rust fungi transferred protein 1* (*RTP1*) transcript was expressed relative to the fungal *elongation factor 1 alpha* in purified fungal infection structures. *RTP1* expression was detected in the hyphal fractions at 2 and 4 dpi, reaching the highest level in the haustorium fraction at 5 dpi and then decreased at 6 and 8 dpi. The EST homologous to *PGTG_11318* were induced from 5 dpi onwards, but was down regulated in sporogenous mycelium (Broeker *et al.,* 2006). The pattern of *PGTG_11318* expression in the current study was thereby confirmed, especially the relative decrease of transcripts at 10 dpi, here hypothesised to be attributed to a developmental shift to sporulation.

The transcript levels of *PGTG_11318* in the APR cultivars, lines and entries were not considered for the fitting of a non-linear equation due to effects that the APR response may have on haustorium formation. The infection process in the susceptible 37-07 line was assumed to be the best representation of haustorium formation on the flag leaf sheaths of wheat. The quantification of *PGTG_11318* transcripts in all trials of the current study fit the Gaussian equation and confirmed this model as descriptive of haustorium formation relative to total biomass. Based on the models of transcript levels, the relative quantity of this

transcript should peak at 5 to 7 dpi in the different trials. However, more time points are needed to improve the model and support this conclusion. The time points from 5 to 7 dpi may therefore be more informative when attempting to distinguish APR lines.

The expression of three haustorium-associated transcripts, *hexose transporter 1* (*HXT1*), *thiamine biosynthesis gene 1* (*THI1)* and *RTP1* in *U. fabae* on broad bean showed parallels to expression analysis for biomass quantification (Voegele and Schmid, 2011). A lag phase, exponential phase and steady-state phase for haustorium formation were observed and appeared to fit a sigmoidal growth curve. However, these results did not present relative transcript quantification and cannot be directly compared to the Gaussian model presented in the current study.

As fungal genes continue to be described and their expression patterns determined, our knowledge of the molecular basis of infection is ever expanding. In the future gene expression markers may be developed for stages or structures of fungal infection. Just as the expression of *RTP1*, *THI1*, *HXT1* (Hacquard *et al.*, 2011; Voegele and Schmid, 2011) and putatively *PGTG_11318* are associated with haustoria, other genes associated with germination, formation of appressoria, sub-stomatal vesicles or sporogenous mycelium may be identified. Expression analysis of such genes will make quantification of infection structures possible without microscopic observations. In the current study, HMC formation was confirmed by microscopic observations as early as 1 dpi (Chapter 4; Figure 4.18), but haustoria were not directly observed and quantification was therefore not possible. However, relative quantification of *PGTG_11318* allowed haustorium formation to be inferred and highlights the potential of this analysis.

Methods presented in this chapter improved on the ability to distinguish between the adult wheat lines after *Pgt* inoculation. The adult plant infection responses could be scored phenotypically at 14 dpi (Chapter 3; Table 3.5). Assessing biomass by chitin quantification and *Pgt-BTUB* transcript quantification allowed APR wheat to be distinguished from susceptible wheat at 10 dpi, 4 days earlier than phenotypic scoring. Assessing haustoria formation by *PGTG_11318* transcript quantification allowed APR wheat to be distinguished from susceptible wheat at 5 dpi, 9 days earlier than phenotypic scoring and 5 days earlier than biomass analysis by RT-qPCR. Quantification of the colony size of 37-07, W1406 and W6979 was likewise possible at 5 dpi (Chapter 4; Figure 4.22), but *PGTG_11318* transcript

quantification has the added benefit of inferring haustoria formation that was not possible by histological observations.

The wheat lines that were the particular focus of the current study were consistently ranked using the applied methods. The methods ranked lines 37-07, W1406 and W6979 from most to least susceptible. The ranking of these lines was supported by chitin quantification and *Pgt-BTUB* transcript quantification at 10 dpi, and *PGTG_11318* transcript quantification at 5 dpi. The ranking was additionally supported by phenotypic scoring of the adult plant infection responses at 14 dpi (Chapter 3; Table 3.5) and the quantified colony sizes at 5 dpi (Chapter 4; Figure 4.22). Based on the adult plant infection responses of the two APR lines in two locations, over three growing seasons, W1406 was scored as 0R, 5R and 10R and W6979 as 0R, 5R, and 40RMR (Prins *et al.,* 2016). These field trials appeared to rank W6979 as equal to, or more susceptible than W1406. Though this contradicts the ranking established in the current study, the APR response in the W1406 and W6979 lines, and the susceptible phenotype of the 37-07 line are confirmed, while the ranking was well supported by all methods.

Distinguishing W1406 and W6979 from 37-07 allowed for the identification of the putative time point for the expression of the APR response. Determination of fungal biomass by chitin quantification and *Pgt-BTUB* transcript quantification both indicated that the APR response started to restrict *Pgt* colonization from 5 dpi, even though the effect was only statistically significant at 10 dpi. Determination of *PGTG_11318* transcript levels indicated that the W1406 and W6979 lines restricted *Pgt* haustorium formation by 5 dpi. When compared to the difference in colony size measured at 5 dpi (Chapter 4; Figure 4.22), all results indicated that the APR response is active by this time point. However, induction of the APR response in the W1406 and W6979 lines must have occurred at an earlier time point. A more sensitive method is required to potentially elucidate the response and differentially expressed transcripts. To understand the APR response in the W1406 and W6979 lines further experimentation will focus on time points preceding 5 dpi, to possibly elucidate APR responses that inhibit *Pgt* colonization.

Chapter 6: An analysis of transcriptomic changes in adult wheat lines upon *Puccinia graminis* f. sp. *tritici* infection

6.1 Introduction

Our understanding of the molecular biology of living organisms has been revolutionised by the development of next-generation sequencing (NGS); called so to distinguish it from first generation sequencing. NGS technologies allows for the simultaneous sequencing of a large number of relatively short reads and include sequencing technology platforms such as Illumina and Ion Torrent. Illumina sequencing is based on the detection of the incorporation of a fluorescently-labelled deoxynucleotide (dNTP) during DNA synthesis. Ion Torrent sequencing measures the incorporation of a dNTP through changes in pH (Liu *et al.,* 2012). More recent developments in NGS have delivered third generation sequencing technologies such as Pacific Biosciences SMRT and Oxford Nanopore sequencing (Kchouk *et al.,* 2017). In the current study, the term NGS shall be used to refer to the Illumina, Ion Torrent and other second generation sequencing platforms.

In studies of plants, their associated pathogens and interactions between plant and pathogen, NGS have accelerated the accumulation of knowledge. This has also greatly improved our understanding of the interaction of wheat (*Triticum aestivum*) with the three *Puccinia* spp. that cause rust diseases: *P. triticina* (*Pt*), *P. striiformis* f. sp. *tritici* (*Pst*) and *P. graminis* f. sp. *tritici* (*Pgt*). The wheat genome has been sequenced (Clavijo *et al.,* 2017), and the assembly and annotation thereof is constantly being improved. Genotyping by sequencing has allowed the mapping of complex traits such *Pgt* resistance in wheat (Bajgain *et al.,* 2016). Resistance gene enrichment sequencing (RenSeq) has allowed the identification of wheat nucleotide-binding and a leucine-rich repeat (NB-LRR) protein encoding genes that confer resistance (Steuernagel *et al*., 2016). The genomes of *Pst*, *Pt* and *Pgt* have also been sequenced (Cantu *et al.,* 2011; Duplessis *et al*., 2011; http://www.broadinstitute.org/annotation/genome/puccinia_group/Info.html). Field pathogenomics has allowed the investigation of the *Pst* population structure in the United Kingdom (Hubbard *et al.,* 2015) and has potential for worldwide application. NGS and associated computational analysis have permitted the identification of numerous candidate effector encoding genes in *Pgt* (Duplessis *et al*., 2011; Saunders *et al*., 2012; Upadhyaya *et al.,* 2015).

The application of NGS to study large scale gene expression changes under variable conditions is called RNA sequencing (RNA-seq). RNA-seq has a number of advantages over other methods such as microarrays. RNA-seq does not require the genome of the analysed

organism to be sequenced and transcripts can be constructed *de novo*. The method is more sensitive and allows transcripts with low copy numbers to be quantified. RNA-seq also does not require any cloning steps. Challenges of RNA-seq are similar to those associated with most NGS techniques. Inherent biases are introduced with the fragmentation of larger transcripts. To ensure sufficient coverage of the transcriptome, higher sequencing depth is required, but this adds costs to the experiment. Bioinformatics and databases need constant improvement to accurately analyse large data sets (Wang *et al.*, 2009). RNA-seq has been widely applied to study changes in the wheat transcriptome upon infection with the *Puccinia* spp. (Dobon *et al.*, 2016; Hao *et al.*, 2016; Rutter *et al.*, 2017; Neugebauer *et al.*, 2018).

The aim of this chapter was to identify differentially expressed (DE) transcripts in the flag leaf sheath of adult wheat upon *Pgt* inoculation. Under investigation were the adult plant resistant (APR) W1406 and W6979 lines, and the susceptible control 37-07 line. The main aim was sub-divided into four objectives. The first objective was to compare the two leading NGS platforms for their capacity to identify similar DE transcripts from the same RNA samples. The second objective was to determine the wheat transcripts associated with the defence response in the APR lines. The third objective was to identify changes in *Pgt* transcript expression on the adult wheat host. The fourth and final objective was to determine how DE transcripts may clarify the genetic basis of the APR response in the W1406 and W6979 lines.

6.2 Materials and methods

6.2.1 Biological material

For RNA-seq, *Pgt*-inoculated wheat samples were generated as described in Chapter 3. The 37-07, W1406 and W6979 wheat lines from the first three adult plant trials (Adult trial 1-3) were used. The flag leaf sheaths of the last internode were collected as previously described and further processed. The 0 days post inoculation (dpi) sample was collected directly after inoculation and samples were thereafter collected at 1 and 3 dpi.

6.2.2 RNA sequencing

6.2.2.1 Total RNA extraction

Total RNA was extracted from 100 mg of flag leaf sheath tissue using the TRIzol™ reagent (Thermo Fisher Scientific, Waltham, Massachusetts, United States of America) as described in Chapter 5 (section 5.2.3.1). RNA quantity and quality were assessed using the NanoDrop 2000 Spectrophotometer (Thermo Fisher Scientific) and 1.0% (w/v) denaturing agarose gel electrophoresis (Sambrook *et al.*, 1989) respectively. Total RNA samples were further purified using the RNAeasy® Mini kit (Qiagen, Hilden, Germany) according to the manufacturer's instructions. An on-column DNase I (RNase-free, 10 units) (Thermo Fisher Scientific) treatment was included. Samples were transported in RNAstable® (Biomatrica, San Diego, California, United States of America) to the respective laboratories for RNA-seq, where it was re-dissolved in nuclease free water. RNA quality was assessed using a 2100 Bioanalyzer (Agilent Technologies, Santa Clara, California, United States) and an RNA integrity number (RIN) > 7 was required before samples were further processed.

6.2.2.2 Illumina sequencing

The 1 and 3 dpi samples from the 37-07, W1406 and W6979 wheat lines from the first biological replicate (Adult trial 1) were sequenced at Cofactor Genomics (St. Louis, Missouri, United States). RNA samples underwent poly-adenine selection and were further prepared according to Illumina guidelines. The cDNA libraries were constructed with TruSeq RNA Library Prep Kit v2 (Illumina, San Diego, California, United States of America) and sequenced on the Illumina HiSeq 2000™ platform (Thermo Fischer Scientific). Single-stranded reads of 75 nucleotides (nt) were generated.

6.2.2.3 Ion Torrent sequencing

The 0, 1 and 3 dpi samples from the 37-07, W1406 and W6979 wheat lines from the first three biological replicates (Adult trials 1-3) were sequenced at the Central Analytical Facility (University of Stellenbosch, South Africa). RNA samples underwent poly-adenine selection and were further prepared according to Ion Torrent guidelines. The cDNA libraries were constructed with Ion Total RNA-Seq Kit v 2 (Thermo Fischer Scientific) and sequenced on the Ion Torrent Proton^{TM} platform (Thermo Fischer Scientific). Single-stranded reads varying between 25-386 nt were generated.

6.2.2.4 Reference transcriptomes

The transcriptome reference sequence of the bread wheat cultivar Chinese Spring TGAC (Ensembl release 35) (Clavijo *et al.,* 2017) and the complete *Pgt* reference transcriptome from *Puccinia* Group Database at the Broad Institute (release 35; Duplessis *et al.,* 2011) were used as reference sequences. These transcriptome references were hosted by Ensembl (https://www.ensembl.org). To test whether there was significant cross-mapping between the two reference transcriptomes the wheat transcriptome reference sequence was aligned to the *Pgt* transcriptome reference sequence using Nucleotide-Nucleotide BLAST v 2.6.0+ with the default E value < 10. Similarly the *Pgt* transcriptome reference sequence was aligned to the wheat transcriptome reference sequence. Cross-mapping sequences from both reference transcriptomes were noted and discarded in further downstream analyses. The bioinformatics pipeline used the merged wheat and *Pgt* transcriptome reference sequences, henceforth simply referred to as the reference transcriptome.

6.2.2.5 Sequencing platform comparison

A subset (from one biological replicate) of the Ion Torrent sequenced samples, corresponding to 1 and 3 dpi from the 37-07, W1406 and W6979 wheat lines' first biological replicate (Adult trial 1), was used for the sequencing platform comparison. RNA for these samples was thus derived from the same inoculated wheat tissue that was used for the Illumina sequencing. For quality control, raw reads from the Illumina dataset and Ion Torrent subset were analysed with FastQC v 0.11.5 (http://www.bioinformatics.babraham.ac.uk/projects/fastqc). FASTX Toolkit v 0.0.14 (http://hannonlab.cshl.edu/fastx_toolkit) was used to trim bases from trailing ends of reads

with a quality score < 20. Read lengths < 75 nt were subsequently discarded. Reads were mapped to the reference transcriptome using Bowtie v 2.3.2 (Langmead and Salzberg, 2012).

Alignment files, generated by Bowtie, for the Illumina and Ion Torrent datasets were separately imported into SeqMonk v 1.40.1 (https://www.bioinformatics.babraham.ac.uk/projects/seqmonk) running R v 3.4.1. DE transcripts were identified using an intensity difference analysis (*p*-value < 0.05). The intensity difference analysis tested whether the read count of any transcript varied significantly from the overall distribution of read counts and tested all pairwise combinations of the imported libraries. The intensity difference analysis may be applied to non-replicated data as represented by the datasets for the sequencing platform comparison. Raw read counts were thereafter $\log_2$ transformed for normalization. Principal component analysis (PCA) was done using ClustVis (Metsalu and Vilo, 2015; https://biit.cs.ut.ee/clustvis) with unit variance scaling and singular value decomposition.

6.2.2.6 Ion Torrent transcriptomic analysis

A schematic representation of the bioinformatics pipeline used for the analysis of the Ion Torrent datasets is presented in Figure 6.1. For quality control, raw reads from the complete Ion Torrent datasets were analysed with FastQC v 0.11.5 and trimmed with FASTX Toolkit v 0.0.14. Bases with a quality score < 20 were trimmed from the trailing end of the strand and resulting reads < 25 nt were discarded. Reads were mapped to the reference transcriptome with Bowtie v 2.3.2 (Langmead and Salzberg, 2012) and mapped reads were quantified with Salmon v 0.9.1 using its alignment-based mode (Patro *et al.*, 2017). The raw sequencing data for the three biological replicates were run independently through this bioinformatics pipeline. The raw data counts from each sample replicate were combined and then analysed for differential expression as described below.

DE transcripts were determined using baySeq v 2.12.0 (Hardcastle and Kelly, 2010) package in R v 3.4.1. Pairwise comparisons were made for wheat lines and time points independently over the course of infection (Figure 6.2). When sample replicates at 0 dpi were analysed against the other time points in the same wheat line, the comparison was referred to as time vs time (Figure 6.2 a). When the inoculated 37-07 line was analysed against an APR line for a given time point, the comparison was referred to as line vs line (Figure 6.2 b). Transcripts were considered as DE if they exhibited a false discovery rate (FDR) < 0.05 at any point over the course of infection and for any comparison. Throughout the DE datasets one was added to

every read count to assure division by zero did not occur for the subsequent calculation of $\log_2$ fold change (FC). Transcripts with a $\log_2$FC > 1.0 were considered induced in the pairwise comparison and $\log_2$FC < -1.0 repressed. Heatmaps were created using Genesis v 1.7.7 (Sturn *et al.,* 2002) and relationships between transcripts and their expression patterns, indicated as $\log_2$FC values, were determined by complete linkage hierarchical clustering. Groups of similarly expressed were summarised as distinct clusters.

DE wheat and *Pgt* transcripts were firstly annotated using BioMart in Ensembl Plants and Fungi respectively. Transcripts were further annotated using Blast2GO v 5.0.13 (Conesa *et al.,* 2005). The BLAST search (blastx-fast) for wheat transcripts was restricted to the Magnoliophyta (taxid: 3398) and for *Pgt* transcripts to the Basidiomycota (taxid: 5204) with an E value cut-off < 0.001. Gene ontology (GO) annotations were determined from BLAST hits. The InterPro (Finn *et al.,* 2017) and associated GO annotations were subsequently retrieved. Multilevel GO distributions based on node scores were determined in Blast2GO. Node scores were calculated from the number of sequences converging at a given GO node and identified the reported GO term (Conesa *et al.,* 2005).

For the identification of NB-LRR protein encoding transcripts, wheat transcripts were scanned for NB-LRR motifs using MEME suite v 4.9.1 (Bailey *et al.,* 2009) using the definitions of Jupe *et al.* (2012). Identified NB-LRR protein encoding transcripts were then classified by NLR-Parser (Steuernagel *et al*., 2015). To identify wheat transcripts with homology to known APR genes, a number of protein domains were identified from InterPro accessions as described by Peng and Yang (2017). For adenosine triphosphate-binding cassette (ABC) transporters, the 'ABC transporter-like domain' (IPR00343) was used. For single domain START kinases, the 'START domain' (IPR002913 and IPR005031) and 'START-like domain superfamily' (IPR023393) were used. Multiple domain START kinases included the 'homeobox-like domain superfamily' (IPR009057) and possibly an additional 'MEKHLA domain' (IPR013978). For hexose transporters, both a 'major facilitator superfamily domain' (IPR020846) and 'sugar transporter conserved site' (IPR005829) were used.

For the identification of effectors from the *Pgt* transcripts, the peptide sequences were imported into EffectorP v 2.0 (Sperschneider *et al.,* 2018; http://effectorp.csiro.au). The identified effector peptide sequences were also imported into LOCALIZER v 1.0.4 (Sperschneider *et al.,* 2017; http://localizer.csiro.au) to identify the putative subcellular

localization within the plant host. The first 20 amino acids were removed from putative effector sequences within LOCALIZER to exclude the effector signal peptide sequence.

6.2.2 Note on transcript abbreviation convention

For in-text reports of the wheat transcript accessions an abbreviated code was used. The Ensembl accession convention for wheat included the TRIAE, CS42 and TGACv1 labels to designate the sequence as originating from *T. aestivum*, cv. Chinese Spring and the TGAC sequencing project. As these labels are common to all wheat accessions, they were removed in the abbreviated code. For example, 4DL_343575_AA1136830.2 in-text corresponds to TRIAE_CS42_4DL_TGACv1_343575_AA1136830.2 Ensembl accession. Full accessions are however reported in the Supplementary Tables as appended to the current study.

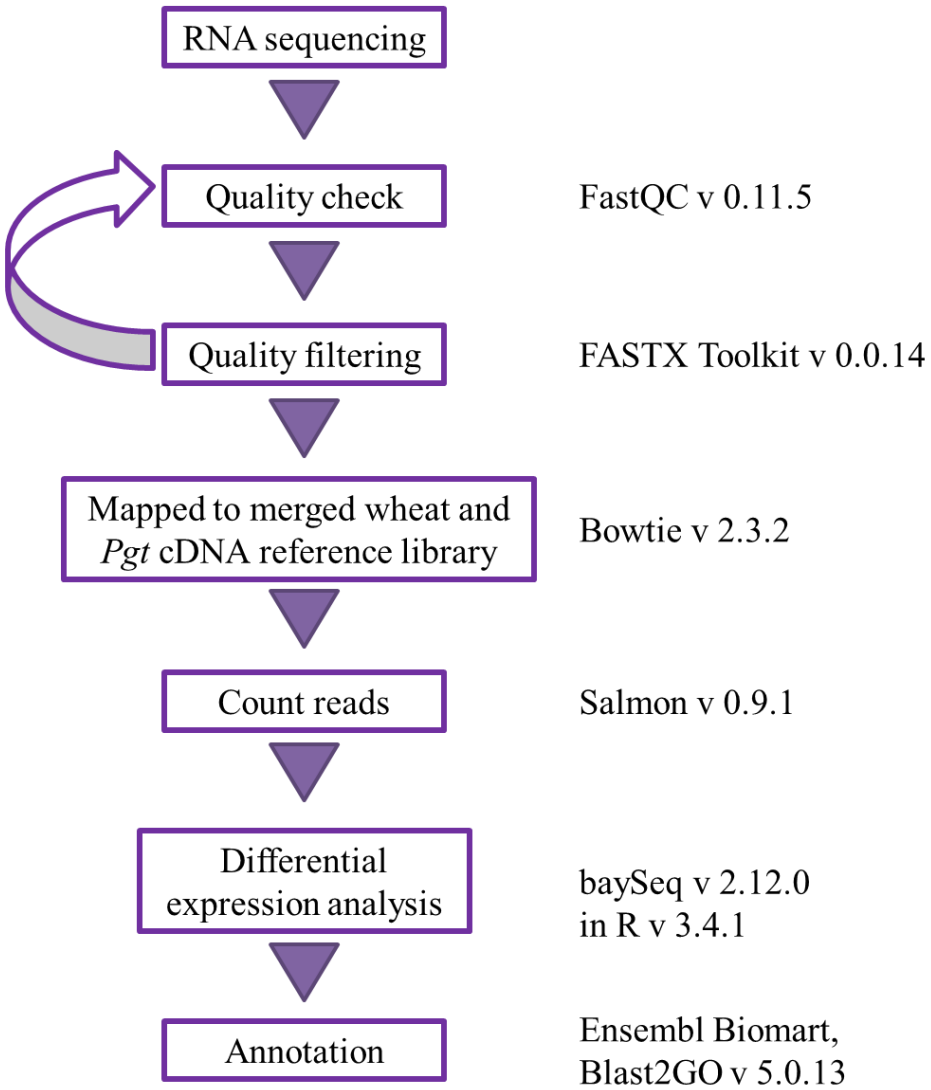

Figure 6.1: Bioinformatics pipeline used in the current study for the analysis of RNA sequencing data. RNA was extracted from triplicated samples at 0, 1 and 3 days post inoculation from adult wheat plants of the 37-07, W1406 and W6979 lines inoculated with *Puccinia graminis* f. sp. *tritici* (*Pgt*). RNA was sequenced using the Ion Torrent Proton™ platform. Steps in the bioinformatics pipeline are noted, with quality checking being repeated after quality filtering. Programmes and versions used for each step are listed to the right.

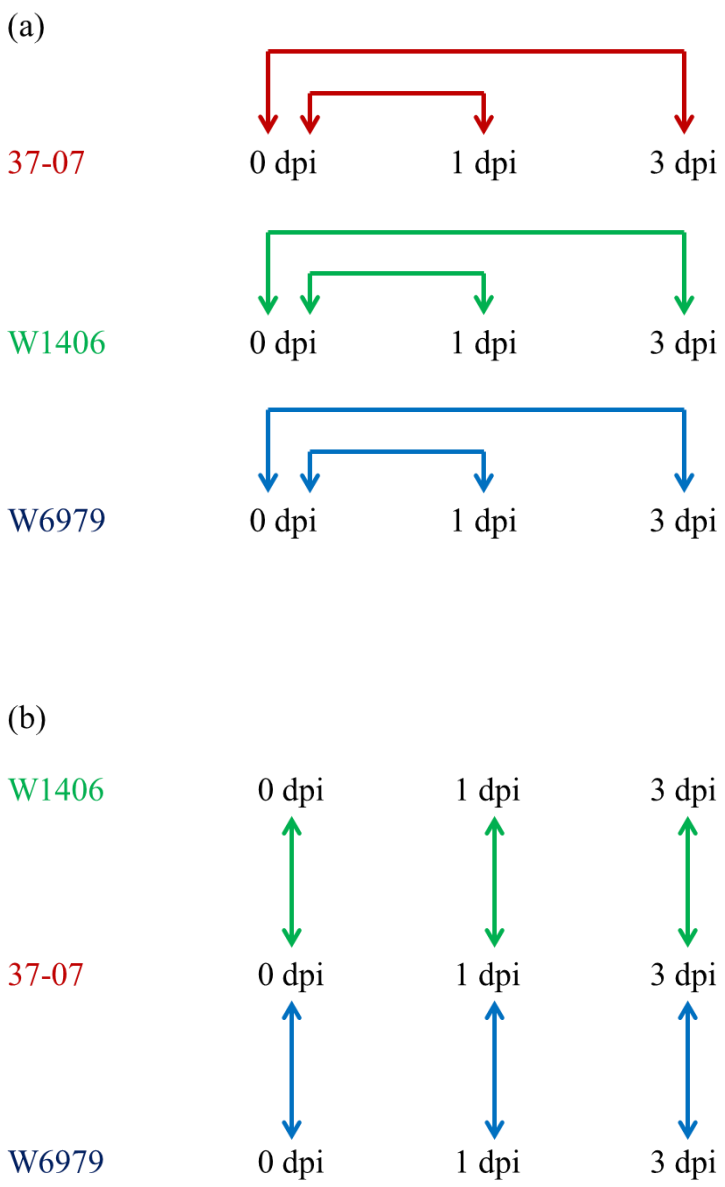

Figure 6.2: Pairwise comparisons for determining differentially expressed transcripts using baySeq with triplicated Ion Torrent datasets. (a) The time vs time comparison analysed 1 and 3 days post inoculation respectively to 0 days post inoculation for each inoculated wheat line. (b) The line vs line comparison analysed the inoculated W1406 and W6979 lines respectively against with the inoculated 37-07 line, at each time point.

6.3 Results

6.3.1 Cross-mapping between wheat and *Puccinia graminis f. sp. tritici* reference transcriptomes

Analysis of wheat and *Pgt* reference transcriptome sequences demonstrated that a small percentage of cross-mapping occurred between the host and pathogen. Results showed that 0.19% of the wheat transcriptome aligned to the *Pgt* transcriptome. Of the *Pgt* transcriptome, 0.24% aligned to the wheat transcriptome. Sequences that cross-mapped coded for histones, tubulins, ubiquitins, peptidyl-prolyl isomerases, glyceraldehyde-3-phosphate dehydrogenases and GTP-binding nuclear proteins. These protein functions are highly conserved in eukaryotes and the genes are expected to share high homology. Included in the cross-mapping reads were also a number of transcripts coding for uncharacterised proteins. Reads aligning to cross-mapping sequences were discarded in further downstream analyses.

6.3.2 Sequencing platform comparison

The number of generated Illumina reads varied from 28.4 to 32.2 million and required no additional quality filtering (Table 6.1). Illumina reads were directly used for mapping to the reference transcriptomes. For the Ion Torrent subset, the mean number of reads was 68.5 million and required quality filtering. Reads shorter than 75 nt were discarded. After filtering, the number of reads in the Ion Torrent subset varied from 43.9 to 73.5 million, with a mean read length of 130 nt. A mean 81.44% (24.4 million) of Illumina reads and 73.05% (42.8 million) of Ion Torrent reads respectively, mapped to the reference transcriptome (Table 6.2).

Using the intensity difference analysis option in SeqMonk, 101 DE transcripts were identified in the Illumina dataset and 530 in the Ion Torrent subset. The PCA of the DE Illumina transcripts showed a cumulative explained variance for the two principal components of 78.9% (Figure 6.3 a) and for the DE Ion Torrent transcripts of 63.5% (Figure 6.3 b). For both PCAs, distinct clusters for 1 and 3 dpi were seen. However, with the Ion Torrent analysis 37-07 at 1 dpi was slightly more removed from the APR lines at that time point than in the Illumina data sets. Of the DE transcripts identified by the two platforms, 97 transcripts were shared (Figure 6.4 a). For the shared DE transcripts, the PCA showed a cumulative explained variance for the two principal components of 81.0% (Figure 6.4 b). Samples from the two different platforms and time points clustered separately.

Table 6.1: Number and lengths of reads for the sequencing platform comparison reported before and after quality trimming. Values for both the Illumina and Ion Torrent platforms are indicated even though the Illumina dataset required no trimming and the number and length of remaining reads are not applicable (na).

Wheat line (days post inoculation)	Total reads (million)	Read length (nucleotides)	Remaining reads (million)	Read length (nucleotides)
Illumina				
37-07 (1)	29.7	75	na	na
37-07 (3)	32.2	75	na	na
W1406 (1)	30.5	75	na	na
W1406 (3)	29.8	75	na	na
W6979 (1)	28.4	75	na	na
W6979 (3)	29.6	75	na	na
Ion Torrent				
37-07 (1)	65.8	25-384	60.6	75-369
37-07 (3)	65.1	25-384	43.9	75-367
W1406 (1)	83.6	25-380	73.5	75-368
W1406 (3)	65.3	25-383	60.7	75-367
W6979 (1)	59.5	25-384	54.1	75-368
W6979 (3)	70.5	25-384	63.0	75-367

Table 6.2: Number and percentage of reads mapped to the reference transcriptomes in the sequencing platform comparison. Reads used for mapping were those that remained after quality control.

Wheat line (days post inoculation)	Remaining reads (million)	Mapped reads (million)	Percentage mapped (%)
Illumina			
37-07 (1)	29.7	23.8	80.33
37-07 (3)	32.2	26.4	82.03
W1406 (1)	30.5	24.6	80.53
W1406 (3)	29.8	24.1	80.91
W6979 (1)	28.4	23.6	83.24
W6979 (3)	29.6	24.1	81.62
Mean	30.0	24.4	81.44
Ion Torrent			
37-07 (1)	60.6	46.6	76.84
37-07 (3)	43.9	36.2	82.43
W1406 (1)	73.5	44.6	60.72
W1406 (3)	60.7	45.2	74.45
W6979 (1)	54.1	37.5	69.35
W6979 (3)	63.0	46.9	74.51
Mean	59.3	42.8	73.05

(a)

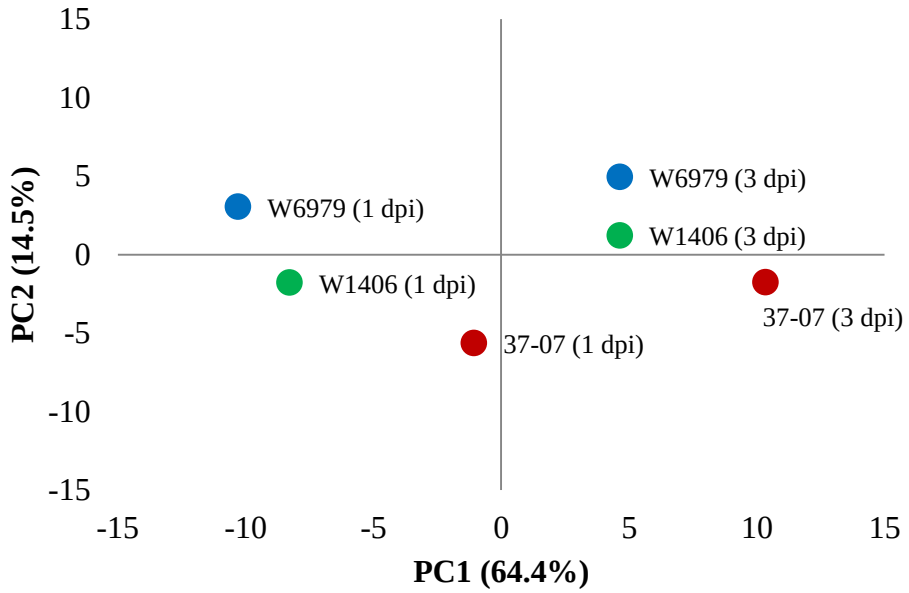

(b)

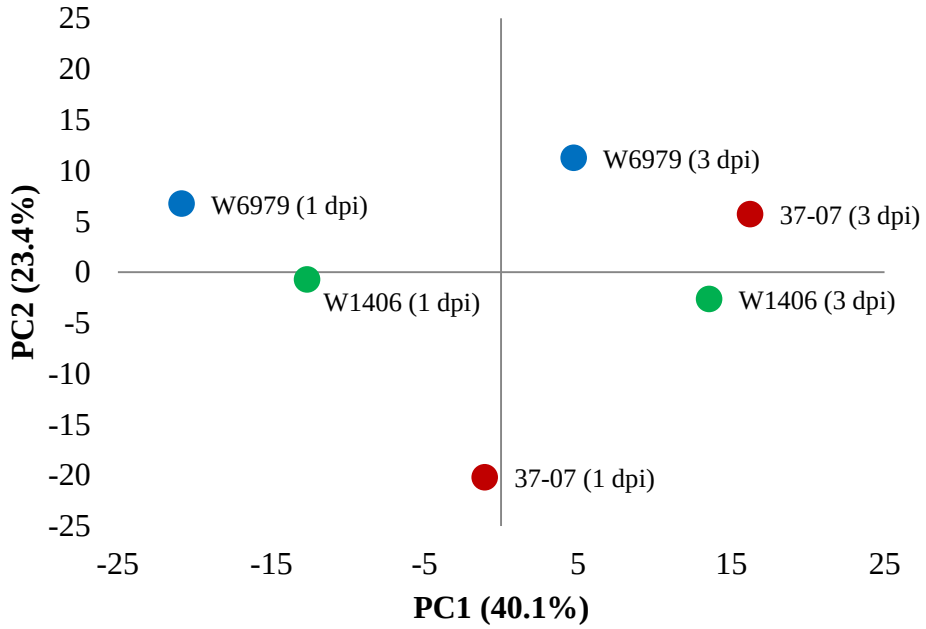

Figure 6.3: Principal component analysis of the differentially expressed transcripts identified by intensity difference analysis. Principal component 1 and 2 (PC1 and PC2) were plotted and percentage variance explained indicated in brackets. The analyses for the 101 DE transcripts identified from the Illumina dataset (a) and the 530 differentially expressed transcripts identified from the Ion Torrent subset (b) are shown separately.

(a)

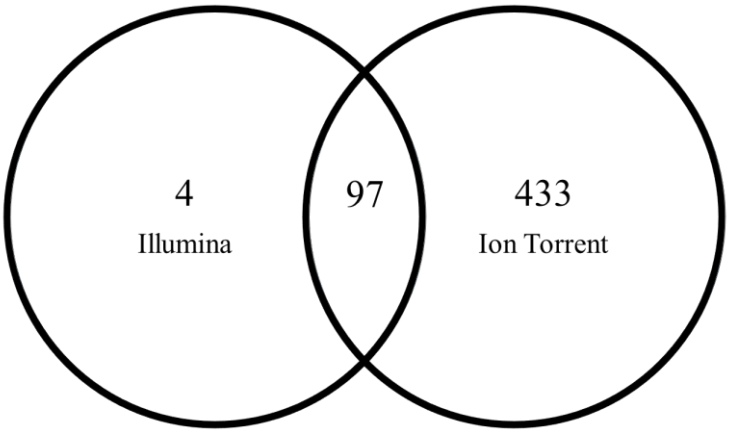

(b)

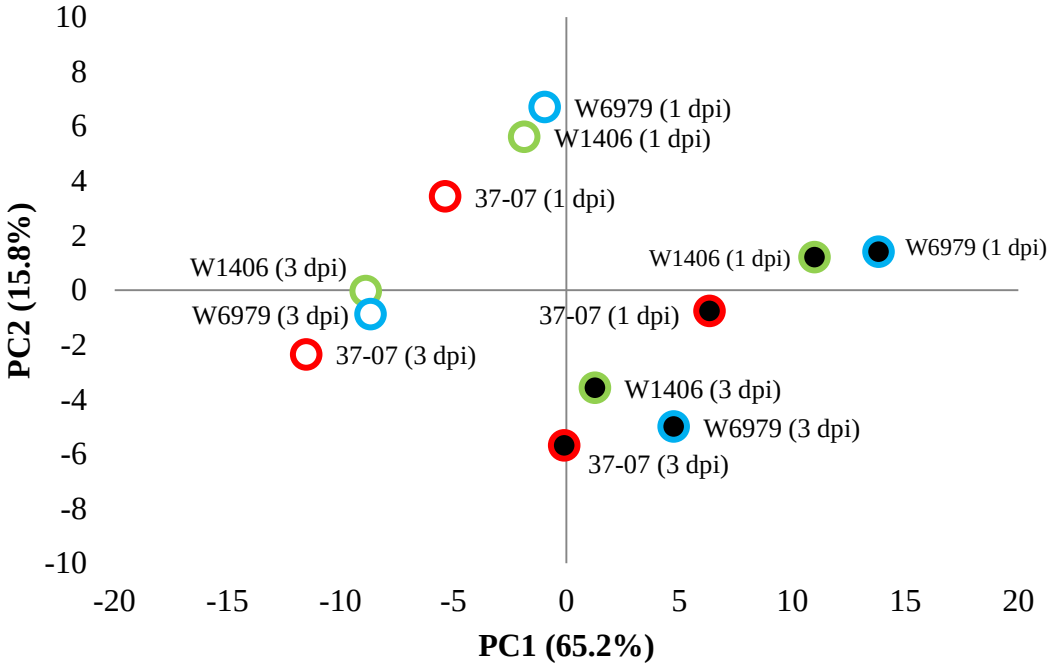

Figure 6.4: Analysis of the shared differentially expressed transcripts identified by intensity difference analysis in the sequencing platform comparison. (a) From the analysis of the Illumina dataset and the Ion Torrent subset a total of 97 differentially expressed transcripts are shared. (b) Principal component analysis of the 97 shared differentially expressed transcripts with percentage variance explained indicated in brackets. The Illumina dataset (○) and Ion Torrent subset (●) are shown separately.

6.3.3 Ion Torrent transcriptomic analysis

For the triplicated Ion Torrent dataset, a mean 61.2 million reads from the 62.0 million raw reads remained after quality filtering (Table 6.3). A mean of 46.1 million (75.66%) of the remaining reads were mapped to the reference transcriptome (Table 6.4).

6.3.3.1 The time vs time comparison

6.3.3.1.1 Differential expression of wheat transcripts

The time vs time comparison reported DE transcripts within each wheat line in relation to 0 dpi. A total of 723 transcripts were DE in the 37-07 dataset, 280 of which were wheat transcripts. In the W1406 dataset a total of 169 DE transcripts were identified, 141 of which were wheat transcripts. Of the 164 DE transcripts in the W6979 dataset, 75 were of wheat origin. The relationship between the different lines with respect to identified DE wheat transcripts is indicated in Figure 6.5.

Clear differences in expression patterns for the DE wheat transcripts were observed over the course of infection. The hierarchical clustering of the DE wheat transcripts and the log_2FC values are reported in Supplementary Tables S1-S3. The hierarchical clustered data for each line was subdivided into five clusters based on the the mean log_2FC for each cluster was reported in Figure 6.6. For each wheat line the log_2FC values were presented with a colour code directly corresponding to the numerical scale. Yellow indicates repressed transcripts and red, green and blue represents induced transcripts for the 37-07, W1406 and W6979 lines respectively. Lighter colour intensity indicates greater log_2FC in the direction of either repression or induction. The largest cluster (E) in the 37-07 line identified 195 transcripts induced at 3 dpi and the second largest cluster (B) showed transcripts induced at 1 dpi, but repressed thereafter (Figure 6.6 a). The largest cluster (C) in W1406 with 99 transcripts, also identified transcripts induced at 3 dpi (Figure 6.6 b). Smaller clusters (D and E) in W1406 showed transcripts induced at 1 dpi, but repressed at 3 dpi. In W6979 the three largest clusters (A-C) indicated a total of 65 transcripts transiently induced at 1 dpi (Figure 6.6 c).

The identities and homologies of the DE wheat transcripts are reported in Supplementary Tables S4-S6 along with associated GO and InterPro accessions. The multilevel distributions of GO accessions are shown in Figures 6.7-6.9 for each line. The GO descriptions indicated a large degree of dissimilarity between lines, but the GO accession corresponding to the ‘oxidation-reduction process’ was the most prevalent in all lines.

Table 6.3: Number and lengths of reads for the triplicated Ion Torrent dataset reported before and after quality trimming. Values for samples from the three independent trials are indicated separately.

Wheat line (days post inoculation)	Total reads (million)	Read length (nucleotides)	Remaining reads (million)	Read length (nucleotides)
Adult trial 1				
37-07 (0)	60.8	25-381	60.4	25-369
37-07 (1)	65.8	25-384	65.7	25-369
37-07 (3)	65.1	25-384	65.0	25-367
W1406 (0)	45.6	25-383	45.3	25-367
W1406 (1)	83.6	25-380	83.4	25-368
W1406 (3)	65.3	25-383	65.1	25-367
W6979 (0)	49.8	25-378	49.5	25-368
W6979 (1)	59.5	25-384	59.3	25-368
W6979 (3)	70.5	25-384	70.4	25-367
Adult trial 2				
37-07 (0)	51.6	25-376	51.3	25-370
37-07 (1)	56.7	25-380	56.4	25-368
37-07 (3)	42.0	25-383	41.7	25-369
W1406 (0)	55.4	25-383	55.1	25-372
W1406 (1)	60.1	25-384	59.7	25-370
W1406 (3)	56.4	25-383	56.1	25-370
W6979 (0)	69.0	25-383	55.2	25-370
W6979 (1)	73.3	25-383	72.8	25-372
W6979 (3)	62.9	25-385	62.6	25-370
Adult trial 3				
37-07 (0)	70.1	25-383	69.7	25-370
37-07 (1)	64.5	25-383	64.0	25-371
37-07 (3)	57.9	25-383	57.4	25-369
W1406 (0)	56.1	25-380	55.8	25-368
W1406 (1)	73.1	25-383	72.5	25-371
W1406 (3)	71.7	25-383	71.2	25-368
W6979 (0)	62.7	25-385	62.4	25-371
W6979 (1)	66.8	25-386	66.4	25-370
W6979 (3)	58.4	25-383	58.0	25-369

Table 6.4: Number and percentage of reads mapped to the reference transcriptomes for the triplicated Ion Torrent dataset. Reads used for mapping were those that remained after quality control.

Wheat line (days post inoculation)	Remaining reads (million)	Mapped reads (million)	Percentage mapped (%)
Adult trial 1			
37-07 (0)	60.4	46.8	77.49
37-07 (1)	65.7	50.4	76.82
37-07 (3)	65.0	54.2	83.46
W1406 (0)	45.3	33.6	74.14
W1406 (1)	83.4	51.7	61.95
W1406 (3)	65.1	48.6	74.57
W6979 (0)	49.5	39.8	80.48
W6979 (1)	59.3	41.4	69.86
W6979 (3)	70.4	52.7	74.83
Adult trial 2			
37-07 (0)	51.3	39.3	76.57
37-07 (1)	56.4	45.2	80.22
37-07 (3)	41.7	32.5	77.88
W1406 (0)	55.1	39.1	71.10
W1406 (1)	59.7	45.2	75.69
W1406 (3)	56.1	44.6	79.50
W6979 (0)	55.2	45.4	82.36
W6979 (1)	72.8	59.4	81.60
W6979 (3)	62.6	50.1	80.14
Adult trial 3			
37-07 (0)	69.7	53.5	76.87
37-07 (1)	64.0	50.1	78.23
37-07 (3)	57.4	41.1	71.65
W1406 (0)	55.8	43.4	77.92
W1406 (1)	72.5	54.4	75.03
W1406 (3)	71.2	48.3	67.80
W6979 (0)	62.4	45.6	73.09
W6979 (1)	66.4	47.3	71.23
W6979 (3)	58.0	42.0	72.40
Mean	61.2	46.1	75.66

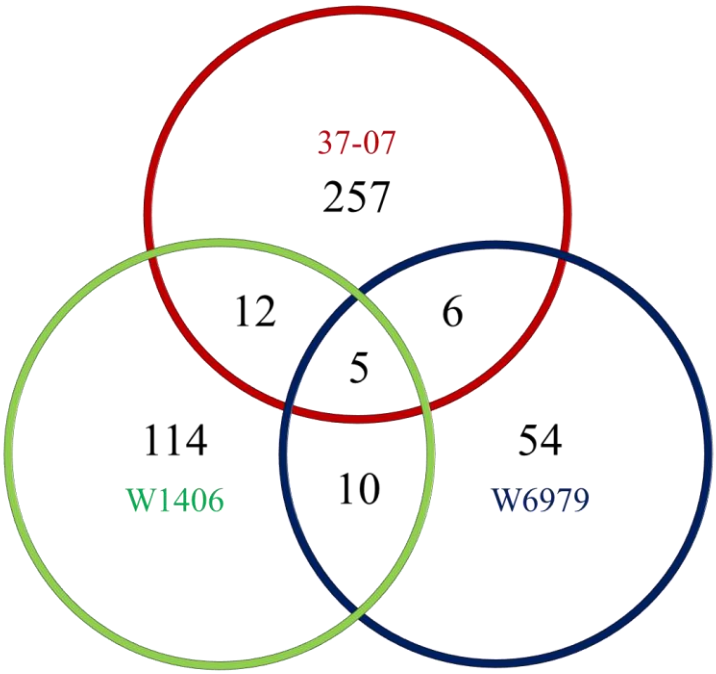

Figure 6.5: Venn diagram showing the number of differentially expressed wheat transcripts in each line for the time vs time comparison. Transcripts were considered differentially expressed with a false discovery rate < 0.05 and a $\log_2$ fold change > 1.0 or $\log_2$ fold change < -1.0 at any time point over the course of infection.

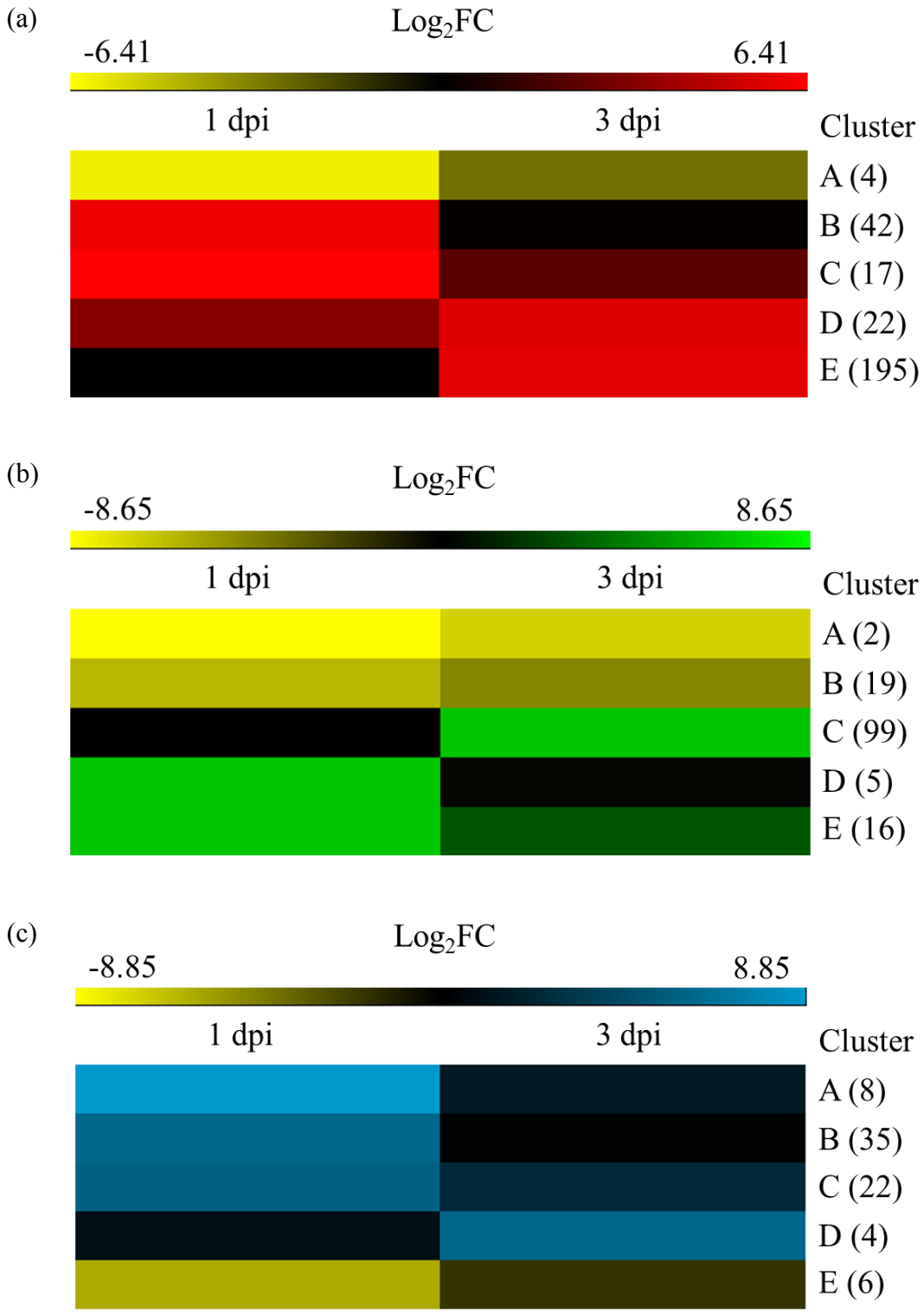

Figure 6.6: Summarised heatmaps of hierarchical clustered wheat transcripts for the time vs time comparison. Colour intensity corresponds to log_2 fold change (FC) values of differentially expressed wheat transcripts at either 1 or 3 days post inoculation (dpi). The 37-07 (a), W1406 (b) and W6979 (c) lines are indicated, with five assigned clusters (A-E) each. In brackets are indicated the number of transcripts in each cluster.

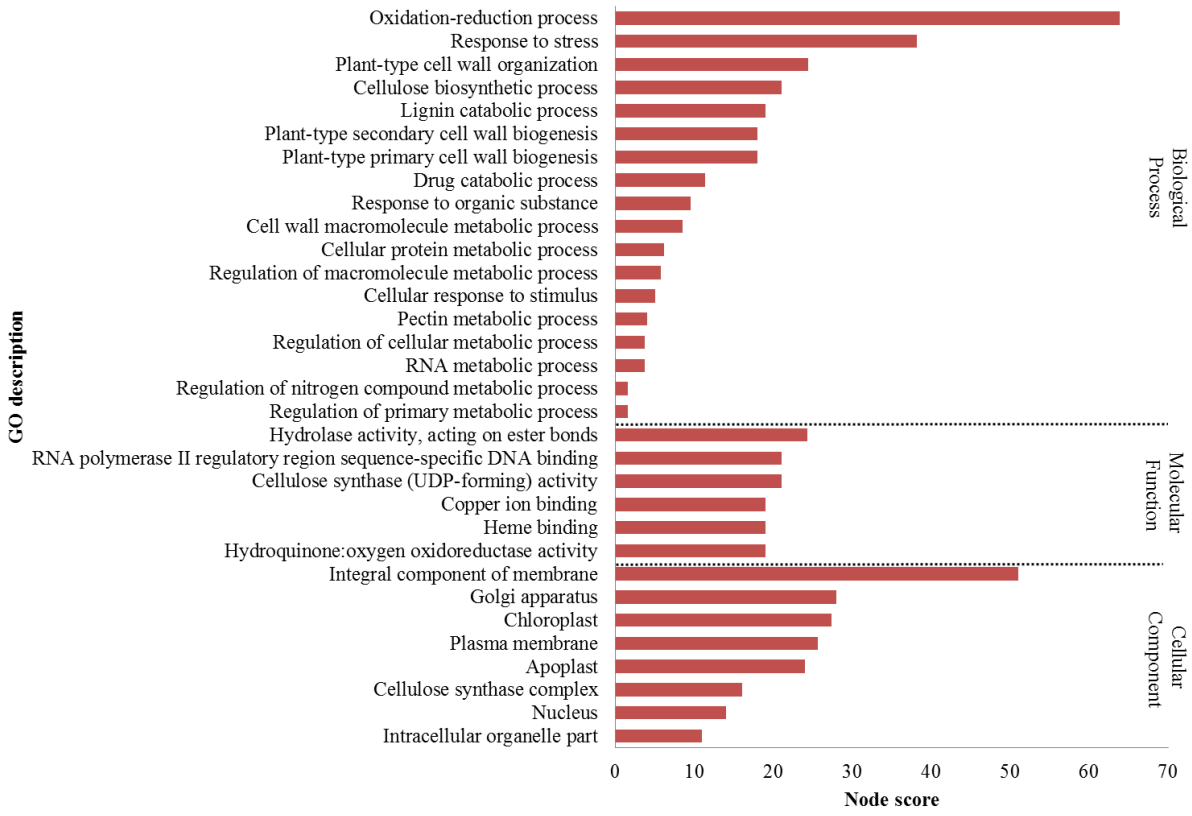

Figure 6.7: Multilevel distribution of gene ontology (GO) annotations in the differentially expressed wheat transcripts in the 37-07 line for the time vs time comparison. Gene ontology descriptions and node scores are reported for gene ontology annotations within the categories of biological process, molecular function and cellular component domains.

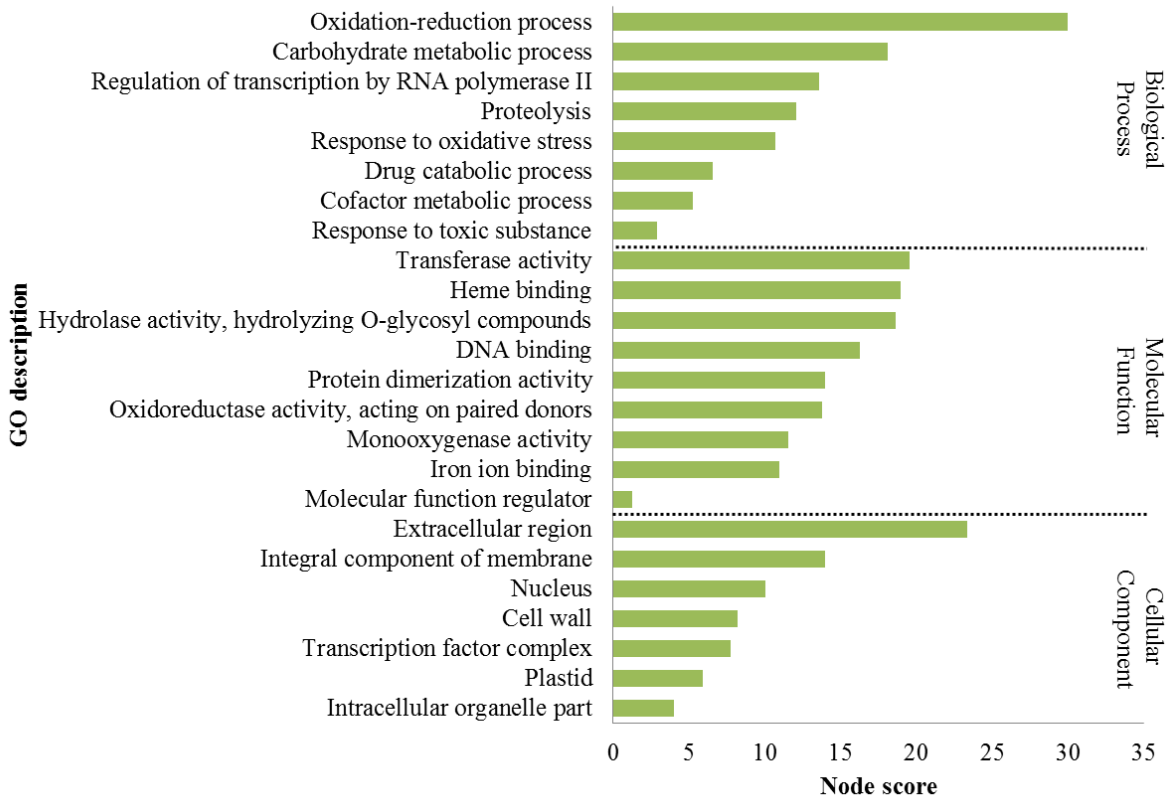

Figure 6.8: Multilevel distribution of gene ontology (GO) annotations in the differentially expressed wheat transcripts in the W1406 line for the time vs time comparison. Gene ontology descriptions and node scores are reported for gene ontology annotations within the categories of biological process, molecular function and cellular component domains.

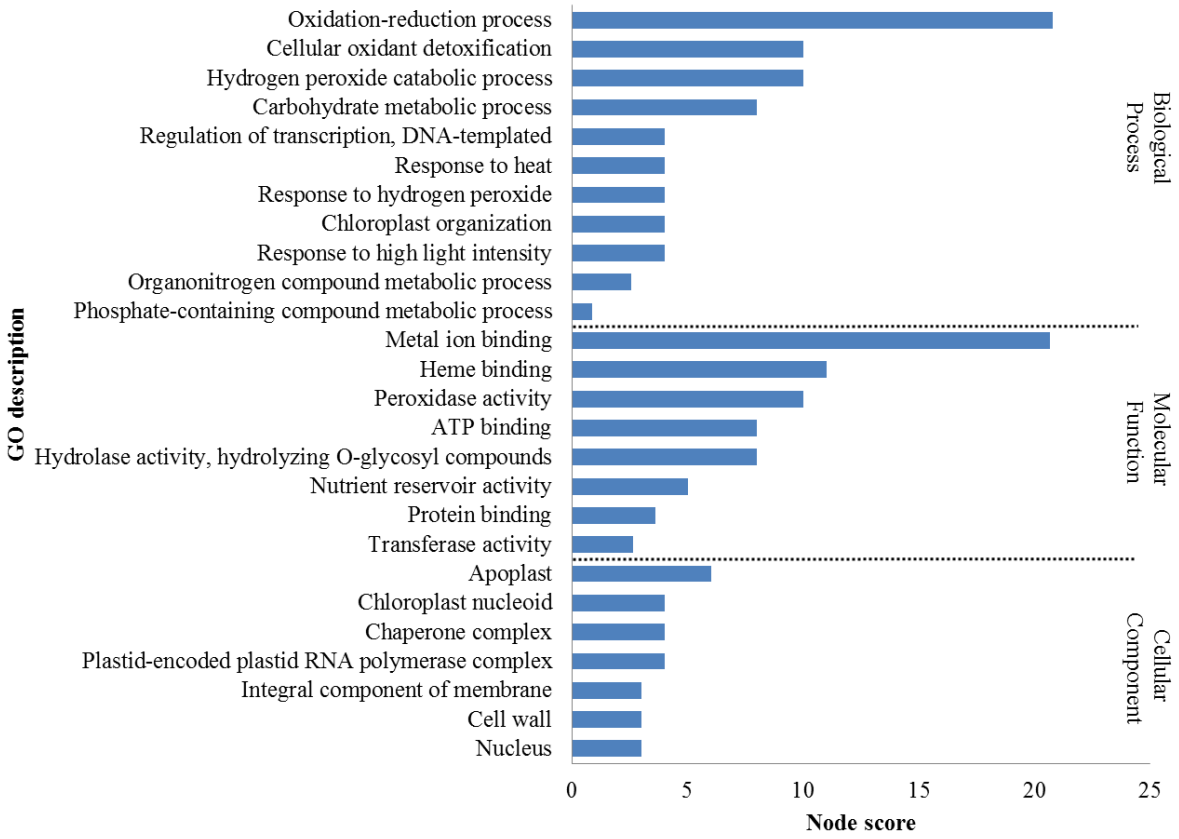

Figure 6.9: Multilevel distribution of gene ontology (GO) annotations in the differentially expressed wheat transcripts in the W6979 line for the time vs time comparison. Gene ontology descriptions and node scores are reported for gene ontology annotations within the categories of biological process, molecular function and cellular component domains.

The defence response in the *Pgt*-inoculated wheat lines was illustrated by the distribution of GO accessions, particularly when focussing on those classified under the biological processes category. In the 37-07 line, the GO descriptions pointing to the maintenance of the plant cell wall dominated and included the cellulose biosynthetic process, plant-type secondary cell wall biogenesis and the pectin metabolic process (Figure 6.7). In contrast, W1406 included diverse GO descriptions such as the regulation of transcription by RNA polymerase II, proteolysis and the response to oxidative stress (Figure 6.8). In W6979 the GO descriptions pointed to the oxidative burst and included cellular oxidant detoxification, hydrogen peroxide catabolic processes and responses to hydrogen peroxide (Figure 6.9).

While a number of DE transcripts were uniquely induced in each wheat line, others were shared. Transcripts encoding sucrose synthases, cellulose synthases and an arginine decarboxylase were unique to 37-07. Two Bowman-Birk trypsin inhibitor-like proteins and two other protease inhibitor-like proteins were encoded by transcripts unique to W1406. Transcripts encoding salicylic acid-binding protein 2-like and a putative invertase inhibitor were unique to W6979. Transcripts that were shared included those encoding chalcone synthase occurring in both 37-07 and W1406 and Wheatwin-1 occurring in both 37-07 and W6979. Glucan endo-1,3-beta-D-glucosidase encoding transcripts occurred in all three lines.

DE transcripts encoding peroxidases were common in all lines, but the expression patterns of these transcripts showed clear differences between lines. In the 37-07 line no transcripts encoding peroxidases were detected at 1 dpi, but numerous were induced at 3 dpi (Figure 6.10 a). W1406 induced peroxidase encoding transcripts either at 1 or 3 dpi but others were induced over the course of infection (Figure 6.10 b). Transcripts encoding peroxidases in W6979 were all induced at 1 dpi, but had much lower expression levels at 3 dpi (Figure 6.10 c).

The time vs time comparison identified few putative resistance-associated protein encoding transcripts. No NB-LRR proteins were DE in any of the wheat lines. ABC transporters, START kinases and hexose transporters were not DE in either 37-07 or W6979. Likewise, ABC transporters and hexose transporters were not DE in W1406. However, W1406 had a single DE transcript (2BL_130389_AA0410180.4) encoding a protein with a START-like domain that was induced at 3 dpi. The function of the encoded peptide is unknown in wheat, but it showed homology to the major latex protein (MLP)-like 423 in *Arabidopsis*.

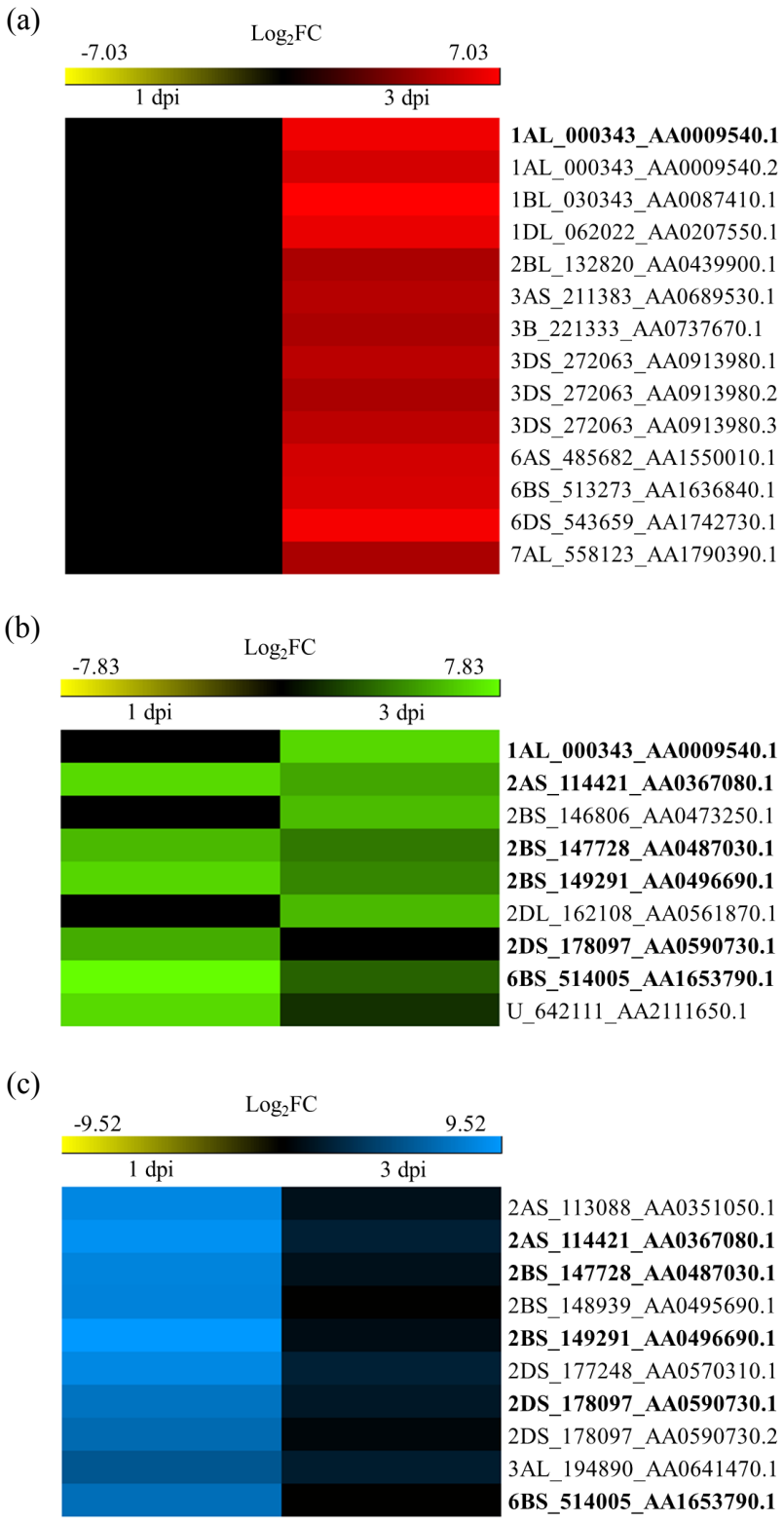

Figure 6.10: Heatmaps of differentially expressed transcripts in time vs time comparison encoding wheat peroxidases. Colour intensity corresponds to log_2 fold change (FC) values of putative peroxidase encoding transcripts at either 1 or 3 days post inoculation (dpi) reported for the 37-07 (a), W1406 (b) and W6979 (c) lines. Transcripts in **bold** are shared between two wheat lines but no transcripts were shared by all three lines.

6.3.3.1.2 Differential expression of *Puccinia graminis f. sp. tritici* transcripts

The relationship between DE *Pgt* transcripts in the different wheat lines is shown in Figure 6.11. A total of 723 transcripts were DE in the 37-07 dataset, 443 of which were *Pgt* transcripts. In the W1406 dataset a total of 169 DE transcripts were identified, 28 of which were *Pgt* transcripts. Of the 164 DE transcripts in the W6979 dataset, 89 were from *Pgt*. Fungal transcripts therefore constituted 61.2% (37-07), 54.2% (W1406) and 16.5% (W6979) of the total DE transcripts in each line.

The induction of *Pgt* transcripts relative to 0 dpi was a near uniform feature of identified expression patterns. The hierarchical clustered DE *Pgt* transcripts and the log_2FC values are reported in Supplementary Tables S7-S9. As before the hierarchical clustered *Pgt* expression data in each line was subdivided into five clusters clusters based on the log_2FC value. The mean log_2FC for each cluster is reported in Figure 6.12 as a summarised heatmap. The log_2FC values for each respective wheat line were presented with colour code as before, with yellow indicating repressed transcripts and red, green and blue representing induced transcripts. The largest cluster (D) of Pgt transcripts in 37-07 identified 232 transcripts induced to higher levels at 3 dpi as compared to 1 dpi (Figure 6.12 a).The second (C) and third (E) largest clusters likewise showed transcripts induced at 3 dpi, but only marginally so at 1 dpi. The largest clusters (D and E) for *Pgt* in W1406 with 21 transcripts in total, identified transcripts induced at similar levels at 1 and 3 dpi (Figure 6.12 b). In contrast, for W6979 all clusters, except cluster A, show lower levels at 3 dpi than 1 dpi, though in some clusters this decrease was only marginal (Figure 6.12 c).

Identities and homologies of DE *Pgt* transcripts are reported in Supplementary Tables S10-S12 along with associated GO and InterPro accessions. The multilevel distributions of GO accessions are shown in Figures 6.13-6.15 for each line. The putative functions of encoded proteins are largely unknown for most *Pgt* transcripts. Of the DE transcripts, 56.9%, 92.9% and 84.3% encoded hypothetical proteins in the 37-07, W1406 and W6979 lines, respectively. Additionally, 16.3% of DE transcripts in 37-07 encoded ribosomal proteins. In contrast, *Pgt* transcripts encoding transcription factors were prominent in W1406 (Figure 6.14). Putative proteins involved in proteolysis and the response to oxidative stress were dominant in W6979 (Figure 6.15).

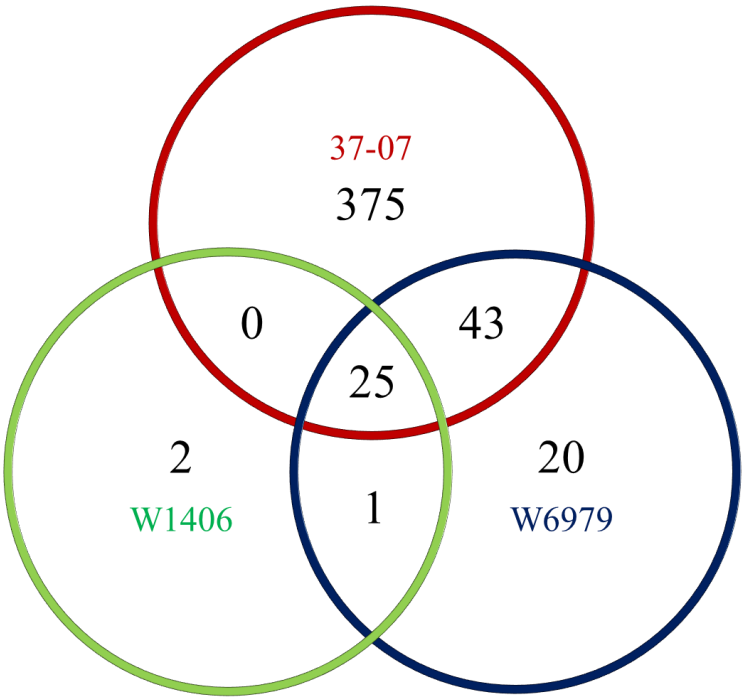

Figure 6.11: Venn diagram showing the differentially expressed *Puccinia graminis* f. sp. *tritici* transcripts in each line for the time vs time comparison. Transcripts were considered differentially expressed with a false discovery rate < 0.05 and a $\log_2$ fold change > 1.0 or $\log_2$ fold change < -1.0 at any time point over the course of infection.

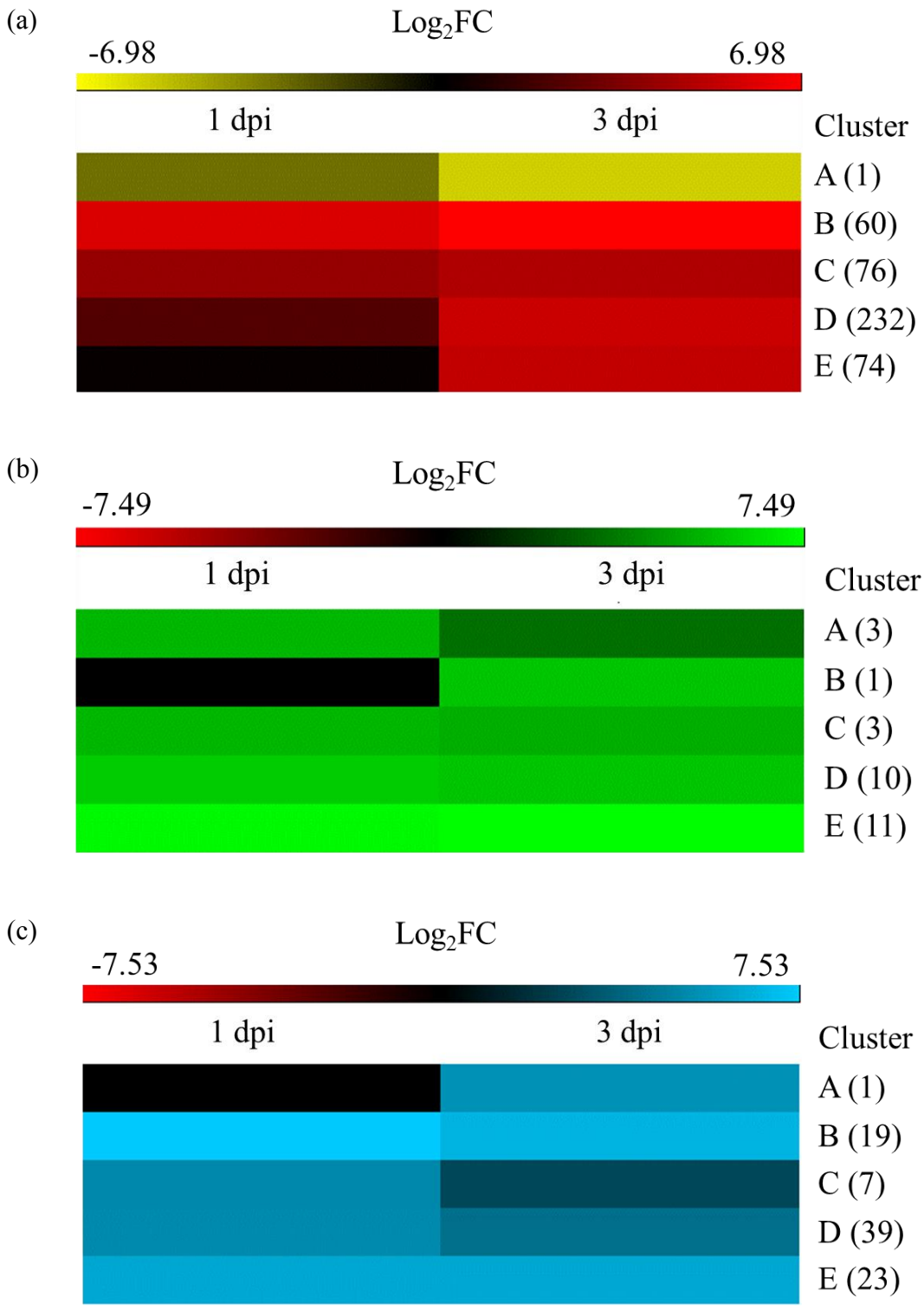

Figure 6.12: Summarised heatmaps of hierarchical clustered *Puccinia graminis* f. sp. *tritici* transcripts for the time vs time comparison. Colour intensity corresponds to log_2 fold change (FC) values of differenttally expressed wheat transcripts at either 1 or 3 days post inoculation (dpi). The 37-07 (a), W1406 (b) and W6979 (c) lines are indicated, with five assigned clusters (A-E) each. In brackets are indicated the number of transcripts in each cluster.

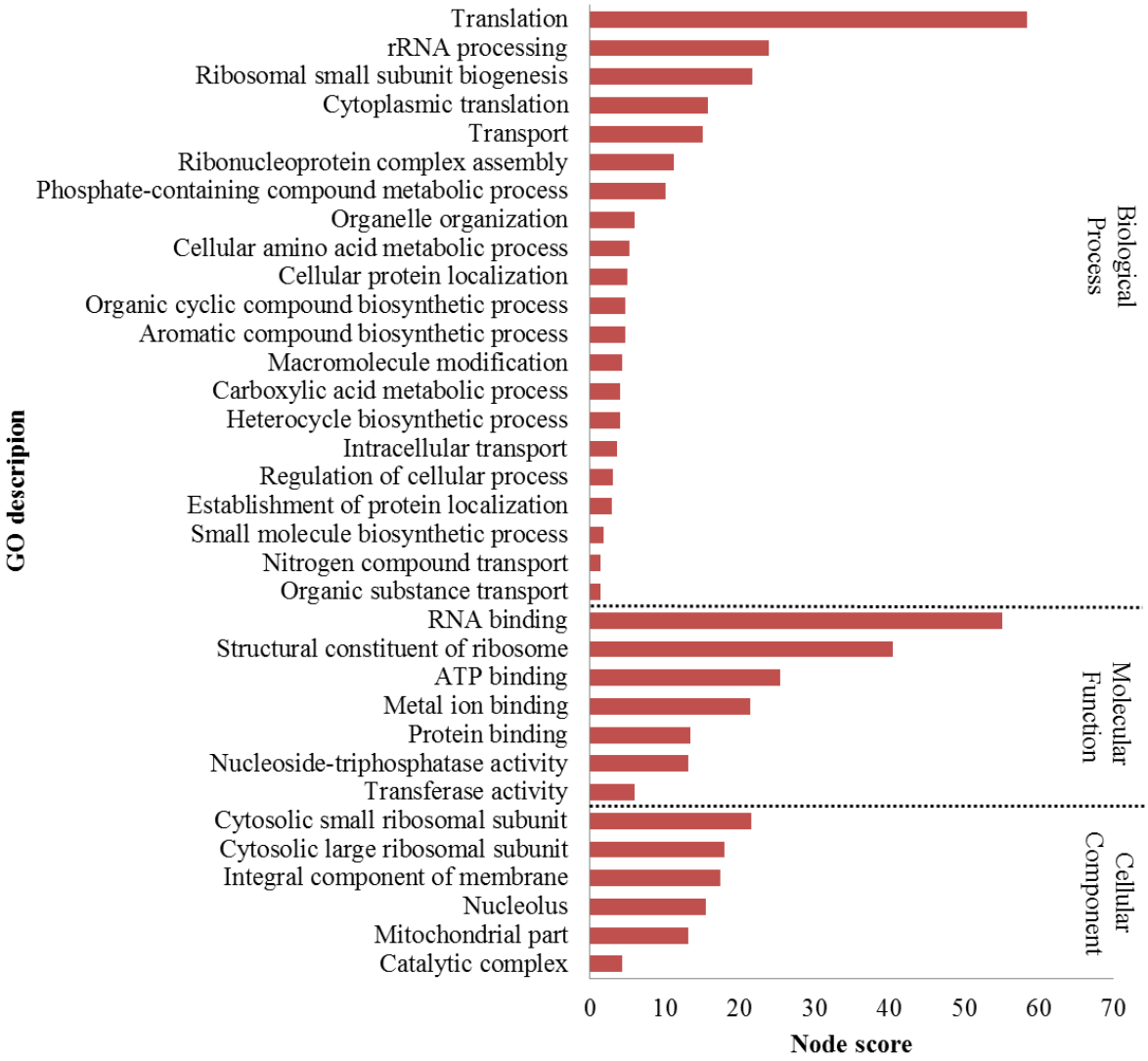

Figure 6.13: Multilevel distribution of gene ontology (GO) annotations in the differentially expressed *Puccinia graminis* f. sp. *tritici* transcripts in the 37-07 line for the time vs time comparison. Gene ontology descriptions and node scores are reported for gene ontology annotations within the biological process, molecular function and cellular component domains.

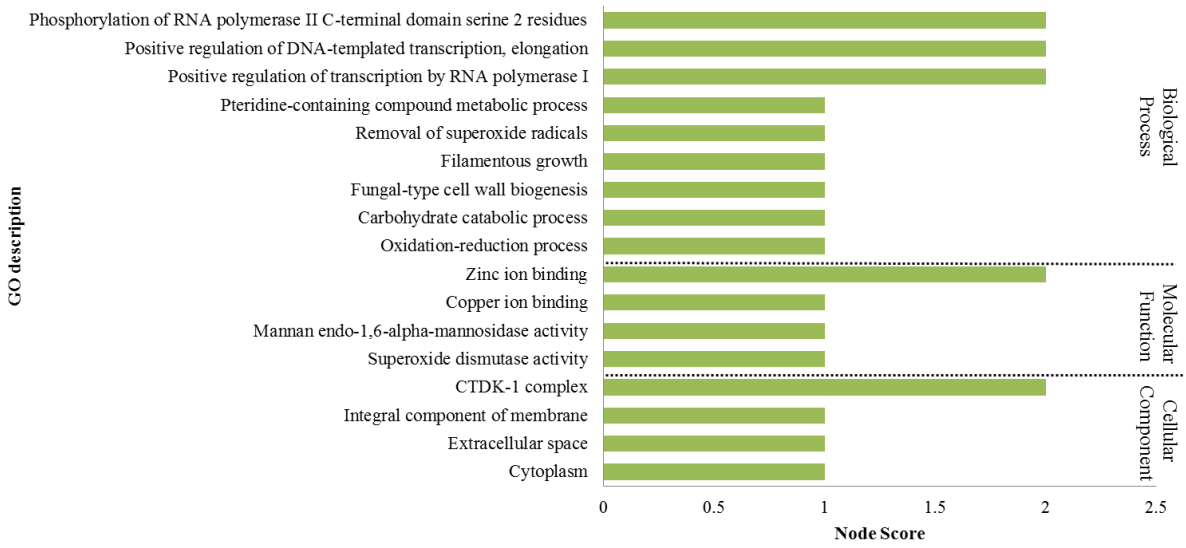

Figure 6.14: Multilevel distribution of gene ontology (GO) annotations in the differentially expressed *Puccinia graminis* f. sp. *tritici* transcripts in the W1406 line for the time vs time comparison. Gene ontology descriptions and node scores are reported for gene ontology annotations within the biological process, molecular function and cellular component domains.

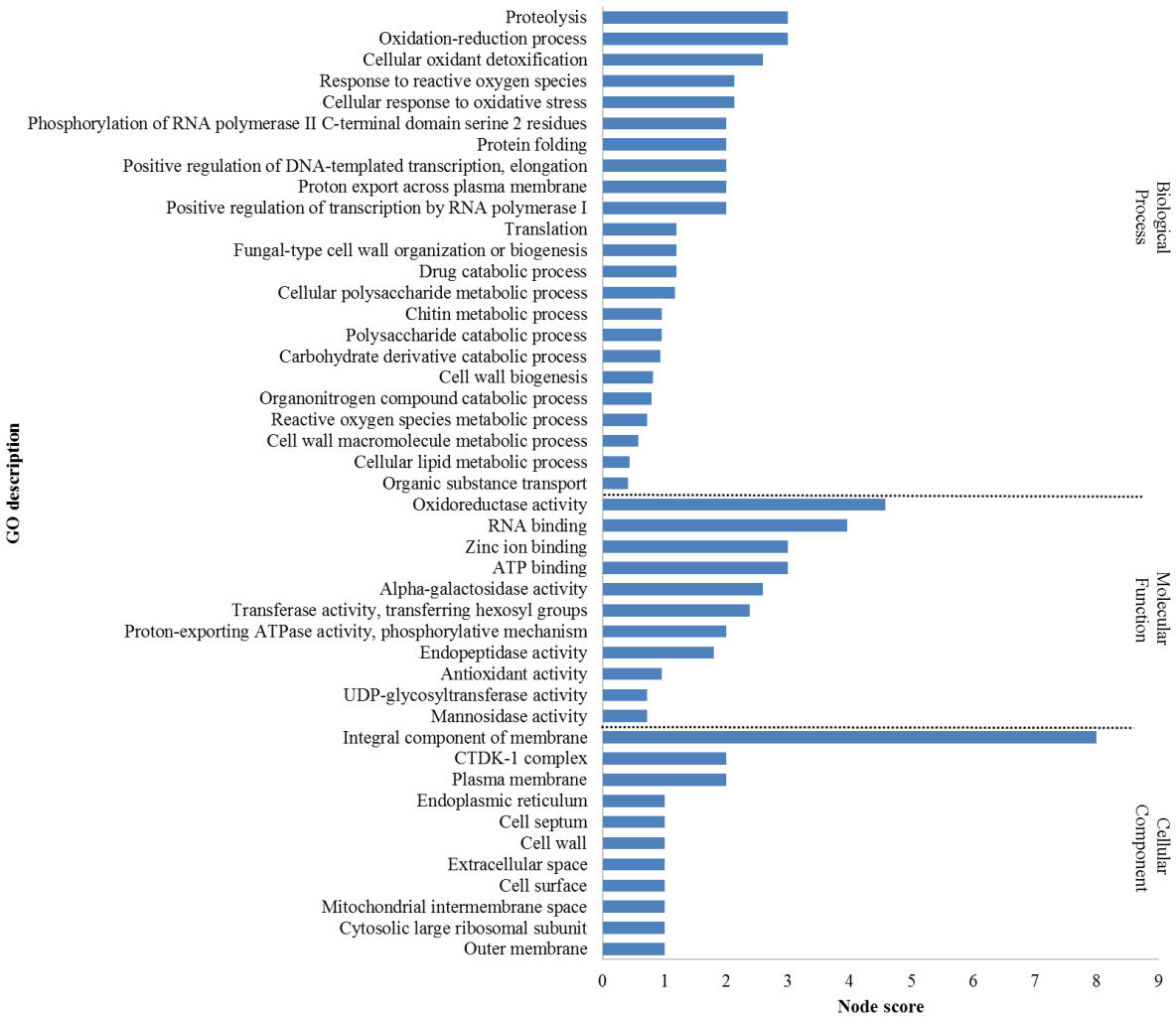

Figure 6.15: Multilevel distribution of gene ontology (GO) annotations in the differentially expressed *Puccinia graminis* f. sp. *tritici* transcripts in the W6979 line for the time vs time comparison. Gene ontology descriptions and node scores are reported for gene ontology annotations within the biological process, molecular function and cellular component domains.

The expression of *Pgt* transcripts showed a number of unique patterns in each of the wheat lines. A large number of annotated transcripts were unique to 37-07 and included an argininosuccinate synthase, a phosphoglycerate kinase and a pyruvate carboxylase. In W6979, transcripts encoding a bleomycin hydrolase, a hypothetical class III chitin synthase and a saccharopepsin were unique. Among the 25 transcripts DE in all three wheat lines only two were annotated, encoding an *L*-iditol 2-dehydrogenase and a copper/zinc superoxide dismutase. The only *Pgt* transcript repressed over the course of infection was a transcript encoding an uncharacterised protein unique to 37-07.

To further classify the DE *Pgt* transcripts, putative effectors and their localization in the host plant were analysed (Supplementary Tables S13-S15). In 37-07, 80 putative effectors were predicted, two in W1406 and 19 in W6979. The relationship of the DE effectors in the different wheat lines is shown in Figure 6.16. The expression of putative effectors over the course of infection was variable and did not group exclusively within any of the previously identified clusters (Figure 6.11), indicating variable expression of effector encoding transcripts.

In parallel with the data for all DE *Pgt* transcripts, most predicted effector transcripts encoded uncharacterised proteins and also a number of ribosomal associated proteins. Of the DE effectors present in the 37-07 line a copper/zinc superoxide dismutase, predicted to be localised to the host mitochondrion, was found. A transcript encoding a TdcF protein, putatively localised to the host chloroplast and mitochondrion, and another encoding unique argininosuccinate synthase were also found. A single effector encoding transcript was unique to W1406 and two to W6979, both encoding uncharacterised proteins. The only effector identified in all three wheat lines (EHS63013) was induced at 1 and 3 dpi. The transcript encoded an uncharacterised protein that was putatively localised to the host nucleus.

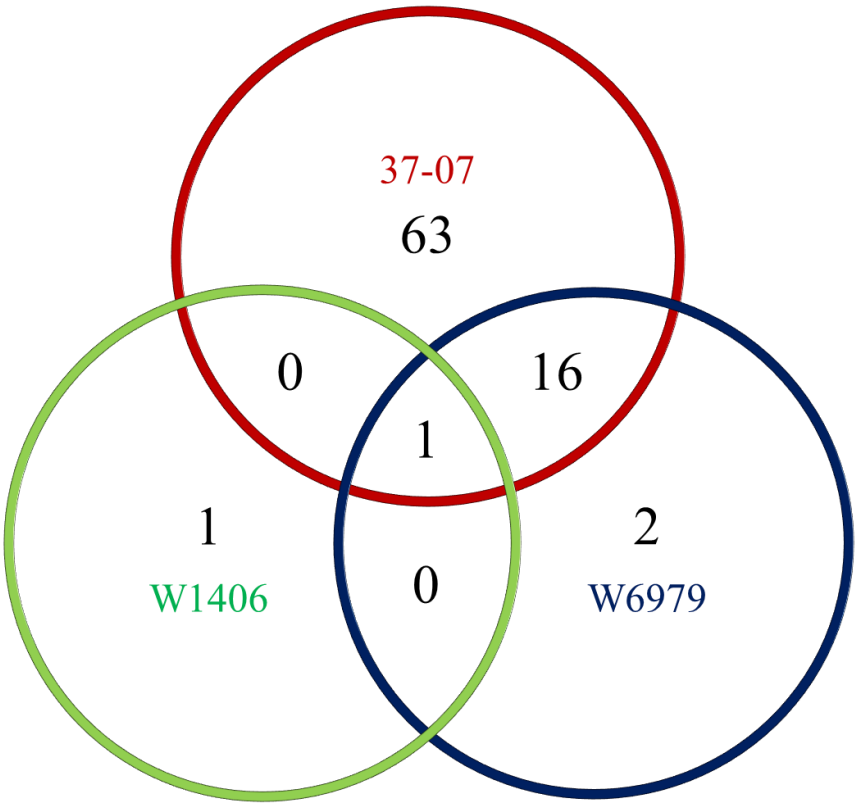

Figure 6.16: Venn diagram of the number of differentially expressed *Puccinia graminis* f. sp. *tritici* transcripts in each wheat line sample for the time vs time comparison that encoded predicted effector proteins. Transcripts were considered differentially expressed with a false discovery rate < 0.05 and a $\log_2$ fold change > 1.0 or $\log_2$ fold change < -1.0 at any time point over the course of infection. Effectors were predicted by EffectorP (Sperschneider *et al.*, 2018).

6.3.3.2 The line vs line comparison

6.3.3.2.1 Differentially expressed wheat transcripts

The line vs line comparison reports DE transcripts within the two APR lines in relation to the susceptible 37-07 line. In the W1406 dataset, 1741 DE wheat transcripts were identified and in W6979, 1432 DE wheat transcripts. The relationship of the two APR lines with respect to the identified DE wheat transcripts is shown in Figure 6.17 and indicated that 448 transcripts were shared.

The hierarchical clustered DE wheat transcripts and the log_2FC values are reported in Supplementary Tables S16 and S17. The hierarchical clustered data for each line was subdivided into nine clusters clusters based on the log_2FC value. The mean log_2FC for each cluster is reported in Figure 6.18 as a summarised heatmap. For each APR lines the log_2FC values were presented on colour code comparable to before. Red indicates repressed transcripts, i.e. those induced in the 37-07 line and green and blue represents induced transcripts in the W1406 and W6979 lines respectively. Lighter colour intensity indicates greater log_2FC in the direction of either one or the other compared wheat lines. The largest cluster (G) in W1406 identified 504 transcripts induced at 3 dpi (Figure 6.18 a). The second and fourth largest clusters (C and D) showed 444 and 165 transcripts respectively that were repressed over the course of infection, but the third largest cluster (H) identified 376 transcripts induced over the course of infection (Figure 6.18 a). In W6979 (Figure 6.18 b) the largest cluster (I) included a total of 429 transcripts repressed over the course of infection, while in the second largest cluster (E) 421 transcripts were induced over the course of infection.

The Ensembl descriptions of DE wheat transcripts are reported in Supplementary Tables S18 and S19 with their associated InterPro accessions. In W1406, 89.4% of the 1741 DE transcripts are uncharacterised and 91.3% of the 1458 DE transcripts from W6979. A number of features of DE transcripts of the time vs time comparison were repeated in the line vs line comparison such as the prominence of peroxidases and identification of a Bowman-Birk trypsin inhibitor-like protein unique to W1406. However, a number of transcripts unique to the line vs line comparison were also found. Transcripts encoding bidirectional sugar transporter (SWEET) proteins were present in both lines, but expression patterns were variable over the course on infection. One SWEET protein encoding transcript was downregulated in the APR lines. Other SWEET protein encoding transcripts in W1406 were

typically not detected at 0 and 1 dpi, but induced at 3 dpi. Contrastingly, the SWEET protein encoding transcripts in W6979 were induced over the course of infection. A transcript encoding a WRKY45-like transcription factor was shared by the two APR lines and was induced to high levels at 1 dpi, but decreased thereafter. Transcripts encoding receptor-like serine/threonine protein kinase 2 were unique to W1406 and highly induced at 3 dpi.

The line vs line comparison identified a number of NB-LRR protein encoding transcripts in the APR lines that are reported in Supplementary Tables S20 and S21. A total of 181 were identified in W1406 and 158 in W6979, with 57 shared (Figure 6.19). The coiled-coil (CC)-NB-LRR subclass made up the majority of identified NB-LRR protein encoding transcripts and accounted for 91.1% in W1406 and 93.0% in W6979. The Toll/interleukin receptor-like (TIR)-NB-LRR subclass was absent. Predicted protein domains in the unclassified NB-LRR protein encoding transcripts showed the loss of a N-terminal domain that resulted in this classification. The chromosomal positions of DE NB-LRR protein encoding transcripts in the APR lines are shown in Figure 6.20. In W1406, the largest number of NB-LRR protein encoding transcripts was predicted to locate to chromosomes 1A, 1D, 2B, 2D and 4B. In W6979 the largest number were predicted to locate to chromosomes 1B, 2B, 3B, 5B and 7A.

To identify possible APR genes, the DE transcripts were searched for predefined InterPro accessions. Four putative ABC transporter transcripts were DE in W1406: 2AL_094030_AA0291350.1, 2AL_094030_AA0291350.2, 2BS_147394_AA0482680.1 and 7AL_556235_AA1758970.1. The expression of these transcripts was variable over the course of infection. Twenty four START domain encoding transcripts were DE and were encoded by 4BS_329705_AA1103430 and were universally repressed over the course of infection. An additional START-like domain encoding transcript, 2AL_094002_AA0290990.1, was induced over the course of infection. No DE putative hexose transporter encoding transcripts were identified in W1406.

For W6979, the DE transcripts were likewise searched for predefined InterPro accessions. Eight DE transcripts encoding putative ABC transporter proteins were encoded by four genes in W6979: 2AS_114278_AA0365810, 2BS_146633_AA0469740, 2BS_147394_AA0482680 and 2DS_177216_AA0569300. Only the two transcripts from the gene on chromosome 2D were induced over the course of infection. No DE putative START domain or hexose transporter encoding transcripts were identified in W6979. None of the identified protein domains coupled to APR were shared between W1406 and W6979.

Figure 6.17: Venn diagram of the number of differentially expressed wheat transcripts in each wheat line sample for the line vs line comparison. Transcripts were considered differentially expressed with a false discovery rate < 0.05 and a $\log_2$ fold change > 1.0 or $\log_2$ fold change < -1.0 at any time point over the course of infection.

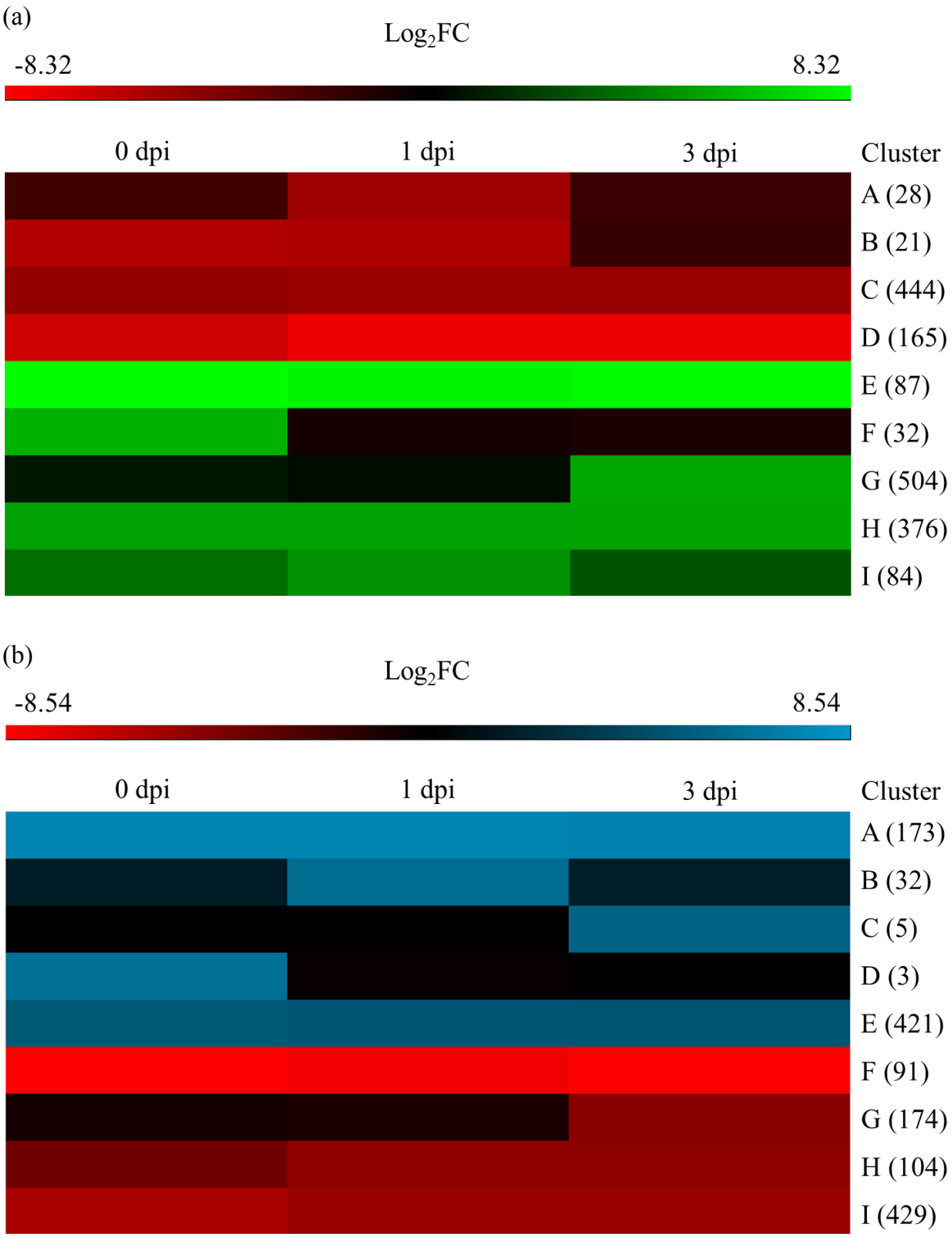

Figure 6.18: Summarised heatmaps of hierarchical clustered wheat transcripts for the line vs line comparison. Colour intensity corresponds to $\log_2$ fold change (FC) values of differentially expressed wheat transcripts at 0, 1 or 3 days post inoculation (dpi). The W1406 (a) and W6979 (b) and transcripts assigned to nine clusters (A-I) each. In brackets are indicated the number of transcripts in each cluster

Figure 6.19: Venn diagram of the number of differentially expressed wheat transcripts in each wheat line for the line vs line comparison that encoded predicted nucleotide-binding and a leucine-rich repeat proteins. Transcripts were considered differentially expressed with a false discovery rate < 0.05 and a $\log_2$ fold change > 1.0 or $\log_2$ fold change < -1.0 at any time point over the course of infection. Nucleotide-binding and a leucine-rich repeat domains were predicted by NLR-Parser (Steuernagel *et al.*, 2015).

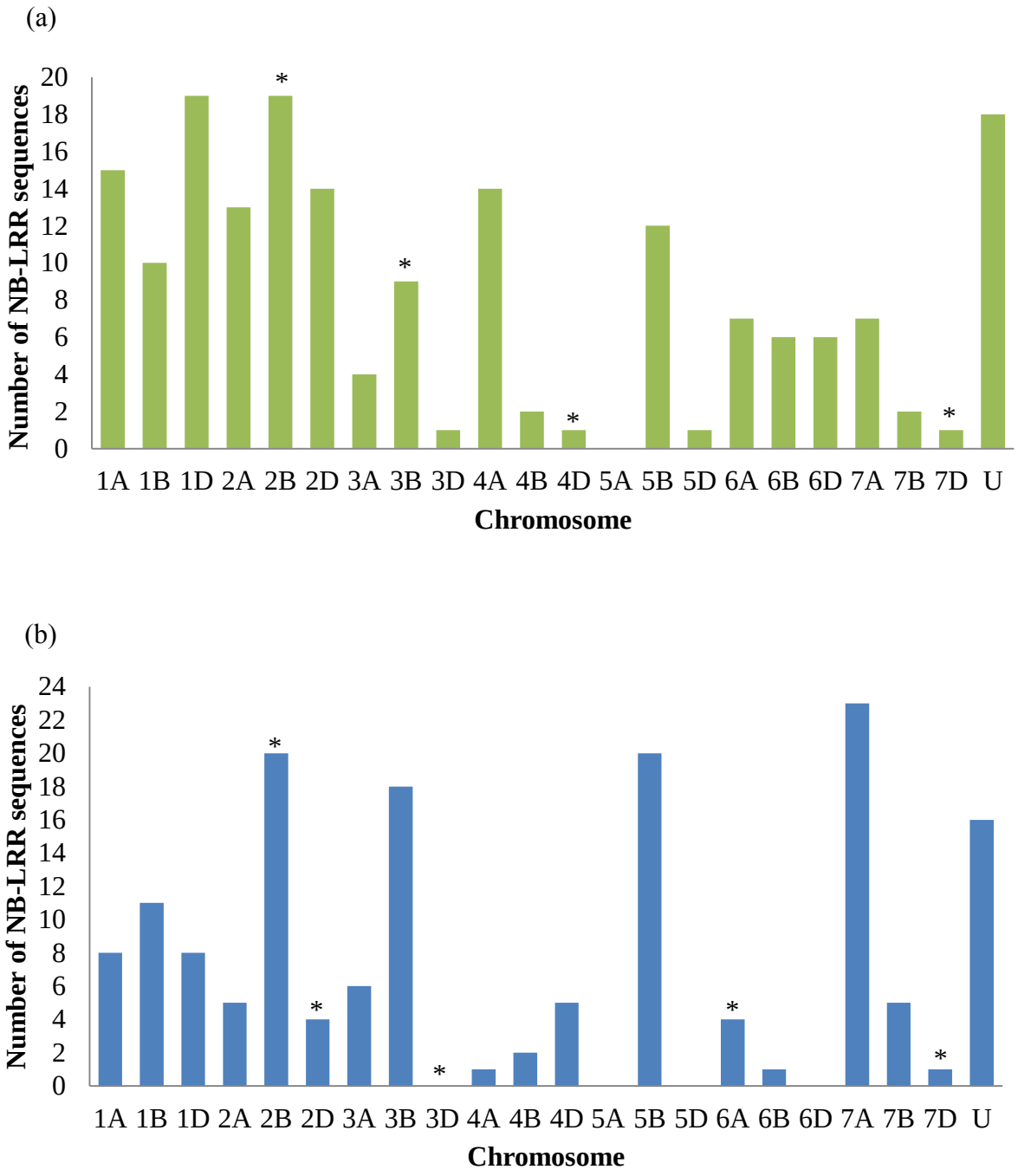

Figure 6.20: Chromosomal distribution of differentially expressed wheat transcripts in each wheat line for the line vs line comparison that encoded predicted nucleotide-binding and a leucine-rich repeat proteins. Chromosomal positions were based on the Centre for Genome Analysis Chinese Spring wheat genome hosted by Ensembl. Unknown chromosome positions are specified as 'Unclassified' (U). Nucleotide-binding and a leucine-rich repeat domains were predicted by NLR-Parser (Steuernagel *et al.*, 2015). The W1406 (a) and W6979 (b) lines are indicated. Chromosomes that are the location of QTL identified by Prins et al. (2016) are indicated with an asterisk (*).

DE transcripts may potentially identify the contribution to gene expression influenced by the stem rust resistance QTL in the APR lines identified by Prins *et al.* (2016). To investigate this hypothesis, DE wheat transcripts were filtered by chromosomal position. Two chromosomes were selected for this approach: 4D for DE transcripts in W1406 and 6A for DE transcripts in W6979. These respective chromosomes were the location of the QTL with the greatest contribution to the APR response of W1406 and W6979 in the field as reported by Prins *et al.* (2016). The expression patterns of DE transcripts originating from these chromosomes are reported in Figures 2.21 and 2.22.

Particular focus was given to induced transcripts encoded by putative resistance genes. However, no DE transcripts originating from chromosome 4D or 6A encoded putative ABC transporters, START kinases or hexose transporters.

A single NB-LRR protein encoding transcript (4DS_361408_AA1167400.1) originating from chromosome 4D was found to be induced in W1406. Another transcript (4DS_361408_AA1167390.1), encoding an uncharacterised protein, was not detected by NB-LRR analysis but showed homology to a putative disease resistance RPP13-like protein 2 isoform X1. Both these putative disease resistance genes were shared with W6979, thereby excluding these transcripts. Other DE transcripts that were induced and may be linked to the defence response included beta-galactosidases, a flavin-containing monooxygenase and non-specific lipid-transfer proteins.

Four NB-LRR protein encoding transcripts originating from chromosome 6A were unique to W6979, but only two were induced (6AL_472855_AA1526610.1 and 6AL_471511_AA1510160.1). These two transcripts encoded proteins with homology to a putative disease resistance RPP13-like protein 3 and Sr13 respectively. Other induced transcripts to be noted encoded an uncharacterised protein (6AL_472536_AA1523250.1) with homology to a chitin elicitor receptor kinase 1 and another (6AS_488347_AA1575210.1) with homology to a leucine-rich repeat receptor-like protein kinase. One characterised transcript (6AS_485239_AA1541390.1) encoded a serine/threonine-protein kinase.

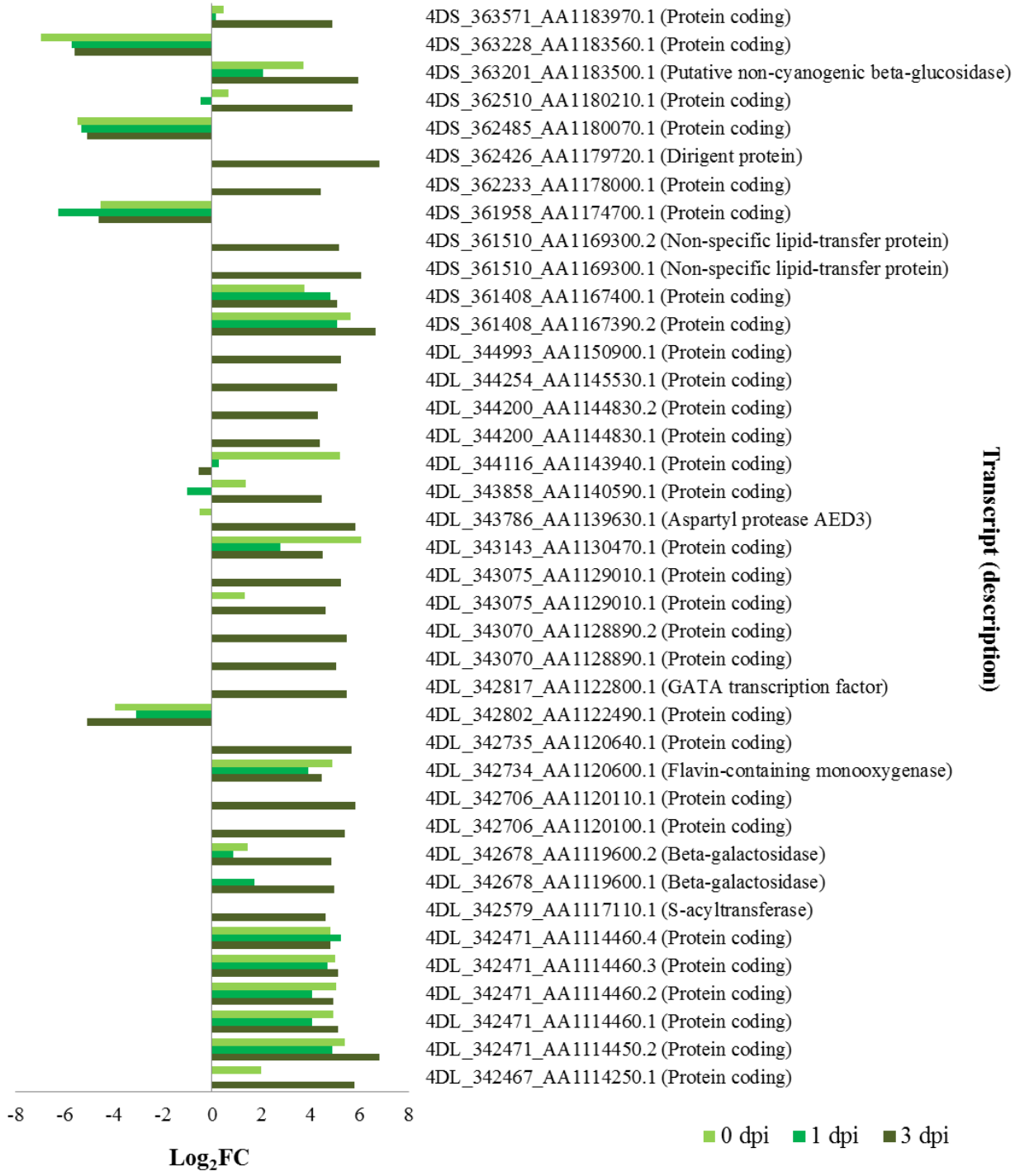

Figure 6.21: Differentially expressed wheat transcripts in the W1406 line in comparison to the 37-07 line located on chromosome 4D. Chromosome positions were based on the Centre for Genome Analysis Chinese Spring wheat genome hosted by Ensembl. Transcript descriptions were derived from Ensembl. Log_2 fold change (FC) values for differentially expressed transcripts are reported for each time point at days post inoculation (dpi).

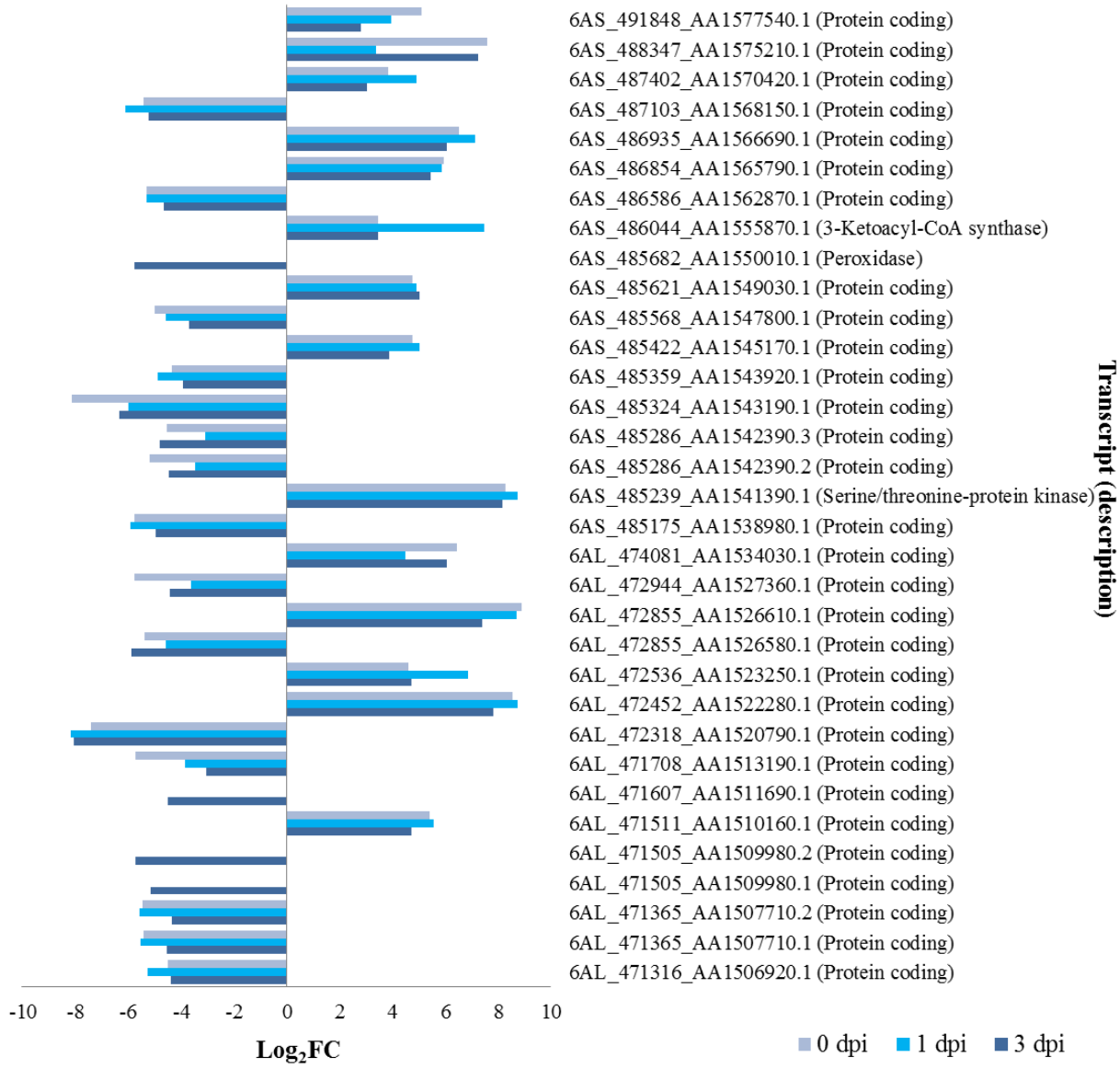

Figure 6.22: Differentially expressed wheat transcripts in the W6979 line in comparison to the 37-07 line located located on chromosome 6A. Chromosome positions were based on the Centre for Genome Analysis Chinese Spring wheat genome hosted by Ensembl. Transcript descriptions were derived from Ensembl. Log_2 fold change (FC) values for differentially expressed transcripts are reported for each time point at days post inoculation (dpi).

6.3.3.2.2 Differentially expressed *Puccinia graminis f. sp. tritici* transcripts

The line vs line comparison delivered few DE *Pgt* transcripts. In the W1406 dataset, a total of 1743 DE transcripts were identified, but only two of these were *Pgt* transcripts. A total of 1458 transcripts were DE in the W6979 dataset, of which 26 were *Pgt* transcripts. *Pgt* transcripts therefore constituted 0.11% (W1406) and 1.78% (W6979) of the total DE transcripts. No DE *Pgt* transcripts were shared between lines. The expression of *Pgt* transcripts over the course of infection are reported in Supplementary Tables S22 and S23 and the Ensembl identities in Supplementary Tables S24 and S25. The majority of DE *Pgt* transcripts were repressed at the tested time points in both APR lines for the line vs line comparison.

The two DE transcripts from W1406 encoded uncharacterised proteins and neither were predicted to be effectors (Supplementary Table S26). In W6979, DE transcripts included one coding for a ribose-phosphate pyrophosphokinase and another for an inosine-5'-monophosphate dehydrogenase. Five putative effectors were predicted from the W6979 dataset (Supplementary Table S27), and all have been previously identified in the time vs time comparison. Four of the putative effector transcripts encoded uncharacterised proteins while the fifth encoded a TdcF protein, predicted to be localised to the host chloroplast and mitochondrion.

6.4 Discussion

The transcriptomic analysis of *Pgt*-inoculated adult wheat lines presented here gave a number of valuable technical insights into the analysis of RNA-seq data. Mapping to a combined wheat and *Pgt* reference transcriptome aimed to distinguish different transcripts or isoforms that are products of alternative gene splicing. Such a transcript-based approach to differential expression has been encouraged over a union exons-based approach (Zhao *et al.,* 2015). The latter collapses transcripts into their respective genes, while the former assigns expression values to each transcript. In the current study, changes in transcript levels were thus presented.

As far as we know, the current comparison of the Illumina and Ion Torrent sequencing platforms was the first for wheat. The DE transcripts from the Ion Torrent subset identified the same transcripts as the Illumina dataset, except for four transcripts found only in the Illumina dataset. The identification of 433 DE transcripts unique to the Ion Torrent subset may be attributed to the higher number of reads in those libraries. As the number of reads in a library increases, the number of reads mapping to any transcript increases, providing improved resolution. An increased number of reads also increases the probability of low copy transcripts being sequenced. Though the Ion Torrent platform had a lower percentage of mapped reads, in terms of absolute number of reads mapped (42.8 vs 24.4 million), the Ion Torrent subset had more mapping reads than the Illumina dataset. For the DE transcripts identified by each sequencing platform, similar relationships between samples were shown by PCA. The same time points from both the Ion Torrent subset and Illumina dataset clustered together, while the two time points (1 and 3 dpi) were distinct from each other, indicating altered gene expression patterns over the course of infection.

For the 97 shared DE transcripts, the Illumina dataset and Ion Torrent subset clustered separately, indicating that the data from these platforms cannot be statistically combined, most likely due to the difference in number of reads in the Ion Torrent libraries. As the number of reads increases, the number of reads mapping to sequences in a reference library also increases, which will lead to a higher read count. Log_2 transformation aims to normalise read counts but the Ion Torrent subset and Illumina dataset still clustered separately. However, the relationship between the samples for a given sequencing platform corresponded well for the 97 shared DE transcripts. Ion Torrent platform was however selected for further

experimentation because of the higher number of reads in the generated libraries and potential to thus identify more DE transcripts.

The two distinct pairwise comparisons used in the current study aimed to address two different biological questions. Firstly, to what extent does gene expression change in wheat over time following inoculation with *Pgt*? This was addressed by the time vs time comparison. Secondly, how does gene expression alter in wheat lines conferring APR to *Pgt* compared to a *Pgt* susceptible wheat line? This in turn was addressed by line vs line comparison. The line vs line comparison identified the largest number of DE transcripts, the majority of which were from wheat. For the time vs time comparison, fewer DE transcripts were identified, but the proportion of *Pgt* transcripts was far greater. The lowest percentage of *Pgt* transcripts within a sampled line was 16.5%, while the highest percentage in the line vs line comparison was a mere 1.78%.

The pairwise comparison of samples therefore must take into consideration the biological question asked. The time vs time comparison avoided genetic differences between wheat lines and purely looked for DE transcripts within a line caused by *Pgt* inoculation. Although no major morphological changes were seen in the flag leaf sheath during the 3 day period under consideration, substantial molecular changes were occurring in response to *Pgt* inoculation, as seen by the DE transcripts.

Although the three wheat lines shared similarities in some features of their response to *Pgt* infection, the DE transcripts differed noticeably, as did expression patterns. In 37-07 and W1406, the majority of wheat transcripts were induced at 3 dpi, but at 1 dpi in W6979. It may be hypothesised that the earlier response in W6979 led to a quantifiably superior APR response as compared to W1406. This hypothesis was supported by adult plant infection responses at 14 dpi (Chapter 3; Table 3.5), colony sises at 5 dpi (Chapter 4; Figure 4.22) and fungal biomass accumulation at 10 dpi (Chapter 5; Figures 5.1 and 5.6) that all indicated that W6979 inhibited *Pgt* development more than W1406. However, it is important to note that W1406 also had transcripts induced at 1 dpi.

Taking the expression of peroxidase encoding transcripts as a general characteristic of the defence response, it appeared that an earlier induction at 1 dpi of peroxidases added a benefit to the APR lines. The expression pattern of peroxidase encoding transcripts was maintained over the course of infection in W1406, but was transient in W6979, with the expression pronounced at 1 dpi. In the susceptible 37-07 line, peroxidase encoding transcripts were

absent at 1 dpi and were only induced at 3 dpi. It remains to be seen if a maintained or transient expression profile was more beneficial as a defence response against *Pgt*, even though the APR response in W6979 was superior to W1406.

The induction peroxidase encoding transcripts appeared to be a common feature of the APR response of wheat to *Puccinia* spp. with the W6979 line showing a transient induction. The induction of *PRA2* and *PR9* (encoding peroxidases) at 6 hpi has also been found by RT-qPCR in the APR line Toropi upon infection with *Pt* (Casassola *et al.,* 2015). However, at 12 hpi, gene expression returned to basal levels and remained so until 3 dpi. The APR response in Toropi therefore includes the induction of peroxidase encoding transcripts as a pre-haustorial defence mechanism. Huang *et al.* (2013) showed that the expression of peroxidase encoding transcripts in the APR cultivar Xingzi 9104 infected with *Pst* is highly induced at 1 dpi, but steadily decreases thereafter.

The *Yr36* APR gene corresponds to the *Wheat Kinase START1* (*WKS1*) gene which encoded a protein kinase shown to phosphorylate and thus inactivate thylakoid associated peroxidases (Gou *et al.,* 2015). Reduced peroxidase activity in the chloroplast leads to the accumulation of H_2O_2 that was hypothesised to lead to a hypersensitive response (HR) to *Pst*. Though such a mechanism was not confirmed in the current study it may likewise be hypothesised that a repressed expression of peroxidase encoding transcripts in W6979, and subsequent decreased enzymatic activity, may also lead to the HR.

In the time vs time comparison, the number of DE *Pgt* transcripts showed a marked difference between the lines. Fewer *Pgt* transcripts in W1406 and W6979 appeared to mirror the adult plant infection responses (Chapter 3; Table 3.5), *Pgt* colony sizes (Chapter 4; Figure 4.22), fungal biomass accumulation (Chapter 5; Figures 5.1 and 5.6) and haustorium formation (Chapter 5; Figure 5.6). It may be hypothesised that the increase in *Pgt* biomass over the course of infection contributed to the differences in copy number of *Pgt* transcripts and thereby presents a quantifiable induction of transcripts. However, all of the techniques used in previous chapters could only distinguish the development of *Pgt* on the wheat lines at 5 dpi and were ineffective at 1 and 3 dpi. RNA-seq may be a more sensitive technique to detect changes in transcript levels due to changes in fungal biomass. However, in *Pst*, as infection proceeded the percentage of mapped fungal reads increased over time, but only significantly from 5 dpi onwards (Dobon *et al.,* 2016).

The limitations of the RT-qPCR markers used in Chapter 5 at early time points were confirmed in the RNA-seq results. The marker for *β-tubulin*, EFP86248 (encoded by *PGTG_12204*), was not DE at any time point, in any line. The marker for haustorium formation, EFP85149 (encoded by *PGTG_11318*) was DE in 37-07 and W6979 at 1 and 3 dpi, but not at any time points in W1406. The RT-qPCR analysis of these transcripts were only informative at 10 and 5 dpi respectively, but not at the earlier time points. The 25 DE *Pgt* transcripts shared by the lines may however be considered in the search for other RT-qPCR markers that may allow for routine quantification of *Pgt* on wheat at earlier time points.

The number of DE *Pgt* transcripts in all three wheat lines was proportionally large in relation to the number of wheat DE genes. Over the course of infection *Pgt* was undergoing developmental changes as infection structures differentiated (Chapter 4). The time vs time comparison therefore reflects *Pgt* development over the course of infection.

The induction of a *Pgt* transcript encoding a superoxide dismutase may indicate that the pathogen is counteracting the oxidative burst of the host. Lanfranco *et al.* (2005) proposed such a mechanism whereby fungal superoxide dismutases may scavenge host O_2^-. Previously, a proteome analysis identified a superoxide dismutase induced in *Pt* during the infection of wheat (Song *et al.,* 2011). Moreover, in 37-07 another superoxide dismutase encoding transcript was induced and classified as a putative effector localised to the host mitochondria. Superoxide dismutases have previously been confirmed as encoded by a number of putative *Pgt* effector genes (Sperschneider *et al.,* 2014). *Pgt* may therefore export superoxide dismutases to the host to directly scavenge O_2^-. The induction of a transcript encoding a putative superoxide dismutase effector unique to 37-07 may indicate the contribution of this effector to wheat susceptibility in this line. This effect however needs to be investigated further.

The line vs line comparison highlighted the considerable genetic differences between 37-07 and the two APR lines. Far more DE wheat transcripts were identified in this comparison, than the time vs time comparison. The uniform induction or repression of transcripts over the course of infection may indicate genes present in one line but absent in the other.

Within the identified NB-LRR protein encoding transcripts, the CC-NB-LRR subclass dominated. As previously reported by Pan *et al.* (2000) and Bai *et al.* (2002), the TIR-NB-LRR subclass appears to be absent in cereals. The TIR-NB-LRR subclass was also absent in

the current study. However, Peng and Yang (2017) have recently found nine putative TIR-NB-LRR proteins in wheat. The chromosomal distribution of 1117 NB-LRR proteins showed the largest numbers on chromosomes 6B, 4A, 7D, 7A and 1B. This differed from the chromosomal distribution of the W1406 and W6979 lines (except for the prominence of 1B in the latter line). Furthermore, the two APR lines differed from one another, except for the prominence of 2B in both.

The prediction of NB-LRR encoding transcripts identified a number of candidate resistance genes for further investigation. However, the current understanding of durable APR genes in particular indicates diverse functions that may exclude NB-LRR proteins. For that purposes, ABC transporters, START kinases and hexose transporters were investigated within the DE transcripts. These protein products have previously been shown to be encoded by APR genes. Peng and Yang (2017) identified 526 ABC transporters and 114 START kinases in wheat. In the current study, 12 putative ABC transporter and 25 putative START kinase encoding transcripts were DE in one or the other line. No putative hexose transporter encoding transcripts were identified. Only two of these transcripts, both encoded by the 2DS_177216_AA0569300 gene, may be linked to the same chromosome as a minor QTL (*QSr.ufs-2D*) identified by Prins *et al.* (2016) in W6979. These two transcripts originated from chromosome 2D and encoded putative ABC transporters that may be further investigated.

To broaden the search for resistance genes in the APR lines and in an attempt to link DE transcripts to QTL locations, the transcripts originating from chromosome 4D for W1406 and 6A for W6979 were further investigated. The respective chromosomes are the location of two QTL, *QSr.ufs-4D* and *QSr.ufs-6A*, identified by Prins *et al.* (2016) with the largest contribution of the APR response in W1406 and W6979 respectively.

DE transcripts from chromosome 4D could not be linked to any known resistance genes or functional resistance domains. The *Sr55* (*Lr67*/*Yr46*/*Pm46*) gene was previously mapped to chromosome 4D (Hiebert *et al.,* 2010). The identification of a QTL in W1406 on chromosome 4D by Prins *et al.* (2016) draws particular attention to the *Sr55* locus. However, in the current study the Ensemble accession 4DL_343575_AA1136830.2 (Genbank accession: ALL26331.2) corresponding to *Sr55* was not detected as DE in W1406. Further fine mapping of *QSr.ufs-4D* will however ultimately exclude or confirm whether it is the *Sr55* QTL.

A number of DE transcripts from chromosome 6A could putatively be linked to known resistance genes or functional resistance domains. The consensus map of Yu *et al.* (2014) for stem rust resistance loci reports five QTL and three designated *Sr* genes (*Sr13*, *Sr26* and *Sr52*) on chromosome 6A. The DE transcript 6AL_471511_AA1510160.1 has high homology with *Sr13* (Genbank accession: *KY825229.1*; Zhang *et al.*, 2017). *Sr13* has been mapped to the long arm of chromosome 6A (McIntosh, 1972). However, Prins *et al.* (2016) mapped *QSr.ufs-6A* in W6979 to the short-arm of chromosome 6A. Also, PTKST is avirulent on seedlings in the presence of *Sr13* (Pretorius *et al.*, 2010), while this *Pgt* race was virulent on W6979 seedlings (Chapter 3; Figure 3.2). *Sr13* is therefore not contributing to the APR response in W6979. Attention was therefore focussed on the short-arm of chromosome 6A. Three candidate transcripts from 6AS, encoding a chitin elicitor receptor kinase 1, a probable leucine-rich repeat receptor-like protein kinase and a serine/threonine-protein kinase, could be potential candidates for *QSr.ufs-6A*.

Linking DE transcripts to chromosomal locations gave only limited insight into the potential genes underlying the QTL for APR. In the current study, *Lr34* (*Yr18*/*Sr57*) will serve as an example of a characterised gene with known chromosomal location. Prins *et al.* (2016) confirmed that *Lr34* contributed to the APR response in both W1406 and W6979. This resistance gene encoded the Ensemble accession 7DS_621754_AA2025300.1. However, this transcript was not DE in any data comparisons. The potential cause for the absence of *Lr34* highlights important considerations when applying gene expression data to QTL analysis. The expression level of *Lr34* may be either too low or biologically variable to be considered as DE within the current statistical parameters. This limitation is inherent to the statistical analysis of RNA-seq data and complicated linking of expression profiles to QTL locations.

To significantly link expression profiles of DE transcripts to QTL, an expression QTL (eQTL) analysis is required. An eQTL analysis combines transcriptomic analysis using microarrays or RNA-seq, with mapping of a QTL in a segregating population (Hansen *et al.*, 2008). The technique has been used on near-isogenic barley lines to identify candidate genes for partial resistance to *P. hordei* (Chen *et al.*, 2010). Near-isogenic lines are often not available and recombinant inbred lines, doubled haploid (DH) or back cross populations may be used. The resolution of any eQTL analysis, however, increases with the size of the population which will accordingly increase the size of trials required. Such an analysis often only considers variation in two alleles at a time, and must be well supported by genotypic and phenotypic data (Ballini *et al.*, 2013). Keeping these considerations in mind, an eQTL

analysis may potentially be undertaken on the DH populations for W1406 and W6979 generated by Prins *et al.* (2016).

PTKST was used for the inoculation of all lines, so DE *Pgt* transcripts in the line vs line comparison cannot be attributed to genetic differences in *Pgt*. As previously noted, histological observations showed no clear differences in the development of *Pgt* infection structures at any time point up to 3 dpi (Chapter 4). It is thus deduced that for this reason the line vs line comparison showed substantially less DE *Pgt* transcripts. Most of DE *Pgt* transcripts were repressed which may indicate that the APR lines are inhibiting *Pgt* development. Lines could not be distinguished at any given time point up to 3 dpi by biomass quantification (Chapter 5; Figures 5.1 and 5.6) but RNA-seq may be a more sensitive technique to detect differences in *Pgt* gene expression at these time points. The line vs line comparison was therefore only of minimal use. Most features of the DE *Pgt* transcripts were already observed in the time vs time comparison, including all of the putative effector encoding transcripts.

The two approaches to DE transcript analysis implemented in the current study gave insights into the adult wheat-*Pgt* interaction. The time vs time comparison was required to accurately describe transcriptional changes in the wheat lines in response to *Pgt* over the course of infection. The comparison also gave insight into *Pgt* development and especially the effector repertoire of the pathogen. The line vs line comparison was required to describe the genetic differences that underpin the APR in the respective wheat lines and was the only approach that effectively allowed putative resistance genes to be discovered. Both of these approaches were therefore required to completely describe the interaction. In wheat a large number of NB-LRR protein encoding transcripts were identified along with some candidate genes showing homology to previously described APR genes that warrant further study. In *Pgt* a number of putative effector encoding transcripts were also found that warrant future testing.

An overview of the APR response in the W1406 and W6979 lines highlighted a number of important considerations. The expression of some transcripts at either 1 or 3 dpi may indicate that these time points define two distinct phases of the APR response. Based on histological observation made in Chapter 3, *Pgt* haustoria were assumed to have formed at 1 dpi in adult wheat plants. The APR response presented here therefore indicates a post-haustorial defence response. However, time points earlier than 1 dpi may help identify a pre-haustorial defence if it exists. DE transcripts indicated that the oxidative burst and HR may be induced in the

APR lines. Histological studies of cell death and the accumulation of reactive oxygen species (ROS) such as H_2O_2 and O_2^- in association with *Pgt* infection sites should be undertaken. Cellular peroxidase activity and ROS levels should likewise be investigated. The confirmation of these defence response may further elucidate the APR response in wheat to *Pgt* infection.

Chapter 7: Conclusions

The current study used various methods to investigate *Puccinia graminis* f. sp. *tritici* (*Pgt*) infection of the two wheat lines W1406 and W6979, both of which express stem rust adult plant resistance (APR). By comparing these lines to the susceptible control 37-07 line, a number of key insights were made regarding *Pgt* development on adult wheat plants, the APR response in general, and APR response in W1406 and W6979 in particular.

Six adult plant wheat trails were completed under greenhouse conditions and a number of different wheat lines, entries and/or cultivars were successfully evaluated. Adult wheat plants were inoculated with the *Pgt* race PTKST according to the method developed by Pretorius *et al.* (2007) and modified by Bender *et al.* (2016). The method reproducibly delivered *Pgt*-inoculated adult wheat plants for sampling. Phenotypic scoring of *Pgt* infection on adult wheat plants is typically done on the flag leaf sheath of the last internode (Roelfs *et al.*, 1992). The sampling of *Pgt*-inoculated flag leaf sheaths was thus a fundamental paradigm of the current study.

Four adult plant wheat trails included the 37-07, W1406 and W6979 lines, that were the main focus of the current study. W1406 and W6979 were susceptible as seedlings to *Pgt* race PTKST, but showed partial resistance in the adult plant trials, confirming the report of Prins *et al.* (2016). Based on phenotypic scores at 14 dpi, W6979 was more effective at restricting *Pgt* development in three trials, but was scored similar to W1406 in one trial. Results contradicted the field observations of Prins *et al.* (2016) which scored similar levels of stem rust infection on W1406 and W6979, except at one location. Results of Soko *et al.* (2018), however, indicated W6979 as more susceptible. It appears that the stem rust APR in W1406 and W6979 may be influenced by environmental conditions, a common feature of APR.

Histological observations allowed the development of *Pgt* to be effectively followed over the course of infection on the flag leaf sheaths of adult wheat plants. Scanning electron microscopy (SEM) and fluorescence microscopy (based on the method of Ayliffe *et al*., 2011) were used to observe *Pgt* development. SEM in particular gave insight into the early development (2 dpi or earlier) of *Pgt*. Epidermal observations indicated that directional growth of germ tubes may not be a feature of *Pgt* development on flag leaf sheaths. Sub-epidermal observations showed the rapid differentiation of the first haustorial mother cell (HMC) from the sub-stomatal vesicle, with no clear primary infection hyphae, all occurring within the sub-stomatal chamber of the host. Since both these findings appear to contradict common assumptions regarding *Puccinia* spp. development it should be further investigated.

Fluorescence microscopy was used to follow *Pgt* development over the course of the infection process up to 10 dpi. All *Pgt* infection structures could be observed, except for haustoria. However, the formation of HMCs is a good indication of the subsequent formation of haustoria, and indicated that the biotrophic relationship was potentially established at 1 dpi, but definitely by 2 dpi. Further optimization is required to improve the processing of inoculated flag leaf sheaths of adult wheat plants, to allow the observation of haustoria.

The histological approach allowed colony size to be monitored as part of the APR response. At 5 dpi, *Pgt* had produced significantly smaller colonies on both W1406 and W6979 compared to those found on 37-07. This directly parallels the observed phenotypic scoring seen at 14 dpi in the greenhouse experiments. However, no quantifiable effect on *Pgt* development could be seen at earlier time points. The inhibition of *Pgt* development at 5 dpi was the first visual indication of a putative post-haustorial defence response in the APR lines.

The fluorescence-based method described by Ayliffe *et al.* (2013) proved appropriate to the examination of *Pgt* biomass accumulation, and the current study was one of the first to apply this method to flag leaf sheaths of adult wheat plants. The method could distinguish the wheat lines at 5 and 10 dpi, but not at any earlier time points. The results directly supported the fluorescence microscopy observations that showed significantly smaller colony sizes in W1406 and W6979 at 5 dpi, compared to 37-07.

Before reverse transcriptase quantitative polymerase chain reaction (RT-qPCR)-based methods were applied to the *Pgt*-inoculated wheat lines, reference gene validation was undertaken. Though stable reference genes were previously reported by Scholtz and Visser (2013) in a study of *Pgt*-inoculated near-isogenic wheat seedlings, the current study was the first to apply this method to a range of *Pgt*-inoculated adult wheat lines and cultivars. The expression of the *18S ribosomal RNA* (*Ta-18S*), *cell division control protein* (*Ta-CDC*) and *transcription elongation factor 1 alpha* (*Ta-TEF*) genes proved stable over the course of infection and may be considered for future RT-qPCR studies.

The relative expression of the *Pgt β-tubulin* (*Pgt-BTUB*) gene, as described by Coram *et al.* (2008), was successfully used to follow biomass accumulation. This study was one of the first to apply this method to *Pgt*-inoculated flag leaf sheaths of adult wheat plants. The method distinguished APR lines, entries and/or cultivars from the susceptible 37-07 line at 5 and 10 dpi, but not at any earlier time points. Relative *Pgt-BTUB* transcript accumulation in the susceptible 37-07 line fitted an exponential growth equation in most trials, thereby indicating

a rapid increase of *Pgt* biomass, particularly between 5 and 10 dpi. For future implementation of this method to monitor *Pgt* development in APR wheat lines, time points after 5 dpi were recommended, and 10 dpi appeared to be the most appropriate choice.

The deductions made using the relative expression of *Pgt-BTUB* are generally supported by the fluorescence-based method for biomass accumulation. It is important to note that both these methods only infer total *Pgt* biomass and do so by different proxies. The pattern of biomass accumulation resolved by the two methods appears different over the course of infection, but important comparisons are possible. Both methods show an increase in biomass over the course of infection, increasing rapidly from 5 dpi onwards and allowing the APR lines to be clearly distinguished at 10 dpi. These therefore methods have equal application in future research.

The *PGTG_11318* gene, encoding an uncharacterised protein, was previously linked to haustorium formation (Broeker *et al.*, 2006; Duplessis *et al.*, 2011) and the relative expression of this gene was used to infer *Pgt* haustorium formation in adult wheat plants. The method was advantageous, as haustoria could not be observed by the histological techniques used. The method could also distinguish APR lines, entries and/or cultivars from the susceptible 37-07 line at 5 dpi, but not at any earlier or later time points. The W1406 and W6979 lines showed a significant difference from the 37-07 line at 5 dpi. The relative transcription of *PGTG_11318* indicated a rapid increase in haustoria from 0 to 5 dpi, paralleling biomass accumulation, but a decrease from 5 to 10 dpi. *PGTG_11318* expression in the susceptible 37-07 line fitted a Gaussian equation in all trials, and indicated 5 to 7 dpi as time interval whereby *Pgt* haustoria formation peaks relative to total *Pgt* biomass. This time interval should be considered for any future investigations that focus on *Pgt* haustoria in adult wheat plants. The pattern of *PGTG_11318* expression appeared to separate *Pgt* development into three distinct phases: establishment, proliferation (with an increase in haustoria formation) and sporulation.

Methods used for the determination of colony size, biomass accumulation and haustorium formation were objective techniques used to support the phenotypic classification of stem rust APR in adult wheat lines. These methods all ranked the wheat lines identically, either at 5 or 10 dpi. W1406 and W6979 showed less *Pgt* development than the 37-07 line, while W1406 was intermediate between 37-07 and W6979. These measurements supported the phenotypic scoring of the adult plant infection response and confirm the expression of an APR response

in W1406 and W6979. Results indicated that by 5 dpi the APR response effectively restricted *Pgt* development. This prompted the selection of time points 0, 1 and 3 dpi for RNA-sequencing (RNA-seq) analysis.

A sequencing platform comparison was undertaken, comparing the Illumina HiSeq 2000™ and Ion Torrent Proton™ platforms. To the best of our knowledge, the current study is the first report of such a comparison in wheat. The majority of differentially expressed (DE) transcripts identified from reads generated by the Illumina platform were also identified from reads generated by the Ion Torrent platform. However, the higher number of reads generated by the Ion Torrent datasets resulted in a greater number of DE transcripts. The Ion Torrent platform was therefore selected for RNA-seq analysis.

The RNA-seq analysis of *Pgt* infection in wheat genotypes expressing APR to stem rust is one of the first reported, especially considering that inoculated flag leaf sheaths from adult wheat plants were used. Two comparative approaches were implemented: a pairwise comparison of either time points or wheat lines. The time vs time comparison identified DE transcripts in the wheat lines over the course of *Pgt* infection, but also changes in *Pgt* transcripts through development of the pathogen. *Pgt* transcripts encoding putative effectors were also identified. DE transcripts identified in the line vs line comparison were deduced to be based on genetic differences between lines, and identified a number of transcripts encoded by APR candidate genes. However, only limited success was obtained with linking candidate transcripts to the chromosomal positions of the quantitative trait loci (QTL) identified by Prins *et al.* (2016).

In the time vs time comparison the DE wheat transcripts were unique to the respective wheat lines. The APR lines not only differed from the susceptible control line, 37-07, but also from each other. Although the APR responses may share common features, they appear to be contributed by entirely different transcripts in W1406 and W6979.

The DE wheat transcripts indicated the oxidative burst as a common feature of *Pgt* infected adult wheat plants. The induction of the oxidative burst occurred as early as 1 dpi in W1406 and W6979, and may be essential for the establishment of the APR response in these lines. This highlights the effectiveness of RNA-seq in identifying putative effects not observed by microscopic techniques, and indicates other avenues that require further investigation. The accumulation of reactive oxygen species in close association with infection sites may validate the presence of the oxidative burst. The hypersensitive response in wheat cells should

likewise be confirmed. Improved methods for the histological study of *Pgt*-inoculated flag leaf sheaths are therefore required.

The investigated wheat lines showed that the nature of the response to *Pgt* inoculation also differed in its distribution over time. Transcripts may be DE at either of the investigated time points (1 and 3 dpi), over the course of infection, but appeared to form part of two distinct phases in the APR responses in W1406 and W6979. The majority of DE transcripts in W1406 were induced at 3 dpi, but in W6979 most of the DE transcripts were induced transiently at 1 dpi. Whether at 1 or 3 dpi, the DE transcripts in W1406 and W6979 indicated an APR response that restricted *Pgt* development. The induction of transcripts at 1 dpi may indicate a pre-haustorial defence mechanism. However, histological observation of HMC formation at 1 dpi implied associated haustorium formation. Until haustorium formation is directly observed and gene expression changes earlier than 1 dpi are measured, a pre-haustorial defence mechanism cannot be confirmed. A pre-haustorial defence mechanism may also be induced at some infection points but not others, another avenue for further investigation. Considering the current gene expression patterns, the presence of a post-haustorial defence mechanism is most likely present in both APR lines.

In summary, it is considered that upon inoculation with *Pgt*, the W1406 and W6979 wheat lines confer an APR response that involves primarily post-haustorial defence mechanisms, restricting the growth of colonies. Two distinct phases of the APR response were observed, at 1 and 3 dpi in the two APR lines, the former being particularly associated with W6979 and the latter with W1406. It was hypothesised that this APR response limits *Pgt* development and results in quantifiable inhibition of *Pgt* development from 5 dpi onwards. W6979 inhibited the *Pgt* infection process more intensely than W1406, indicating that the induction of an earlier defence mechanisms at 1 dpi may have made a contribution to the stronger APR response in W6979. The inhibition of *Pgt* development by the APR responses eventually leads to phenotypically observable adult plant infection responses in W1406 and W6979. The current study therefore delivered a multifaceted description of the APR in W1406 and W6979, and gave insights into the defence response based on multiple QTL that additively contribute to resistance. Findings contributed to a broader understanding of the APR response in wheat and its effects on *Pgt* development.

References

Acevedo, M, Jackson, EW, Sturbaum, A, Ohm, HW and Bonman, JM. 2010. An improved method to quantify *Puccinia coronata* f. sp. *avenae* DNA in the host *Avena sativa*. *Canadian Journal of Plant Pathology* 32 (2): 215-224.

Andolfo, G, Jupe, F, Witek, K, Etherington, GJ, Ercolano, MR and Jones, JDG. 2014. Defining the full tomato NB-LRR resistance gene repertoire using genomic and cDNA RenSeq. *BMC Plant Biology* 14: 120.

Anguelova-Merhar, VS, Van der Westhuizen, AJ and Pretorius, ZA. 2001. β-1,3-Glucanase and chitinase activities and the resistance response of wheat to leaf rust. *Journal of Phytopathology* 149: 381-384.

Atienza, SG, Jafary, H and Niks, RE. 2004. Accumulation of genes for susceptibility to rust fungi for which barley is nearly a nonhost results in two barley lines with extreme multiple susceptibility. *Planta* 220 (1): 71-79.

Axtell, MJ and Staskawicz, BJ. 2003a. Initiation of RPS2-specified disease resistance in *Arabidopsis* is coupled to the AvrRpt2-Directed Elimination of RIN4. *Cell* 112: 369-377.

Axtell, MJ, Chisholm, ST, Dahlbeck, D and Staskawicz, BJ. 2003b. Genetic and molecular evidence that the *Pseudomonas syringae* type III effector protein AvrRpt2 is a cysteine protease. *Molecular Microbiology* 49 (6): 1537-1546.

Ayliffe, M, Devilla, R, Mago, R, White, R, Talbot, M, Pryor A and Leung H. 2011. Nonhost resistance of rice to rust pathogens. *Molecular Plant-Microbe Interactions* 24 (10): 1143-1155.

Ayliffe, M, Periyannan, SK, Feechan, A, Dry, I, Schumann, U, Wang, M, Pryor, A and Lagudah, E. 2013. A simple method for comparing fungal biomass in infected plant tissues. *Molecular Plant-Microbe Interactions* 26 (6): 658-667.

Bai, J, Pennill, LA, Ning, J, Lee, SW, Ramalingam, J, Webb, CA, Zhao, B, Sun, Q, Nelson, JC, Leach, JE and Hulbert, SH. 2002. Diversity in nucleotide binding site-leucine-rich repeat genes in cereals. *Genome Research* 12 (12): 1871-1884.

Bailey, TL, Boden, M, Buske, FA, Frith, M, Grant, CE, Clementi, L, Ren, J, Li, WW and Noble, WS. 2009. MEME SUITE: Tools for motif discovery and searching. *Nucleic Acids Research* 37 (supplement 2): W202-W208.

Bajgain, P, Rouse, MN, Tsilo, TJ, Macharia, GK, Bhavani, S, Jin, Y and Anderson, JA. 2016. Nested association mapping of stem rust resistance in wheat using genotyping by sequencing. *PLOS ONE* 11 (5): e0155760.

Ballini, E, Lauter, N and Wise, R. 2013. Prospects for advancing defense to cereal rusts through genetical genomics. *Frontiers in Plant Science* 4: 117.

Barber MS and Ride JP. 1994. Levels of elicitor-active β (1-4) linked N-acetyl-D-glucosamine oligosaccharides in the lignifying tissue of wheat. *Physiological and Molecular Plant Pathology* 45: 37-45.

Baum, BR and Savile, DB. 1985. Rusts (Uredinales) of Triticeae: Evolution and extent of coevolution, a cladistic analysis. *Botanical journal of the Linnean Society* 91 (3): 367-394.

Beckett, A, Tatnell, JA and Taylor, N. 1990. Adhesion and pre-invasion behaviour of urediniospores of *Uromyces viciae-fabae* during germination on host and synthetic surfaces. *Mycological Research* 94 (7): 865-875.

Belkhadir, Y, Nimchuk, Z, Hubert, DA, Mackey, D and Dangl, JL. 2004. *Arabidopsis* RIN4 negatively regulates disease resistance mediated by RPS2 and RPM1 downstream or independent of the NDR1 signal modulator and is not required for the virulence functions of bacterial type III effectors AvrRpt2 or AvrRpm1. *The Plant Cell* 16: 2822-2835.

Bender, CM, Prins, R and Pretorius, ZA. 2016. Development of a greenhouse screening method for adult plant response in wheat to stem rust. *Plant Disease* 100 (8): 1627-1633.

Bettgenhaeuser, J, Gilbert, B, Ayliffe, M and Moscou, MJ. 2014. Nonhost resistance to rust pathogens-a continuation of continua. *Frontiers in plant science* 5: 664.

Bhattacharya, S. 2017. Deadly new wheat disease threatens Europe's crops. *Nature* 542 (7640): 145-146.

Bozkurt, O, Unver, T and Akkaya, MS. 2007. Genes associated with resistance to wheat yellow rust disease identified by differential display analysis. Physiological and Molecular Plant Pathology 71(4-6): 251-259.

Bolton, MD, Kolmer, JA, Xu, WW and Garvin, DF. 2008. *Lr34*-mediated leaf rust resistance in wheat: Transcript profiling reveals a high energetic demand supported by transient

recruitment of multiple metabolic pathways. *Molecular Plant-Microbe Interactions* 21 (12): 1515-1527.

Boyd, LA and Minchin, PN. 2001. Wheat mutants showing altered adult plant disease resistance. *Euphytica* 122: 361-368.

Broeker, K, Bernard, F and Moerschbacher, BM. 2006. An EST library from *Puccinia graminis* f. sp. *tritici* reveals genes potentially involved in fungal differentiation. *Federation of European Microbiological Societies Microbiology Letters* 256: 273-281.

Browder, LE. 1971. Pathogenic specialization in cereal rust fungi, especially *Puccinia recondita* f. sp. *tritici*: Concepts, methods of study and application. *Technical Bulletin of the United States Department of Agriculture* 1432: 45.

Brown, GN. 1997. The inheritance and expression of leaf chlorosis associated with gene *Sr2* for adult plant resistance to wheat stem rust. *Euphytica* 95 (1): 67-71.

Bruce, M, Neugebauer, KA, Joly, DL, Migeon, P, Cuomo, CA, Wang S, Akhunov, E, Bakkeren, G, Kolmer JA and Fellers, JP. 2014. Using transcription of six *Puccinia triticina* races to identify the effective secretome during infection of wheat. *Frontiers in Plant Science* 4: 520.

Brueggeman, R, Rostoks, N, Kudrna, D, Kilian, A, Han, F, Chen, J, Druka, A, Steffenson, B and Kleinhofs, A. 2002. The barley stem rust-resistance gene *Rpg1* is a novel disease-resistance gene with homology to receptor kinases. *Proceedings of the National Academy of Sciences, USA* 99 (14): 9328-9333.

Bustin, SA, Benes, V, Garson, JA, Hellemans, J, Huggett, J, Kubista, M, Mueller, R, Nolan, T, Pfaffl, MW, Shipley, GL, Vandesompele, J and Wittwer, CT. 2009. The MIQE guidelines: Minimum information for publication of quantitative real-time PCR experiments. *Clinical Chemistry* 55 (4): 611-622.

Cantu, D, Govindarajulu, M, Kozik, A, Wang, M, Chen, X, Kojima, KK, Jurka, J, Michelmore, RW and Dubcovsky, J. 2011. Next generation sequencing provides rapid access to the genome of *Puccinia striiformis* f. sp. *tritici*, the causal agent of wheat stripe rust. *PLOS ONE* 6 (8): e24230.

Cantu, D, Segovia, V, MacLean, D, Bayles, R, Chen, X, Kamoun, S, Dubcovsky, J, Saunders, DGO and Uauy, C. 2013. Genome analyses of the wheat yellow (stripe) rust pathogen *Puccinia striiformis* f. sp. *tritici* reveal polymorphic and haustorial expressed secreted proteins as candidate effectors. *BMC Genomics* 14: 270.

Casassola, A, Brammer SP, Chaves MS, Martinelli JA, Stefanato F and Boyd LA. 2015. Changes in gene expression profiles as they relate to the adult plant leaf rust resistance in the wheat cv. Toropi. *Physiological and Molecular Plant Pathology* 89: 49-54.

Catanzariti, AM, Dodds PN, Lawrence, GJ, Ayliffe, MA and Ellis JG. 2006. Haustorially expressed secreted proteins from flax rust are highly enriched for avirulence elicitors. *Plant Cell* 18: 243-56.

Césari, S, Bernoux, M, Moncuquet, P, Kroj, T and Dodds, PN. 2014a. A novel conserved mechanism for plant NLR protein pairs: The "integrated decoy" hypothesis. *Frontiers in Plant Science* 5: 606.

Césari, S, Kanzaki, H, Fujiwara, T, Bernoux, M, Chalvon, V, Kawano, Y, Shimamoto, K, Dodds, PN, Terauchi, R and KrojT. 2014b. The NB-LRR proteins RGA4 and RGA5 interact functionally and physically to confer disease resistance. *The European Molecular Biology Organization Journal* 33: 1941-1959.

Césari, S, Thilliez, G, Ribot, C, Chalvon, V, Michel, C, Jauneau, A, Rivas, S, Alaux, L, Kanzaki, H, Okuyama, Y, Morel, J, Fournier, E, Tharreau, D, Terauchi, R and Thomas Kroja, T. 2013. The rice resistance protein pair RGA4/RGA5 recognizes the *Magnaporthe oryzae* effectors AVR-Pia and AVR1-CO39 by direct binding. *Plant Cell* 25: 1463-1481.

Chaturvedi, R, Krothapalli, K, Makandar, R, Nandi, A, Sparks, AA, Roth, MR, Welti, R and Shah, J. 2008. Plastid ω3-fatty acid desaturase-dependent accumulation of a systemic acquired resistance inducing activity in petiole exudates of *Arabidopsis thaliana* is independent of jasmonic acid. *The Plant Journal* 54 (1): 106-117.

Chen, J, Upadhyaya, NM, Ortiz, D, Sperschneider, J, Li, F, Bouton, C, Breen, S, Dong, C, Xu, B, Zhang, X, Mago, R, Newell, K, Xia, X, Bernoux, M, Taylor, JM, Steffenson, B, Jin, Y, Zhang, P, Kanyuka, K, Figueroa, M, Ellis, JG, Park, RF, Peter N. Dodds, PN. 2017. Loss of *AvrSr50* by somatic exchange in stem rust leads to virulence for *Sr50* resistance in wheat. *Science* 358 (6370): 1607-1610.

Chen, X, Coram, T, Huang, X, Wang, M and Dolezal, A. 2013. Understanding molecular mechanisms of durable and non-durable resistance to stripe rust in wheat using a transcriptomics approach. *Current Genomics* 14 (2): 111-126.

Chen, X, Niks, RE, Hedley, PE, Morris, J, Druka, A, Marcel, TC, Vels, A and Waugh, R. 2010. Differential gene expression in nearly isogenic lines with QTL for partial resistance to *Puccinia hordei* in barley. *BMC Genomics* 11 (1): 629.

Chen, X, Shi, T, Yang, J, Shi, W, Gao, X, Chen, D, Xu, X, Xu, J, Talbot, NJ and Peng, Y. 2014. *N*-glycosylation of effector proteins by an α-1,3-mannosyltransferase is required for the rice blast fungus to evade host innate immunity. *The Plant Cell* 26: 1360-1376.

Chern, MS, Fitzgerald, HA, Yadav, RC, Canlas, PE, Dong, X and Ronald, PC. 2001. Evidence for a disease-resistance pathway in rice similar to the *NPR1*-mediated signaling pathway in *Arabidopsis*. *The Plant Journal* 27 (2): 101-113.

Chisholm, ST, Dahlbeck, D, Krishnamurthy, N, Day, B, Sjolander, K and Staskawicz, BJ. 2005. Molecular characterization of proteolytic cleavage sites of the *Pseudomonas syringae* effector AvrRpt2. *Proceedings of the National Academy of Sciences, USA* 102 (6): 2087-2092.

Chomczynski, P and Sacchi, N. 1987. Single-step method of RNA isolation by acid guanidiniumthiocyanate-phenol-chloroform extraction. *Analytical Biochemistry* 162 (1): 156-159.

Chong, J, Kang, Z, Kim, WK and Rohringer, R. 1992. Multinucleate condition of *Puccinia striiformis* in colonies isolated from infected wheat leaves with macerating enzymes. *Canadian Journal of Botany* 70 (1): 222-224.

Clarke, JM and Richards, RA. 1988. The effects of glaucousness, epicuticular wax, leaf age, plant height, and growth environment on water loss rates of excised wheat leaves. *Canadian Journal of Botany* 73: 961-967.

Clavijo, BJ, Venturini, L, Schudoma, C, Accinelli, GG, Kaithakottil, G, Wright, J, Borrill, P, Kettleborough, G, Heavens, D, Chapman, H, Lipscombe, J, Barker, T, Lu, F, McKenzie, N, Raats, D, Ramirez-Gonzalez, RH, Coince, A, Peel, N, Percival-Alwyn, L, Duncan, O, Trösch, J, Yu, G, Bolser, DM, Namaati, G, Kerhornou, A, Spannagl, M, Gundlach, H, Haberer, G, Davey, RP, Fosker, C, Di Palma, FM, Phillips, AL, Millar, AH, Kersey, PJ,

Uauy, C, Krasileva, KV, David Swarbreck, D, Bevan, MW and Clark, MD. 2017. An improved assembly and annotation of the allohexaploid wheat genome identifies complete families of agronomic genes and provides genomic evidence for chromosomal translocations. *Genome Research* 27 (5): 885-896.

Clement, JA, Martin, SG, Porter, R, Butt, TM and Beckett, A. 1993. Germination and the role of extracellular matrix in adhesion of urediniospores of *Uromyces viciae-fabae* to synthetic surfaces. *Mycological Research* 97 (5): 585-593.

Clement, JA, Porter, R, Butt, TM and Beckett, A. 1994. The role of hydrophobicity in attachment of urediniospores and sporelings of *Uromyces viciae-fabae*. *Mycological Research* 98 (11): 1217-1228.

Colebrook, EH. 2010. The localisation of Pseudomonas-induced acquired resistance in barley. PhD thesis. University of East Anglia, United Kingdom.

Colebrook, EH, Creissen, G, McGrann, GRD, Dreos, R, Lamb, C and Boyd, LA. 2012. Broad-spectrum acquired resistance in barley induced by the *Pseudomonas* pathosystem shares transcriptional components with *Arabidopsis* systemic acquired resistance. *Molecular Plant-Microbe Interactions* 25 (5): 658-667.

Collins, NC, Niks, RE and P. Schulze-Lefert, P. 2007. Resistance to cereal rusts at the plant cell wall—what can we learn from other host-pathogen systems? *Australian Journal of Agricultural Research* 58: 476-489.

Collins, TJ, Moerschbacher, BM and Read, ND. 2001. Synergistic induction of wheat stem rust appressoria by chemical and topographical signals. *Physiological and Molecular Plant Pathology* 58: 259-266.

Conesa, A, Götz, S, García-Gómez, JM, Terol, J, Talón, M and Robles, M. 2005. Blast2GO: A universal tool for annotation, visualization and analysis in functional genomics research. *Bioinformatics* 21 (18): 3674-3676.

Coram, TE, Settles, ML and Chen, X. 2008. Transcriptome analysis of high-temperature adult-plant resistance conditioned by *Yr39* during the wheat-*Puccinia striiformis* f. sp. *tritici* interaction. *Molecular Plant Pathology* 9 (4): 479-493.

Dangl, JL and Jones, JDG. 2001. Plant pathogens and integrated defence responses to infection. *Nature* 411: 826-833.

Dawson, AM, Bettgenhaeuser, J, Gardiner, M, Green, P, Hernández-Pinzón, I, Hubbard, A and Moscou, MJ. 2015. The development of quick, robust, quantitative phenotypic assays for describing the host-nonhost landscape to stripe rust. *Frontiers in Plant Science* 6: 876.

Dawson, AM, Ferguson, JN, Gardiner, M, Green, P, Hubbard, A and Moscou, MJ. 2016. Isolation and fine mapping of *Rps6*: An intermediate host resistance gene in barley to wheat stripe rust. *Theoretical and Applied Genetics* 129 (4): 831-843.

Day, B, Dahlbeck, D, Huang, J, Chisholm, ST, Li, D and Staskawicz, BJ. 2005. Molecular basis for the RIN4 negative regulation of RPS2 disease resistance. *The Plant Cell* 17: 1292-1305.

Dean, R, Van Kan, JAL, Pretorius, ZA, Hammond-Kosack, KE, Di Pietro, A, Spanu, PD, Rudd, JJ, Dickman, M, Kahmann, R, Ellis, J and Foster, GD. 2012. The top 10 fungal pathogens in molecular plant pathology. *Molecular Plant Pathology* 13 (4): 414-430.

Deising, H, Nicholson, RL, Haug, M, Howard, RJ and Mendgen, K. 1992. Adhesion pad formation and the involvement of cutinase and esterases in the attachment of uredospores to the host cuticle. *Plant Cell* 4: 1101-1111.

Dempsey, DA and Klessig, DF. 2012. SOS - Too many signals for systemic acquired resistance? *Trends in Plant Science* 17 (9): 538-545.

Deslandes, L, Olivier, J, Peeters, N, Feng, DX, Khounlotham, M, Boucher, C, Somssich, I, Genin, S and Marco, Y. 2003. Physical interaction between RRS1-R, a protein conferring resistance to bacterial wilt, and PopP2, a type III effector targeted to the plant nucleus. *Proceedings of the National Academy of Sciences, USA* 100 (13): 8024-8029.

Dickinson, S. 1949. Studies in the physiology of obligate parasitism: II. The behaviour of the germ-tubes of certain rusts in contact with various membranes. *Annals of Botan*y 13 (50): 219-236.

Dixon, MS, Golstein, C, Thomas, CM, Van der Biezen, EA and Jones, JDG. 2000. Genetic complexity of pathogen perception by plants: The example of *Rcr3*, a tomato gene required

specifically by *Cf-2*. *Proceedings of the National Academy of Sciences, USA* 97 (16): 8807-8814.

Dobon, A, Bunting, DC, Cabrera-Quio, LE, Uauy, C and Saunders, DGO. 2016. The host-pathogen interaction between wheat and yellow rust induces temporally coordinated waves of gene expression. *BMC Genomics* 17 (1): 380.

Dodds, PN, Catanzariti, A, Lawrence, GJ and Ellis, JG. 2007. Avirulence proteins of rust fungi: Penetrating the host-haustorium barrier. *Australian Journal of Agricultural Research* 58: 512-517.

Dodds, PN, Lawrence, GJ, Catanzariti, A, Teh, T, Wang, CA, Ayliffe, MA, Kobe, B and Ellis, JG. 2006. Direct protein interaction underlies gene-for-gene specificity and coevolution of the flax resistance genes and flax rust avirulence genes. *Proceedings of the National Academy of Sciences, USA* 103 (23): 8888-8893.

Dorey, S, Baillieul, F, Pierrel, MA, Saindrenan, P, Fritig, B and Kauffmann, S. 1997. Spatial and temporal induction of cell death, defense genes, and accumulation of salicylic acid in tobacco leaves reacting hypersensitively to a fungal glycoprotein elicitor. *Molecular Plant-Microbe Interactions* 10 (5): 646-655.

Duplessis, S, Cuomo, CA, Lin, Y, Aerts, A, Tisserant, E, Veneault-Fourrey, C, Joly, DL, Hacquard, S, Amselem, J, Cantarel, BL, Chiu, R, Couthinho, PM, Feau, N, Field, M, Frey, P, Gelhaye, E, Goldberg, J, Grabherr, MG, Kodira, CD, Kohler, A, Kües, U, Lindquist, EA, Lucas, SM, Mago, R, Mauceli, E, Morin, E, Murat, C, Pangilinan, JL, Park, R, Pearson, M, Quesneville, H, Rouhier, N, Sakthikumar, S, Salamov, AA, Schmutz, J, Selles, B, Shapiro, H, Tangay, P, Tuskan, GA, Van de Peer, Y, Henrissat, B, Rouzé, P, Ellis, JG, Dodds, PN, Schein, JE, Zhong, S, Hamelin, RC, Grigoriev, IV, Szabo, LJ and Martin, F. 2011. Obligate biotrophy features unraveled by the genomic analysis of the rust fungi. *Proceedings of the National Acadamy of Sciences, USA* 108 (22): 9166-9171.

Durrant, WE and Dong, X. 2004. Systemic acquired resistance. *Annual Review of Phytopathology* 42: 185-209.

Dwight, Z, Palais, R and Wittwer, CT. 2011. uMELT: Prediction of high-resolution melting curves and dynamic melting profiles of PCR products in a rich web application. *Bioinformatics* 27 (7): 1019-1020.

Ehrlich, HG and Ehrlich, MA. 1963. Electron microscopy of the host-parasite relationships in stem rust of wheat. *American Journal of Botany* 50 (2): 123-130.

Ellis, JG, Lagudah, ES, Spielmeyer, W and Dodds, PN. 2014. The past, present and future of breeding rust resistant wheat. *Frontiers in Plant Science* 5: 641.

Emanuelsson, O, Nielsen, H, Brunak, S and Von Heijne, G. 2000. Predicting subcellular localization of proteins based on their N-terminal amino acid sequence. *Journal of Molecular Biology* 300 (4): 1005-1016.

Evans, IP. 1907. The Cereal Rusts I. The Development of their Uredo mycelia. *Annals of Botany* 21 (84): 441-466.

Favret, EA and Pidal, B. 2013. Wheat leaves: The surface disposition of their epicuticular wax. *Microscopy and Microanalysis* 19 (S2): 150-151.

Felix, G, Duran, JD Volko, S and Boller, T. 1999. Plants have a sensitive perception system for the most conserved domain of bacterial flagellin. The Plant Journal 18 (3): 265-276.

Feuillet, C, Travella, S, Stein, N, Albar, L, Nublat, A and Keller, B. 2003. Map-based isolation of the leaf rust disease resistance gene *Lr10* from the hexaploid wheat (*Triticum* aestivum L.) genome. *Proceedings of the National Academy of Sciences, USA* 100: 15253-15258.

Finn, RD, Attwood, TK, Babbitt, PC, Bateman, A, Bork, P, Bridge, AJ, Chang, HY, Dosztányi, Z, El-Gebali, S, Fraser, M, Gough, J, David Haft, D, Holliday, GL, Huang, H, Huang, X, Letunic, I, Lopez, R, Lu, S, Marchler-Bauer, A, Mi, H, Mistry, J, Natale, DA, Necci, M, Nuka, G, Orengo, CA, Park, Y, Pesseat, S, Piovesan, D, Potter, SC, Rawlings, ND, Redaschi, N, Richardson, L, Rivoire, C, Sangrador-Vegas, A, Sigrist, C, Sillitoe, I, Smithers, B, Squizzato, S, Sutton, G, Thanki, N, Thomas, PD, Tosatto, SCE, Wu, CH, Xenarios, I, Yeh, L, Young, S and Mitchell, AL. 2017. InterPro in 2017 - Beyond protein family and domain annotations. *Nucleic Acids Research* 45 (D1): D190-D199.

Flor, HH. 1971. Current status of the gene-for-gene concept. *Annual Review of Phytopathology* 9 (1): 275-296.

French, RC. 1992. Volatile chemical germination stimulators of rust and other fungal spores. *Mycologia* 84 (3): 277-288.

Fu, D, Uauy, C, Distelfeld, A, Blechl, A, Epstein, L, Chen, X, Sela, H, Fahima, T and Dubcovsky J. 2009. A kinase-START gene confers temperature-dependent resistance to wheat stripe rust. *Science* 323: 1357-1359.

Gambone, K. 2016. *Mapping stem rust resistance genes in 'Kingbird'.* PhD thesis. Kansas State University.

Gao, L, Chen, W, Liu, T and Liu, B. 2013. An immunofluorescence assay for the detection of wheat rust species using monoclonal antibody against urediniospores of *Puccinia triticina*. *Journal of Applied Microbiology* 115 (4): 1023-1028.

Gao, L, Yu, HX, Kang, XH, Shen, HM, Li, C, Liu, TG, Liu, B and Chen, WQ. 2016. Development of SCAR markers and an SYBR green assay to detect *Puccinia striiformis* f. sp. *tritici* in infected wheat leaves. *Plant Disease* 100 (9): 1840-1847.

Garnica, DP, Upadhyaya, NM, Dodds, PN and Rathjen JP. 2013. Strategies for wheat stripe rust pathogenicity identified by transcriptome sequencing. *PLOS ONE* 8 (6): e67150.

Gautam, P and Stein, J. 2011. Induction of systemic acquired resistance to *Puccinia sorghi* in corn. *International Journal of Plant Pathology* 2 (1): 43-50.

Giménez, MJ, Pistón, F and Atienza, SG. 2011. Identification of suitable reference genes for normalization of qPCR data in comparative transcriptomic analyses in the Triticeae. *Planta* 233: 163-173.

Glazebrook, J, Zook, M, Mert, F, Kagan, I, Rogers, EE, Crute, IR, Holub, EB, Hammerschmidt, R and Ausubelt, FM. 1997. Phytoalexin-deficient mutants of *Arabidopsis* reveal that pad4 encodes a regulatory factor and that four pad genes contribute to downy mildew resistance. *Genetics* 146: 381-392.

Gou, JY, Li, K, Wu, K, Wang, X, Lin, H, Cantu, D, Uauy, C, Dobon-Alonso, A, Midorikawa, T, Inoue, K and Sánchez, J. 2015. Wheat stripe rust resistance protein WKS1 reduces the ability of the thylakoid-associated ascorbate peroxidase to detoxify reactive oxygen species. *The Plant Cell* 27 (6): 1755-1770.

Gozzo, F and Faoro, F. 2013. Systemic acquired resistance (50 years after discovery): Moving from the lab to the field. *Journal of Agricultural and Food Chemistry* 61 (51): 12473-12491.

Gurr, SJ and Rushton, PJ. 2005. Engineering plants with increased disease resistance: How are we going to express it? *Trends in Biotechnology* 23 (6): 283-290.

Gustafson, GD and Shaner, G. 1982. Influence of plant age on the expression of slow-mildewing resistance in wheat. *Phytopathology* 72 (7): 746-749.

Hacquard, S, Delaruelle, C, Legué, V, Tisserant, E, Kohler, A, Frey, P, Martin, F and Duplessis, S. 2010. Laser capture microdissection of uredinia formed by *Melampsora larici-populina* revealed a transcriptional switch between biotrophy and sporulation. *Molecular Plant-Microbe Interactions* 23 (10): 1275-1286.

Hacquard, S, Veneault-Fourrey, C, Delaruelle, C, Frey, P, Martin, F and Duplessis, S. 2011. Validation of *Melampsora larici-populina* reference genes for *in planta* RT-quantitative PCR expression profiling during time-course infection of poplar leaves. *Physiological and Molecular Plant Pathology* 75 (3): 106-112.

Hahn, M and Mendgen, K. 1997. Characterization of *in planta*-induced rust genes isolated from a haustorium-specific cDNA library. *Molecular Plant-Microbe Interactions* 10 (4): 427-437.

Hahn, M, Neef, U, Struck, C, Göttfert, M and Mendgen, K. 1997. A putative amino acid transporter is specifically expressed in haustoria of the rust fungus *Uromyces fabae*. *Molecular Plant-Microbe Interactions* 10 (4): 438-445.

Hansen, BG, Halkier, BA and Kliebenstein, DJ. 2008. Identifying the molecular basis of QTLs: eQTLs add a new dimension. *Trends in Plant Science* 13 (2): 72-77.

Hansen, JG. 2017. Caution: Risk of wheat stem rust in Mediterranean basin in the forthcoming 2017 crop season following outbreaks on Sicily in 2016. [online] *Global Rust Reference Center*. Available at: http://wheatrust.org/news-and-events/news-item/artikel/caution-risk-of-stem-rust-in-eastern-mediterranean-basin-in-the-forthcoming-2017-season-due-to-ou/ [accessed 20-02-2017].

Hao, Y, Wang, T, Wang, K, Wang, X, Fu, Y, Huang, L and Kang, Z. 2016. Transcriptome analysis provides insights into the mechanisms underlying wheat plant resistance to stripe rust at the adult plant stage. *PLOS ONE* 11 (3): e0150717.

Hardcastle, T.J. and Kelly, K.A. 2010. baySeq: Empirical Bayesian methods for identifying differential expression in sequence count data. *BMC Bioinformatics* 11 (1): 422.

Hardham, AR. 2001. Cell biology of fungal infection of plants. Howard RJ and Gow, NAR (editors). *Biology of the fungal cell Volume VIII The Mycota*: 91-123.

Hellemans, J, Mortier, G, De Paepe, A, Speleman, F and Vandesompele, J. 2007. qBase relative quantification framework and software for management and automated analysis of real-time quantitative PCR data. *Genome Biology* 8 (2): R19.

Herrera-Foessel, SA, Lagudah, ES, Huerta-Espino, J, Hayden, MJ, Bariana, HS, Singh, D and Singh, RP. 2011. New slow-rusting leaf rust and stripe rust resistance genes *Lr67* and *Yr46* in wheat are pleiotropic or closely linked. *Theoretical and Applied Genetics* 122 (1): 239-249.

Herrera-Foessel, SA, Singh, RP, Lillemo, M, Huerta-Espino, J, Bhavani, S, Singh, S, Lan, C, Calvo-Salazar, V and Lagudah, ES. 2014. *Lr67*/*Yr46* confers adult plant resistance to stem rust and powdery mildew in wheat. *Theoretical and Applied Genetics* 127 (4): 781-789.

Hiebert, CW, Kolmer, JA, McCartney, CA, Briggs, J, Fetch, T, Bariana, H, Choulet, F, Rouse, MN and Spielmeyer, W. 2016. Major gene for field stem rust resistance co-locates with resistance gene *Sr12* in 'Thatcher' wheat. *PLOS ONE* 11 (6): e0157029.

Hiebert, CW, Thomas, JB, McCallum, BD, Humphreys, DG, DePauw, RM, Hayden, MJ, Mago, R, Schnippenkoetter, W and Spielmeyer, W. 2010. An introgression on wheat chromosome 4DL in RL6077 (Thatcher* 6/PI 250413) confers adult plant resistance to stripe rust and leaf rust (*Lr67*). *Theoretical and Applied Genetics* 121 (6): 1083-1091.

Hoch, HC, Staples, RC, Whitehed, B, Comeau, J and Wolf, ED. 1987. Signaling for growth orientation and cell differentiation by surface topography in *Uromyces*. *Science* 235: 1659-1663.

Horton, P, Park, KJ, Obayashi, T, Fujita, N, Harada, H, Adams-Collier, CJ and Nakai, K. 2007. WoLF PSORT: Protein localization predictor. *Nucleic Acids Research* 35 (S2): W585-W587.

Hu, G and Rijkenberg, FHJ. 1998. Scanning electron microscopy of early infection structure formation by *Puccinia recondita* f. sp. *tritici* on and in susceptible and resistant wheat lines. *Mycological Research* 102 (4): 391-399.

Huang, X, Ma, J, Chen, X, Wang, X, Ding, K, Han, D, Qu, Z, Huang, L and Kang, Z. 2013. Genes involved in adult plant resistance to stripe rust in wheat cultivar Xingzi 9104. *Physiological and Molecular Plant Pathology* 81: 26-32.

Hubbard, A, Lewis, CM, Yoshida, K, Ramirez-Gonzalez, RH, De Vallavieille-Pope, C, Thomas, J, Kamoun, S, Bayles, R, Uauy, C and Saunders, DGO, 2015. Field pathogenomics reveals the emergence of a diverse wheat yellow rust population. *Genome Biology* 16 (1): 23.

Hückelhoven, R, Dechert, C and Kogel, K. 2001. Non-host resistance of barley is associated with a hydrogen peroxide burst at sites of attempted penetration by wheat powdery mildew fungus. *Molecular Plant Pathology* 2 (4): 199-205.

Hughes, FL and Rijkenberg, FHJ. 1985. Scanning electron microscopy of early infection in the uredial stage of *Puccinia sorghi* in *Zea mays*. *Plant Pathology* 34: 61-68.

Hulbert, S and Pumphrey, M. 2014. A time for more booms and fewer busts? Unraveling cereal-rust interactions. *Molecular Plant-Microbe Interactions* 27 (3): 207-214.

Hurd-Karrer, AM and Rodenhiser, HA. 1947. Structures corresponding to appressoria and substomatal vesicles produced on nutrient-solution agar by cereal rusts. *American Journal of Botany* 34 (7): 377-384.

Ito, Y, Kaku, H and Shibuya, N. 1997. Identification of a high-affinity binding protein for N-acetylchitooligosaccharide elicitor in plasma membrane of suspension-cultured rice cells by affinity labelling. *The Plant Journal* 12 (2): 347-356.

Jackson, EW, Avant, JB, Overturf, KE and Bonman, JM. 2006. A quantitative assay of *Puccinia coronata* f. sp. *avenae* DNA in *Avena sativa*. *Plant Disease* 90 (5): 629-636.

Jarosch, B, Jansen, M and Schaffrath, U. 2003. Acquired resistance functions in *mlo* barley, which is hypersusceptible to *Magnaporthe grisea*. *Molecular Plant-Microbe Interactions* 16 (2): 107-114.

Jarošová, J and Kundu, JK. 2010. Validation of reference genes as internal control for studying viral infections in cereals by quantitative real-time RT-PCR. *BMC Plant Biology* 10 (1): 46.

Jin, Y. 2011. Role of *Berberis* spp. as alternate hosts in generating new races of *Puccinia graminis* and *P. striiformis*. *Euphytica* 179: 105-108.

Jin, Y, Szabo, LJ, Pretorius, ZA, Singh, RP, Ward, R and Fetch, T. 2008. Detection of virulence to resistance gene *Sr24* within race TTKS of *Puccinia graminis* f. sp. *tritici*. *Plant Disease* 92 (6) 923-926.

Johal, GS, Gray, J, Gruis, D and Briggs, S. P. 1995. Convergent insights into mechanism determining disease and resistant response in plant-fungal interactions. *Canadian Journal of Botany* 73 (supplement 1): 468-474.

Johansen, DA. 1940. *Plant microtechnique*. McGraw-Hill Book Company.

Johnson, R. 1979. Letter to the Editor: The concept of durable resistance. *Phytopathology*, 69 (3): 198-199.

Johnson, T. 1934. A tropic response in germ tubes of urediospores of *Puccinia graminis tritici*. *Phytopathology* 24: 80-82.

Jones, JDG and Dangl, JL. 2006. The plant immune system. *Nature* 444 (16): 323-329.

Jones, P, Binns, D, Chang, HY, Fraser, M, Li, W, McAnulla, C, McWilliam, H, Maslen, J, Mitchell, A, Nuka, G and Pesseat, S. 2014. InterProScan 5: Genome-scale protein function classification. *Bioinformatics* 30 (9): 1236-1240.

Joshi, RK and Nayak, S. 2010. Gene pyramiding - A broad spectrum technique for developing durable stress resistance in crops. *Biotechnology and Molecular Biology Reviews*, 5 (3): 51-60.

Jupe, F, Pritchard, L, Etherington, GJ, MacKenzie, K, Cock, PJA, Frank Wright, F, Sharma, SK, Bolser, D, Bryan, GJ, Jones, JDG and Hein, I. 2012. Identification and localisation of the NB-LRR gene family within the potato genome. *BMC Genomics* 13: 75.

Jupe, F, Witek, K, Verweij, W, Sliwka, J, Pritchard, L, Etherington, GJ, Maclean, D, Cock, PJA, Leggett, RM, Bryan, GJ, Cardle, L, Hein, I and Jones, JDG. 2013. Resistance gene enrichment sequencing (RenSeq) enables reannotation of the NB-LRR gene family from sequenced plant genomes and rapid mapping of resistance loci in segregating populations. *The Plant Journal* 76: 530-544.

Kaku, H, Nishizawa, Y, Ishii-Minami, N, Akimoto-Tomiyama, C, Dohmae, N, Takio, K, Minami, E and Shibuya, N. 2006. Plant cells recognize chitin fragments for defence

signalling through a plasma membrane receptor. *Proceedings of the National Academy of Science, USA* 103 (29): 11086-11091.

Käll, L, Krogh, A and Sonnhammer, EL. 2007. Advantages of combined transmembrane topology and signal peptide prediction - The Phobius web server. *Nucleic Acids Research* 35 (S2): W429-W432.

Kchouk, M, Gibrat, JF and Elloumi, M. 2017. Generations of sequencing technologies: From first to next generation. *Biology and Medicine* 9: 3.

Keith, RC, Keith, LWM, Hernández-Guzmán, G, Uppalapati, SR and Bender, CL. 2003. Alginate gene expression by *Pseudomonas syringae* pv. tomato DC3000 in host and non-host plants. *Microbiology* 149: 1127-1138.

Kemen, E, Kemen, AC, Rafiqi, M, Hempel, U, Mendgen, K, Hahn, M and Voegele, RT. 2005. Identification of a protein from rust fungi transferred from haustoria into infected plant cells. *Molecular Plant-Microbe Interactions* 18: 1130-1139.

Klarzynski, O, Plesse, B Joubert, J, Yvin, J, Kopp, M, Kloareg, B and Fritig, B. 2000. Linear β-1,3 glucans are elicitors of defense responses in tobacco. *Plant Physiology* 124: 1027-1037.

Kloppers, FJ and Pretorius ZA. 1997. Effects of combinations amongst genes *Lr13*, *Lr34* and *Lr37* on components of resistance in wheat to leaf rust. *Plant Pathology* 46: 737-750.

Koiattukudy, PE. 1985. Enzymatic penetration of the plant cuticle by fungal pathogens. *Annual Review of Phytopatholgy* 23: 223-250.

Kolmer, JA, Ordonez, ME and Groth, JV. 2009. *The Rust Fungi. Encyclopedia of Life Sciences.* John Wiley and Sons.

Kou, Y and Wang, S. 2010. Broad-spectrum and durability: Understanding of quantitative disease resistance. *Current Opinion in Plant Biology* 13 (2): 181-185.

Krattinger, SG, Lagudah, ES, Spielmeyer, W, Singh, RP, Huerta-Espino, J, McFadden, H, Bossolini, E, Selter, LL and Keller, B. 2009. A putative ABC transporter confers durable resistance to multiple fungal pathogens in wheat. *Science* 323: 1360-1363.

Krattinger, SG, Sucher, J, Selter, LL, Chauhan, H, Zhou, B, Tang, M, Upadhyaya, NM, Mieulet, D, Guiderdoni, E, Weidenbach, D and Schaffrath, U. 2016. The wheat durable,

multipathogen resistance gene *Lr34* confers partial blast resistance in rice. *Plant Biotechnology Journal*.14: 1261-1268.

Krogh, A, Larsson, B, Von Heijne, G and Sonnhammer, EL. 2001. Predicting transmembrane protein topology with a hidden Markov model: Application to complete genomes. *Journal of Molecular Biology* 305 (3): 567-580.

Lan, C, Rosewarne, GM, Singh, RP, Herrera-Foessel, SA, Huerta-Espino, J, Basnet, BR, Zhang, Y and Yang, E. 2014. QTL characterization of resistance to leaf rust and stripe rust in the spring wheat line Francolin# 1. *Molecular Breeding* 34 (3): 789-803.

Lanfranco, L, Novero, M and Bonfante, P. 2005. The mycorrhizal fungus *Gigaspora margarita* possesses a CuZn superoxide dismutase that is up-regulated during symbiosis with legume hosts. *Plant Physiology* 137 (4): 1319-1330.

Langmead, B and Salzberg, SL. 2012. Fast gapped-read alignment with Bowtie 2. *Nature Methods* 9 (4): 357.

Le Roux, J and Rijkenberg, FHJ. 1987. Occurrence and pathogenicity of *Puccinia graminis* f. sp. *tritici* in South Africa during the period 1981-1985. *Phytophylactica* 19 (4): 467-472.

Lennox, CL and Rijkenberg, FHJ. 1989. Scanning electron microscopy study of infection structure formation of *Puccinia graminis* f. sp. *tritici* in host and non-host cereal species. *Plant Pathology* 38 (4): 547-556.

Lennox, CL and Rijkenberg, FHJ. 1994. Towards an understanding of the expression of stem rust resistance gene *Sr5*. *Journal of Phytopathology* 140 (2): 165-171.

Leonard, KJ and Szabo, LJ. 2005. Stem rust of small grains and grasses caused by *Puccinia graminis*. *Molecular Plant Pathology* 6 (2): 99-111.

Lewis, BG and Day, JR. 1972. Behaviour of uredospore germ-tubes of *Puccinia graminis tritici* in relation to the fine structure of wheat leaf surfaces. *Transactions of the British Mycological Society* 58 (I): 139-145.

Lewis, CM, Persoons, A, Bebber, DP, Kigathi, RN, Maintz, J, Findlay, K, Bueno-Sancho, V, Corredor-Moreno, P, Harrington, SA, Kangara, N, Berlin, A, García, R, Germán, SE, Hanzalová, A, Hodson, DP, Hovmøller, MS, Huerta-Espino, J, Imtiaz, M, Mirza, JI, Justesen, AF, Niks, RE, Omrani, A, Patpour, M, Pretorius, ZA, Roohparvar, R, Sela, H, Singh, RP,

Steffenson, B, Visser, B, Fenwick, PM, Thomas, J, Wulff, BBH and Saunders, DGO. 2018. Potential for re-emergence of wheat stem rust in the United Kingdom. *Communications Biology* 1 (1): 13.

Li, K, Hegarty, J, Zhang, C, Wan, A, Wu, J, Guedira, GB, Chen, X, Muñoz-Amatriaín, M, Fu, D and Dubcovsky, J. 2016. Fine mapping of barley locus *Rps6* conferring resistance to wheat stripe rust. *Theoretical and Applied Genetics* 129 (4): 845-859.

Li, X, Kapos, P and Zhang, Y. 2015. NLRs in plants. *Current Opinion in Immunology* 32: 114-121.

Li, Z, Lan, C, He, Z, Singh, RP, Rosewarne, GM, Chen, X and Xia, X. 2014. Overview and application of QTL for adult plant resistance to leaf rust and powdery mildew in wheat. *Crop Science* 54: 1907-1925.

Liu, B, Xue, X, Cui, S, Zhang, X, Han, Q, Zhu, L, Liang, X, Wang, X, Huang, L, Chen, X and Kang, Z. 2010. Cloning and characterization of a wheat β-1, 3-glucanase gene induced by the stripe rust pathogen *Puccinia striiformis* f. sp. *tritici*. *Molecular Biology Reports* 37 (2): 1045.

Liu, L, Li, Y, Li, S, Hu, N, He, Y, Pong, R, Lin, D, Lu, L and Law, M. 2012. Comparison of next-generation sequencing systems. *Journal of Biomedicine and Biotechnology*: doi:10.1155/2012/251364.

Loutre, C, Wicker, T, Travella, S, Galli, P, Scofield, S, Fahima, T, Feuillet, C and Keller, B. 2009. Two different CC-NBS-LRR genes are required for *Lr10*-mediated leaf rust resistance in tetraploid and hexaploid wheat. *The Plant Journal* 60: 1043-1054.

Lowe, I, Cantu, D and Dubcovsky, J. 2011. Durable resistance to the wheat rusts: Integrating systems biology and traditional phenotype-based research methods to guide the deployment of resistance genes. *Euphytica* 179 (1): 69-79.

Lukasik, E and Takken, FLW. 2009. STANDing strong, resistance proteins instigators of plant defence. *Current Opinion in Plant Biology* 12: 427-436.

Mackey, D, Belkhadir, Y, Alonso, JM, Ecker, JR and Dangl JL. 2003. *Arabidopsis* RIN4 is a target of the type III virulence effector AvrRpt2 and modulates RPS2-mediated resistance. *Cell* 112: 379-389.

Mago, R, Lawrence, GJ and Ellis, JG. 2011. The application of DNA marker and doubled-haploid technology for stacking multiple stem rust resistance genes in wheat. *Molecular Breeding* 27 (3): 329-335.

Makandar, R, Essig, JS, Schapaugh, MA, Trick, HN and Shah, J. 2006. Genetically engineered resistance to *Fusarium* head blight in wheat by expression of *Arabidopsis NPR1*. *Molecular Plant-Microbe Interactions* 19 (2): 123-129.

Malamy, J, Sánchez-Casas, P, Henning, J, Guo, A and Klessig, DF. 1996. Dissection of the salicylic acid signaling pathway. *Molecular Plant-Microbe Interactions* 9: 474-482.

Maré, A. 2017. *Development of wheat lines with complex resistance to rusts and Fusarium head blight.* PhD thesis. University of the Free State, South Africa.

Mauch, F, Mauch-Mani, B and Boller, T. 1988. Antifungal hydrolases in pea tissue II. Inhibition of fungal growth by combinations of chitinase and β-1,3-glucanase. *Plant Physiology* 88, 936-942.

McDonald, BA and Linde, C. 2002. The population genetics of plant pathogens and breeding strategies for durable resistance. *Euphytica* 124 (2): 163-180.

McIntosh, RA. 1972. Cytogenetical studies in wheat VI. Chromosome location and linkage studies involving *Sr13* and *Sr8* for reaction to *Puccinia graminis* f. sp. *tritici*. *Australian Journal of Biological Sciences* 25 (4): 765-774.

McIntosh, RA, Dubcovsky, J, Rogers, W, Morris, C, Appels, R and Xia, X. 2016. *Catalogue of gene symbols for wheat: 2015-2016 supplement.*

McIntosh, RA, Wellings, CR and Park, RF. 1995. *Wheat rusts: An atlas of resistance genes.*

Melichar, JPE, Berry, S, Newell, C, MacCormack, R and Boyd LA. 2008. QTL identification and microphenotype characterization of the developmentally regulated yellow rust resistance. *Theoretical and Applied Genetics* 117: 391-399.

Mendgen, K. 1981. Nutrient uptake in rust fungi. *Phytopathology* 71 (9): 983-989.

Mendgen, K, Schneider, A, Sterk, M and Fink, W. 1988. The differentiation of infection structures as a result of recognition events between some biotrophic parasites and their hosts. *Journal of Phytopathology* 123 (3): 259-272.

Mendgen, K, Wirsel, SGR, Jux, A, Hoffmann, J and Boland, W. 2006. Volatiles modulate the development of plant pathogenic rust fungi. *Planta* 224: 1353-1361.

Mentlak, TA, Kombrink, A, Shinya, T, Ryder, LS, Otomo, I, Saitoh, H, Terauchi, R, Nishizawa, Y, Shibuya, N, Thomma, BPHJ and Talbot, NJ. 2012. Effector-mediated suppression of chitin-triggered immunity by *Magnaporthe oryzae* is necessary for rice blast disease. *The Plant Cell* 24: 322-335.

Metsalu, T and Vilo, J. 2015. ClustVis: A web tool for visualizing clustering of multivariate data using Principal Component Analysis and heatmap. *Nucleic Acids Research* 43 (W1): W566-W570.

Meyers, BC, Dickerman, AW, Michelmore, RW, Sivaramakrishnan, S, Sobral, BW and Young, ND. 1999. Plant disease resistance genes encode members of an ancient and diverse protein family within the nucleotide-binding superfamily. *The Plant Journal* 20 (3): 317-332.

Meyers, BC, Kozik, A, Griego, A, Kuang, H and Michelmore, RW. 2003. Genome-wide analysis of NBS-LRR-encoding genes in *Arabidopsis*. *The Plant Cell* 15: 809-834.

Miya, A, Albert, P, Shinya, T, Desaki, Y, Ichimura, K, Shirasu, K, Narusaka, Y, Kawakami, N, Kaku, H and Shibuya, N. 2007. CERK1, a LysM receptor kinase, is essential for chitin elicitor signaling in *Arabidopsis*. *Proceedings of the National Academy of Sciences, USA* 104 (49): 19613-19618.

Moerschbacher, BM, Noll, U, Gorrichon, L and Reisener, HJ. 1990. Specific inhibition of lignification breaks hypersensitive resistance of wheat to stem rust. *Plant Physiology*, 93 (2): 465-470.

Moldenhauer, J, Moerschbacher, BM and Van der Westhuizen, AJ. 2006. Histological investigation of stripe rust (*Puccinia striiformis* f. sp. *tritici*) development in resistant and susceptible wheat cultivars. *Plant Pathology* 55: 469-474.

Moldenhauer, J, Pretorius, ZA, Moerschbacher, BM, Prins, R and Van der Westhuizen, AJ. 2008. Histopathology and PR-protein markers provide insight into adult plant resistance to stripe rust of wheat. *Molecular Plant Pathology* 9 (2): 137-145.

Moore, JW, Herrera-Foessel, S, Lan, C, Schnippenkoetter, W, Ayliffe, M, Huerta-Espino, J, Lillemo, M, Viccars, L, Milne, R, Periyannan, S, Kong, X, Wolfgang Spielmeyer, W, Talbot,

M, Bariana, H, Patrick, JW, Dodds, P, Singh, R and Evans Lagudah, L. 2015. A recently evolved hexose transporter variant confers resistance to multiple pathogens in wheat. *Nature Genetics* 47 (12): 1494.

Mur, LA, Naylor, G, Warner, SA, Sugars, JM, White, RF and Draper, J. 1996. Salicylic acid potentiates defence gene expression in tissue exhibiting acquired resistance to pathogen attack. *The Plant Journal* 9 (4): 559-571.

Mur, LAJ, Kenton, P, Lloyd, AJ, Ougham, H and Prats, E. 2008. The hypersensitive response; the centenary is upon us but how much do we know? *Journal of Experimental Botany* 59 (3): 501-520.

Mysore, KS and Ryu C. 2004. Nonhost resistance: How much do we know? *Trends in Plant Science* 9 (2): 97-104.

Narusaka, M, Shirasu, K, Noutoshi, Y, Kubo, Y, Shiraishi, T, Iwabuchi, M and Narusaka, Y. 2009. RRS1 and RPS4 providea dual *Resistance*-gene system against fungal and bacterial pathogens. *The Plant Journal* 60: 218-226.

Neugebauer, KA, Bruce, M, Todd, T, Trick, HN and Fellers, JP. 2018. Wheat differential gene expression induced by different races of *Puccinia triticina*. *PLOS ONE* 13 (6): e0198350.

Niks, RE. 1986. Variation of mycelial morphology between species and formae speciales of rust fungi of cereals and grasses. *Canadian Journal of Botany* 64: 2976-2983.

Niks, RE and Thierry C. Marcel, TC. 2009. Nonhost and basal resistance: How to explain specificity? *New Phytologist* 182: 817-828.

Njau, PN, Bhavani, S, Huerta-Espino, J, Keller, B and Singh, RP. 2013. Identification of QTL associated with durable adult plant resistance to stem rust race Ug99 in wheat cultivar 'Pavon 76'. *Euphytica* 190 (1): 33-44.

Nowara, D, Gay, A, Lacomme, C, Shaw, J, Ridout, C, Douchkov, D, Hensel, G, Kumlehn, J and Schweizera, P. 2010. HIGS: Host-induced gene silencing in the obligate biotrophic fungal pathogen *Blumeria graminis*. *The Plant Cell* 22: 3130-3141

Nunes CC and Dean, RA. 2012. Host-induced gene silencing: A tool for understanding fungal host interaction and for developing novel disease control strategies. *Molecular Plant Pathology* 13 (5): 519-529.

Nürnberger, T, Brunner, F, Kemmerling, B and Piater, L. 2004. Innate immunity in plants and animals: Striking similarities and obvious differences. *Immunological Reviews* 198: 249-266.

Olivera Firpo, PD, Newcomb, M, Flath, K, Sommerfeldt, N, Szabo, LJ, Carter, M, Luster, DG and Jin, Y. 2017. Characterization of *Puccinia graminis* f. sp. *tritici* isolates derived from an unusual wheat stem rust outbreak in Germany in 2013. *Plant Pathology* 66 (8): 1258-1266.

Olivera, P, Newcomb, M, Szabo, LJ, Rouse, M, Johnson, J, Gale, S, Luster, DG, Hodson, D, Cox, JA, Burgin, L, Hort, M, Gilligan, CA, Patpour, M, Justesen, AF, Hovmøller, MS, Woldeab, G, Hailu, E, Hundie, B, Tadesse, K, Pumphrey, M, Singh, RP and Jin, Y. 2015. Phenotypic and genotypic characterization of race TKTTF of *Puccinia graminis* f. sp. *tritici* that caused a wheat stem rust epidemic in southern Ethiopia in 2013-14. *Phytopathology* 105 (7): 917-928.

Pan, Q, Wendel, J and Fluhr, R. 2000. Divergent evolution of plant NBS-LRR resistance gene homologues in dicot and cereal genomes. *Journal of Molecular Evolution* 50 (3): 203-213.

Panwar, V, Brent McCallum, B and Bakkeren, G. 2013. Endogenous silencing of *Puccinia triticina* pathogenicity genes through *in planta*-expressed sequences leads to the suppression of rust diseases on wheat. *The Plant Journal* 73: 521-532.

Paolacci, AR, Tanzarella, OA, Porceddu, E and Ciaffi, M. 2009. Identification and validation of reference genes for quantitative RT-PCR normalization in wheat. *BMC Molecular Biology* 10 (1): 11.

Papadopoulou, K, Melton, R.E, Leggett, M, Daniels, MJ and Osbourn, AE. 1999. Compromised disease resistance in saponin-deficient plants. *Proceedings of the National Academy of Sciences, USA* 96 (22): 12923-12928.

Pardey, PG, Beddow, JM, Kriticos, DJ, Hurley, TM, Park, RF, Duveiller, E, Sutherst, RW, Burdon, JJ and D. Hodson, D. 2013. Right-sizing stem-rust research. *Science* 340: 147-148.

Park, R, Fetch, T, Hodson, D, Jin, Y, Nazari, K, Prashar, M and Pretorius, ZA. 2011. International surveillance of wheat rust pathogens: Progress and challenges. *Euphytica* 179 (1): 109-117.

Park, RF. 2007. Stem rust of wheat in Australia. *Australian Journal of Agricultural Research* 58 (6): 558-566.

Passardi, F, Penel, C and Dunand, C. 2004. Performing the paradoxical: How plant peroxidases modify the cell wall. *Trends in plant science* 9 (11): 534-540.

Patpour, M, Hovmøller, MS and Justesen, AF, Newcomb, M, Olivera, Jin, PY, Szabo, LJ, Hodson, D, Shahin, AA, Wanyera, R, Habarurema, I and Wobibi, S. 2016. Emergence of virulence to *SrTmp* in the Ug99 race group of wheat stem rust, *Puccinia graminis* f. sp. *tritici*, in Africa. *Plant Disease* 100 (2): 522.

Patro, R, Duggal, G, Love, MI, Irizarry, RA and Kingsford, C. 2017. Salmon provides fast and bias-aware quantification of transcript expression. *Nature Methods* 14 (4): 417.

Peng, FY and Yang, RC. 2017. Prediction and analysis of three gene families related to leaf rust (*Puccinia triticina*) resistance in wheat (*Triticum aestivum* L.). *BMC Plant Biology* 17 (1): 108.

Periyannan, S, Milne, RJ, Figueroa, M, Lagudah, ES and Dodds, PN. 2017. An overview of genetic rust resistance: From broad to specific mechanisms. *PLOS Pathogens* 13 (7): e1006380.

Petersen, TN, Brunak, S, Von Heijne, G and Nielsen, H. 2011. SignalP 4.0: Discriminating signal peptides from transmembrane regions. *Nature Methods* 8 (10): 785-786.

Petre, B, Lorrain, C, Saunders, DGO, Win, J, Sklenar, J, Duplessis, S, Kamoun, S. 2016. Rust fungal effectors mimic host transit peptides to translocate into chloroplasts. *Cellular Microbiology* 18 (4): 453-465.

Petre, B, Saunders, DGO, Sklenar, J, Lorrain, C, Win, J, Duplessis, S and Kamoun, S. 2015. Candidate effector proteins of the rust pathogen *Melampsora larici-populina* target diverse plant cell compartments. *Molecular Plant-Microbe Interactions* 28 (6): 689-700.

Pfaffl, MW. 2001. A new mathematical model for relative quantification in real-time RT-PCR. *Nucleic Acids Research* 29 (9): 2002-2007.

Pliego, C, Nowara, D, Bonciani, G, Gheorghe, DM, Xu, R, Surana, R, Whigham, E, Nettleton, D, Bogdanove, AJ, Wise, RP, Schweizer, P, Bindschedler, LV and Spanu PD. 2013. Host-induced gene silencing in barley powdery mildew reveals a class of ribonuclease-like effectors. *Molecular Plant-Microbe Interactions* 26 (6): 633-642.

Pretorius, ZA, Bender, CM, Visser, B and Terefe, T. 2010. First report of a *Puccinia graminis* f. sp. *tritici* race virulent to the *Sr24* and *Sr31* wheat stem rust resistance genes in South Africa. *Plant Disease* 94 (6): 784.

Pretorius, ZA, Pienaar, L and Prins, R. 2007. Greenhouse and field assessment of adult plant resistance in wheat to *Puccinia striiformis* f. sp. *tritici*. *Australasian Plant Pathology* 36: 552-559.

Pretorius, ZA, Prins, R, Malaker, PK, Barma, NCD, Hakim, MA, Thapa, D, Bansal, U, Cisar, GL and Park, RF. 2015. Assessing the vulnerability of wheat germplasm from Bangladesh and Nepal to Ug99 stem rust. *Phytoparasitica* 43(5): 637-645.

Pretorius, ZA, Singh, RP and Wagoire, WW. 2000. Detection of virulence to wheat stem rust resistance gene *Sr31* in *Puccinia graminis* f.sp. *tritici* in Uganda. *Plant Disease* 84 (2): 203.

Pretorius, ZA, Szabo, LJ, Boshoff, WHP, Herselman, L and Visser, B. 2012. First report of a new TTKSF race of wheat stem rust (*Puccinia graminis* f. sp. *tritici*) in South Africa and Zimbabwe. *Plant Disease* 96 (4): 590-590.

Pretsch, K, Kemen, A, Kemen, E, Geiger, M, Mendgen, K and Voegele, RT. 2013. The rust transferred proteins - A new family of effector proteins exhibiting protease inhibitor function. *Molecular Plant Pathology* 14 (1): 96-107.

Prins, R, Dreisigacker, S, Pretorius, ZA, Van Schalkwyk, H, Wessels, E, Smit, C, Bender, CM, Singh, D and Boyd, LA. 2016. Stem rust resistance in a geographically diverse collection of spring wheat lines collected from across Africa. *Frontiers in Plant Science* 7: 973.

Puthoff, DP, Neelam, A, Ehrenfried, ML, Scheffler, BE, Ballard, L, Song, Q, Campbell, KB, Cooper, B and Tucker, ML. 2008. Analysis of expressed sequence tags from *Uromyces appendiculatus* hyphae and haustoria and their comparison to sequences from other rust fungi. *Phytopathology* 98 (10): 1126-1135.

Ray DK, Mueller ND, West PC and Foley JA. 2013. Yield trends are insufficient to double global crop production by 2050. *PLOS ONE* 8 (6): e66428.

Read, ND, Kellock, LJ, Collins, TJ and Gundlach, AM. 1997. Role of topography sensing for infection-structure differentiation in cereal rust fungi. *Planta* 202 (2): 163-170.

Rep, M. 2005. Small proteins of plant-pathogenic fungi secreted during host colonization. *Federation of European Microbiological Societies Microbiology Letters* 253: 19-27.

Rinaldi, C, Kohler, A, Frey, P, Duchaussoy, F, Ningre, N, Couloux, A, Wincker, P, Le Thiec, D, Fluch, S, Martin, F and Duplessis, S. 2007. Transcript profiling of poplar leaves upon infection with compatible and incompatible strains of the foliar rust *Melampsora larici-populina*. *Plant Physiology* 144 (1): 347-366.

Rinaldo, A, Gilbert, B, Boni, R, Krattinger, SG, Singh, D, Park, RF, Lagudah, E and Ayliffe, M. 2017. The *Lr34* adult plant rust resistance gene provides seedling resistance in durum wheat without senescence. *Plant Biotechnology Journal* 15: 894-905.

Risk, JM, Selter, LL, Chauhan, H, Krattinger, SG, Kumlehn, J, Hensel, G, Viccars, LA, Richardson, TM, Buesing, G, Troller, A and Lagudah, ES. 2013. The wheat *Lr34* gene provides resistance against multiple fungal pathogens in barley. *Plant Biotechnology Journal* 11 (7): 847-854.

Roderick, HW and Thomas, BJ. 1997. Infection of ryegrass by three rust fungi (*Puccinia coronata*, *P. graminis* and *P. loliina*) and some effects of temperature on the establishment of the disease and sporulation. *Plant Pathology* 46 (5): 751-761.

Roelfs, AP. 1982. Effects of barberry eradication on stem rust in the United States. *Plant Disease* 66: 177-181.

Roelfs, AP and Martens, JW. 1988. An international system of nomenclature for *Puccinia graminis* f. sp. *tritici*. *Phytopathology* 78: 526-533.

Roelfs, AP, Singh, RP and Saari, EE. 1992. *Rust diseases of wheat: Concepts and methods of disease management*. Hettel, GP (editor). CIMMYT.

Rohringer R, Kim WK, Samborsky DJ and Howes, NK. 1977. Calcofluor: An optical brightener for fluorescence microscopy of fungal plant parasites in leaves. *Phytopathology* 67: 808-810.

Ross, AF. 1961a. Localized acquired resistance to plant virus infection in hypersensitive hosts. *Virology* 14: 329-339.

Ross, AF. 1961b. Systemic acquired resistance induced by localized virus infections in plants. *Virology* 14: 340-358.

Rouse, MN, Nirmala, J, Jin, Y, Chao, S, Fetch, TG, Pretorius, ZA and Hiebert, CW. 2014. Characterization of *Sr9h*, a wheat stem rust resistance allele effective to Ug99. *Theoretical and Applied Genetics* 127 (8): 1681-1688.

Rubiales, D and Niks, RE. 1995. Characterization of *Lr34*, a major gene conferring nonhypersensitive resistance to wheat leaf rust. *Plant Disease* 79 (12): 1208-1212.

RustTracker.org. 2016. Pathotype Tracker - Where is Ug99? Status Summary: Ug99 Lineage - February 2016. [online] Available at: http://rusttracker.cimmyt.org/?page_id=22 [accessed 20-02-2017].

Rutkoski, JE, Poland, JA, Singh, RP, Huerta-Espino, J, Bhavani, S, Barbier, H, Rouse, MN, Jannink, J and Sorrells, ME. 2014. Genomic selection for quantitative adult plant stem rust resistance in wheat. *The Plant Genome* 7 (3).

Rutter, WB, Salcedo, A, Akhunova, A, He, F, Wang, S, Liang, H, Bowden, RL and Akhunov, E. 2017. Divergent and convergent modes of interaction between wheat and *Puccinia graminis* f. sp. *tritici* isolates revealed by the comparative gene co-expression network and genome analyses. *BMC Genomics* 18 (1): 291.

Salcedo, A, Rutter, W, Wang, S, Akhunova, A, Bolus, S, Chao, S, Anderson, N, De Soto, MF, Rouse, M, Szabo, L, Bowden, RL, Dubcovsky, J and Akhunov, E. 2017. Variation in the *AvrSr35* gene determines *Sr35* resistance against wheat stem rust race Ug99. *Science* 358 (6370): 1604-1606.

Sambrook, J, Fritsch, EF and Maniatis, T. (1989) *Molecular Cloning: A Laboratory Manual, Edition 2*. Cold Spring Harbor Laboratory Press, Cold Spring Harbor.

Sankaran, S, Mishra, A, Ehsani, R and Davis, C. 2010. A review of advanced techniques for detecting plant diseases. *Computers and Electronics in Agriculture* 72 (1): 1-13.

Saunders, DGO, Win, J, Liliana M, Cano, LM, Szabo, LJ, Kamoun, S and Raffaele. 2012. Using hierarchical clustering of secreted protein families to classify and rank candidate effectors of rust fungi. *PLOS ONE* 7(1): e29847.

Saunders, DGO. 2015. Hitchhiker's guide to multi-dimensional plant pathology. *New Phytologis*t 205: 1028-1033.

Schena, L, Nigro, F, Ippolito, A and Gallitelli, D. 2004. Real-time quantitative PCR: A new technology to detect and study phytopathogenic and antagonistic fungi. *European Journal of Plant Pathology* 110 (9): 893-908.

Scholtz, JJ and Visser, B. 2013. Reference gene selection for qPCR gene expression analysis of rust-infected wheat. *Physiological and Molecular Plant Pathology* 81: 22-25.

Schwessinger, B and Zipfel, C. 2008. News from the frontline: Recent insights into PAMP-immunity in plants. *Current Opinion in Plant Biology* 11: 389-395.

Segovia, V, Hubbard, A, Craze, M, Bowden, S, Wallington, E, Bryant, R, Greenland, A, Bayles, R and Uauy, C. 2014. *Yr36* confers partial resistance at temperatures below 18°C to UK isolates of *Puccinia striiformis*. *Phytopathology* 104 (8): 871-878.

Setten, LM, Lendoiro, N and Favret, EA. 2015. Wheat leaf rust fungus: RIMAPS analysis to detect germ-tube orientation pattern. *Microscopy and Microanalysis* 21: 227-228.

Shabab, M, Shindo, T, Gu, C, Kaschani, F, Pansuriya, T, Chintha, R, Harzen, A, Colby, T, Kamoun, S and Van der Hoorn, RAL. 2008. Fungal effector protein AVR2 targets diversifying defense-related Cys proteases of tomato. *The Plant Cell* 20: 1169-1183.

Sharma, S, Shiveta, S, Hirabuchi, A, Yoshida, K, Fujisaki, K, Ito, A, Uemura, A, Terauchi, R, Kamoun, S, Sohn, KH, Jones JDG and Saitoh, H. 2013. Deployment of the *Burkholderia glumae* type III secretion system as an efficient tool for translocating pathogen effectors to monocot cells. *The Plant Journal* 74: 701-712.

Sherwood, RT and Vance, CP. 1976. Histochemistry of papillae formed in reed canarygrass leaves in response to noninfecting pathogenic fungi. *Phytopathology* 66: 503-510.

Shimizu, T, Nakano, T, Takamizawa, D, Desaki, Y, Ishii-Minami, N, Nishizawa, Y, Minami, E, Okada, K, Yamane, H, Kaku, H and Shibuya, N. 2010. Two LysM receptor molecules,

CEBiP and OsCERK1, cooperatively regulate chitin elicitor signaling in rice. *The Plant Journal* 64 (2): 204-14.

Shinya, T, Motoyama, N, Ikeda, A, Wada, M, Kamiya, K, Hayafune, M, Kaku, H and Shibuya, N. 2012. Functional characterization of CEBiP and CERK1 homologs in *Arabidopsis* and rice reveals the presence of different chitin receptor systems in plants. *Plant and Cell Physiology* 53 (10): 1696-1706.

Singh, RP, Hodson, DP, Huerta-Espino, J, Jin, Y, Njau, P, Wanyera, R, Herrera-Foessel, SA and Ward, RW. 2008. Will stem rust destroy the world's wheat crop? Sparks, DL (editor). *Advances in Agronomy* 98: 271-309.

Singh, RP, Hodson, DP, Jin, Y, Huerta-Espino, J, Kinyua, MG, Wanyera, R, Njau, P and Ward, RW. 2006. Current status, likely migration and strategies to mitigate the threat to wheat production from race Ug99 (TTKS) of stem rust pathogen. *Centre for Agriculture and Bioscience Reviews: Perspectives in Agriculture, Veterinary Science, Nutrition and Natural Resources* 1 (54): 1-13.

Singh, RP, Hodson, DP, Jin, Y, Lagudah, ES, Ayliffe, MA, Bhavani, S, Rouse, MN, Pretorius, ZA, Szabo, LJ, Huerta-Espino, J, Basnet, BR, Lan, C and Hovmøller, MS. 2015. Emergence and spread of new races of wheat stem rust fungus: Continued threat to food security and prospects of genetic control. *Phytopathology* 105 (7): 872-884.

Skipp, RA, Harder, DE and Samborski, DJ. 1974. Electron microscopy studies on infection of resistant (*Sr6* gene) and susceptible near-isogenic wheat lines by *Puccinia graminis* f. sp. *tritici*. *Canadian Journal of Botany* 52 (12): 2615-2620.

Skottrup, P, Frøkiær, H, Hearty, S, O'Kennedy, R, Hejgaard, J, Nicolaisen, M and Justesen, AF. 2007. Monoclonal antibodies for the detection of *Puccinia striiformis* urediniospores. *Mycological Research* 111 (3): 332-338.

Soko, T, Bender, CM, Renee Prins, R and Pretorius, ZA. 2018. Yield loss associated with different levels of stem rust resistance in bread wheat. *Plant Disease*: doi:10.1094/PDIS-02-18-0307-RE.

Song, X, Christof Rampitsch, C, Soltani, B, Mauthe, W, Linning, R, Banks, T, McCallum, B and Bakkeren, G. 2011. Proteome analysis of wheat leaf rust fungus, *Puccinia triticina*, infection structures enriched for haustoria. *Proteomics* 11: 944-963.

Sørensen, CK, Justesen, AF and Hovmøller, MS. 2012. 3-D imaging of temporal and spatial development of *Puccinia striiformis* haustoria in wheat. *Mycologia* 104 (6): 1381-1389.

Sperschneider, J, Catanzariti, AM, DeBoer, K, Petre, B, Gardiner, DM, Singh, KB, Dodds, PN and Taylor, JM. 2017. LOCALIZER: Subcellular localization prediction of both plant and effector proteins in the plant cell. *Scientific Reports* 7: 44598.

Sperschneider, J, Dodds, PN, Gardiner, DM, Singh, KB and Taylor, JM. 2018. Improved prediction of fungal effector proteins from secretomes with EffectorP 2.0. *Molecular Plant Pathology*: doi:10.1111/mpp.12682.

Sperschneider, J, Gardiner, DM, Dodds, PN, Tini, F, Covarelli, L, Singh, KB, Manners, JM and Taylor, JM. 2015. EffectorP: Predicting fungal effector proteins from secretomes using machine learning. *New Phytologist* 210 (2): 743-761.

Sperschneider, J, Ying, H, Dodds, PN, Gardiner, DM, Upadhyaya, NM, Singh, KB, Manners JM and Taylor, JM. 2014. Diversifying selection in the wheat stem rust fungus acts predominantly on pathogen-associated gene families and reveals candidate effectors. *Frontiers in Plant Science* 5: 372.

Spoel, SH, Koornneef, A, Claessens, SM, Korzelius, JP, Van Pelt, JA, Mueller, MJ, Buchala, AJ, Métraux, JP, Brown, R, Kazan, K and Van Loon, LC. 2003. NPR1 modulates cross-talk between salicylate- and jasmonate-dependent defense pathways through a novel function in the cytosol. *The Plant Cell* 15 (3): 760-770.

Stakman, EC, Stewart, DM and Loegering, WQ. 1962. *Identification of physiologic races of Puccinia graminis var. tritici.* USDA ARS.

Staples, RC, Grambow, HJ, Hoch, HC and Wynn, WK. 1983. Contact with membrane grooves induces wheat stem rust uredospore germlings to differentiate appressoria but not vesicles. *Phytopathology* 73 (10): 1436-1439.

Stein, M, Dittgen, J, Sánchez-Rodríguez, C, Hou, B, Molina, A, Schulze-Lefert, P, Lipka, V and Somerville, S. 2006. *Arabidopsis* PEN3/PDR8, an ATP binding cassette transporter, contributes to nonhost resistance to inappropriate pathogens that enter by direct penetration. *The Plant Cell* 18: 731-746.

Steuernagel, B, Jupe, F, Witek, K, Jones, JDG and Wulff, BBH. 2015. NLR-parser: Rapid annotation of plant NLR complements. *Bioinformatics* 31 (10): 1665-1667.

Steuernagel, B, Periyannan, SK, Hernández-Pinzón, I, Witek, K, Rouse, MN, Yu, G, Hatta. A, Ayliffe, M, Bariana, H, Jones, JDG, Lagudah, ES and Wulff, BBH. 2016. Rapid cloning of disease-resistance genes in plants using mutagenesis and sequence capture. *Nature Biotechnology* 34: 652-655.

Sticher, L, Mauch-Mani, B and Métraux, JP. 1997. Systemic acquired resistance. *Annual Review of Phytopathology* 35: 235-270.

Struck, C, Ernst, M and Hahn, M. 2002. Characterization of a developmentally regulated amino acid transporter (AAT1p) of the rust fungus *Uromyces fabae. Molecular Plant Pathology* 3 (1): 23-30.

Struck, C, Hahn, M and Mendgen, K. 1996. Plasma membrane H^+-ATPase activity in spores, germ tubes, and haustoria of the rust fungus *Uromyces viciae-fabae*. *Fungal Genetics and Biology* 20: 30-35.

Sturn, A, Quackenbush, J and Trajanoski, Z. 2002. Genesis: Cluster analysis of microarray data. *Bioinformatics* 18 (1): 207-208.

Sucher, J, Boni, R, Yang, P, Rogowsky, P, Büchner, H, Kastner, C, Kumlehn, J, Krattinger, SG and Keller, B. 2017. The durable wheat disease resistance gene *Lr34* confers common rust and northern corn leaf blight resistance in maize. *Plant Biotechnology Journal* 15 (4): 489-496.

Tanaka, S, Brefort, T, Neidig, N, Djamei, A, Kahnt, J, Vermerris, W, Koenig, S, Feussner, K, Feussner, I and Kahmann, R. 2014. A secreted *Ustilago maydis* effector promotes virulence by targeting anthocyanin biosynthesis in maize. *eLife* 3: e01355.

Tarr, DEK and Alexander HM. 2009. *TIR-NBS-LRR* genes are rare in monocots: Evidence from diverse monocot orders. *BMC Research Notes* 2 (1): 197.

Taylor, S, Wakem, M, Dijkman, G, Alsarraj, M and Nguyen, M. 2010. A practical approach to RT-qPCR - Publishing data that conform to the MIQE guidelines. *Methods* 50 (4): S1-S5.

Terefe, TG, Visser, B and Pretorius, ZA. 2016. Variation in *Puccinia graminis* f. sp. *tritici* detected on wheat and triticale in South Africa from 2009 to 2013. *Crop Protection* 86: 9-16.

Terhune, BT and Hoch, HC. 1993. Substrate hydrophobicity and adhesion of *Uromyces* urediospores and germlings. *Experimental Mycology* 17 (4): 241-252.

Thomma, BPHJ, Nelissen, I, Eggermont, K and Broekaert, WF. 1999. Deficiency in phytoalexin production causes enhanced susceptibility of *Arabidopsis* thaliana to the fungus Alternaria brassicicola. *The Plant Journal* 19 (2): 163-171.

Thordal-Christensen, H, Zhang, Z, Wei, Y and Collinge, DB. 1997. Subcellular localization of H_2O_2 in plants. H_2O_2 accumulation in papillae and hypersensitive response during the barley-powdery mildew interaction. *The Plant Journal* 11 (6): 1187-1194.

Tiburzy, R, Noll, U and Reisener, HJ. 1990. Resistance of wheat to *Puccinia graminis* f. sp. *tritici*: Histological investigation of resistance caused by the *Sr5* gene. *Physiological and Molecular Plant Pathology* 36 (2): 95-108.

Tulloch AP. 1973. Composition of leaf surface waxes of *Triticum* species: Variation with age and tissue. *Phytochemistry* 12 (9): 2225-2232.

Tyagi, S, Mir, RR, Kaur, H, Chhuneja, P, Ramesh, B, Balyan, HS and Gupta, PK. 2014. Marker-assisted pyramiding of eight QTLs/genes for seven different traits in common wheat (*Triticum aestivum* L.). *Molecular Breeding* 34 (1): 167-175.

Uddin, MN and Marshall, DR. 1988. Variation in epicuticular wax content in wheat. *Euphytica* 38 (1): 3-9.

United States Department of Agriculture (USDA). November 2018. *World Agricultural Production, Circular Series, WAP* 11-18.

Upadhyaya, NM, Garnica, DP, Karaoglu, H, Sperschneider, J, Nemri, A, Xu, B, Mago, R, Cuomo, CA, Rathjen, JP, Park, RF, Ellis, JG and Dodds, PN. 2015. Comparative genomics of Australian isolates of the wheat stem rust pathogen *Puccinia graminis* f. sp. *tritici* reveals extensive polymorphism in candidate effector genes. *Frontiers in Plant Science* 5: 759.

Upadhyaya, NM, Mago, R, Staskawicz, BJ, Ayliffe, MA, Ellis, JG and Dodds, PN. 2014. A bacterial type III secretion assay for delivery of fungal effector proteins into wheat. *Molecular Plant-Microbe Interactions* 27 (3): 255-264.

Van den Burg, HA, Harrison, SJ, Joosten, MHAJ, Vervoort, J and DeWit PJGM. 2006. *Cladosporium fulvum* Avr4 protects fungal cell walls against hydrolysis by plant chitinases accumulating during infection. *Molecular Plant-Microbe Interactions* 19 (12): 1420-1430.

Van den Burg, HA, Westerink, N, Francoijs, KJ, Roth, R, Woestenenk E, Boeren, S, de Wit, PJ, Joosten, MH and Vervoort, J. 2003. Natural disulphide bond-disrupted mutants ofAVR4 of the tomato pathogen *Cladosporium fulvum* are sensitive to proteolysis, circumvent Cf-4-mediated resistance, but retain their chitin binding ability. *The Journal of Biological Chemistry* 278: 27340-27346.

Van der Biezen, EA and Jones, JDG. 1998a. Plant disease resistance proteins and the gene-for-gene concept. *Trends in Biochemical Science* 23: 454-456.

Van der Biezen, EA and Jones, JDG. 1998b.The NB-ARC domain: A novel signalling motif shared by plant resistance gene products and regulators of cell death in animals. *Current Biology* 8 (7): R226-R227.

Van der Hoorn, RAL and Kamoun, S. 2008. From guard to decoy: A new model for perception of plant pathogen effectors. *The Plant Cell* 20: 2009-2017.

Van Loon, LC. 1997. Induced resistance in plants and the role of pathogenesis-related proteins. *European Journal of Plant Pathology* 103 (9): 753-765.

Van Loon, LC, Rep, M and Pieterse, CMJ. 2006. Significance of inducible defence-related proteins in infected plants. *Annual Review Phytopathology* 44: 135-162.

Vandesompele, J, De Preter, K, Pattyn, F, Poppe, B, Van Roy, N, De Paepe, A and Speleman, F. 2002. Accurate normalization of real-time quantitative RT-PCR data by geometric averaging of multiple internal control genes. *Genome Biology* 3 (7): 0034.1-0034.11.

Visser, B, Herselman, L, Park, RF, Karaoglu, H, Bender, CM and Pretorius, ZA. 2011. Characterization of two new *Puccinia graminis* f. sp. *tritici* races within the Ug99 lineage in South Africa. *Euphytica* 179 (1): 119-127.

Vleeshouwers, VG and Oliver, RP. 2014. Effectors as tools in disease resistance breeding against biotrophic, hemibiotrophic, and necrotrophic plant pathogens. *Molecular Plant-Microbe Interactions* 27 (3): 196-206.

Voegele, RT and Mendgen, KW. 2011. Nutrient uptake in rust fungi: How sweet is parasitic life? *Euphytica* 179 (1): 41-55.

Voegele, RT and Schmid, A. 2011. RT real-time PCR-based quantification of *Uromyces fabae in planta*. *Federation of European Microbiological Societies Microbiology Letters* 322: 131-137.

Voegele, RT, Hahn, M and Mendgen, K. 2009. The uredinales: Cytology, biochemistry, and molecular biology. Deising, HB. (editor). *Plant Relationships Volume V The Mycota*: 69-98.

Voegele, RT, Struck, C, Hahn, M and Mendgen, K. 2001. The role of haustoria in sugar supply during infection of broad bean by the rust fungus *Uromyces fabae*. *Proceedings of the National Academy of Sciences, USA* 98 (14): 8133-8138.

Voigt, CA and Wilhelm Schäfer, W and Salomon, S. 2005. Secreted lipase of *Fusarium graminearum* is a virulence factor required for infection of cereals. *The Plant Journal* (2005) 42: 364-375.

Wang, C, Huang, L, Buchenauer, H, Han, Q, Zhang, H and Kang, Z. 2007. Histochemical studies on the accumulation of reactive oxygen species (O_2^- and H_2O_2) in the incompatible and compatible interaction of wheat-*Puccinia striiformis* f. sp. *tritici*. *Physiological and Molecular Plant Pathology* 71 (4): 230-239.

Wang, C, Huang, L, Zhang, H, Han, Q, Buchenauer, H and Kang, Z. 2010. Cytochemical localization of reactive oxygen species (O_2^- and H_2O_2) and peroxidase in the incompatible and compatible interaction of wheat-*Puccinia striiformis* f. sp. *tritici*. *Physiological and Molecular Plant Pathology* 74: 221-229.

Wang, X, McCallum, BD, Fetch, T, Bakkeren, G and Saville, BJ. 2015. *Sr36*- and *Sr5*-mediated resistance response to *Puccinia graminis* f. sp. *tritici* is associated with callose deposition in wheat guard cells. *Phytopathology* 105 (6): 728-737.

Wang, X, Richards, J, Gross, T, Druka, A, Kleinhofs, A, Steffenson, B Acevedo, M and Brueggeman, R. 2013. The rpg4-mediated resistance to wheat stem rust (*Puccinia graminis*) in barley (*Hordeum vulgare*) requires Rpg5, a second NBS-LRR gene, and an actin depolymerization factor. *Molecular Plant-Microbe Interactions* 26 (4): 407-418.

Wang, Z, Gerstein, M and Snyder, M. 2009. RNA-Seq: A revolutionary tool for transcriptomics. *Nature Reviews Genetics* 10 (1): 57.

Wanyera, R, Kinyua, MG, Jin, Y and Singh, RP. 2006. The spread of stem rust caused by *Puccinia graminis* f. sp. *tritici*, with virulence on *Sr*31 in wheat in eastern Africa. *Plant Disease* 90: 113.

Wesp-Guterres, C, Martinelli, JA, Graichen, FAS and Chaves, MS. 2013. Histopathology of durable adult plant resistance to leaf rust in the Brazilian wheat variety Toropi. *European Journal of Plant Pathology* 137: 181-196.

Wiethölter, N, Horn, S, Reisige, K, Beike, U and Moerschbacher, BM. 2003. *In vitro* differentiation of haustorial mother cells of the wheat stem rust fungus, *Puccinia graminis* f. sp. *tritici*, triggered by synergistic action of chemical and physical signals. *Fungal Genetics and Biology* 38 (3): 320-326.

Williams, PG. 1971. A new perspective of the axenic culture of *Puccinia graminis* f. sp. *tritici* from uredospores. *Phytopathology* 61: 994-1002.

Williams, SJ, Sohn, KH, Wan, L, Bernoux, M, Sarris, PF, Segonzac, C, Ve, T, Ma, Y, Saucet, SB, Ericsson, DJ, Casey, LW, Lonhienne, T, Winzor, DJ, Zhang, X, Coerdt, A, Parker, JE, Dodds, PN, Kobe, B and Jones, JDG. 2014. Structural basis for assembly and function of a heterodimeric plant immune receptor. *Science* 344: 299-303.

Wu, C, Krasileva, KV, Banfield, MJ, Terauchi, R and Kamoun, S. 2015. The "sensor domains" of plant NLR proteins: More than decoys? *Frontiers in Plant Science* 6: 134.

Wynn, WK and Wilmot, VA. 1977. Growth of germ tubes of the wheat stem rust fungus on leaves and leaf replicas. *Annual Proceedings of the American Phytopathological Society* 4: 129.

Wynn, WK. 1976. Appressorium formation over stomates by bean rust fungus: Response to a surface contact stimulus. *Phytopathology* 66 (2): 136-146.

Yamaguchi, T, Akira Yamada, A, Hong, N, Ogawa, T, Ishii, T and Shibuyaa, N. 2000. Differences in the recognition of glucan elicitor signals between rice and soybean: β-glucan fragments from the rice blast disease fungus *Pyricularia oryzae* that elicit phytoalexin biosynthesis in suspension-cultured rice cells. *The Plant Cell* 12: 817-826.

Yin, C and Hulbert, S. 2011. Prospects for functional analysis of effectors from cereal rust fungi. *Euphytica* 179: 57-67.

Yin, C, Chen, X, Wang, X, Han, Q, Kang, Z and Hulbert, S.H. 2009. Generation and analysis of expression sequence tags from haustoria of the wheat stripe rust fungus *Puccinia striiformis* f. sp. *tritici*. *BMC Genomics* 10 (1): 626.

Yin, C, Downey, SI, Klages-Mundt NL, Ramachandran, S, Chen, X, Szabo, LJ, Pumphrey, M and Hulbert, SH. 2015. Identification of promising host-induced silencing targets among genes preferentially transcribed in haustoria of *Puccinia*. *BMC Genomics* 16: 579.

Yu, LX, Barbier, H, Rouse, MN, Singh, S, Singh, RP, Bhavani, S, Huerta-Espino, J and Sorrells, ME. 2014. A consensus map for Ug99 stem rust resistance loci in wheat. *Theoretical and Applied Genetics* 127 (7): 1561-1581.

Zadoks, JC, Chang, TT and Konzak, CF. 1974. A decimal code for the growth stages of cereals. *Weed Research* 14 (6): 415-421.

Zhang, H, Wang, C, Cheng, Y, Chen, X, Han, Q, Huang, L, Wei, G and Kang, Z. 2012. Histological and cytological characterization of adult plant resistance to wheat stripe rust. *Plant Cell Reports* 31 (12): 2121-2137.

Zhang, W, Chen, S, Abate, Z, Nirmala, J, Rouse, MN and Dubcovsky, J. 2017. Identification and characterization of *Sr13*, a tetraploid wheat gene that confers resistance to the Ug99 stem rust race group. *Proceedings of the National Academy of Sciences, USA*: doi/10.1073/pnas.1706277114.

Zhao, S, Xi, L and Zhang, B. 2015. Union exon based approach for RNA-seq gene quantification: To be or not to be? *PLOS ONE* 10 (11): e0141910.

Zipfel, C. 2014. Plant pattern-recognition receptors. *Trends in Immunology* 35 (7): 345-351.

Zurn, JD, Dugyala, S, Borowicz, P, Brueggeman, R and Acevedo, M. 2015. Unraveling the wheat stem rust infection process on barley genotypes through relative qPCR and fluorescence microscopy. *Phytopathology* 105 (5): 707-712.